THE INFLUENCE OF IRON AND SULFUR MINERALS ON SUB-ICE BIOGEOCHEMICAL PROCESSES AT LAKE BONNEY, ANTARCTICA AND BENCH GLACIER, ALASKA

by

August James Steigmeyer

A dissertation submitted in partial fulfillment
of the requirements for the degree

of

Doctor of Philosophy

in

Earth Sciences

MONTANA STATE UNIVERSITY
Bozeman, Montana

July 2024

©COPYRIGHT

by

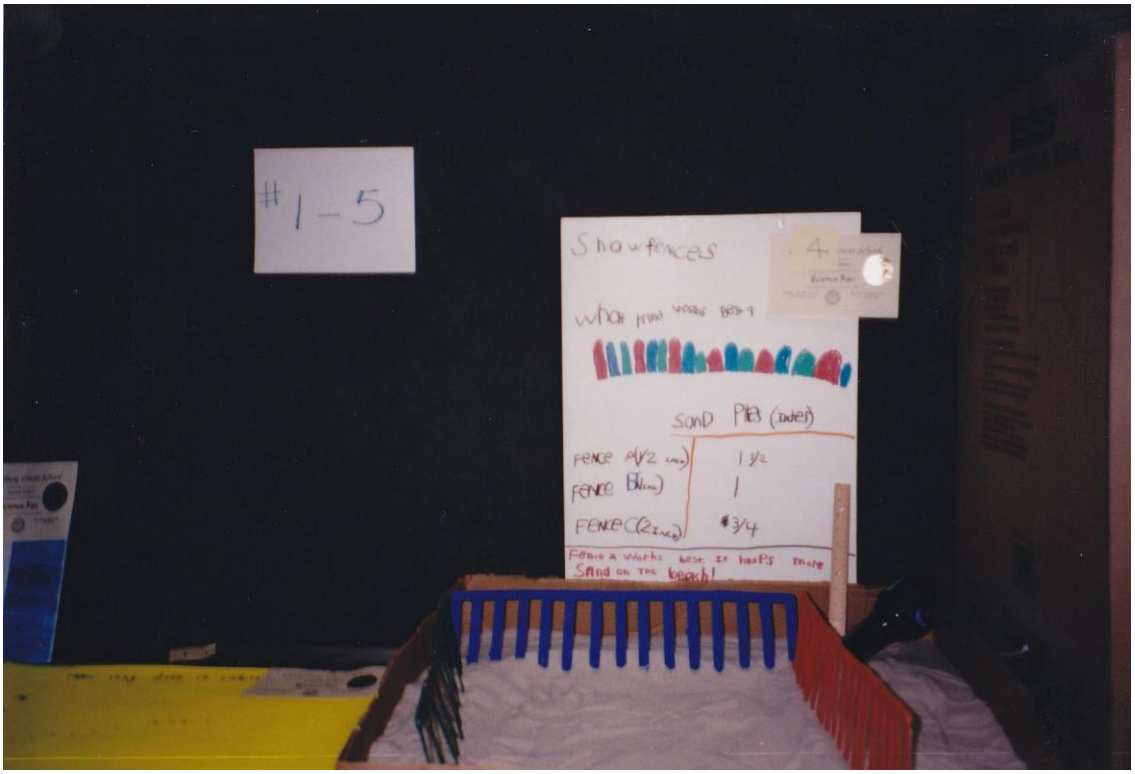
August James Steigmeyer

2024

All Rights Reserved

DEDICATION

For Mom, Dad, Joe, and Hannah whose support over the last 35 years carried me to this point.



"It is a capital mistake to theorize before one has data. Insensibly one begins to twist facts to suit theories, instead of theories to suit facts."

– Sherlock Holmes, *A Scandal in Bohemia*.

"Facts are meaningless. You can use facts to prove anything that's even remotely true."

– Homer Simpson.

ACKNOWLEDGEMENTS

I would first like to acknowledge my advisor Mark Skidmore for his guidance and support throughout my graduate program, for his help in the lab and with data analyses, and the many hours spent editing and advising on this dissertation. I would also like to thank my committee members Dave Bowen, Eric Boyd, and Jean Dixon for their support and guidance throughout my PhD program.

I want to thank John Priscu for inviting me to join the LTER Limnology Team in the McMurdo Dry Valleys, Antarctica. This fieldwork made the research in this dissertation possible, and I am extremely grateful for the opportunity to see Lake Bonney in person. The successful sample collection in Antarctica also would not have been possible without the guidance and expertise of Wei Li and the McMurdo Dry Valleys LTER.

Several people assisted with or conducted key analyses. Wei Li helped design and set up the Lake Bonney water/sediment incubations described in Chapter 3. John Dore conducted the ethane gas measurements described in Chapter 3. Maria Fernandes-Martins assembled the Bench Glacier isolate genome and identified the 16S sequence in Chapter 5. Tim Campbell ran the Mastersizer to obtain data on grain size for experiments in Chapters 3 and 5. Sara Zacher operated the Scanning Electron Microscope described in Chapter 5.

Research was supported by NESSF award 80NSSC18K1266 to John Priscu, John Dore, and Mark Skidmore and by the NASA Earth and Space Science Fellowship award (PLANET18F-0194) to August Steigmeyer. Dissertation writing and preparation was supported by the Montana State University Graduate Completion Award to August Steigmeyer.

TABLE OF CONTENTS

1. DISSERTATION OBJECTIVES AND OUTLINE 1

Dissertation Objectives 1
Theme 1: Sub-ice Methane Production from the Abiotic Reaction of Iron-Bearing Minerals and Organosulfur Compounds 1
Theme 2: Microbial Oxidation of Sulfur Sourced from Iron-sulfide Minerals in Subglacial Environments 2
Significance to Astrobiology 3
Dissertation Outline 5
Chapter 2 – Introduction: McMurdo Dry Valleys, East Antarctica 5
Chapter 3 – Abiotic Methane Sources in a Perennially Ice-Covered Antarctic Lake 6
Chapter 4 – Sulfur Oxidizing Organisms in Subglacial Systems 6
Chapter 5 – Sulfur Oxidation by a Novel Subglacial Bacterium 6
Chapter 6 – Concluding Remarks 7
References 7

2. THEME 1 INTRODUCTION 10

The McMurdo Dry Valleys and Lake Bonney, East Antarctica 10
The Antarctic Ice Sheet 10
The McMurdo Dry Valleys 11
Lake Bonney 17
Evolution of Present-Day Taylor Valley (TV) Lakes 19
Present Day Lake Bonney 26
Hydrology 26
Water Column 28
Water Flows 30
Sediments 34
Biogeochemistry 35
Present Day Taylor Glacier 36
Glacial Ice 36
Subglacial Brine 38
Glacial Sediment Flux to West Lake Bonney 39
Blood Falls Outflow 40
Potential Sources of Methane in Lake Bonney 41
Biological Methanogenesis in Lake Bonney 41
Biological Methanogenesis in the Subglacial Brine 44
Methane in Taylor Glacier Sediments 46
Legacy Thermogenic Methane 48
Methanogenesis from Reactions Between Organosulfur Compounds and Minerals in the LB Water Column 49

TABLE OF CONTENTS CONTINUED

References 52

3. ABIOTIC METHANE SOURCES IN A PERENNIALLY ICE-COVERED ANTARCTIC LAKE 67

Introduction 67
Methane Sources in Lake Bonney, East Antarctica 69
Methods 72
Field Site 72
Sample Collection 76
Water Column Methane Isotopic Analyses 78
Concentration and Isotopic Composition of Methane Released from TG Basal Ice 78
Glacial Sediment Comminution Simulation 79
Experiments with TG Sediments and WLB Natural Waters and Organosulfur Compounds 80
Results 82
CH_4 Concentration and Isotope Profiles in WLB and ELB 82
Direct Methane Sources from Taylor Glacier 86
Incubations of WLB Water DMS and DMSO, with TG Sediments 87
Discussion 89
Potential Direct Sources of Methane to the WLB Water Column 89
Methylotrophic Methanogenesis 91
Taylor Glacier Basal Ice Melt and Comminuted Basal Ice Sediments 93
Methanogenesis from Organosulfur Compound-Mineral Reactions 95
Estimating the Magnitude of Organosulfur Compound-Mineral Reactions as a Contributor to the WLB Methane Pool 98
Legacy Methane 100
Legacy Biological Methane 101
Legacy Thermogenic Methane 102
Deposition of Legacy Methane into WLB 108
Potential Impact of Organosulfur-Mineral Reactions on ELB Methane Pool 115
Conclusions 118
References 119

4. THEME 2 INTRODUCTION 130

Sulfur Oxidizing Organisms in Subglacial Systems 130
Subglacial Environments as Microbial Biomes 130

TABLE OF CONTENTS CONTINUED

Microbial Influence on Subglacial Geochemistry 133
Environmental Influence on Microbial Biomass, Activity, and Community Structure 134
Influence of Substrates on Subglacial Microbial Diversity 136
Influence of Pyrite on Subglacial Microbial Diversity 137
Subglacial Sulfur Oxidation 138
Bench Glacier, Alaska 142
Glacial Hydrology 144
Bedrock Composition and Subglacial Sediments 145
Pyrite Content 146
References 147

5. SULFUR OXIDATION BY A SUBGLACIAL BACTERIUM 152

Introduction 152
Methods 155
Study Site and Sample Collection 155
Sulfur Oxidizers Enrichment Cultures and Dilution Series 157
Genetic Characterization of the Isolate 162
Isolate Activity with Pyrite as Sole Source of Thiosulfate 163
Results 166
Genetic Characterization of a Thiosulfate Oxidizing Organism 166
Pyrite Analyses 171
Bench Glacier isolate utilization of thiosulfate sourced from pyrite 173
Discussion 176
Identification and Isolation of a Thiosulfate-Oxidizing Organism 176
Genetic Characterization of the Bench Isolate 184
Global Distribution and Adaptability of *Polaromonas* 187
Conclusions 188
References 189

6. CONCLUSION 196

Concluding Remarks 196
References 200

REFERENCES CITED 202

LIST OF TABLES

Table Page

1. Table 3.1. Summary of concentrations and isotopic signatures of methane from lake water measurements and lab experiments to determine potential sources. West Lake Bonney (WLB), The Narrows, and East Lake Bonney (WLB) water measurements are from samples collected from the listed depths in 2017. Location designation references Fig. 3.5. TG = Taylor Glacier. DMS = dimethyl sulfide. DMSO = dimethyl sulfoxide. ND = not determined. Methane concentrations determined with a gas chromatograph (limit of detection = 3nM). Gas isotope values measured with a Cavity Ring-Down Spectrometer..... 86

2. Table 3.2. Grain size distribution for Taylor Glacier basal ice sediment. 87

3. Table 3.3 Calculations for hypothetical WLB/ELB methane mixing model 117

4. Table 5.1. Media composition for Bench Glacier enrichment cultures, dilution series, and pyrite experiments 159

5. Table 5.2. Statistics associated wit the assembly of the Bench Glacier *Polaromonas sp.* isolate 168

6. Table 5.3. Percent similarity in sequence identity of select genes (*soxB* and *cbbl*) in the Bench Glacier isolate when compared to *Polaromonas* isolates in NCBI Genome Database. *soxB* is a key gene in the sulfur oxidation pathway and *cbbl* is a key gene in the Calvin Cycle..... 170

7. Table 5.4. Grain size distribution of pyrite used in Bench Glacier isolate pyrite utilization experiments. 171

8. Table 5.5 Comparison of sulfate production rates during aqueous pyrite oxidation. “Biotic” incubation indicates sulfur-oxidizing organisms were present in aqueous media with pyrite. “Abiotic” incubations contained no organisms, only pyrite. All three studies were conducted in aerobic media. The media in the present study had a pH ~8, while the other two studies had media pH of ~7. 179

LIST OF FIGURES

Figure Page

1. Fig. 2.1 (A) Map of the McMurdo Dry Valleys (MDV), Antarctica. Blue square on inset map shows approximate location of the MDV Dry Valleys on the Antarctic continent. (B) Satellite image of Taylor Valley showing the three major valley floor lakes and Taylor Glacier. McMurdo Dry Valleys map from the LTER (https://lternet.edu/site/mcmurdo-dry-valleys-lter/). Inset map from NASA (https://earthobservatory.nasa.gov/images/6087/high-resolution-mosaic-of-antarctica). Taylor Valley satellite image from Google Earth. 13

2. Fig. 2.2 (A) Map of the Lake Bonney basin and Taylor Glacier. “WLB” = West Lake Bonney. “ELB” = East Lake Bonney. Red arrow indicates location and viewing direction of panel B photograph. (B) View from WLB surface ice looking northwest towards the Taylor Glacier terminus. Satellite image in (A) from Google Earth. 18

3. Fig. 3.1 Map of the Lake Bonney basin and Taylor Glacier. “WLB” = West Lake Bonney. “ELB” = East Lake Bonney. 70

4. Fig. 3.2 Methane concentration profiles for (A) West Lake Bonney and (B) East Lake Bonney. Data from Li et al. (2020). 71

5. Fig. 3.3 Dissolved oxygen, conductivity, and temperature profiles for (A) West Lake Bonney and (B) East Lake Bonney. Measurements conducted by the MCM LTER project at Locations B and D (Fig. 1) in 2017 (Priscu, 2023). Conductivity and temperature were measured with a SBE 25 Sealogger CTD probe. Dissolved oxygen was determined on discrete samples using a Winkler Titration (limit of detection = 0.09 mg O_2 L^{-1}). 74

6. Fig. 3.4 Annual conductivity profile data from 1998-2922 for (A) West Lake Bonney water column and (B) East Lake Bonney water column. Dotted line indicates the depth of the chemocline in each lobe. Profile data are from November each year: 1998-2022 (Priscu, 2023). 75

LIST OF FIGURES CONTINUED

7. Fig. 3.5 (TOP) Sampling sites at Lake Bonney, Taylor Valley, East Antarctica. Red letters indicate borehole locations for lake water sampling. Red dot indicates location of Taylor Glacier basal ice sampling (Montross et al., 2014). TG = Taylor Glacier. WLB = West Lake Bonney. ELB = East Lake Bonney. "The Narrows" is the contraction and bedrock sill that divides the two lobes. (BOTTOM) Table of analytes determined at each sampling location. Conductivity, temperature, and dissolved oxygen are determined annually by the McMurdo Dry Valleys Long Term Environmental Research (MCM LTER) project at Locations B and D (https://mcm.lternet.edu/limnological-data). Concentration profiles for dimethyl sulfide (DMS) and dimethyl sulfoxide (DMSO) were measured by Lee et al. (2004). 76

8. Fig. 3.6 Annual Lake Bonney water column height from 1991-2022 measured in meters above sea level (MASL). Measurements conducted by the MCM LTER (Doran and Gooseff, 2023). 82

9. Fig. 3.7 (TOP) Lake water sampling locations at Lake Bonney. (BOTTOM) Methane concentration profiles at each sampling location in 2017. Methane concentrations determined with a gas chromatograph (limit of detection = 3nM). Note the order of magnitude change in methane concentration for the x-axis between locations A/B and locations C/D. Brown shapes indicate the lake bottom depth at each sampling location but do not represent precise bathymetry..... 83

10. Fig. 3.8 Methane concentration, $\delta^{13}C–CH_4$ and $\delta^{2}H\text{-}CH_4$ values in depth profiles for West Lake Bonney at Location B (Fig. 3.5). Methane concentrations determined with a gas chromatograph (limit of detection = 3nM). Gas isotope values measured with a Cavity Ring-Down Spectrometer. 84

11. The $\delta^{13}C\text{-}CH_4$ values measured in ELB in 2017 were also similar to the methane at Locations A and B in WLB: -29.3 ± 1.9 ‰ and -29.6 ± 3.2 ‰ (Fig. 3.9, Table 3.1). 84

12. The $\delta^{2}H\text{-}CH_4$ value measured at 24m for Location A was -141.0 ± 0.1, which was similar to $\delta^{2}H\text{-}CH_4$ values at Location B, which were -142.2 ± 0.1 and -141.5 ± 0.1 for 20 and 25m, respectively. The methane at Location D in ELB had different $\delta^{2}H\text{-}CH_4$ signatures relative to the same depths in WLB, of -169.9 ± 0.1 and -164.3 ± 0.1 for 20m and 25m, respectively (Fig. 3.9, Table 3.1). 85

LIST OF FIGURES CONTINUED

13. Fig. 3.10 Methane produced over 72h when 5g of dried, milled (<63 μm) of Taylor Glacier (TG) basal sediments were added to 28ml of West Lake Bonney (WLB) water from 20m and 25m from Location B (see Fig. 6) and incubated in the dark for 72h at 5ºC. Methane concentrations at each time point represent cumulative values per gram of sediment. TG sediments added to ultrapure water acted as the control. Error bars indicated standard deviation from the mean (n=3). 88

14. Fig. 3.11 Methane produced when 5g of dried, milled (<63 μm) Taylor Glacier (TG) basal sediments were added to 28ml of 200nM solutions of either dimethyl sulfide (DMS) or dimethyl sulfoxide (DMSO) then incubated in the dark for 48h at 5ºC. TG sediments (5g) in ultrapure water served as the control. Error bars indicated standard deviation from the mean (n=3)..... 89

15. Fig. 3.12 Isotopic composition methane produced from comminution of Taylor Glacier (TG) sediment and methane released from melting TG basal ice, compared to the isotopic composition of methane in the West Lake Bonney (WLB) water column. Dotted lines indicate only $\delta^{13}C–CH_4$ measurements are available. Base figure adapted from Milkov & Etiope (2018). 90

16. Fig. 3.13 Methane, dimethyl sulfide (DMS), and dimethyl sulfoxide (DMSO) concentrations in (A) West Lake Bonney and (B) East Lake Bonney. Methane samples were collected in 2017 from Locations B and D (Fig. 1). Samples for DMS and DMSO quantification were collected in 1999 from Locations B and D (Fig. 1) as reported in Lee et al. (2004). Note the order of magnitude change in methane concentration for the x-axis in panels (A) and (B). Methane concentrations determined with a gas chromatograph (limit of detection = 3nM) 91

17. Fig. 3.14 Major fluvial inputs to West Lake Bonney (WLB). A) Seasonal, subaerial proglacial streams that flow into the peripheral moats that form on WLB during the summer melt season (Welch et al., 2010). B) Modelled Taylor Glacier englacial and subglacial flow paths for brine delivery into WLB (adapted from Lawrence et al., 2020). Satellite images from Google Earth. 109

LIST OF FIGURES CONTINUED

18. Fig. 3.15 Annual conductivity data for the West Lake Bonney water column at the MCM LTER sampling site (~600m east of Taylor Glacier terminus). A) Complete conductivity profiles from November of each year. All depth values are adjusted to the 2017 lake level. B) Enlargement of the anomalous section of the conductivity profile with brackets indicating the range of years in each cluster. Data from Priscu, 2023. 111

19. Fig. 3.16 Annual conductivity data for the West Lake Bonney water column at Location B (Fig. 3.7). (A) Complete conductivity profiles from November of each year. All depth values are referenced to the 2017 lake level. (B) Enlargement of the 21-30m section of the profile with the migrating anomaly labeled for select years. Data from Priscu, 2023. 112

20. Fig. 3.17 (A) Annual temperature profile data for 1998-2022 for the West Lake Bonney water column Location B, Fig.3.7, measured in November each year. (Priscu, 2023). All depth values are referenced to the 2017 lake level. Dotted line indicates the depth of the chemocline (B) Enlargement of the 19 – 25m depth of the conductivity profile immediately below the chemocline with brackets indicating the range of years in each cluster. 114

21. Fig. 5.2 Example of pyrite experimental flask setup with pyrite-filled dialysis bag suspended in media. 165

22. Fig. 5.3 Dilution series from active thiosulfate oxidizer enrichment culture containing sediments from Bench Glacier (BG). A subsample from the BG enrichment culture was passaged into new media in a serial dilution (10^{-1} to 10^{-4}). The uninoculated control incubations were also diluted in series. Media was incubated at 4°C in the dark, with an aerobic headspace. Timepoint 0 was the start of the incubation and timepoint 1 was one month after the start. Thiosulfate and sulfate concentrations determined with ion chromatography (limit of detection: 1μM). 167

23. Fig. 5.4 KEGG pathway mapping of A) sulfur oxidation (Sox) pathway and B) carbon fixation pathway (Calvin Cycle) for Polaromonas isolate from Bench Glacier sediments. Green-filled boxes indicate that a gene is present in isolate genome. 169

24. Fig. 5.5 Pyrite grain surfaces from control incubation dialysis bag (A), and live incubation dialysis bag (B). Images captured with Scanning Electron Microscopy (SEM)..... 172

LIST OF FIGURES CONTINUED

25. Fig. 5.8 Cell counts in the aqueous phase for “live” incubations in the pyrite utilization experiment. Error bars represent standard deviation between the three replicate incubations. 175

26. Fig. 5.9 Cells associated with precipitate formed in pyrite utilization experiment media inoculated with Polaromonas sp. The cells were stained with SYBR Gold nucleic acid gel stain (Invitrogen) and appear bright green when imaged with epifluorescence microscopy. 176

ABSTRACT

This research investigated the influence of iron- and sulfur-containing minerals on biogeochemical processes in two contrasting glaciated catchments. In Theme 1, I explored the role of iron-bearing minerals in an abiotic methanogenesis reaction as a possible source to an unexplained methane pool in Lake Bonney (LB), Antarctica. In Theme 2, I examined the effect of iron-sulfide minerals on biological activity in subglacial sediments from Bench Glacier (BG), Alaska. The presence of iron and sulfur minerals potentially drives abiotic and biotic processes in both glaciated systems, though the magnitude of these processes is not fully understood.

Theme 1 considers the methane in LB's water column, which has isotopic values consistent with an abiotic (thermogenic) source. Peak methane concentration occurs just below the depth of subglacial brine inflow from adjacent Taylor Glacier (TG). My experiments indicate direct basal ice melt, rock comminution, and methane production from the reaction of TG sediment with organosulfur compounds are not major sources of methane to LB. The likely source is crustally-derived methane supplied to the subglacial environment at TG, trapped by the overlying ice, then carried to the lake within subglacial brine outflows. My work also demonstrated how naturally occurring organosulfur compounds in LB will produce methane when reacted with TG glacial sediments at close to *in situ* temperature. Though this reaction is unlikely a major methane source in western LB, isotopic analysis of dissolved methane in LB's eastern lobe indicate this process may be occurring in the lake.

For Theme 2, I isolated a species of *Polaromonas* which oxidizes thiosulfate to sulfate under aerobic conditions at near subglacial temperatures. This is the first demonstration of sulfur oxidation in this genus, and it is only the second organism with this ability to be isolated from a subglacial environment. My experiments showed this species can utilize thiosulfate sourced solely from the abiotic oxidation of the iron-sulfide mineral pyrite in an aqueous setting. This is the first time a glacial isolate has been shown to exhibit this capability.

CHAPTER ONE

DISSERTATION OBJECTIVES AND OUTLINE

Dissertation Objectives

Environments beneath ice sheets and glaciers are biogeochemically and hydrologically dynamic, producing trace elements, nutrients, organic compounds, and gases that can have a significant impact on downstream ecosystems. In subglacial systems containing liquid water, flowing ice generates fine-grained sediments from abrasion and crushing of the bedrock, releasing trapped gasses, and exposing fresh mineral surfaces that support a range of geochemical and microbiological processes. Historically, the sediments beneath ice sheets and glaciers were thought to be devoid of life, but research in the last two decades has revealed diverse, active subglacial microbial communities that drive mineral weathering, carbon transformations and elemental cycling beneath the ice. The interplay between glacial dynamics, subglacial hydrology and biogeochemical processes is not fully understood and new processes, both abiotic and biotic, continue to be uncovered in these environments. This study examines two sub-ice ecosystems where iron and sulfur bearing minerals influence biogeochemical reactions. The research has two themes:

Theme 1: Sub-ice Methane Production from the Abiotic Reaction of Iron-Bearing Minerals and Organosulfur Compounds

The water column of perennially ice-covered Lake Bonney, Antarctica contains a pool of methane that is supersaturated relative to atmospheric concentrations. The source of methane in the anaerobic waters below the chemocline is unclear, with no evidence for biological

methanogenesis at those depths. The methane concentration peak occurs at the depth of subglacial inflow from the adjacent Taylor Glacier, suggesting a possible connection. Additionally, concentrations of organic, dimethylated sulfur compounds in the water column are among the highest recorded in a natural system and previous laboratory studies demonstrated that these compounds can react with iron-bearing minerals to produce methane. The objectives for Theme 1 were:

1. Examine potential direct sources of methane to Lake Bonney associated with subglacial processes at Taylor Glacier.
2. Determine whether naturally occurring organosulfur compounds from the lake react with iron-bearing minerals in Taylor Glacier basal sediments and generate methane.

Theme 2: Microbial Oxidation of Sulfur Sourced from Iron-sulfide Minerals in Subglacial Environments

Redox-active minerals in sediments underlying glaciers supports microbial activity in subglacial environments. This appears especially true for sediment that contains pyrite (FeS_2). The abiotic oxidation of pyrite at a circumneutral pH produces thiosulfate, which can be used as an electron donor by sulfur-oxidizing microorganisms. Pyrite is ubiquitous in many lithologies and so is common in subglacial sediments, but only one organism capable of thiosulfate oxidation has previously been isolated from a subglacial system: a species of *Thiobacillus* from pyritic sediments of Robertson Glacier in the Canadian Rockies. Mineralogical, chemical, and genetic evidence indicate sulfur oxidizers are also likely present in the subglacial sediments of Bench Glacier, Alaska. The objectives for Theme 2 were:

1. Investigate the presence of sulfur-oxidizing microbes in the subglacial sediments of Bench Glacier and isolate an organism(s).

2. Determine if the sulfur oxidizer isolate(s) can utilize thiosulfate sourced solely from the abiotic oxidation of pyrite.

Significance to Astrobiology

This research was funded, in part, by a NASA Earth and Space Science Fellowship. It has potential significance in understanding how life may exist beyond Earth and how we might approach differentiating abiotic processes from biological activity.

Subsurface and subglacial bodies of liquid water have been identified or inferred on Jovian moons (Baker et al., 2005) and Enceladus (McKay et al., 2008). These lunar systems are dark, cold, subglacial environments where the presence and survival of microbial lifeforms is likely dependent on bedrock minerology, carbon sources, and redox dynamics. Though it is unclear whether life could have developed on these moons, if there is life present, it may exhibit molecular, chemical, and physical signatures like those of lifeforms identified in subglacial water bodies on Earth, such as Antarctic subglacial lakes. The study of microbial metabolisms from terrestrial subglacial systems in both polar and alpine settings can provide guidance in the search for life elsewhere in the solar system.

Aqueous subglacial environments share common physical attributes, but chemical properties are unique to each system and can have a significant effect on microbial community composition (Skidmore et al., 2005; Stibal et al., 2012). Microbial activity can, in turn, influence the solute composition in a subglacial system (Christner et al., 2014; Purcell et al., 2014; Skidmore et al., 2005), providing chemical signatures that could be used to identify the presence of similar metabolisms in an extraterrestrial setting. Understanding how local geochemical

factors influence microbial community composition and associated metabolisms in subglacial environments could aid in the identification of potential biosignatures on other planetary bodies.

Methane was detected on Mars (Webster et al., 2015) and is considered a potential biosignature for life beneath the surface (Kral et al., 2014; Kral et al., 2016; Sauterey et al., 2022; Wormald et all., 2022). The source of Martian methane is unknown, with several potential biotic and abiotic origins (Sinha et al., 2021). The stable isotopic composition of methane gas can be used to distinguish its source (Whiticar et al., 1999). This isotopic approach has been tested using analogue Martian conditions on Earth (Novak et al., 2011; Sinha and Kral, 2015; Sinha et al., 2021) and directly applied at Gale Crater on Mars (House et al., 2022). The isotopic compositions of methane sources, however, are not rigid and continue to be defined as unconventional methanogenic pathways and site-specific biogeochemical conditions expand our understanding of methane dynamics in natural systems (Milkov and Etiope, 2018; Klintzsch et al., 2023). The research presented in Theme 1 of the dissertation examines the stable isotopic composition of the methane pool in Lake Bonney while considering potential biological, chemical, and geologic sources, both contemporary and ancient. A similar approach could be applied to characterizing methane detected on another planetary body and assessing whether it signifies the presence of life.

Chemoautotrophic microbes may represent the most likely form of life on Mars or Jovian moons, where subsurface conditions could provide liquid water, inorganic sources of carbon, and redox pairings for energy (Michalski et al., 2013; Westall et al., 2015; Jebbar et al., 2020). Subglacial environments on Earth were previously thought to be devoid of life, but research over the last 20 years has determined that microbes are not only present in these systems but

constitute a phylogenetically and metabolically diverse community (e.g. Tranter et al., 2002; Skidmore et al., 2005; Christner et al., 2014; Hawkings et al., 2020). Microbial communities in similar environments beyond Earth would be defined by local geochemical conditions, which serve as a predictor for possible microbial metabolisms. Theme 2 of this research explored the existence of microbial sulfur oxidizers beneath Bench Glacier, Alaska, based on prior research indicating the presence of pyrite minerals and chemical signatures for pyrite oxidation (Skidmore et al., 2005). Determining the identity of chemoautotrophic microbes from subglacial systems that are active at low (~ 4^{o}C) temperatures improves our understanding of the diversity of organisms with such capabilities. The research in Theme 2 demonstrates that our knowledge of life in subglacial systems on Earth is still expanding and that subglacial geomicrobiology requires understanding how physical, chemical, and biological processes are interconnected and unique to each system. The interplay between these factors will define whether life could exist in a similar environment beyond Earth, and the form that life may take.

Dissertation Outline

This dissertation consists of six chapters. Chapters 2 and 3 are the introduction and research section, respectively, for Theme 1 (Lake Bonney, Antarctica). Chapters 3 and 4 are the introduction and research section, respectively, for Theme 2 (Bench Glacier, Alaska).

Chapter 2 – Introduction: McMurdo Dry Valleys, East Antarctica

This chapter provides context for the research at Lake Bonney, including the geologic history of the region, the history the lake and its evolution through time, contemporary biophysiochemical conditions in the lake basin, including methane in the lake water column. The

goal of this chapter was to evaluate the likely sources of methane in the lake, based on its history and current ecosystem, to inform the research questions addressed in Chapter 3.

Chapter 3 – Abiotic Methane Sources in a Perennially Ice-Covered Antarctic Lake

This chapter describes the field and laboratory work I conducted to address Theme 1. I discuss the potential methane sources I assessed and their relative potential contributions to the methane pool, based on my experimental data.

Chapter 4 – Sulfur Oxidizing Organisms in Subglacial Systems

This chapter provides background on the relationship between subglacial physiochemical conditions and microbial diversity beneath glaciers, particularly regarding the influence of pyrite. I discuss current evidence for microbial sulfur oxidation in subglacial systems in a global context. The chapter then outlines the history and current conditions of Bench Glacier and prior research indicating the likely presence of sulfur oxidizers in it subglacial sediments, leading to its selection for my research.

Chapter 5 – Sulfur Oxidation by a Novel Subglacial Bacterium

This chapter describes the lab work I conducted to address Theme 2. I discuss the enrichment, isolation, and genetic characterization of a sulfur oxidizer from the Bench Glacier sediments. I then describe experiments where the isolate was incubated with pyrite as its sole source of thiosulfate to assess the potential for this metabolism in the pyritic sediments of Bench Glacier. The significance of the isolate's genus is also discussed.

Chapter 6 – Concluding Remarks

In this chapter I summarize the findings at each research site and discuss them in relation to the overarching theme of iron and sulfur bearing minerals in glaciated systems.

References

Baker, V. R., Dohm, J. M., Fairén, A. G., Ferré, T. P., Ferris, J. C., Miyamoto, H., & Schulze-Makuch, D. (2005). Extraterrestrial hydrogeology. *Hydrogeology Journal*, *13*, 51-68.

Christner, B. C., Priscu, J. C., Achberger, A. M., Barbante, C., Carter, S. P., Christianson, K., Michaud, A.B., Mikucki, J.A., Mitchell, J.A., & Vick-Majors, T. J. (2014). A microbial ecosystem beneath the West Antarctic ice sheet. Nature, 512(7514), 310-313.

Hawkings, J. R., Skidmore, M. L., Wadham, J. L., Priscu, J. C., Morton, P. L., Hatton, J. E., Gardner, C.B., Kohler, T.J., Stibal, M., Bagshaw, E.A., Steigmeyer, A.J., Barker, J., Dore, J.E., Lyons, W.B., Tranter, M., Specer, R.G., & the SALSA Science Team. (2020). Enhanced trace element mobilization by Earth's ice sheets. Proceedings of the National Academy of Sciences, 117(50), 31648-31659.

House, C. H., Wong, G. M., Webster, C. R., Flesch, G. J., Franz, H. B., Stern, J. C., Pavlov, A., Atreya, S.K., Eigenbrode, J.L., Gilbert, A., Hofmann, A.E., Millan, M., Steele, A., Glavin, D.P., Malespin, C.A., & Mahaffy, P. R. (2022). Depleted carbon isotope compositions observed at Gale crater, Mars. *Proceedings of the National Academy of Sciences*, *119*(4), e2115651119.

Jebbar, M., Hickman-Lewis, K., Cavalazzi, B., Taubner, R. S., Rittmann, S. K. M., & Antunes, A. (2020). Microbial diversity and biosignatures: an icy moons perspective. *Space Science Reviews*, *216*(1), 10.

Klintzsch, T., Geisinger, H., Wieland, A., Langer, G., Nehrke, G., Bizic, M., Greule, M., Lenhart, K., Borsch, C., Schroll, M., & Keppler, F. (2023). Stable carbon isotope signature of methane released from phytoplankton. *Geophysical research letters*, *50*(12), e2023GL103317.

Kral, T. A., Birch, W., Lavender, L. E., & Virden, B. T. (2014). Potential use of highly insoluble carbonates as carbon sources by methanogens in the subsurface of Mars. *Planetary and Space Science*, *101*, 181-185.

Kral, T. A., Goodhart, T. H., Harpool, J. D., Hearnsberger, C. E., McCracken, G. L., & McSpadden, S. W. (2016). Sensitivity and adaptability of methanogens to perchlorates: Implications for life on Mars. *Planetary and Space Science*, *120*, 87-95.

McKay, C. P., Porco, C. C., Altheide, T., Davis, W. L., & Kral, T. A. (2008). The possible origin and persistence of life on Enceladus and detection of biomarkers in the plume. *Astrobiology*, *8*(5), 909-919.

Michalski, J. R., Cuadros, J., Niles, P. B., Parnell, J., Deanne Rogers, A., & Wright, S. P. (2013). Groundwater activity on Mars and implications for a deep biosphere. *Nature Geoscience*, *6*(2), 133-138.

Milkov, A. V., & Etiope, G. (2018). Revised genetic diagrams for natural gases based on a global dataset of> 20,000 samples. Organic geochemistry, 125, 109-120.

Novak, R. E., Mumma, M. J., & Villanueva, G. L. (2011). Measurement of the isotopic signatures of water on Mars; Implications for studying methane. *Planetary and Space Science*, *59*(2-3), 163-168.

Purcell, A. M., Mikucki, J. A., Achberger, A. M., Alekhina, I. A., Barbante, C., Christner, B. C., Ghosh, D., Michaud, A.B., Mitchell, A.C., Priscu, J.C., Scherer, R., Skidmore, M.L., Vic-Majors, T.J., & Wissard Science Team. (2014). Microbial sulfur transformations in sediments from Subglacial Lake Whillans. Frontiers in Microbiology, 5, 594.

Sauterey, B., Charnay, B., Affholder, A., Mazevet, S., & Ferrière, R. (2022). Early Mars habitability and global cooling by H2-based methanogens. *Nature Astronomy*, *6*(11), 1263-1271.

Skidmore, M., Anderson, S. P., Sharp, M., Foght, J., & Lanoil, B. D. (2005). Comparison of microbial community compositions of two subglacial environments reveals a possible role for microbes in chemical weathering processes. *Applied and environmental microbiology*, *71*(11), 6986-6997.

Stibal, M., Wadham, J. L., Lis, G. P., Telling, J., Pancost, R. D., Dubnick, A., Sharp, M.J., Lawson, E.C., Butler, C.E.H., Hasan, F., Tranter, M. & Anesio, A. M. (2012). Methanogenic potential of Arctic and Antarctic subglacial environments with contrasting organic carbon sources. Global Change Biology, 18(11), 3332-3345.

Tranter, M., Sharp, M. J., Lamb, H. R., Brown, G. H., Hubbard, B. P., & Willis, I. C. (2002). Geochemical weathering at the bed of Haut Glacier d'Arolla, Switzerland—a new model. *Hydrological processes*, *16*(5), 959-993.

Webster, C. R., Mahaffy, P. R., Atreya, S. K., Flesch, G. J., Mischna, M. A., Meslin, P. Y., Farley K.A., Conrad, P.G., Christensen, L.E., Pavlov A.A., Martín-Torres, J, & MSL Science Team. (2015). Mars methane detection and variability at Gale crater. *Science*, *347*(6220), 415-417.

Westall, F., Foucher, F., Bost, N., Bertrand, M., Loizeau, D., Vago, J. L., Kminek, G., Gaboyer, F., Campbell, K.A., Breheret, J.G., Gautret, P., & Cockell, C. S. (2015). Biosignatures on Mars: what, where, and how? Implications for the search for martian life. *Astrobiology*, *15*(11), 998-1029.

Whiticar, M. J. (1999). Carbon and hydrogen isotope systematics of bacterial formation and oxidation of methane. Chemical Geology, 161(1-3), 291-314.

CHAPTER TWO

THEME 1 INTRODUCTION

The McMurdo Dry Valleys and Lake Bonney, East Antarctica

The Antarctic Ice Sheet

The Antarctic Ice Sheet (AIS) contains the largest mass of freshwater on Earth, encompassing an area of ~12.8 million km^2 with a total ice volume of ~25.4 million km^3, which would cause global sea levels to rise ~58 m in a complete melt scenario (Benn & Evans, 2010; Fretwell et al., 2013). The AIS is divided into three unequal parts: the ~522,000 km^2 Antarctic Peninsula, the ~1.97 million km^2 West Antarctic Ice Sheet (WAIS), and the ~10.35 million km^2 East Antarctic Ice Sheet (EAIS) (Bindschadler, 2006; Siegert, 2008; Benn & Evans, 2010). The WAIS is an extensional province with a thin crust and a warm upper mantle that is primarily below sea level (Siegert, 2008; Goodge, 2020). Sectors of the WAIS are underlain by the West Antarctic Rift System, containing individual rift basins, fault systems, and young volcanic activity, which favor relatively higher geothermal heat flow (Dziadek et al., 2017). The elevated geothermal heat flux beneath parts of the WAIS ($105 \pm 13 mW/m^2$) are a contributory factor in driving the dynamic ice streams and generating an active subglacial hydrological system including lakes in this region (Fisher et al., 2015). Conversely, the EAIS is comparatively stable, having maintained a relatively consistent ice mass since ~700 ka, with only modest ice sheet advance and retreat (Petit et al., 1999; Siegert, 2008). The EAIS is underlain by a cratonic lithosphere (~200 km thick), with the ice sheet largely defined by the South Polar Plateau, a relatively flat (~4000 m) dome from which ice flows radially to the coast (Siegert, 2008;

Goodge, 2020; Benn & Evans, 2010). This ice flow is impeded in the Ross Sea region of the EAIS by the Transantarctic Mountain range.

The division between the WAIS and EAIS is formed by the Transantarctic Mountains (TAM), which rise to elevations from 2,500-4,500 m above sea level (asl) and extend over 3,200 km from Oates Land on the Ross Sea to the Pensacola Mountains that abut the Ronne Ice Shelf on the Weddell Sea (Benn & Evans, 2010, Goodge, 2020). The TAM are an intraplate mountain belt formed primarily during an uplift in the flank of the West Antarctic Rift System during the late Mesozoic and early Cenozoic (Sugden et al., 1995; Goodge, 2020). The mountains are a relatively young feature, underlain by remnants of a pre-Devonian range that is covered by a Devonian-Jurassic sedimentary sequence (Sugden et al., 1995; Elliot, 2013; Goodge, 2020). This sequence was subsequently covered by basaltic (dolerite) rocks and intruded by sills during the early Jurassic, then by basaltic rocks and glacial tills during the upper Cenozoic (Elliot, 2013). The TAM act as a barrier between the EAIS and the Ross Sea region of the continent. Lateral ice flows from the polar ice cap rise to over 2,500m asl as they are dammed against the TAM, preventing most ice movement into the Ross Sea, aside from a few individual outlet glaciers (Goodge, 2020). The buttressing effect of the TAM also impedes ice advance into the McMurdo Dry Valleys along the Ross Sea, resulting in the largest ice-free region on the continent (Bomblies et al., 2001).

The McMurdo Dry Valleys

The McMurdo Dry Valleys (MDV) of East Antarctica are a cold polar desert, comprising an area of ~2000 km^2 between the Transantarctic Mountains and McMurdo Sound (Gooseff et al., 2011; Fig. 2.1A). The MDV experience little precipitation and no permanent ice cover aside

from alpine glaciers on the valley sides and perennially ice-covered valley floor lakes (Monaghan et al., 2005; Fountain et al., 2014). Sublimation exceeds precipitation at lower elevations causing relatively ice and snow-free conditions on the valley floor (Fountain et al., 1998). The valleys are underlain primarily by ice-cemented permafrost, with dry-frozen (ice-free) permafrost along the valley walls, and some areas of buried massive ice (ground ice) in alpine sections (Bockheim et al., 2007; Swanger et al., 2010; Fountain et al., 2014).

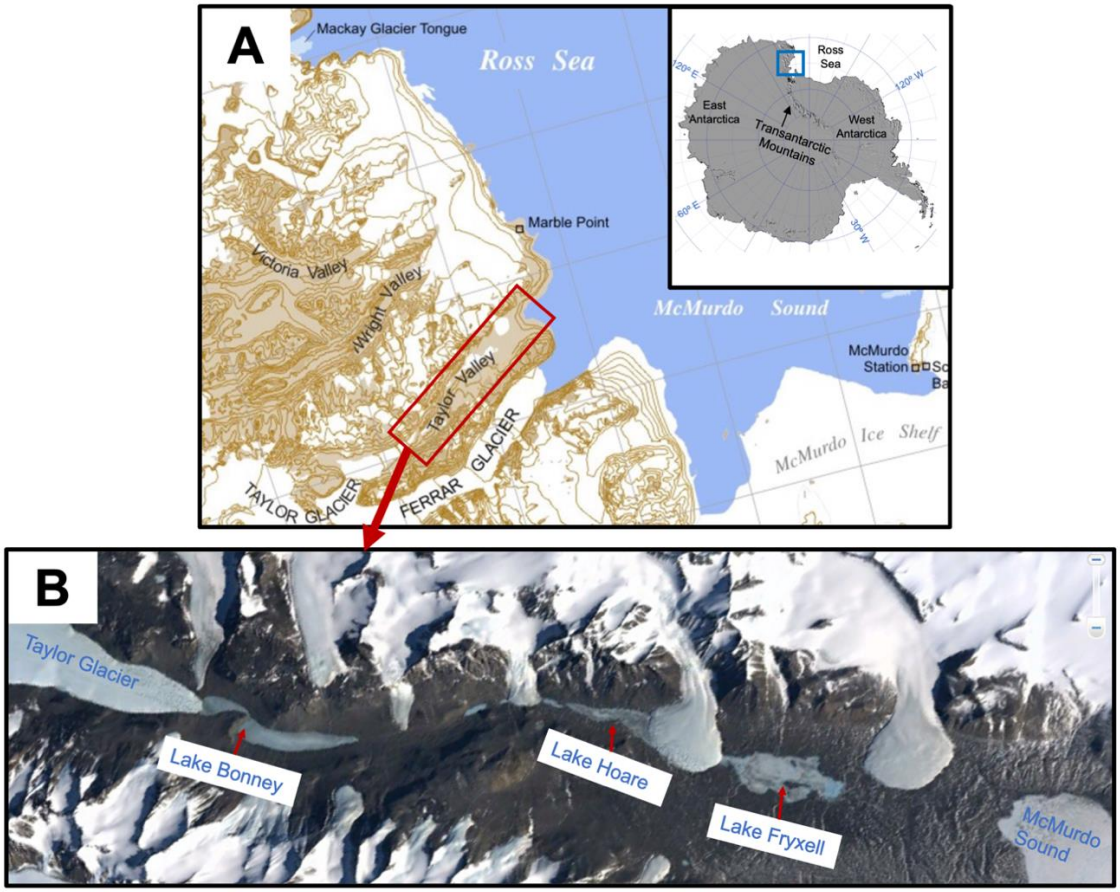


Fig. 2.1 (A) Map of the McMurdo Dry Valleys (MDV), Antarctica. Blue square on inset map shows approximate location of the MDV Dry Valleys on the Antarctic continent. (B) Satellite image of Taylor Valley showing the three major valley floor lakes and Taylor Glacier. McMurdo Dry Valleys map from the LTER (https://lternet.edu/site/mcmurdo-dry-valleys-lter/). Inset map from NASA (https://earthobservatory.nasa.gov/images/6087/high-resolution-mosaic-of-antarctica). Taylor Valley satellite image from Google Earth.

The hydrologic cycle of the MDV is driven predominantly by surface energy balance, due to the low annual precipitation (Gooseff et al., 2011; Myers et al., 2020, Cross et al., 2022). Lake water levels in the MDV are highly sensitive to variations in air temperature, albedo, and wind speeds (Fountain et al., 1998; Cross et al., 2022). A thin snow cover on glacier surfaces, for example, significantly increases albedo in the summer and with air temperatures near or below freezing, there is insufficient energy to melt the snow and glacial runoff will cease almost

entirely (Cross et al., 2022). Therefore, the valley hydrology is not driven by precipitation, but by climate conditions that influence energy exchange with ice surfaces. Warmer temperatures and 24 hours of sunlight during the summer months leads to liquid water on the glaciers, the formation of valley streams, and melting lake ice along the basins' edges (Gooseff et al., 2011). Variations in solar aspect and topographic shading lead to significant fluctuations in surface energy balance on a diurnal timescale, but climate is ultimately the largest influence on hydrologic cycling (Gooseff et al., 2011). The MDV have two distinct climate regimes: a maritime climate closer to the Ross Sea that is defined by cooler, wetter conditions and an inland climate that is typically drier and warmer, influenced by continental factors (Chinn et al., 1993; Fountain et al., 1998; Higgins et al., 2000). The microclimate transition from coastal areas toward the continent interior is particularly pronounced in Taylor Valley, which is nearest the coast (Fountain et al., 2010).

Taylor Valley (TV) extends approximately 125 km east-west (162º-163ºE longitude) from Taylor Dome on the EAIS, through the TAM to McMurdo Sound on the Ross Sea (77º30'–77º45'S latitude) (Higgins et al., 2000) (See Figure 2.1B). The valley is situated between the Kukri Hills to the south and the Asgard Range to the north. The mean precipitation, in the form of snow, ranges from 50mm annually in the Ross Sea region to only ~3mm annually at the western end of the valley (Doran et al., 2002; Fountain et al., 2010; Myers et al., 2020), emphasizing the microclimate transition from maritime to continental climate influence. Mean annual air temperatures in the valley range from -14.7 to -23°C (Myers et al., 2020). Snowfall usually sublimates in the valley, instead of melting (Fountain et al., 1998; Welch et al., 2010). During the summer melt season, liquid water is present on the valley sides and floor for ~4-12

weeks, in the form of meltwater streams originating at the alpine glaciers and flowing into the valley lakes (Welch et al., 2010). There are three major lake basins in TV: (upvalley from the Ross Sea) Fryxell, Hoare, and Bonney (Fig. 2.1B). The lakes are closed basin, perennially ice-covered systems that receive inputs primarily through ephemeral streams of alpine glacial and snow melt (Myers et al. 2020). Since there is no outflow the lake volume changes based on the difference between glacial meltwater inflow and water loss through evaporation or ice sublimation (Clow et al., 1988; Chinn, 1993). Ice cover on the lakes is typically 3-5m thick but experiences an annual melt window from December through February that leads to open-water moats at the lake edge (Myers et al., 2020). However, annual lake losses to ice ablation and evaporation from the moats is negligible, so lake level changes are overwhelmingly indicators of local climatic changes (Bomblies et al., 2001). The eastern portion of the valley (Fryxell and Hoare basins) is influenced by marine air masses moving upvalley from the Ross Ice Shelf, especially during the austral summer months (Lyons et al., 2000), while the western part of the valley (Bonney Basin) is affected more by continental air masses, leading to warmer, sunnier, and drier conditions at Lake Bonney (LB) in the summer (Welch et al., 2010). Typically, winds are calm and up-valley from the Ross Sea in summer, while the winter winds are very strong and down-valley from the continental interior (Nylen et al., 2004). The average temperature at LB increases by ~17ºC during katabatic wind events in the winter and the relative humidity decreases by 25% (Nylen et al., 2004), leading to higher lake ice sublimation rates in the winter at LB (0.17 m season^{-1}), compared to Hoare and Fryxell (0.10 m season^{-1}) (Dugan et al., 2013).

Down-valley winds can warm adiabatically as they descend into the western part of TV, leading to increasing air temperature on a scale of hours (Nylen et al., 2004). These Foehn winds

can directly influence ice melt rates in the valley and, subsequently, lake water levels. For example, Foehn winds were more prevalent in TV during the 2001-02 summer than in prior seasons (Doran et al., 2008), likely due to low cloud cover (Castendyk et al., 2016) and lower mean sea level pressure in the Ross Sea Region (Doran et al., 2008). These winds likely contributed to the dramatic increase in glacier melt that summer, which subsequently led to a rapid rise in lake levels (0.5-1m across the TV lakes) that effectively reversed the previous decade of gradual lake level decline (Doran et al., 2008).

The Taylor Valley lakes are annual sampling sites for the McMurdo Long-Term Ecological Research (MCM LTER) program, which has been collecting physical, chemical, and biological data from the valley ecosystems annually since 1993. The LTER selected the valleys for study because they represent one of the few mostly ice-free regions on the continent. An Antarctic landscape with exposed geology, ephemeral streams, glaciers, ice-covered lakes, and a microbially-dominated biological community (Fountain et al., 2014) allows researchers to observe the interactions between physiochemical and biological components of a relatively simple and stable ecosystem, which exists under temperatures far colder than any previously established LTER program (Jennings-Mays & Wharton, 1996; Lyons et al., 2001). The relatively ice-free conditions in the valley also preserve geomorphic and geochemical signs of past lake levels, which can help establish a paleoclimate record for the region (Hall and Denton, 2000; Berger et al., 2013, Myers et al., 2021; Cross et al, 2022). The abundance of paleoclimatic and contemporary hydrogeological data on LB collected through the LTER program provides the context for the research presented in Chapter 3 investigating potential sources for the methane in the deeper waters of LB.

Lake Bonney

Lake Bonney (LB) is situated ~25km inland from the Ross Sea at the western end of Taylor Valley, between the Bonney and Nussbaum Riegels (Higgins et al., 2000; Patriarche et al., 2021). The 7 km long lake is comprised of two perennially ice-covered, ~40m-deep lobes with steep bathymetry (Doran et al., 2008; Fig. 2.2A). The two basins, West Lake Bonney (WLB) and East Lake Bonney (ELB), are hydrologically connected via The Narrows, a 50m-wide contraction over a bedrock sill, where the water depth decreases to ~16-18m (Lyons et al., 2000; Winslow et al., 2014; Spigel et al., 2018). The lake is bounded by steep valley sides formed by the Asgard Mountain Range to the North and the Kukri Hills to the south. The western end of WLB abuts the terminus of Taylor Glacier (Fig. 2.2) which, along with five alpine glaciers above the valley, is a water source to the basin.

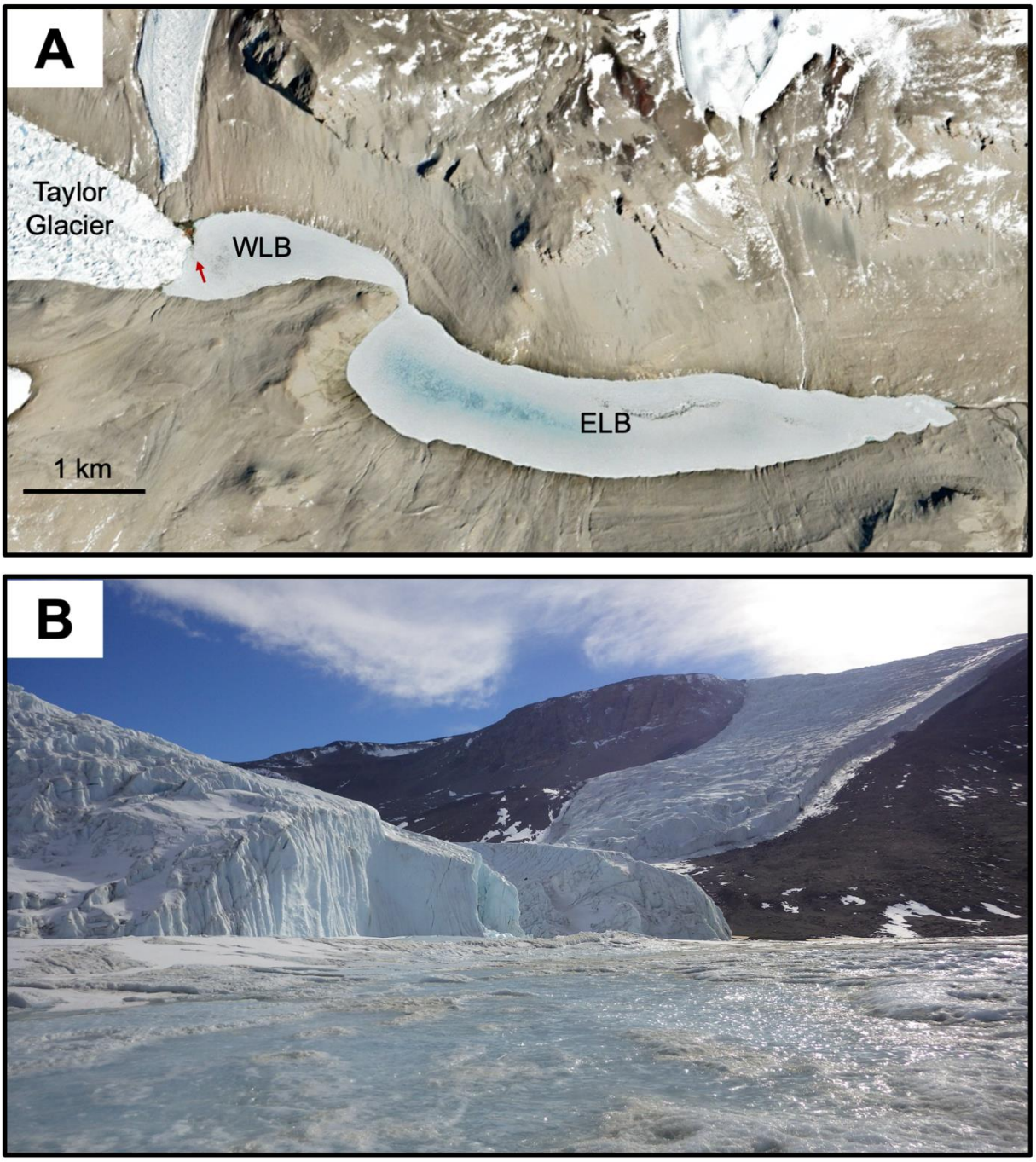


Fig. 2.2 (A) Map of the Lake Bonney basin and Taylor Glacier. “WLB” = West Lake Bonney. “ELB” = East Lake Bonney. Red arrow indicates location and viewing direction of panel B photograph. (B) View from WLB surface ice looking northwest towards the Taylor Glacier terminus. Satellite image in (A) from Google Earth.

Evolution of Present-Day Taylor Valley (TV) Lakes

Constructing a paleoclimate history for the McMurdo Dry Valleys region is more difficult than in other areas of the continent due to a limited amount of regional ice storing long-term climate records (Hall et al., 2017). Ice cores from Taylor Dome and valley glaciers provide some information on past temperatures and precipitation (e.g. Steig et al., 2000; Aciego et al., 2007; Baggenstos et al., 2018), which is combined with paleoclimate proxies within the lakes, sediments, and valley floor to establish a chronology of lake development. For example, historical lake level changes have primarily been reconstructed through analyses of paleodeltas that formed where streams entered the lake during a higher stand and left sediment deposits, which appear as present-day landforms on the valley slopes and floor. Radiocarbon dating of algal mats and optically stimulated luminescence dating of quartz grains in the deltas help determine the age of these deposits (Hall and Denton, 2000; Berger et al., 2013).

Most knowledge of subsurface geology in Taylor Valley comes from the Dry Valley Drilling Project (DVDP) in the late 1970s, which bored four ~200-320m cores into the valley floor between the mouth of McMurdo Sound and the Lake Hoare basin, ~17km westward (Elston and Bressler, 1981). The presence of deep-water benthic foraminifera at the Miocene-Pliocene boundary in the cores suggests a 600-900-meter-deep fjord filled at least the eastern part of TV between 7-4.6 ma (Elston and Bressler, 1981). This was during a period where subsidence of greater than 400m led to marine intrusions from the Ross Sea between 9 and 3.5 ma, based on the age of marine sediments at the mouth of TV (Sugden et al., 1995) and the late Miocene-early Pliocene deposits indicative of a deep-water fjord found in the DVDP cores (Elston and Bressler, 1981). Renewed crustal uplift in TV < 3.5 ma would gradually create a negative slope towards the Ross Sea resulting in fjord drainage (Sugden et al., 1995). Coarser

grained, cobble and boulder-bearing diamictite in the DVDP core strata above the Miocene-Pliocene boundary were glacially-derived and showed evidence of subaerial weathering, suggesting a shallowing of the fjord between 7 and 4.6 ma (Elston and Bressler, 1981).

During the Last Glacial Maximum in Antarctica (~28.5-12.8 ka BP), colder mean annual temperatures (4-9°C lower than present) led to ice sheet thickening and advance (Hall et al., 2015), with both the East and West Antarctic Ice Sheets grounding zones extending about 500km further into the Ross Sea than the present-day position (Anderson et al., 2014). Ice from the Ross Ice Shelf (RIS) flowed inland through the MDV, creating an ice dam that allowed for the formation of a glacially dammed lake, Glacial Lake Washburn (GLW), which filled Taylor Valley, with a water level as high as 350 masl (Denton and Marchant, 2000). The ice sheet likely retreated from the mouth of Taylor Valley between 7,800 and 6000 years BP (Cunningham et al., 1999; Hall et al, 2006; Hall et al., 2013; Anderson et al., 2017) possibly coinciding with an increase in regional temperatures between 12,000 and 6,000 BP (Steig et al., 2000). Loss of the ice dam would have resulted in the draining of GLW (Myers et al., 2020), potentially leading to the formation of smaller lakes in valley floor depressions, the precursor basins to modern Lakes Fryxell, Hoare, and Bonney (Myers et al., 2021). Water basins in TV fluctuated in size and depth until settling at or below the current water levels, forming the three contemporary TV lakes (Myers et al., 2021). Myers et al. (2020) estimate, based on permafrost age calculations and paleotemperature records from Taylor Dome, that maximum lake levels in TV occurred around 12ka BP then dropped significantly around 8ka BP after the RIS ice dam collapse. Hall and Denton (2000) and Berger et al. (2013) postulate that a lack of ^{14}C dateable material in the

paleodeltas from the late Holocene implies that the Taylor Valley lakes have been at or below their current levels for the last 5,000 years.

The DVDP did not drill in the Lake Bonney Basin, so stratigraphic data showing the extent of the marine incursion west of Lake Hoare are unavailable. However, large areas of subsurface brines have since been identified throughout the MDV and are likely remnants of the marine incursion and fjord system (Lyons et al., 2005; Mikucki et al., 2015). Mikucki et al. (2015) identified two contemporary systems of subsurface, brine-saturated sediments in TV: one that connects the eastern portion of the valley to the ocean, and another beneath Taylor Glacier (Mikucki et al., 2015). Lyons et al. (2005) suggest overdeepenings carved from past glacial advances in TV trapped seawater as the fjord drained, possibly forming a saltwater lake near what is now the Bonney Basin. Lyons et al. (2005) further hypothesize that one of the past advances of Taylor Glacier (Hendy et al., 1977) possibly overrode the salt lake in the early Quaternary, trapping Miocene-Pliocene era seawater and sediments beneath the glacier. The brine system beneath TG is unique in the valley because it comprises an active subglacial hydrologic system that forms supraglacial outflows at the TG terminus.

Blood Falls is an iron-rich brine that has overflowed a northern section of the TG terminus periodically since at least 1911, when the phenomenon was first observed, and has long been theorized to be sourced from a relict marine deposit beneath the glacier (Keys et al., 1979). During the summer melt season, subglacial outflows release a reddish brine on the glacier surface, allowing for sampling of brine from the subglacial reservoir (Mikucki et al., 2004). Dissolved ion ratios (Na:Cl, Mg:Cl) and ^{36}Cl values in the Blood Falls brine match those of seawater (Lyons et al., 2005), albeit brine that has undergone cryoconcentration over time.

Additionally, greater than 70% of bacterial clones and isolates from the brine are closely related to previously described marine phylotypes, based on 16S rRNA gene homology (Mikucki and Priscu, 2007). These data are consistent with marine deposition and suggest the brine-saturated sediments were overridden by TG during a glacial advance (Mikucki et al., 2004). Brine also exists beneath the terminus of Canada Glacier in the floor of TV, but there is no discharge point, suggesting that the glacier has overridden brine saturated sediments rather than there being an active subglacial drainage system (Mikucki et al., 2015), making the TG subglacial hydrology unique in the valley. This is discussed further below, in the "Present Day Taylor Glacier" section.

The age of the WLB bottom waters has been estimated at between 15 and 26 kyr (Doran et al., 2014), suggesting co-existence with GLW. The high deep-water concentrations of He, and N_2 and Ar are too high to suggest atmospheric equilibration but too low to have been concentrated by ice removal, so they indicate these waters were under a permanent ice cover with no atmospheric contact where the gases could accumulate over time (Poreda et al., 2004). Ar isotope ratios in WLB waters above 13m and throughout the water column of ELB are atmospheric, suggesting relatively recent contact with the atmosphere as they were deposited by valley streams into the lake's peripheral moats (Warrier et al., 2015). Together, these gas data suggest that WLB has been perennially ice-covered for much longer than ELB.

Helium concentrations in the deepest part of WLB are 500 times higher than in ELB, which suggests that WLB was ice-covered without seasonal open moats for thousands of years while ELB lacked a permanent ice cover until ~200 years BP (Hall et al., 2017). There may have been intermittent periods of ice cover on ELB following a cooling trend ~1200 years BP (Warrier et al., 2015). While ion ratios in WLB resemble seawater (suggesting a marine source), ELB ion

ratios appear to be the result of additional salts leaching from valley soils and/or concentration by evaporation (Spiegel and Priscu, 1996). Additionally, unlike WLB, ELB has a >1m thick layer of salt at the sediment/water interface, consisting of dihydrohalite, halite, gypsum, and aragonite, suggesting an extended period of contact with the atmosphere where evaporation exceeded fluvial input (Poreda et al., 2004).

The spillover from WLB could have been caused by an advance of Taylor Glacier during a warming period (Warrier et al., 2015). Increased accumulation at Taylor Dome occurred during the Mid-Holocene climatic optimum ~5,000 years BP, which would have caused a delayed response at Taylor Glacier around 2,000 years later (Steig et al., 2000). He diffusion rates from the lake sediment, Cl profiles, and multiple isotope tracer profiles in the WLB and ELB lake water columns suggest flow from WLB to ELB over the sill likely occurred 3,000 ± 500 years BP (Poreda et al., 2004; Warrier et al., 2015), which correlates with the postulated timing of a TG advance following the Mid-Holocene climatic optimum (Warrier et al., 2015). After lake water overflowed from the WLB basin, water inputs exceeded evaporation in ELB and the lake level rose until it reached the depth of the sill (~13m) and surface ice formed, limiting gas exchange with the atmosphere. Diffusion modelling based on ^{4}He and ^{40}Ar dissolved gas ages in the ELB water column suggest the spillover was likely not continuous, confined to warm periods, until ~150-250yrs BP when the lakes reached similar elevations above the sill (Warrier et al., 2015). At this point the ELB water column was permanently stratified, isolating the deep-water brine from the atmosphere (Poreda et al., 2004). These data suggest that the rise in WLB lake levels occurred at the end of, or after, the previous climate optimum (4-8kya BP) wherein Antarctica experienced the highest temperatures since the last ice age (Warrier.et al., 2015). The Taylor

Dome ice core record shows a cooling period, beginning ~3000 yr BP (Steig et al., 2000) when the WLB overflow supposedly occurred. This seeming discrepancy could be explained by either enhanced meltwater inflows to WLB towards the end of the climate optimum, or that perhaps localized climate factors (e.g. katabatic wind activity and/or fewer clouds) led to increased melting in the Lake Bonney basin despite overall cooling trends in the region (Poreda et al., 2004). The local temperatures could have been warmer, the more arid climate may have led to less snowfall and therefore a lower albedo on the glaciers (Doran et al., 2008), or down-valley winds could have affected glacier mass balance.

Katabatic wind activity could account for increased localized melting in the Lake Bonney basin despite a regional cooling trend. Katabatic winds are dry, fast-moving air currents that flow down mountain slopes. On the Antarctic continent there is an inversion of air temperature patterns, as the ice sheet and glaciers cool air close to the ice surface, with warmer air above. The cooler air is denser, so it tends to sink/flow downslope from the Antarctic Plateau, in the interior, to the ice sheet margins. As these winds are channeled by landforms (e.g. the Taylor Valley) they increase in speed. High-speed katabatic wind enhance vertical mixing of air above the ice, reducing the surface/air temperature inversion caused by the ice-cooled surface, leading to a sensible heat flux from the air to the ice, increasing ablation (Poreda et al., 2004) and thus meltwater flows to the lake.

The last few decades have seen climatic and local weather changes that have led to an increase in hydrologic flows into the Lake Bonney basin. There was little change in the annual inflow to LB between 1903 and 1973 with only a ~3% increase over that time (Bomblies et al., 2001). Between 1969 and 1993, changing cloud cover patterns coupled with a gradual warming

trend increased solar radiation and air temperatures in the Lake Bonney basin, leading to greater meltwater generation (Bomblies et al., 2001). The level of Lake Bonney rose by ~5m, between 1963 and 1990, primarily as freshwater input that thickened the layer above the chemocline (Spigel & Priscu, 1996). Over the same period, the maximum temperature in WLB increased slightly from 2.0 to 3.1°C (shifting from 8.5 to 9.5m depth), while the maximum temperature in ELB decreased from 7.0 to 6.3°C but occurred at approximately the same depth (14.5m).

Taylor Valley underwent a subsequent cooling period from 1993-2001, during which time there was relatively little glacier melt and low stream flows (McKnight et al., 1999). This led to a decline in lake levels by ~0.006 to 0.08 m yr^{-1} (Doran et al., 2008). The cooler period ended dramatically during the 2001-02 austral summer, which was the warmest on record for the MDV (Lyons et al., 2005; Doran et al., 2008). Stream discharge was 33 times higher than previous years, seeps or subsurface discharges appeared on the valley floor where they had not been observed before, and Cl^- concentrations in the surface waters of the lakes were the lowest ever recorded due to freshwater dilution (Lyons et al., 2005). The overall Chlorophyl *a* concentrations in the photic zone of Lake Bonney were up 150% from the previous year, likely indicating a larger flux of nutrients from inflow streams combined with a thinning ice cover leading to increased irradiance (Foreman et al., 2004; Lyons et al., 2006). Lake levels in TV increased between 0.54 and 1.01m during the 2001-02 summer, effectively reversing the prior 14 years of lake level decreases (Doran et al., 2008). Lake levels across the valley have continued to increase since 2001-02, with Lake Bonney's water level rising by ~0.2 m yr^{-1} from 2004 to 2020 (Patriarche et al., 2021, Cross et al., 2022).

Present Day Lake Bonney

Hydrology

Precipitation at Lake Bonney is 1-3mm yr^{-1} of low density (100 kg m^{-3} water equivalent) snow, so it is a negligible source of water to the lake (Fountain et al., 2010, Myers et al., 2020, Cross et al., 2022), making proglacial streams the predominant source of inflows. About 20m of the TG terminus is submerged in the WLB water column (Spigel & Priscu, 1998) and though TG is a cold-based glacier, it advances towards WLB by 3-4m yr^{-1} (Pettit et al., 2014). TG movement leads to glacial ice melt into the lake as well as subglacial and englacial brine flows (Badgeley et al., 2017; Lawrence et al., 2020). Additional subglacial inputs come from Blood Falls (Spigel and Priscu, 1996; Mikucki et al., 2004, Lyons et al., 2005; Spigel et al., 2018; Lawrence et al., 2020). Subglacial sources account for approximately 20% of inflow to LB (Doran et al., 2014). The bulk of inflow to WLB comes from glacial meltwater streams on the valley floor (Welch et al., 2010; Cross et al., 2020).

Valley meltwater streams form during the summer months and flow into the surface waters of both WLB and ELB (Welch et al., 2010), accounting for >60-78% of inflow (Fountain et al., 1999; Doran et al., 2014). The proglacial streams that flow into WLB and ELB tend to be steeper, rockier, and carry a higher sediment load than others in the valley (Welch et al., 2010). The geochemistry of streams in the Bonney basin resembles that of global streams and rivers in arid regions and/or draining from evaporitic environments (Welch et al., 2010). The two proglacial streams, Santa Fe and Lyon, that flow from TG into WLB have higher total dissolved solids (TDS), 235 and 452 mg/L, respectively, relative to other streams in the valley, likely due to relict salt deposits under the TG terminus (Lyons et al., 2005). These are the highest TDS

values in TV aside from the Blood Falls outflow (34,400 mg/L) (Welch et al., 2010). Though only 10s of meters away, Lawson Stream, which flows from the alpine Rhone Glacier southward into WLB, has a relatively low TDS of 23.4 mg/L, showing greater similarity to waters from mixed crystalline silicate rock-dominated and sedimentary rock-dominated watersheds (Welch et al., 2010). Proglacial stream inputs to ELB originate from Alpine glaciers Matterhorn and Hughes, with additional inflow from Priscu Stream, a second-order stream that flows to the eastern tip of ELB (Welch et al., 2010).

Water generally flows from LB's west lobe (WLB) to the east lobe (ELB), although there is evidence of hydrologic transport in both directions across the sill (Spigel & Priscu, 1998; Spigel et al., 2018). The chemocline in WLB has remained at the height of the sill since at least 1991, suggesting the sill acts as a barrier to the flow of deeper saline waters, but water is exchanged between the two lobes above the depth of the sill (~17m) as indicated by similarity in dissolved ion concentrations and ratios (Spigel et al., 2018). Water flux from WLB to ELB is approximately 100m^3/yr (Poreda et al., 2004), which is ~0.0001% of Lake Bonney's 79 million m^3 total volume (Priscu, 2016). There is no ouflow from ELB and little to no groundwater flow from the water column.

Much of Taylor Valley is ice-cemented below the active layer (upper 20-45cm of the valley floor) but imaging from AEM surveys indicates groundwater connectivity in the form of two subsurface brine systems, one connecting Lake Hoare and Lake Fryxell and a separate system beneath Taylor Glacier, connected to Lake Bonney (Mikucki et al., 2015). However, while the groundwater flows appear to deposit brine from TG to WLB, there does not appear to be much groundwater outflow from the lake itself (Mikucki et al., 2015). There is also no surface

outflow from ELB, so the lake is considered a closed basin (Spigel & Priscu, 1998; Lawrence et al., 2020).

Water does leave the LB "closed basin," but loss is minimal. Lake surface ice melts and moats form along the periphery of LB during the summer, but most of the ice melt percolates back into the lake (Dugan et al., 2013) and evaporative losses from the moats are negligible, so these processes are not considered contributors to water loss (Spigel and Priscu, 1998; Dugan et al., 2013; Cross et al., 2022). The primary mode of water loss from the system is sublimation of lake ice (Chinn et al., 1993), which is estimated to be 0.37-0.74 m yr^{-1} for LB (Dugan et al., 2013; Cross et al., 2022). However, new ice also forms at the water/ice interface, so surface ice thickness typically varies <1m yr^{-1}, dependent on air temperature, wind speeds, and shallow water temperatures, which are driven by the amount of shortwave radiation penetrating the ice (Obryk et al., 2016). The water loss through sublimation is, therefore, essentially at an equilibrium with new ice formation on a decadal scale (Obryk et al., 2016).

Water Column

The maximum depths in WLB and ELB are ~43m and ~41m, respectively (Spigel et al., 2018; Patriarche et al., 2020). The lake ice is 3-5m thick, and gas exchange with the atmosphere is extremely limited, only occurring during the melt season when the edges of the lake are ice free (Welch et al., 2010). Sunlight penetration during the austral summer allows for photosynthetic activity (Kong et al., 2014) and the waters are oxygenated down to ~20m in WLB and ~25m in ELB (Li et al., 2020). The water column is stable in both lobes due to a high salinity gradient that forms strong chemoclines at ~18m and ~20m in WLB and ELB, respectively (Spigel et al., 2018; Li et al., 2020).

The water column in both lobes is increasingly saline with depth, with the deepest waters reaching salinities 3-4 times higher than seawater (Spigel & Priscu, 1996; Spigel et al., 2018). The shallow waters in WLB and ELB above the chemocline are freshwater (~1000 kg/m^3) but density increases to 1.1-1.2 times that of seawater near the water-sediment interface (Spigel & Priscu, 1996). The halocline and pycnocline occur just below the depth of the sill and have been remained constant at that depth since at least 1991 (Spigel et al., 2018). The steep salinity and density gradients create a highly stratified and stable water column. Concentration profiles for various dissolved compounds follow similar patterns to salinity and density profiles, indicating a clear chemical distinction between the upper and lower depths of the lake. Collectively, the depth of the halocline, pycnocline, and steepest chemical gradients form the chemocline.

There are no thermohaline convective cells to create water circulation (Spigel & Priscu, 1998) so mixing between the hypolimnion and epilimnion is inhibited, but limited water circulation occurs. Turbulent mixing can occur above the chemocline during high streamflow events in the summer (Foreman et al., 2004), through wind-induced ice movement creating internal waves in the winter (Lawrence et al., 2020), and in The Narrows due to the complex water exchange between WLB and ELB (Spigel & Priscu, 1998). Some circulation below the chemocline occurs between ~17m and 25m near the glacier face due to melting ice (Spigel et al., 2018). Salinity and density profiles in LB are nearly identical because salinity exerts such a strong influence on lake water density (Lawrence et al., 2020). The influence of temperature on density is therefore small and can be used as a proxy for water movements (Spigel & Priscu, 1998).

Water Flows

Cooler waters near the glacier disseminate eastward towards the sill, indicating inflows from TG (Spigel et al., 2018). Salinity and density profiles are relatively consistent horizontally across WLB, but temperatures within 100m of the glacier front are 2-3 degrees colder than more eastern portions of the water column, emphasizing the strong influence of the glacier on the westernmost sector of the lake (Spigel et al., 2018). Water inputs from TG likely occur between 17 and 25m in WLB, based on temperature anomalies and changes in density (Spigel & Priscu, 1998; Lawrence et al., 2020; Li et al., 2020), as well as increases in the concentration of compounds such as He, dissolved inorganic carbon, and total iron, which reflect the higher concentrations in the Blood Falls brine, relative to the lake water (Mikucki et al 2004; Doran et al., 2014). Additionally, the Eh values in the surface waters of WLB are ~750 mV but drop to 240 mV, the same value recorded in Blood Falls, below the WLB chemocline (Mikucki et al., 2004). Glacial inflows come from three primary sources: melting terminus ice, Blood Falls (surface inflows through peripheral lake moats), and direct subglacial brine inflows. Ice melt below the chemocline in WLB is identified by relatively thin (~20cm thick) horizontal oscillations in temperature and salinity profiles between 17 and 25m, which dissipate with increasing distance from the glacier (Spigel et al., 2018). Glacial ice melt is differentiated from brine inflows by the magnitude of horizontal oscillations and the density of the incoming water, relative to the average density of the lake water: 1060-1090 kg m^{-3} from 18-23m (Lawrence et al., 2020). Larger intrusions of anomalously cold water (~1m thick) with densities similar to that of the Blood Falls brine (1100 kg m^{-3}) between 18 and 23m near the glacier terminus are interpreted as direct subglacial brine inflows (Spigel et al., 2018; Lawrence et al., 2020). This is further supported by a significant temperature change at 21m in the water column near the

glacier, dropping from -1ºC to between -3 and -4º C (Lawrence et al., 2020). The TG subglacial brine temperature has been measured at as low as -7ºC (Badgeley et al., 2017), so mixing with warmer lake water results in the observed average temperature of -3.7ºC in the likely area of inflow (Lawrence et al., 2020). Further, the temperature and density anomalies measured by Spigel et al. (2018) and Lawrence et al. (2020) correspond with the subglacial flow paths inferred by Badgeley et al. (2017).

Hydraulic potential modelling suggests subglacial brines are routed either to the north end of the terminus to Blood Falls before entering the lake, or to the middle and southern sections of the terminus where they flow directly into the water column (Badgeley et al., 2017). This model is supported by temperature and density measurements collected by the autonomous underwater vehicle *Endurance* from 2008-2009 (Spigel et al., 2018). *Endurance* sampled 36 locations in WLB within a ~200x400m sampling grid along the middle and southern sections of the TG terminus. The large temperature decreases and instability in the density profile were observed around 21m at each sampling location from the glacier front to at least 100m east from the terminus (Spigel et al., 2018). Annual sampling by the MCM LTER near the center of the WLB basin has also demonstrated abnormally cold temperatures around 21m (adjusted depth) since 1993 (Li et al., 2020; Lawrence et al., 2020), suggesting that the glacial inflows travel horizontally eastward for at least 600m away from the glacier terminus. Brine inflows occur throughout the year, even during the winter season (Lawrence et al., 2020). Strong katabatic wind events in the winter are followed by short periods of temperature anomalies in the water column. This suggests that extreme wind speeds (>37m s^{-1}) could be causing pressure on the glacier face, leading to subglacial brine “pulses” into the lake (Lawrence et al., 2020). The depths

for winter brine pulses commonly occur at depths shallower than 21m, including above the chemocline, but likely sink below the chemocline due to density differences (Lawrence et al., 2020). Wind events also cause internal waves in the lake, which may induce mixing, especially at depths where the density gradient has been disrupted by brine inflows, allowing for the geochemical transport of brine further into the lake (Lawrence et al., 2020).

Net flow across The Narrows is west to east, though there is some exchange in both directions (Spigel and Priscu, 1998; Spigel et al., 2018). Spigel et al. (2018) estimate that 80-90% of fresh meltwater input to Lake Bonney is derived from proglacial meltwater streams emanating from Taylor Glacier and Rhone Glacier in the western basin. The surface areas of WLB and ELB are 23% and 77%, respectively, of the total lake surface area, so a large portion of water input to WLB must flow to ELB to maintain hydrostatic equilibrium in the system (Spigel et al., 2018). The bulk of water exchange is, therefore, occurring from west to east. The exchange largely occurs above the WLB chemocline as the sill typically blocks denser, deeper waters from flowing eastward. Spigel and Priscu (1998) suggest that upper waters of the WLB chemocline layer are carried to ELB, due to the strong west-east flow. The mixing of upper WLB chemocline waters with freshwater inputs would explain a pervasive curve in the conductivity and density profiles at ~19m for ELB (Spigel et al., 2018). Transport of upper chemocline waters could also be offsetting diffusion, maintaining the sharp division between the hypolimnion and epilimnion in WLB. There have been episodes of “chemocline leakage,” however, where the depth of the WLB chemocline has risen above the depth of the sill, allowing waters below 17m to flow out of WLB (Doran et al., 2014).

The apparent ^{14}C age of dissolved inorganic carbon (DIC) increases with depth in WLB, but in ELB the oldest DIC is found at and immediately below the chemocline (~20m, adjusted to 2017 lake level), with younger DIC below 25m (Doran et al., 2014). This suggests that older, more saline water from WLB passed over the sill and sank to a depth of equal density in ELB (Spigel and Priscu, 1998; Doran et al., 2014). Chemocline leakage has occurred in the past and continues in the present, but the process is likely sporadic with varying magnitude (Doran et al., 2014). Present-day chemocline leakage could occur following an advance of TG or a large inflow of subglacial brine, both of which could raise the chemocline above the depth of the sill (Doran et al., 2014). The horizontal oscillations below the chemocline in WLB measured by Spigel et al., (2018) are caused by glacial meltwater and subglacial outflow. The inflows form horizontal intrusions, due to the density stratification of the hypolimnion, which would raise the water in layers above them, including the chemocline (Spigel et al., 2018).

The amount of annual terminus ice melt into WLB is difficult to estimate as TG advances and calving do not occur homogenously over time (Spigel et al., 2018). The glacier terminus advanced approximately 100 ± 11m between 1976 and 1996 (Fountain et al., 2004) which suggests a flow rate of ~5m yr^{-1} (Spigel et al., 2018). Measurements of surface ice velocity within 500m of the terminus estimate the glacier is moving between 5.1 and 5.3 m yr^{-1} (Pettit et al., 2014). Spigel et al. (2018) estimated ice melt between 3.4m yr^{-1} and 7.0m yr^{-1} in 2008 and 2009, respectively, based on the approximate horizontal area over which the temperature anomaly was observed below the chemocline and the amount of freshwater required to cause the concurrent salinity changes. Further, the total dissolved solids (TDS) decreased between 17m and 40m in the WLB basin by 33.3 x 10^6 kg from 1990 to 2009 (Spigel et al., 2018). The

estimated rate of ice melt required for this 19-year change is 8.0 m yr^{-1}, based on the assumed area of the glacier face in contact with the lake water beneath the lake ice and the measured decrease in lake water salinity over that time as a proxy for freshwater volume (Spigel et al., 2018).

Sediments

Aeolian transport processes are important in Taylor Valley, with episodic wind events where wind speeds are 25-35m s^{-1} (Šabacká et al., 2012). Such events blow significant abiotic and biotic material; dust, soil, microbial mats and weathered rock onto the ice surface of LB (Šabacká et al., 2012) which is then transported through the ice to the sediments (Adams et al 1998). Brief sedimentary description of five, 5cm sections of a 3.55m core of Lake Bonney sediments indicates the upper 5-10cm is silt/sand with a few pebbles, composed primarily of microbial mat and terrigenous materials, from 50-55cm, the sediment contains large clasts and sand/soil-like terrigenous materials, and similarly at 350-355cm depth (Tang et al., 2013). The shallow sediments (< 3.55 m) of Lake Bonney (Tang et al., 2013) likely originated from the walls of Taylor Valley, rather than from beneath Taylor Glacier, as He isotope ratios suggest sediment exposure to cosmic radiation, which could not occur under TG (Poreda et al., 2004). Tang et al., (2013) do not provide a coring location or details on the core stratigraphy, outside of the five 5cm sections, thus precluding further analysis of LB sediments. The composition of deeper sediments (>3.55m) in LB remains unknown, but the upper TV is filled with a mixture of glaciogenic sediments, as documented in a much deeper core of the valley fill sediments recovered ~ 10km down valley from LB on the southern shore of Lake Hoare (Powell, 1981). Here, 165m of sediment was recovered, and described as largely diamicton (58%), with the

remaining sediments being graded beds of gravel, sand and mud, 'varved' muds and silts, weathered iron-oxide horizons and lenses, and carbonate-evaporite beds (Chapman-Smith, 1975).

Additional sediment flux to WLB comes from Taylor Glacier. Flow rates at the TG terminus are primarily (~90%) controlled by basal ice deformation (Pettit et al., 2014), discussed further below. Highly deformable basal ice is flowing at speeds up to 3 m yr^{-1} at the TG terminus, which would result in a substantial sediment flux to WLB (Pettit et al., 2014). However, both the bulk sediment content of the basal ice and the portion of basal ice that melts out forming proglacial moraine are unknown, making it difficult to determine how much sediment reaches the water column (Pettit et al., 2014).

Biogeochemistry

The upper and lower layers of LB are separated by a chemocline/oxycline at ~18m in WLB and 20m in ELB (Li et al., 2020). Mean temperatures above the chemocline are 3-5°C, decreasing with depth to -5°C and -2°C at the bottom of WLB and ELB, respectively (Spigel & Priscu, 1998). The pH is basic (8-9) in the upper waters and neutral to slightly acidic (6-7) in the deeper waters (Lee et al., 2004). Sunlight penetrates the ice-cover (<5% passes through), creating a photic zone in the hypolimnion (Lee et al., 2004). Phytoplankton (chlorophytes, chrysophytes, and cryptophytes) are present in the upper layers, with Chlorophyll *a* peak concentrations occurring at 14m (4µg/L) and 19m (3µg/L) in WLB and ELB, respectively (Lee et al., 2004). Salinity increases with depth from <10 to >120 g salt/kg solution near the lake bottom, which is over 3 times higher than seawater (Spigel and Priscu, 1996).

Present Day Taylor Glacier

Taylor Glacier (TG) is an outlet glacier of Taylor Dome (TD) on the East Antarctic Ice Sheet. TG extends 100km from TD to its terminus at the western edge of Lake Bonney (Pettit et al., 2014). The movement of TG is primarily influenced by ice volume changes in the Taylor Dome region of the EAIS (Higgins et al., 2000), but local basal conditions beneath TG do affect the glacier's movement. Taylor Glacier overrides frozen, unconsolidated, marine-based sediments, with the glacier margins defined by 20-30m high ice cliffs (Pettit et al., 2014). Although there is an overdeepening point where the basal ice may reach a localized pressure melting point, leading to basal sliding, the glacier 6km downstream from this point is likely frozen to the bed (Higgins et al., 2000; Kavanaugh et al., 2009; Pettit et al., 2014). However, the measured surface velocity ~5m/yr (Fountain et al., 2004; Pettit et al., 2014) is nearly two orders of magnitude faster than what would be expected for deformation of cold, thin ice with a low surface slope (~0.1 for TG) (Pettit et al., 2014). This discrepancy is potentially explained by the TG basal ice (possibly >15m thick), which is easily deformable, accounting for over 85% of the total glacier ice deformation, based on modelling (Pettit et al., 2014). The clean ice (meteoric) is acting as a stiff material, flowing somewhat like a plug flow over the 40-times softer, more deformable basal ice (Pettit et al., 2014).

Glacial Ice

Taylor Glacier ice thickness increases from 80m at the terminus to 470m at an overdeepening point in the bed ~8km up glacier (Hubbard et al., 2004). Clean meteoric ice overlies an estimated 10-15m of basal ice (Pettit et al., 2014). Surface velocities within ~500m of the Taylor Glacier terminus have been measured at between 2 and 10 m yr^{-1} (Pettit et al., 2014;

Telling et al., 2017; Fitzsimons et al., 2024). Pettit et al. (2014) suggested that basal ice deformation accounted for 85-90% of the measured surface velocity of Taylor Glacier. Estimates by Fitzsimons et al. (2024) attribute a slightly lower proportion, ~60% of the surface velocity at TG, to deformation within the basal ice sequences, and ~15% was attributed to sliding at interfaces within the basal ice sequence. In both studies, however, the authors found that TG movement is primarily controlled by deformation in the basal ice.

Ice in the basal zone of TG consists of three distinct facies: clean englacial ice, stratified ice with two subfacies, and coarse gravel at the base with interstitial ice in the pore spaces (Samyn et al., 2008; Montross et al., 2014; Fitzsimons et al., 2024). The stratified ice contains layers of alternating clean and debris-rich ice, then massive, unstructured facies comprised of densely-packed debris in a clean-ice matrix. The highest debris content in the unstructured facies is ~32% volume (Fitzsimons et al., 2024). The highest strain rate occurs within the debris-rich ice and the lowest occurs in ice with <0.02% debris (Samyn et al., 2008; Fitzsimons et al., 2024). The presence of subglacial and englacial brines (Badgeley et al., 2017) and finely stacked laminae in the sediment-rich ice (Pettit et al., 2014; Fitzsimons et al., 2024) suggest regelation as the primary mode of debris entrainment in the basal ice (Fitzsimons et al., 2024).

The debris content (Pettit et al., 2004; Fitzsimons et al., 2024) and high strain rate in the stratified ice (Samyn et al., 2008) leads to increased abrasion, creating silt-sized particles and striated clasts similar to those observed in temperate glacier environments, which suggests glacial comminution processes similar to those beneath temperate glaciers (Fitzsimons et al., 2024). The exact depth of the basal ice layer is not known, but a distinct boundary is visible between the top of the basal ice and the bottom of the clean ice, suggesting a rigid meteoric ice

layer over the deformable, sediment-rich ice layer (Pettit et al., 2014). The lower boundary of the basal ice is likely frozen to the bed across much of TG, due to temperatures as low as -18°C, except at the point of bed overdeepening where the 470m-thick ice may be at the pressure melting point (Hubbard et al., 2004). This may be due in part to the subglacial brine present beneath Taylor Glacier which has a significantly lower freezing point than freshwater. Additional areas at the bed may experience localized basal ice melt due to liquid brine flows (Hubbard et al., 2004; Badgeley et al., 2017). While basal sliding may occur in these areas of melt at the bed, the contribution to the observed annual surface velocity of TG was estimated to be from <0.2% (Pettit et al., 2014). Most ice flow, and therefore sediment comminution, likely occurs at the interface between the upper basal and lower clean ice layers.

Variations in surface ice speeds suggest the basal layer varies in thickness across the bed and must be 20-40 times softer than clean glacier ice to account for the surface ice velocities measured, according to Glen's Flow Law (Glen, 1958; Pettit et al., 2014). Modeled basal temperature at the base of the glacier tongue is colder along the margins (-16 to -18ºC) and warms to -7.8ºC at the overdeepening along the glacier center line, due to insulation from thicker ice overtop and frictional heating from glacier movement (Hubbard et al., 2004). For the glacier to move at the speeds measured by Pettit et al. (2014) with the basal temperatures inferred by Hubbard et al. (2004), the basal sediments would have to be saturated with brine at a salinity of at least 125% of seawater to lower the freezing point of brine below -7ºC (Badgeley et al., 2017).

Subglacial Brine

The temperatures at the bed of TG are below the pressure melting point for fresh water (Hubbard et al., 2004), yet data from ice-penetrating radar, radio echo sounding, and transient

electromagnetic surveys of TG suggest an extensive zone of liquid is present beneath the glacier tongue (Hubbard et al., 2004; Mikucki et al., 2015; Foley et al., 2016; Badgeley et al., 2017). The salinity of the englacial and subglacial brine, estimated from radio echo sounding scattering is ~3.5 times that of seawater (Badgeley et al., 2017), which is supported by direct measurements of the downstream discharge at Blood Falls (Lyons et al., 2005). The combination of easily deformable basal ice and pressurized, flowing liquid beneath the ice explain how the velocity of TG exceeds what would normally be expected for a cold-based glacier (Pettit et al., 2014; Badgeley et al., 2017).

Hubbard et al. (2004) first detected an area of saturated sediments and/or liquid beneath TG that was 400-1000m wide, located 3-6km upglacier from the terminus in an overdeepening at the bed. Mikucki et al. (2015) and Foley et al. (2016) subsequently used airborne electromagnetic (AEM) surveys (a more sensitive approach for quantitating volume and salinity of brine, compared to the radar used by Hubbard et al., 2004) and found a horizontally continuous region of brine extending from the TG terminus to at least 6 km upglacier, where ice thickness of > 350 m prevented further AEM analysis (Mikucki et al., 2015; Foley et al., 2016). The brine-saturated sediment layer extends 10s of meters below the ice-sediment interface of TG with an estimated volume of at least 1.5 km^3 over the measured area (Mikucki et al., 2015). Based on conservative estimates of porosity, the volume of liquid water beneath TG is likely greater than that of all TV surface lakes combined (Mikucki et al., 2015, Foley et al., 2016).

Glacial Sediment Flux to West Lake Bonney

The terminus of TG is partially in contact with WLB, so melting basal ice results in a sediment flux to the lake. About 700m of the glacier terminus is in direct contact with the lake at

a water depth of ~21m, which results in about 14,700m^3 of ice melt per meter of advancement annually (Bomblies et al., 2001). Although the direct ice melt into the lake has little impact on water levels in WLB (<0.5cm/yr, Bomblies et al., 2001) it is unclear how much this melt contributes to sediment flux. Pettit et al. (2014) argue that because the basal ice is thick and deformable, moving at speeds up to 3m/yr at the terminus, the sediment flux to WLB is non-negligible. Basal ice at the terminus is ~4m thick and is composed of a sequence of distinct ice facies (Pettit et al., 2014). Bands of clean ice intermix with stratified debris-rich basal ice, some of which have >50% debris by volume (Pettit et al., 2014). Pettit et al. (2014) calculated that a 10m-thick layer of basal ice with an average of 5% by volume of sediment flowing at an average of 2m/yr would equate to a flux of 1m^3/yr of sediment per meter of terminus. It is difficult to determine the bulk sediment content of the ice, though, and it is not clear how much of the basal ice melts into the lake and what portion is deposited in proglacial moraines (Pettit et al., 2014). Debris-rich basal ice flowing at speeds around 3m a^{-1} should result in a sediment flux to the glacier margins and terminus (Pettit et al., 2004). Based on debris content and flow rate, there would be an estimated sediment flux between 0.5 and 1m^3 a^{-1} to each meter of the glacier terminus (Pettit et al., 2004; Fitzsimons et al., 2024). The limited debris and lack of moraines along the periphery of TG is not consistent with the predicted sediment flux, which suggests that most of the debris is washed into Lake Bonney via the proglacial streams (Fitzsimons et al., 2024).

Blood Falls Outflow

Additional brine inputs from TG flow from Blood Falls through periodic discharges onto the glacier/lake surface and into the WLB water column (Mikucki et al., 2004). The

geochemistry of the brine discharge is similar to seawater except it is enriched in products associated with weathering, such as H_4SiO_4 and Li^+ and depleted in K^+ and Rb^+, relative to seawater, possibly due to adsorption by clay minerals in the subglacial sedimentary environment (Lyons et al., 2019). The brine discharge accounts for 95% of the total Cl flux to the lake (Lyons et al., 1998) and contributes organic carbon, microbes, and iron to the lake (Mikucki et al., 2004). The density of the discharge (1,100 kg m^{-3}) (Keys, 1979; Micucki et al., 2004; Lawrence et al., 2020) is identical to the deep waters of WLB, so it will sink below the chemocline at 15m. The total iron concentration at around 25m in WLB, near the glacier terminus, is over 50µM with Blood Falls identified as the likely source (Mikucki et al., 2004).

Potential Sources of Methane in Lake Bonney

Methane in the water columns of WLB and ELB is supersaturated relative to the atmosphere, between the depths of 12 and 35m (Li et al., 2020). The peak methane concentrations occur in WLB at 25m (354 nmol CH_4 L^{-1}), and in ELB at 22m (33.5 nmol CH_4 L^{-1}), below the respective chemoclines of both lobes where the waters are sub-oxic. The exact source(s) of this methane are unknown, with multiple possible abiotic and biotic processes supplying methane (Li et al., 2020). Determining the potential methane sources in LB requires understanding the geologic history of the lake, contemporary physical, chemical, and biological processes, and methane sources beyond conventional methanogenesis.

Biological Methanogenesis in Lake Bonney

Methanogenesis was previously thought to occur only in anoxic environments, but recent research has shown aerobic methanogenesis is possible in oligotrophic marine and freshwater

systems (e.g. Bogard et al., 2014; Damm et al., 2010; Grossart et al., 2011; Karl et al., 2008). Damm et al. (2010) demonstrated that metabolic lysis of organosulfur compounds by certain phytoplankton may produce methane. The demethylation of other methylated organic compounds such as methyl amines has been shown as a potential source of methane in other lakes (Bižic-Ionescu et al. 2018). Bacteria using the C-P lyase pathway produce methane as a byproduct under oxic conditions, utilizing various methylated organic compounds such as methylphosphonate (MPn) (e.g. Metcalf et al. 2012; Wang et al. 2017). Similarly, Li et al., (2020) demonstrated experimentally that the amendment of oxic waters from WLB and ELB with methylphosphonate (MPn) generated methane through microbial activity from the native lake microbial community at 5ºC in the dark, suggesing *in situ* methanogenesis via the carbon-phosphorus (C-P) lyase pathway is possible in the oxic waters of WLB and ELB.

Aerobic methanogenesis is likely a major source of the methane in the oxygenated surface waters from 12 to 20m, however, the highest concentrations of methane occur below 20m where the waters are sub-oxic (Li et al., 2020), which could suggest microbial methanogenesis. Methanogenic lineages were detected in archaeal OTUs from the oxygenated zone of the WLB water column (Vick-Majors et al., 2014) but the closest sequence matches (*Methanomicrobia* and *Methanobacteria*) are only known to produce methane under anaerobic conditions (Ferry, 2010; Offre et al., 2013; Vick-Majors et al., 2014) so it was suggested that they were transported to the aerobic epilimnion of WLB from another environment (Vick-Majors et al., 2014). Allochthonous cell deposits occur as surface soil particles that are transported through the ice to the WLB water column (Fritsen and Priscu, 1999), but the methanogenic sequences detected in the upper waters of the lake do not match any OTUs observed in the soil surrounding

WLB (Vick-Majors et al., 2014), leading the authors to speculate that they may have diffused upward from the anoxic waters and/or sediments of WLB.

Microbial methanogenesis has previously been measured in the anoxic waters of MDV Lakes Vanda, in Wright Valley (Saxton et al., 2021), Hoare, in Taylor Valley (Lawson Knoepfle et al., 2009), and Fryxell in Taylor Valley (Karr et al., 2005; Saxton et al., 2016). Lake Fryxell (~16km east of LB) contains archaeal methanogenic lineages in the sediments (Smith et al., 1993; Karr et al., 2006) and methane concentrations at the sediment/water interface of ~1mM, decreasing towards the surface in a diffusional profile (Saxton et al., 2016). The methane concentration profile in WLB is not consistent with a simple diffusion gradient of methane sourced from the sediments (Li et al., 2020). The concentration profile suggests the sediments may be a methane source, but the highest concentrations are between 20 and 25m depth, in the 40m deep water column (Li et al., 2020).

Sub-ice sediments with suitable organic carbon, anoxic conditions, and a lack of higher-energy-yielding redox couplings can provide an environment habitable for methanogens (Wadham et al., 2012). Sulfate reduction is more energetically favorable than methanogenesis, so sulfate reducers typically outcompete methanogens for H_2 and acetate substrates (Boyd et al., 2014), leading to sulfate reduction generally being the dominant process in anoxic marine environments (Mitterer, 2010). When sulfate reduction is not present, methanogenesis becomes more viable (Boyd et al., 2010). Despite high concentrations of sulfate in the bottom waters of WLB, no hydrogen sulfide has been detected in the water column, so sulfate reduction is unlikely (Ward et al., 2003), reducing competition for any potential methanogens. High salinity, however, constrains methanogenesis (Waldron et al., 2007) so this would impact any potential

biogenic methane production in LB below the chemocline, where salinity approaches four times that of seawater. Indeed, 16S rRNA gene-based pyrosequencing found the majority of bacterial OTUs in the bottom waters of WLB are closely related to known halophiles, while there is no evidence for methanogens (Kwon et al., 2017; Lee et al., 2023). Further, the methanogenesis marker gene *mcrA* was absent in metagenomic sequence libraries from waters below the LB chemocline (Li et al., 2020). DNA was also extracted from five discrete horizons from in a 3.55m-long sediment core from WLB, and 16S rRNA gene sequencing of the samples revealed no OTUs closely associated with known methanogens (Tang et al., 2013). Collectively these data indicate biological methanogenesis is unlikely in the bottom waters or sediments of Lake Bonney, but the methane concentration profile measured by Li et al. (2020) suggests the lake sediments may be a methane source. Therefore, a plausible alternate abiotic source would be from geogenic/ thermogenic sources beneath the lake sediments (discussed below).

Biological Methanogenesis in the Subglacial Brine

The microbial community structure and geochemical conditions in the brine beneath Taylor Glacier suggest both traditional methanogenesis and methanogenesis from non-traditional substrates are not possible. Although detailed geochemical measurements of the Blood Falls englacial brine are available, no data on methane concentration have been published (Lyons et al., 2019). The community structure of the brine is most consistent with other iron and sulfur-rich systems, with abundant sequences closely related to known iron and sulfur oxidizers (Mikucki and Priscu, 2007; Campen et al., 2019). The high availability of more energetically favorable electron acceptors and a relatively slow rate of metabolism measured in the brine also makes it unlikely that energy sources would be depleted enough for the less energetically favorable

methanogenesis to occur (Mikucki et al., 2004; Murray et al., 2012). The dominance of iron and sulfur reducers in Blood Falls (Mikucki et al., 2004) would likely lead to competition for H_2 and acetate, which would make anaerobic methanogenesis difficult (Lovley and Phillips, 1987; Oremland and Polcin, 1982; Schönheit et al., 1982). Non-traditional biological methanogenesis pathways were also considered.

Anaerobic methylotrophic methanogenesis uses non-competitive substrates, such as methylamine, and has been observed in Lake Vanda, another hypersaline (>10 times seawater) McMurdo Dry Valleys lake (Saxton et al., 2021) and the saline (~1.2 times seawater) Ace Lake in the Vestfold Hills of East Antarctica (Franzmann et al., 1992). The Ace Lake methylotrophic methanogen was isolated and identified as the archaeon *Methanococcoides burtoni sp.* (Franzmann et al., 1992). *M. burtoni* was capable of growth in media with pH ~6.6-8.3 under anaerobic conditions (Franzmann et al., 1992). The pH of the Blood Falls brine is ~6 (Mikucki et al., 2009) and the englacial brine has a more variable pH from 7-9 (Campen et al., 2019), while both are anaerobic (Campen et al., 2019). However, it is unlikely that *M. burtoni*, or similar methylotrophic archaea are present in the TG subglacial brine. Methylotrophic methanogenesis is most commonly associated with archaea (Bueno de Mesquita et al., 2023) and archaeal DNA sequences in the TG subglacial brine were the lowest in abundance, following bacteria and eukaryotes in both Blood Falls and brine from an englacial conduit of TG (Campen et al., 2019). The physiochemical conditions in the brine are also not conducive to alternative methanogenic pathways.

Aerobic methanogenesis via microbial methylphosphonate (MPn) degradation occurs in the epilimnion of Lake Bonney because the water is P-deficient and the bacteria are utilizing

MPn as an alternate phosphorous source (Li et al., 2020), but the concentration of phosphate in the subglacial brine is sufficient to support microbial activity (Lyons et al., 2019). Also, no detectable oxygen is present in the brine (Mikucki et al., 2009; Lyons et al., 2019) so aerobic methylphosphonate degradation, like that observed in the epilimnion of WLB (Li et al., 2020), is not likely (Karl et al., 2008). Methanogenesis from microbial degradation of dimethylsulfide (DMS) and dimethylsulfoxide (DMSO) occurs in marine environments (Florez-Leiva et al., 2013), but DMS and DMSO are produced by photosynthetic organisms (Lee et al., 2004), which cannot exist in a subglacial environment and were absent from genetic analyses of the brine (Campen et al., 2019). Collectively these data indicate biological methanogenesis in the englacial brine is unlikely.

Methane in Taylor Glacier Sediments

Microbial methane production has previously been measured or inferred in subglacial environments in the Canadian Rockies (Boyd et al., 2010), the High Arctic (Skidmore et al., 2000), Iceland (Burns et al., 2018), the Yukon (Sapper et al., 2023) and beneath the Greenland and West Antarctic ice sheets (Dieser et al., 2014; Michaud et al., 2017; Christiansen and Jørgensen, 2018). The presence of active methanogens in subglacial sediments has previously been determined through genetic proxies (metabolic biomarkers for methanogenesis, 16S rRNA gene phylotypes related to known methanogens) and enrichment culturing (Boyd et al., 2010), the autofluorescence of coenzyme F_{420} in methanogenic cells and enrichments (Stibal et al., 2012) and inferred by measuring the isotopic signature of the methane (e.g. Burns et al., 2018; Sapper et al., 2023).

Prior research on microbial diversity within the basal ice of Taylor Glacier did not produce any archaeal sequences (Doyle and Christner 2022), indicating biological methanogenesis in basal ice would be unlikely as methane source to LB. However, published data on the gas content of basal ice from Taylor Glacier did not include any methane measurements (Montross et al., 2014), so it is possible there may be (stored) methane in the basal ice. If methane exists beneath TG, there are three potential sources: relict biological methane from ancient marine sediments overridden by the glacier, crustally-derived methane seeping up from underlying rocks, or methane released from the glacial comminution of bedrock and sediments. Given TG is cold-based with minimal contemporary basal sliding the latter source seems unlikely to be significant. Stored methane, "sealed" in the sediments, brine, and ice beneath TG is certainly possible.

The presence of the subglacial brine beneath the glacier suggests it advanced over marine-deposited sediments sometime after the Taylor Valley fjord drained, likely in the early Quaternary, ~2-3 ma (Lyons et al., 2005). Its furthest advance was possibly more than 10 km eastward of its current position between 70 and 130 ka (Higgins et al., 2000), followed by periods of variable retreat and advance until becoming relatively stable at its current position during the Last Glacial Maximum in Antarctica, ~28.5-12.8 ka (Hall et al., 2015). There is no evidence for major TG advances beyond the current margins for ~11,000 ka (Kavanaugh et al., 2009). The region of brine-saturated sediment has, therefore, been "sealed" by overlying ice for at least 12.8 thousand years, perhaps as much as 2-3 million years. This is a significant amount of time for methane from the marine sediments, or from deeper in the underlying rocks, to seep into the subglacial brine and/or be incorporated into the basal ice. Isotopic analysis of subglacial

methane in other glacial systems has shown examples that are clearly microbial in origin (e.g. Dieser et al., 2014; Michaud et al., 2017) but numerous studies indicate abiotic methane sources are also likely contributors to the methane gas flux (e.g. Burns et al., 2018; Lamarche-Gagnon et al., 2019; Sapper et al., 2023).

Legacy Thermogenic Methane

There are two primary crustal sources of abiotic methane emanating from beneath glaciers and ice sheets, thermogenic methane related to hydrocarbon production in sedimentary basins and inorganic reactions of Fischer-Tropsch type in geothermal systems (Etiope and Klusman, 2002; Wadham et al., 2012; Burns et al., 2018). This crustally-derived methane is supplied to the subglacial environment via gas permeable faults and fractured rocks and is trapped by the overlying ice, rather than being released directly to the atmosphere. An additional subglacial abiotic methane source is through the glacial comminution of methane-containing subglacial bedrock, e.g. shale and other sedimentary rocks, and sediments derived from such lithologies (Gill-Olivas et al., 2023).

The underlying bedrock of the McMurdo Dry Valleys consists of a Precambrian basement complex of metasediments, overlain by Devonian-age sedimentary rocks including sandstones and siltstones of the Beacon Supergroup (Sugden et al., 1995; Hall et al., 2000; Cox et al., 2012) Ferrar dolerite sills of Jurassic age intrude the basement complex and the Beacon Supergroup (Sugden et al., 1995; Hall et al., 2000; Cox et al., 2012). The valley walls and mountain ranges have visible bands of sandstone and dolerite and much of the valley floor soil and rocks are derived from weathering of the Ferrar dolerite and Beacon supergroup sandstone (Tamppari et al., 2012; Goordial et al., 2016). Methane can be found in igneous rocks (Potter and Konnerup-

Madsen, 2003; Milkov and Etiope, 2018), including dolerite (Jeffrey and Kaplan, 1988; McElwain et al., 2005). Sandstones have also been found to contain methane (You and Flemings, 2018). However, the most likely lithological source is shale deposits beneath TG. Hamilton and Hayes (1963) identified carbonaceous shale within the cliffs and mountains adjacent to TG. The unit was considered widespread in the regions north of lower TG (Hamilton and Hayes, 1963). Glacial grinding of bedrock shales was found to be an abiotic source of methane beneath Robertson Glacier in the Canadian Rockies and may represent the largest source of methane in subglacial systems with carbon-rich bedrock (MacDonald et al., 2018). The rocks underlying TG are therefore a potential source of thermogenically-derived methane.

Methanogenesis from Reactions Between Organosulfur Compounds and Minerals in the LB Water Column

Abiotic methane production from organosulfur compounds including methionine, dimethyl sulphoxide (DMSO), and dimethylsulphoniopropionate (DMSP) in the presence of ferrihydrite and hydrogen peroxide has been demonstrated under oxic ambient temperature conditions in the laboratory (Althoff et al., 2014). Sulphoxides have been suggested as potential precursors to methane formed in oxic and suboxic waters, perhaps providing an explanation for the "oceanic methane paradox" (Althoff et al., 2014) and may also be a contributory source to the supersaturated methane pool in LB. Methane production has been recorded in solutions containing DMS or DMSO, iron-bearing minerals, and hydrogen peroxide (Herscu-Kluska, 2008; Althoff et al., 2014). In one proposed series of reactions, hydroxyl radicals (formed either by radiolysis of water or through the Fenton Reaction) oxidize organic compounds containing hetero-bonded methyl groups (e.g. DMSO) to produce methyl radicals, which are then reduced by hydrogen peroxide to methane (Herscu-Kluska, 2008). DMSO, when compared to other

methylated organic compounds, yielded the highest methane production from these reactions (Althoff et al., 2014). The production of methane from DMSO can occur from pH 3-8 and under anaerobic conditions (Herscu-Kluska, 2008; Althoff et al., 2014). The methane concentration peak in WLB occurs at ~25m, just below the subglacial inflow from TG, where the water is sub-oxic, with a pH around 6 (Li et al., 2020). It is possible, then, that iron-bearing minerals deposited into WLB through subglacial inflow from TG catalytically decompose hydrogen peroxide to generate hydroxyl radicals (Fenton Reaction), which then react with DMSO to produce methyl radicals, which are then reduced by hydrogen peroxide to methane (Eberhardt and Colina, 1988; Herscu-Kluska, 2008).

Fenton's Reaction: $Fe^{2+} + H_2O_2 \rightarrow Fe^{3+} + \cdot OH + OH^-$

DMSO Reaction: $\cdot OH + CH_3SOCH_3 \rightarrow \cdot CH_3 + CH_3SOOH$

Methyl Radical Reaction: $\cdot CH_3 + H_2O_2 \rightarrow CH_4 + HO_2$

The hydrogen peroxide (H_2O_2) in Fenton's Reaction can be formed from the interaction of water with crushed pyrite at a circumneutral pH. Crushing and abrasion of pyrite fractures the S-S bonds, forming S^- sites on the mineral surface (Nesbitt et al., 1998). The unstable S^- sites then acquire an electron from Fe^{2+} ions on the mineral surface (Gill-Olivas et al., 2023; Reaction 1 below). The Fe^{3+} from Reaction 1 then splits water, producing hydroxyl radicals (Gill-Olivas et al., 2023; Reaction 2). Finally, the hydroxyl radicals from Reaction 2 combine to form hydrogen peroxide (Gill-Olivas et al., 2023; Reaction 3).

Reaction 1: $Fe^{2+}_{surface} + S^{-}_{surface} \rightarrow Fe^{3+}_{surface} + S^{2-}_{surface}$

Reaction 2: $Fe^{3+}_{surface} + H_2O \rightarrow Fe^{2+}_{surface} + \bullet OH + H^{+}$

Reaction 3: $\bullet OH + \bullet OH \rightarrow H_2O_2$

Concentrations of Dimethylsulfide (DMS) and Dimethylsulfoxide (DMSO) in LB are among the highest concentrations recorded in a natural system (Lee et al., 2004). DMS and DMSO are biogenic gases produced by phytoplankton (Lee et al., 2001). The compounds may serve several purposes, including acting as free radical scavengers (Lee et al., 2004). DMS concentrations at the bottom of WLB are as high as those typically associated with phytoplankton blooms (Lee et al., 2004), but there is no evidence of phytoplankton biomass or activity below the chemocline (Lizotte et al., 1996). These sulfur compounds are likely produced by phytoplankton in the surface waters, then lost to the epilimnion through sedimentation of particulate matter. The particulate forms are then microbially transformed into dissolved forms, which would explain the high dissolved DMS and DMSO concentrations in the bottom waters (Lee et al., 2004). Around 22m in WLB, the DMSO concentration begins to decrease concurrent with an increase in DMS, a phenomenon which does not occur in ELB. Lee et al. (2004) suggest that because conditions in WLB are more reducing (325-400 mV) than ELB (550-650mV), the reduction of DMSO to DMS may be a more energetically favorable metabolism. The high levels of dimethylsulfide (DMS) and DMSO in the water column of Lake Bonney (Lee et al. 2004) in concert to the iron rich brines derived from subglacial brine discharge (Mikucki et al. 2004, 2015) may provide the substrate for methane-yielding abiotic reactions in a natural environmental setting.

References

Aciego, S. M., Cuffey, K. M., Kavanaugh, J. L., Morse, D. L., & Severinghaus, J. P. (2007). Pleistocene ice and paleo-strain rates at Taylor Glacier, Antarctica. Quaternary Research, 68(3), 303-313.

Adams, E. E., Priscu, J. C., Fritsen, C. H., Smith, S. R., & Brackman, S. L. (1998). Permanent ice covers of the McMurdo Dry Valley Lakes, Antarctica: bubble formation and metamorphism. Ecosystem dynamics in a polar desert: the McMurdo dry valleys, Antarctica, 72, 281-295.

Althoff, F., Benzing, K., Comba, P., McRoberts, C., Boyd, D. R., Greiner, S., & Keppler, F. (2014). Abiotic methanogenesis from organosulphur compounds under ambient conditions. Nature Communications, 5(1), 4205.

Anderson, J. B., Conway, H., Bart, P. J., Witus, A. E., Greenwood, S. L., McKay, R. M., Hall, B.L., Ackert, R.P., Licht, K., Jakobsson, M., & Stone, J. O. (2014). Ross Sea paleo-ice sheet drainage and deglacial history during and since the LGM. Quaternary Science Reviews, 100, 31-54.

Anderson, J. T., Wilson, G. S., Fink, D., Lilly, K., Levy, R. H., & Townsend, D. (2017). Reconciling marine and terrestrial evidence for post LGM ice sheet retreat in southern McMurdo Sound, Antarctica. Quaternary Science Reviews, 157, 1-13.

Badgeley, J. A., Pettit, E. C., Carr, C. G., Tulaczyk, S., Mikucki, J. A., Lyons, W. B., & MIDGE Science Team. (2017). An englacial hydrologic system of brine within a cold glacier: Blood Falls, McMurdo Dry Valleys, Antarctica. Journal of Glaciology, 63(239), 387-400.

Baggenstos, D., Severinghaus, J. P., Mulvaney, R., McConnell, J. R., Sigl, M., Maselli, O., Petit, J., Grente, B., & Steig, E. J. (2018). A horizontal ice core from Taylor Glacier, its implications for Antarctic climate history, and an improved Taylor Dome ice core time scale. Paleoceanography and Paleoclimatology, 33(7), 778-794.

Benn, D., & Evans, D. J. (2010). Glaciers and glaciation. Routledge.

Berger, G. W., Doran, P. T., & Thomsen, K. J. (2013). Micro-hole and multigrain quartz luminescence dating of Paleodeltas at Lake Fryxell, McMurdo Dry Valleys (Antarctica), and relevance for lake history. Quaternary Geochronology, 18, 119-134.

Bindschadler, R. (2006). The environment and evolution of the West Antarctic ice sheet: setting the stage. Philosophical Transactions of the Royal Society A: Mathematical, Physical and Engineering Sciences, 364(1844), 1583-1605.

Bižić-Ionescu, M., Ionescu, D., Günthel, M., Tang, K. W., & Grossart, H. P. (2018). Oxic methane cycling: New evidence for methane formation in oxic lake water. Biogenesis of hydrocarbons, 1-22.

Bogard, M. J., Del Giorgio, P. A., Boutet, L., Chaves, M. C. G., Prairie, Y. T., Merante, A., & Derry, A. M. (2014). Oxic water column methanogenesis as a major component of aquatic CH4 fluxes. Nature communications, 5(1), 5350.

Bockheim, J. G., Campbell, I. B., & McLeod, M. (2007). Permafrost distribution and active-layer depths in the McMurdo Dry Valleys, Antarctica. Permafrost and periglacial processes, 18(3), 217-227.

Bomblies, A., McKnight, D. M., & Andrews, E. D. (2001). Retrospective simulation of lake-level rise in Lake Bonney based on recent 21-year record: indication of recent climate change in the McMurdo Dry Valleys, Antarctica. Journal of Paleolimnology, 25, 477-492.

Boyd, E. S., Skidmore, M., Mitchell, A. C., Bakermans, C., & Peters, J. W. (2010). Methanogenesis in subglacial sediments. Environmental microbiology reports, 2(5), 685-692.

Boyd, E. S., Hamilton, T. L., Havig, J. R., Skidmore, M. L., & Shock, E. L. (2014). Chemolithotrophic primary production in a subglacial ecosystem. Applied and environmental microbiology, 80(19), 6146-6153.

Bueno de Mesquita, C. P., Wu, D., & Tringe, S. G. (2023). Methyl-based methanogenesis: an ecological and genomic review. *Microbiology and Molecular Biology Reviews*, *87*(1), e00024-22.

Burns, R., Wynn, P. M., Barker, P., McNamara, N., Oakley, S., Ostle, N., Stott, A.W., Tuffen, H., Zhou, Z., Tweed. F.S., Chesler, A., & Stuart, M. (2018). Direct isotopic evidence of biogenic methane production and efflux from beneath a temperate glacier. Scientific reports, 8(1), 17118.

Campen, R., Kowalski, J., Lyons, W. B., Tulaczyk, S., Dachwald, B., Pettit, E., Welch, K.A., & Mikucki, J. A. (2019). Microbial diversity of an Antarctic subglacial community and high-resolution replicate sampling inform hydrological connectivity in a polar desert. *Environmental Microbiology*, *21*(7), 2290-2306.

Castendyk, D. N., Obryk, M. K., Leidman, S. Z., Gooseff, M., & Hawes, I. (2016). Lake Vanda: A sentinel for climate change in the McMurdo Sound Region of Antarctica. Global and Planetary Change, 144, 213-227.Castendyk, D. N., Obryk, M. K., Leidman, S. Z., Gooseff, M., & Hawes, I. (2016). Lake Vanda: A sentinel for climate change in the McMurdo Sound Region of Antarctica. Global and Planetary Change, 144, 213-227. Castendyk, D. N., Obryk, M. K., Leidman, S. Z., Gooseff, M., & Hawes, I. (2016). Lake Vanda: A sentinel for climate change in the McMurdo Sound Region of Antarctica. Global and Planetary Change, 144, 213-227.

Chapman-Smith, M. (1975). Geologic log of DVDP 12. Lake Leon, Taylor Valley: Dry Valley Drilling Project Bulletin, (5), 61-70.

Chinn, T. J. (1993). Physical hydrology of the dry valley lakes. Physical and biogeochemical processes in Antarctic lakes, 59, 1-51.

Christiansen, J. R., & Jørgensen, C. J. (2018). First observation of direct methane emission to the atmosphere from the subglacial domain of the Greenland Ice Sheet. Scientific reports, 8(1), 16623.

Clow, G. D., McKay, C. P., Simmons Jr, G. M., & Wharton Jr, R. A. (1988). Climatological observations and predicted sublimation rates at Lake Hoare, Antarctica. Journal of Climate, 1(7), 715-728.

Cox, S., Turnbull, I. M., Isaac, M. J., Townsend, D., & Lyttle, B. S. (2012). Geology of southern Victoria land Antarctica. Institute of Geological & Nuclear Sciences 1:250 000 Geological Map 22, 1-140.

Cross, J. M., Fountain, A. G., Hoffman, M. J., & Obryk, M. K. (2022). Physical Controls on the Hydrology of Perennially Ice-Covered Lakes, Taylor Valley, Antarctica (1996–2013). Journal of Geophysical Research: Earth Surface, 127(12), e2022JF006833.

Cunningham, W. L., Leventer, A., Andrews, J. T., Jennings, A. E., & Licht, K. J. (1999). Late Pleistocene-Holocene marine conditions in the Ross Sea, Antarctica: evidence from the diatom record. The Holocene, 9(2), 129-139.

Damm, E., Helmke, E., Thoms, S., Schauer, U., Nöthig, E., Bakker, K., & Kiene, R. P. (2010). Methane production in aerobic oligotrophic surface water in the central Arctic Ocean. Biogeosciences, 7(3), 1099-1108.

Denton, G. H., & Marchant, D. R. (2000). The geologic basis for a reconstruction of a grounded ice sheet in McMurdo Sound, Antarctica, at the last glacial maximum. Geografiska Annaler: Series A, Physical Geography, 82(2-3), 167-211.

Dieser, M., Broemsen, E. L., Cameron, K. A., King, G. M., Achberger, A., Choquette, K., Hagedorn, B., Sletten, R., Junge, K., & Christner, B. C. (2014). Molecular and biogeochemical evidence for methane cycling beneath the western margin of the Greenland Ice Sheet. The ISME Journal, 8(11), 2305-2316.

Doran, P. T., McKay, C. P., Clow, G. D., Dana, G. L., Fountain, A. G., Nylen, T., & Lyons, W. B. (2002). Valley floor climate observations from the McMurdo Dry Valleys, Antarctica, 1986–2000. Journal of Geophysical Research: Atmospheres, 107(D24), ACL-13.

Doran, P. T., McKay, C. P., Fountain, A. G., Nylen, T., McKnight, D. M., Jaros, C., & Barrett, J. E. (2008). Hydrologic response to extreme warm and cold summers in the McMurdo Dry Valleys, East Antarctica. Antarctic Science, 20(5), 499-509.

Doran, P. T., Kenig, F., Knoepfle, J. L., Mikucki, J. A., & Lyons, W. B. (2014). Radiocarbon distribution and the effect of legacy in lakes of the McMurdo Dry Valleys, Antarctica. Limnology and Oceanography, 59(3), 811-826.

Doyle, S. M., & Christner, B. C. (2022). Variation in bacterial composition, diversity, and activity across different subglacial basal ice types. The Cryosphere, 16(10), 4033-4051.

Dugan, H. A., Obryk, M. K., & Doran, P. T. (2013). Lake ice ablation rates from permanently ice-covered Antarctic lakes. Journal of Glaciology, 59(215), 491-498.

Dziadek, R., Gohl, K., Diehl, A., & Kaul, N. (2017). Geothermal heat flux in the Amundsen Sea sector of West Antarctica: New insights from temperature measurements, depth to the bottom of the magnetic source estimation, and thermal modeling. Geochemistry, Geophysics, Geosystems, 18(7), 2657-2672.

Eberhardt, M. K., & Colina, R. (1988). The reaction of OH radicals with dimethyl sulfoxide. A comparative study of Fenton's reagent and the radiolysis of aqueous dimethyl sulfoxide solutions. The Journal of Organic Chemistry, 53(5), 1071-1074.

Elliot, D. H. (2013). The geological and tectonic evolution of the Transantarctic Mountains: a review. Geological Society, London, Special Publications, 381(1), 7-35.

Elston, D. P., & Bressler, S. L. (1981). Magneto-stratigraphic studies in neogene deposits of Taylor Valley and McMurdo Sound, Antarctica. Journal of the Royal Society of New Zealand, 11(4), 481-486.

Etiope, G., & Klusman, R. W. (2002). Geologic emissions of methane to the atmosphere. Chemosphere, 49(8), 777-789.

Ferry, J. G. (2010). The chemical biology of methanogenesis. Planetary and Space Science, 58(14-15), 1775-1783.

Fisher, A. T., Mankoff, K. D., Tulaczyk, S. M., Tyler, S. W., Foley, N., & WISSARD Science Team. (2015). High geothermal heat flux measured below the West Antarctic Ice Sheet. Science Advances, 1(6), e1500093.

Fitzsimons, S., Samyn, D., & Lorrain, R. (2024). Deformation, strength and tectonic evolution of basal ice in Taylor Glacier, Antarctica. *Journal of Geophysical Research: Earth Surface*, *129*(4), e2023JF007456.

Foley, N., Tulaczyk, S., Auken, E., Schamper, C., Dugan, H., Mikucki, J., Virginia, R., & Doran, P. (2016). Helicopter-borne transient electromagnetics in high-latitude environments: An application in the McMurdo Dry Valleys, Antarctica. Geophysics, 81(1), WA87-WA99.

Foreman, C. M., Wolf, C. F., & Priscu, J. C. (2004). Impact of episodic warming events. Aquatic Geochemistry, 10, 239-268.

Fountain, A. G., Dana, G. L., Lewis, K. J., Vaughn, B. H., & Mcknight, D. H. (1998). Glaciers of the McMurdo Dry Valleys, Southern Victoria Land, Antarctica. Ecosystem Dynamics in a Polar Desert: The McMurdo Dry Valleys, Antarctica, 72, 65-75.

Fountain, A. G., Lyons, W. B., Burkins, M. B., Dana, G. L., Doran, P. T., Lewis, K. J., McKnight, D.M, Moorhead, D.L., Parsons, A.N, Priscu, J.C., Wall, D.H., Wharton, R.A., & Virginia, R. A. (1999). Physical controls on the Taylor Valley ecosystem, Antarctica. Bioscience, 49(12), 961-971.

Fountain, A. G., Neumann, T. A., Glenn, P. L., & Chinn, T. (2004). Can climate warming induce glacier advance in Taylor Valley, Antarctica?. Journal of Glaciology, 50(171), 556-564.

Fountain, A. G., Nylen, T. H., Monaghan, A., Basagic, H. J., & Bromwich, D. (2010). Snow in the McMurdo dry valleys, Antarctica. International Journal of Climatology: A Journal of the Royal Meteorological Society, 30(5), 633-642.

Fountain, A. G., Levy, J. S., Gooseff, M. N., & Van Horn, D. (2014). The McMurdo Dry Valleys: a landscape on the threshold of change. Geomorphology, 225, 25-35.

Franzmann, P. D., Springer, N., Ludwig, W., De Macario, E. C., & Rohde, M. (1992). A methanogenic archaeon from Ace Lake, Antarctica: Methanococcoides burtonii sp. nov. *Systematic and Applied Microbiology*, *15*(4), 573-581.

Fretwell, P., Pritchard, H. D., Vaughan, D. G., Bamber, J. L., Barrand, N. E., Bell, R., Bianchi,C., Bingham,R.G., Blankenship, D.D., Casassa, G., Catania, G., Callens,D., Conway, H., Cook,A.J., Corr, H.F.J., Damaske, D., Damm,V., Ferraccioli, F., Forsberg,R., Fujita,S., Gim,Y., Gogineni,P., Griggs,J.A., Hindmarsh,R.C.A., Holmlund,P., Holt,J.W., Jacobel,R.W., Jenkins,A., Jokat,W., Jordan,T., King,E.C., Kohler,J., Krabill,W., Riger-Kusk,M., Langley,K.A., Leitchenkov,G., Leuschen,C., Luyendyk, B.P., Matsuoka,K., Mouginot,J., Nitsche,F.O., Nogi,Y., Nost,O.A., Popov,S.V., Rignot,E., Rippin,D.M., Rivera,A., Roberts,J., Ross,N., Siegert,M.J., Smith,A.M., Steinhage,D., Studinger,M., Sun,B., Tinto,B.K., Welch,B.C., Wilson,D., Young,D.A., Xiangbin,C., & Zirizzotti, A. (2013). Bedmap2: improved ice bed, surface and thickness datasets for Antarctica. The cryosphere, 7(1), 375-393.

Fritsen, C. H., & Priscu, J. C. (1999). Seasonal change in the optical properties of the permanent ice cover on Lake Bonney, Antarctica: consequences for lake productivity and phytoplankton dynamics. Limnology and Oceanography, 44(2), 447-454.

Gill-Olivas, B., Telling, J., Skidmore, M., & Tranter, M. (2023). Abrasion of sedimentary rocks as a source of hydrogen peroxide and nutrients to subglacial ecosystems. Biogeosciences, 20(5), 929-943.

Glen, J. W. (1958). The flow law of ice: A discussion of the assumptions made in glacier theory, their experimental foundations and consequences. IASH Publications, 47(171), e183.

Goodge, J. W. (2020). Geological and tectonic evolution of the Transantarctic Mountains, from ancient craton to recent enigma. Gondwana Research, 80, 50-122.

Gooseff, M. N., McKnight, D. M., Doran, P., Fountain, A. G., & Lyons, W. B. (2011). Hydrological connectivity of the landscape of the McMurdo Dry Valleys, Antarctica. Geography Compass, 5(9), 666-681.

Goordial, J., Davila, A., Lacelle, D., Pollard, W., Marinova, M. M., Greer, C. W., DiRuggiero, J., McKay, C.P., & Whyte, L. G. (2016). Nearing the cold-arid limits of microbial life in permafrost of an upper dry valley, Antarctica. The ISME journal, 10(7), 1613-1624.

Grossart, H. P., Frindte, K., Dziallas, C., Eckert, W., & Tang, K. W. (2011). Microbial methane production in oxygenated water column of an oligotrophic lake. Proceedings of the National Academy of Sciences, 108(49), 19657-19661.

Hall, B. L., & Denton, G. H. (2000). Radiocarbon chronology of Ross Sea drift, eastern Taylor Valley, Antarctica: Evidence for a grounded ice sheet in the Ross Sea at the last glacial maximum. Geografiska Annaler: Series A, Physical Geography, 82(2-3), 305-336.

Hall, B. L., Hendy, C. H., & Denton, G. H. (2006). Lake-ice conveyor deposits: geomorphology, sedimentology, and importance in reconstructing the glacial history of the Dry Valleys. Geomorphology, 75(1-2), 143-156.

Hall, B. L., Denton, G. H., Stone, J. O., & Conway, H. (2013). History of the grounded ice sheet in the Ross Sea sector of Antarctica during the Last Glacial Maximum and the last termination. Geological Society, London, Special Publications, 381(1), 167-181.

Hall, B. L., Denton, G. H., Heath, S. L., Jackson, M. S., & Koffman, T. N. (2015). Accumulation and marine forcing of ice dynamics in the western Ross Sea during the last deglaciation. Nature Geoscience, 8(8), 625-628.

Hall, C. M., Castro, M. C., Kenig, F., & Doran, P. T. (2017). Constraining the recent history of the perennially ice-covered Lake Bonney, East Antarctica using He, Kr and Xe concentrations. Geochimica et Cosmochimica Acta, 209, 233-253.

Hamilton, W., & Hayes, P. T. (1963). Type Section of the Beacon Sandstone of Antarctica. Geological Survey Professional Paper (No. 456-A).

Hendy, C. H., Wilson, A. T., Popplewell, K. B., & House, D. A. (1977). Dating of geochemical events in Lake Bonney, Antarctica, and their relation to glacial and climate changes. New Zealand Journal of Geology and Geophysics, 20(6), 1103-1122.

Herscu-Kluska, R., Masarwa, A., Saphier, M., Cohen, H., & Meyerstein, D. (2008). Mechanism of the reaction of radicals with peroxides and dimethyl sulfoxide in aqueous solution. Chemistry–A European Journal, 14(19), 5880-5889.

Higgins, S. M., Hendy, C. H., & Denton, G. H. (2000). Geochronology of Bonney drift, Taylor Valley, Antarctica: evidence for interglacial expansions of Taylor Glacier. Geografiska Annaler: Series A, Physical Geography, 82(2-3), 391-409.

Hubbard, A., Lawson, W., Anderson, B., Hubbard, B., & Blatter, H. (2004). Evidence for subglacial ponding across Taylor Glacier, Dry Valleys, Antarctica. Annals of Glaciology, 39, 79-84.

Jeffrey, A. W. A., & Kaplan, I. R. (1988). Hydrocarbons and inorganic gases in the Gravberg-1 well, Siljan Ring, Sweden. Chemical Geology, 71(1-3), 237-255.

Jennings-Mays, S.E., & Wharton, J.R. (1996). McMurdo Dry Valleys Long-Term Ecological Research (LTER): An overview of 1994-1995 research activities. Antarctic Journal of the United States, 30, 275-275.

Karl, D. M., Beversdorf, L., Björkman, K. M., Church, M. J., Martinez, A., & Delong, E. F. (2008). Aerobic production of methane in the sea. Nature Geoscience, 1(7), 473-478.

Karr, E. A., Ng, J. M., Belchik, S. M., Sattley, W. M., Madigan, M. T., & Achenbach, L. A. (2006). Biodiversity of methanogenic and other Archaea in the permanently frozen Lake Fryxell, Antarctica. Applied and Environmental Microbiology, 72(2), 1663-1666.

Kavanaugh, J. L., Cuffey, K. M., Morse, D. L., Bliss, A. K., & Aciego, S. M. (2009). Dynamics and mass balance of Taylor Glacier, Antarctica: 3. State of mass balance. Journal of Geophysical Research: Earth Surface, 114(F4).

Keys, J. R. (1979). Saline discharge at the terminus of Taylor Glacier. Antarctic Journal of the US, 14, 82–85.

Kong, W., Li, W., Romancova, I., Prášil, O., & Morgan-Kiss, R. M. (2014). An integrated study of photochemical function and expression of a key photochemical gene (psbA) in photosynthetic communities of Lake Bonney (McMurdo Dry Valleys, Antarctica). FEMS Microbiology Ecology, 89(2), 293-302.

Kwon, M., Kim, M., Takacs-Vesbach, C., Lee, J., Hong, S. G., Kim, S. J., Priscu, J.C., & Kim, O. S. (2017). Niche specialization of bacteria in permanently ice-covered lakes of the McMurdo Dry Valleys, Antarctica. Environmental microbiology, 19(6), 2258-2271.

Lamarche-Gagnon, G., Wadham, J. L., Sherwood Lollar, B., Arndt, S., Fietzek, P., Beaton, A. D., Tedstone, A.J., Telling, J., Bagshaw, E., Hawkings, J.R., Kohler, T.J., Zarsky, J.D., Moowlem, M.C., Anesio, A.M., & Stibal, M. (2019). Greenland melt drives continuous export of methane from the ice-sheet bed. Nature, 565(7737), 73-77.

Lawrence, J. P., Doran, P. T., Winslow, L. A., & Priscu, J. C. (2020). Subglacial brine flow and wind-induced internal waves in Lake Bonney, Antarctica. Antarctic Science, 32(3), 223-237.

Lawson Knoepfle, J., Doran, P. T., Kenig, F., Lyons, W. B., & Galchenko, V. F. (2009). Particulate organic and dissolved inorganic carbon stable isotopic compositions in Taylor Valley lakes, Antarctica: the effect of legacy. Hydrobiologia, 632, 139-156.

Lee, P. G., Park, C., Moon, C. H., Park, M. O., & Gwon, K. Y. (2001). Biomass and species composition of phytoplankton and zooplankton along the salinity gradients in the Seomjin River Estuary. The Sea: Journal of the Korean Society of Oceanography, 6(2), 93-102.

Lee, P. A., Priscu, J. C., DiTullio, G. R., Riseman, S. F., Tursich, N., & de Mora, S. J. (2004). Elevated levels of dimethylated-sulfur compounds in Lake Bonney, a poorly ventilated Antarctic lake. Limnology and Oceanography, 49(4), 1044-1055.

Levy, J. S., Fountain, A. G., O'Connor, J. E., Welch, K. A., & Lyons, W. B. (2013). Garwood valley, Antarctica: a new record of last glacial maximum to Holocene glaciofluvial processes in the McMurdo dry valleys. Bulletin, 125(9-10), 1484-1502.

Li W., Dore J.E., Steigmeyer, A.J., Cho, Y-J., Kim, O-S., Liu, Y., Morgan-Kiss, R.M., Skidmore, M.L., Priscu, J.C. (2020). Methane production in the oxygenated water column of a perennially ice-covered Antarctic lake. Limnology and Oceanography, 65(1), 143-156.

Li, W., Chiuchiolo, A., Lawrence, J., Takacs-Vesbach, C., Morgan-Kiss, R., & Priscu, J.C. (In Preparation). Flux of particulate organic matter to the sediments of Lak Bonney, a permanently ice-covered Antarctic lake.

Lizotte, M. P., Sharp, T. R., & Priscu, J. C. (1996). Phytoplankton dynamics in the stratified water column of Lake Bonney, Antarctica: I. Biomass and productivity during the winter-spring transition. Polar Biology, 16, 155-162.

Lovley, D. R., & Phillips, E. J. (1987). Competitive mechanisms for inhibition of sulfate reduction and methane production in the zone of ferric iron reduction in sediments. Applied and Environmental Microbiology, 53(11), 2636-2641.

Lyons, W., Fountain, R., Priscu, J. C.,Neumann, K., & Welch, K. A. (2000). Importance of landscape position and legacy: the evolution of the lakes in Taylor Valley, Antarctica. Freshwater Biology, 43(3), 355-367.

Lyons, W. B., Welch, K. A., Priscu, J. C., Laybourn-Parry, J., Moorhead, D., McKnight, D. M., Doran, P.T., & Tranter, M. (2001). The Mcmurdo Dry Valleys Long-Term Ecological Research Program: New understanding of the biogeochemistry of the Dry Valley Lakes: A review. Polar Geography, 25(3), 202-217.

Lyons, W. B., Welch, K. A., Snyder, G., Olesik, J., Graham, E. Y., Marion, G. M., & Poreda, R. J. (2005). Halogen geochemistry of the McMurdo Dry Valleys lakes, Antarctica: clues to the origin of solutes and lake evolution. Geochimica et Cosmochimica Acta, 69(2), 305-323.

Lyons, W. B., Mikucki, J. A., German, L. A., Welch, K. A., Welch, S. A., Gardner, C. B., Tulaczyk, S.M; Pettit, E.C., Kowalski, J., & Dachwald, B. (2019). The geochemistry of englacial brine from Taylor Glacier, Antarctica. Journal of Geophysical Research: Biogeosciences, 124(3), 633-648.

Macdonald, M. L., Wadham, J. L., Telling, J., & Skidmore, M. L. (2018). Glacial erosion liberates lithologic energy sources for microbes and acidity for chemical weathering beneath glaciers and ice sheets. *Frontiers in Earth Science*, *6*, 416476.

McElwain, J. C., Wade-Murphy, J., & Hesselbo, S. P. (2005). Changes in carbon dioxide during an oceanic anoxic event linked to intrusion into Gondwana coals. Nature, 435(7041), 479-482.

McKnight, D. M., Niyogi, D. K., Alger, A. S., Bomblies, A., Conovitz, P. A., & Tate, C. M. (1999). Dry valley streams in Antarctica: ecosystems waiting for water. Bioscience, 49(12), 985-995.

Metcalf, W. W., Griffin, B. M., Cicchillo, R. M., Gao, J., Janga, S. C., Cooke, H. A., Circelloo, B.T., Evans, B.S., Martens-Habbena, W.Stahl, D.A., & Van Der Donk, W. A. (2012). Synthesis of methylphosphonic acid by marine microbes: a source for methane in the aerobic ocean. Science, 337(6098), 1104-1107.

Michaud, A. B., Dore, J. E., Achberger, A. M., Christner, B. C., Mitchell, A. C., Skidmore, M. L., Vick-Majors, T., & Priscu, J. C. (2017). Microbial oxidation as a methane sink beneath the West Antarctic Ice Sheet. Nature Geoscience, 10(8), 582-586.

Mikucki, J. A., Foreman, C. M., Sattler, B., Berry Lyons, W., & Priscu, J. C. (2004). Geomicrobiology of Blood Falls: an iron-rich saline discharge at the terminus of the Taylor Glacier, Antarctica. Aquatic Geochemistry, 10, 199-220.

Mikucki, J. A., & Priscu, J. C. (2007). Bacterial diversity associated with Blood Falls, a subglacial outflow from the Taylor Glacier, Antarctica. Applied and Environmental Microbiology, 73(12), 4029-4039.

Mikucki, J. A., Pearson, A., Johnston, D. T., Turchyn, A. V., Farquhar, J., Schrag, D. P., Anbar, A.D., Priscu, J.C., & Lee, P. A. (2009). A contemporary microbially maintained subglacial ferrous" ocean". Science, 324(5925), 397-400.

Mikucki, J. A., Auken, E., Tulaczyk, S., Virginia, R. A., Schamper, C., Sørensen, K. I., Doran, P.T., Dugan, H., & Foley, N. (2015). Deep groundwater and potential subsurface habitats beneath an Antarctic dry valley. Nature Communications, 6(1), 6831.

Milkov, A. V., & Etiope, G. (2018). Revised genetic diagrams for natural gases based on a global dataset of > 20,000 samples. Organic Geochemistry, 125, 109-120.

Mitterer, R. M. (2010). Methanogenesis and sulfate reduction in marine sediments: A new model. Earth and Planetary Science Letters, 295(3-4), 358-366.

Monaghan, A. J., Bromwich, D. H., Powers, J. G., & Manning, K. W. (2005). The climate of the McMurdo, Antarctica, region as represented by one year of forecasts from the Antarctic Mesoscale Prediction System. Journal of Climate, 18(8), 1174-1189.

Montross, S., Skidmore, M., Christner, B., Samyn, D., Tison, J. L., Lorrain, R., Doyle, S. & Fitzsimons, S. (2014). Debris-rich basal ice as a microbial habitat, Taylor Glacier, Antarctica. Geomicrobiology Journal, 31(1), 76-81.

Murray, A. E., Kenig, F., Fritsen, C. H., McKay, C. P., Cawley, K. M., Edwards, R., Kuhn, E., McKnnight, D.M., Ostrom, N.E., Peng, V., Ponce, A., Priscu, J.C., Samarkin, V., Townsend, A.T., Wagh, P., Young, S.A., Yung, P.T., & Doran, P. T. (2012). Microbial life at− 13 C in the brine of an ice-sealed Antarctic lake. Proceedings of the National Academy of Sciences, 109(50), 20626-20631.

Myers, M. E., Doran, P. T., & Myers, K. F. (2020). Summer valley-floor snowfall in Taylor Valley, Antarctica from 1995–2017. The Cryosphere Discussions, 2020, 1-24.

Myers, K. F., Doran, P. T., Tulaczyk, S. M., Foley, N. T., Bording, T. S., Auken, E., Dugan, H.A., Mikucki, J.A., Foged, N., Grombacher, D. & Virginia, R. A. (2021). Thermal legacy of a large paleolake in Taylor Valley, East Antarctica, as evidenced by an airborne electromagnetic survey. The Cryosphere, 15(8), 3577-3593.

Nesbitt, H. W., Bancroft, G. M., Pratt, A. R., & Scaini, M. J. (1998). Sulfur and iron surface states on fractured pyrite surfaces. American Mineralogist, 83(9-10), 1067-1076.

Nylen, T. H., Fountain, A. G., & Doran, P. T. (2004). Climatology of katabatic winds in the McMurdo dry valleys, southern Victoria Land, Antarctica. Journal of Geophysical Research: Atmospheres, 109(D3).

Obryk, M. K., Doran, P. T., Hicks, J. A., McKay, C. P., & Priscu, J. C. (2016). Modeling the thickness of perennial ice covers on stratified lakes of the Taylor Valley, Antarctica. Journal of Glaciology, 62(235), 825-834.

Offre, P., Spang, A., & Schleper, C. (2013). Archaea in biogeochemical cycles. Annual Review of Microbiology, 67, 437-457.

Oremland, R. S., & Polcin, S. (1982). Methanogenesis and sulfate reduction: competitive and noncompetitive substrates in estuarine sediments. Applied and Environmental Microbiology, 44(6), 1270-1276.

Patriarche, J. D., Priscu, J. C., Takacs-Vesbach, C., Winslow, L., Myers, K. F., Buelow, H., Morgan-Kiss, R.M, & Doran, P. T. (2021). Year-round and long-term phytoplankton dynamics in Lake Bonney, a permanently ice-covered Antarctic lake. Journal of Geophysical Research: Biogeosciences, 126(4), e2020JG005925.

Petit, J. R., Jouzel, J., Raynaud, D., Barkov, N. I., Barnola, J. M., Basile, I., Bender, M., Chappellaz, J., Davis, M., Delaygue, G., Delmotte, M., Kotylakov, V.M., Legrand, M., Lipenkov, V.Y., Lorius, C., Pepin, L., Ritz, C., Saltzman, E., & Stievenard, M. (1999). Climate and atmospheric history of the past 420,000 years from the Vostok ice core, Antarctica. Nature, 399(6735), 429-436.

Pettit, E. C., Whorton, E. N., Waddington, E. D., & Sletten, R. S. (2014). Influence of debris-rich basal ice on flow of a polar glacier. Journal of Glaciology, 60(223), 989-1006.

Poreda, R. J., Hunt, A. G., Lyons, W. B., & Welch, K. A. (2004). The helium isotopic chemistry of Lake Bonney, Taylor Valley, Antarctica: Timing of late Holocene climate change in Antarctica. Aquatic Geochemistry, 10, 353-371.

Powell, R. D. (1981). Sedimentation conditions in Taylor Valley, Antarctica, inferred from textural analysis of DVDP cores. Dry Valley Drilling Project, 33, 331-349.

Potter, J., & Konnerup-Madsen, J. (2003). A review of the occurrence and origin of abiogenic hydrocarbons in igneous rocks. Geological Society, London, Special Publications, 214(1), 151-173.

Priscu, J. 2016. McMurdo Dry Valleys Depths, Areas, Volumes Measured by Jeffrey Schmok ver 5. Environmental Data Initiative. https://doi.org/10.6073/pasta/631a5c32f27e37a8094e2e18e4dec63c (Accessed 2024-05-02).

Šabacká, M., Priscu, J. C., Basagic, H. J., Fountain, A. G., Wall, D. H., Virginia, R. A., & Greenwood, M. C. (2012). Aeolian flux of biotic and abiotic material in Taylor Valley, Antarctica. Geomorphology, 155, 102-111.

Samyn, D., Svensson, A., & Fitzsimons, S. J. (2008). Dynamic implications of discontinuous recrystallization in cold basal ice: Taylor Glacier, Antarctica. *Journal of Geophysical Research: Earth Surface*, *113*(F3).

Saxton, M. A., Samarkin, V. A., Schutte, C. A., Bowles, M. W., Madigan, M. T., Cadieux, S. B., Pratt, L.M., & Joye, S. B. (2016). Biogeochemical and 16S rRNA gene sequence evidence supports a novel mode of anaerobic methanotrophy in permanently ice-covered Lake Fryxell, Antarctica. Limnology and Oceanography, 61(S1), S119-S130.

Saxton, M. A., Samarkin, V. A., Madigan, M. T., Bowles, M. W., Sattley, W. M., Schutte, C. A., & Joye, S. B. (2021). Sulfate reduction and methanogenesis in the hypersaline deep waters and sediments of a perennially ice-covered lake. Limnology and Oceanography, 66(5), 1804-1818.

Sapper, S. E., Jørgensen, C. J., Schroll, M., Keppler, F., & Christiansen, J. R. (2023). Methane emissions from subglacial meltwater of three alpine glaciers in Yukon, Canada. Arctic, Antarctic, and Alpine Research, 55(1), 2284456.

Schönheit, P., Kristjansson, J. K., & Thauer, R. K. (1982). Kinetic mechanism for the ability of sulfate reducers to out-compete methanogens for acetate. Archives of Microbiology, 132, 285-288.

Siegert, M. J. (2008). Antarctic subglacial topography and ice-sheet evolution. Earth Surface Processes and Landforms: The Journal of the British Geomorphological Research Group, 33(4), 646-660.

Skidmore, M. L., Foght, J. M., & Sharp, M. J. (2000). Microbial life beneath a high Arctic glacier. Applied and Environmental Microbiology, 66(8), 3214-3220.

Smith, R. L., Miller, L. G., & Howes, B. L. (1993). The geochemistry of methane in Lake Fryxell, an amictic, permanently ice-covered, Antarctic lake. Biogeochemistry, 21, 95-115.

Spigel, R. H., & Priscu, J. C. (1996). Evolution of temperature and salt structure of Lake Bonney, a chemically stratified Antarctic lake. Hydrobiologia, 321, 177-190.

Spigel, R. H., & Priscu, J. C. (1998). Physical limnology of the McMurdo Dry Valleys lakes. Ecosystem Dynamics in Polar Desert: the McMurdo Dry Valleys, Antarctica, 72, 153-187.

Spigel, R. H., Priscu, J. C., Obryk, M. K., Stone, W., & Doran, P. T. (2018). The physical limnology of a permanently ice-covered and chemically stratified Antarctic lake using high resolution spatial data from an autonomous underwater vehicle. Limnology and Oceanography, 63(3), 1234-1252.

Steig, E. J., Morse, D. L., Waddington, E. D., Stuiver, M., Grootes, P. M., Mayewski, P. A., Twickler, M.S., & Whitlow, S. I. (2000). Wisconsinan and Holocene climate history from an ice core at Taylor Dome, western Ross Embayment, Antarctica. Geografiska Annaler: Series A, Physical Geography, 82(2-3), 213-235.

Stibal, M., Wadham, J. L., Lis, G. P., Telling, J., Pancost, R. D., Dubnick, A., Sharp, M., Lawson, E., Butler, C., Hasan, F., Tranter, M., & Anesio, A. M. (2012). Methanogenic potential of Arctic and Antarctic subglacial environments with contrasting organic carbon sources. Global Change Biology, 18(11), 3332-3345.

Sugden, D. E., Denton, G. H., & Marchant, D. R. (1995). Landscape evolution of the Dry Valleys, Transantarctic Mountains: tectonic implications. Journal of Geophysical Research: Solid Earth, 100(B6), 9949-9967.

Swanger, K. M., Marchant, D. R., Kowalewski, D. E., & Head III, J. W. (2010). Viscous flow lobes in central Taylor Valley, Antarctica: origin as remnant buried glacial ice. Geomorphology, 120(3-4), 174-185.

Tamppari, L. K., Anderson, R. M., Archer, P. D., Douglas, S., Kounaves, S. P., McKay, C. P., Ming, D.W., Moore, Q., Quinn, J.E., Smith, P.H., Stroble, S., & Zent, A. P. (2012). Effects of extreme cold and aridity on soils and habitability: McMurdo Dry Valleys as an analogue for the Mars Phoenix landing site. Antarctic Science, 24(3), 211-228.

Tang, C., Madigan, M. T., & Lanoil, B. (2013). Bacterial and archaeal diversity in sediments of west Lake Bonney, McMurdo Dry Valleys, Antarctica. Applied and Environmental Microbiology, 79(3), 1034-1038.

Vick-Majors, T. J., Priscu, J. C., & Amaral-Zettler, L. A. (2014). Modular community structure suggests metabolic plasticity during the transition to polar night in ice-covered Antarctic lakes. The ISME Journal, 8(4), 778-789.

Wadham, J. L., Arndt, S., Tulaczyk, S., Stibal, M., Tranter, M., Telling, J., Lis, G.P., Lawson, E., Ridgwell, A., Dubnick, A., Sharp, M.J., Anesio, A.M., & Butler, C. E. H. (2012). Potential methane reservoirs beneath Antarctica. Nature, 488(7413), 633-637.

Waldron, P. J., Petsch, S. T., Martini, A. M., & Nüsslein, K. (2007). Salinity constraints on subsurface archaeal diversity and methanogenesis in sedimentary rock rich in organic matter. Applied and Environmental Microbiology, 73(13), 4171-4179.

Wang, Q., Dore, J. E., & McDermott, T. R. (2017). Methylphosphonate metabolism by Pseudomonas sp. populations contributes to the methane oversaturation paradox in an oxic freshwater lake. Environmental Microbiology, 19(6), 2366-2378.

Ward, B. B., Granger, J., Maldonado, M. T., & Wells, M. L. (2003). What limits bacterial production in the suboxic region of permanently ice-covered Lake Bonney, Antarctica?. Aquatic Microbial Ecology, 31(1), 33-47.

Warrier, R. B., Castro, M. C., Hall, C. M., Kenig, F., & Doran, P. T. (2015). Reconstructing the evolution of Lake Bonney, Antarctica using dissolved noble gases. Applied Geochemistry, 58, 46-61.

Welch, K. A., Lyons, W. B., Whisner, C., Gardner, C. B., Gooseff, M. N., McKnight, D. M., & Priscu, J. C. (2010). Spatial variations in the geochemistry of glacial meltwater streams in the Taylor Valley, Antarctica. Antarctic Science, 22(6), 662-672.

Winslow, L. A., Dugan, H. A., Buelow, H. N., Cronin, K. D., Priscu, J. C., Takacs-Vesbach, C., & Doran, P. T. (2014). Autonomous year-round sampling and sensing to explore the physical and biological habitability of permanently ice-covered Antarctic lakes. Marine Technology Society Journal, 48(5), 8-17.

You, K., & Flemings, P. B. (2018). Methane hydrate formation in thick sandstones by free gas flow. Journal of Geophysical Research: Solid Earth, 123(6), 4582-4600.

CHAPTER THREE

ABIOTIC METHANE SOURCES IN A PERENNIALLY ICE-COVERED ANTARCTIC LAKE

Introduction

Methane is derived from microbial, thermogenic, and abiogenic sources. Most of the methane in Earth's atmosphere is of biotic origin, which includes contemporary bacterial activity, the release of relict methane from ancient microbial activity, and the thermal degradation of fossilized organic matter (kerogen) in rock and sediments (e.g. Whiticar, 1999; Etiope et al., 2011; Tazaz et al., 2013, Milkov and Etiope, 2018). Abiogenic methane is produced through inorganic reactions including those during volcanic activity, water-rock interactions, and serpentinization (Etiope et al., 2011; Tazaz et al., 2013). The source of observed methane can be inferred by measuring the stable isotopic composition of the constituent elements of the gas, with the intersection of $\delta^{13}C\text{-}CH_4$ and $\delta^{2}H\text{-}CH_4$ values typically used as the indicator for the likely source. Microbially-produced methane is generally more enriched in ^{12}C, leading to more negative $\delta^{13}C\text{-}CH_4$ values (-100 ‰ to -50‰) compared to thermogenic or abiogenic methane (> -50‰) (Whiticar, 1999). These isotopic boundaries, however, are not rigid. Recent studies have expanded the range of both potential abiotic and biotic methane sources (e.g. Milkov and Etiope, 2018).

Contemporary discoveries of previously unknown methanogenic processes, as well as observations of methanogenesis under variable environmental conditions, have expanded our understanding of methane formation and the relationship between methane isotopic composition

and its origin (e.g. Penger et al., 2012; Tazaz et al., 2013; Milkov and Etiope, 2018). Methanogens were long considered to be obligate anaerobes, conducting the final step in a series of dissimilatory reactions to break down organic compounds (Garcia, 1990; Whiticar, 1999). Methanogenesis using methylated compounds in oxic environments, however, is now known to be active in marine and freshwater systems (e.g. Repeta et al., 2016; Sosa et al., 2017; Wang et al., 2017; Li et al., 2020; Wang et al., 2021). Fermentation produces methane with an isotopic signature in a distinct range within the larger isotopic boundaries of biogenic methane (e.g. Penger et al., 2012; Milkov and Etiope, 2018). Recent work has shown abiotic methane in petroleum systems with $\delta^{13}C\text{-}CH_4$ values as low as -75‰, well within the range previously considered to be indicative of microbial methane (Milkov and Etiope; 2018). Conversely, Tazaz et al. (2013) measured biogenic methane produced from algal mat samples in a high salinity environment with $\delta^{13}C\text{-}CH_4$ values as high as -35‰, values that would traditionally be considered an abiotic isotopic signature. The initial methods for determining methane sources, as well as the range of potential sources in natural systems (Schoell, 1980; Whiticar, 1999) have been revised and expanded significantly in the last 20 years following closer examination of unique biogeochemical settings (e.g. Etiope and Sherwood-Lollar, 2013; Milkov and Etiope, 2018).

The presence and cycling of methane have been researched extensively in cold environments such as permafrost (e.g. Sebacher et al., 1986; Rivkina et al., 2007), and deep-sea marine sediments (e.g. Cragg et al., 1990; Newberry et al., 2004), but only in the last couple decades have perennially ice-covered aqueous systems been investigated as potential methane reservoirs (e.g. Wadham et al., 2008; Boyd et al., 2010; Stibal et al., 2012). Genetic and

geochemical evidence suggest the presence of active methanogenesis beneath glaciers, ice sheets, and cold lakes in alpine and polar regions (Coolen et al., 2004; Boyd et al., 2010; Stibal et al., 2012; Dieser et al., 2014; Burns et al., 2018). Perennially ice-covered Lakes Fryxell, Hoare, and Bonney in the McMurdo Dry Valleys of Antarctica have methane present in their water columns, but while in the former two there is evidence for active methanogenesis (Karr et al., 2006; Lawson et al., 2009; Saxton et al., 2016), Lake Bonney shows no evidence for this at depths of peak methane concentrations (Tang et al., 2013; Tang et al., 2017; Li et al., 2020). Therefore, abiotic source(s) of methane in Lake Bonney are logical alternatives. These sources/abiotic processes have not previously been investigated, but likely depend on a combination of glaciologic, hydrologic and local geochemical processes, including the availability of organic compounds.

Methane Sources in Lake Bonney, East Antarctica

The water column of Lake Bonney (LB), McMurdo Dry Valleys, East Antarctica contains methane concentrations that are supersaturated relative to the atmosphere. Lake Bonney consists of two ~40m-deep lobes separated by a contraction and bedrock sill (Fig. 3.1).

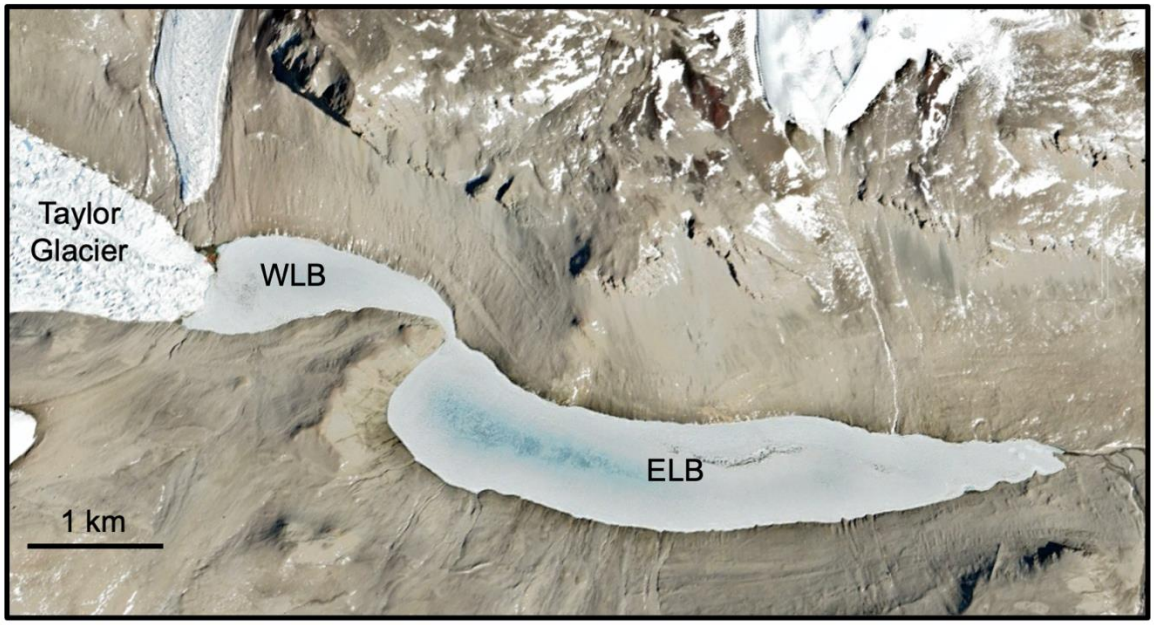


Fig. 3.1 Map of the Lake Bonney basin and Taylor Glacier. “WLB” = West Lake Bonney. “ELB” = East Lake Bonney.

The methane concentration peaks occur in West Lake Bonney (WLB) at 25m and in East Lake Bonney (ELB) at 22m (Fig. 3.2).

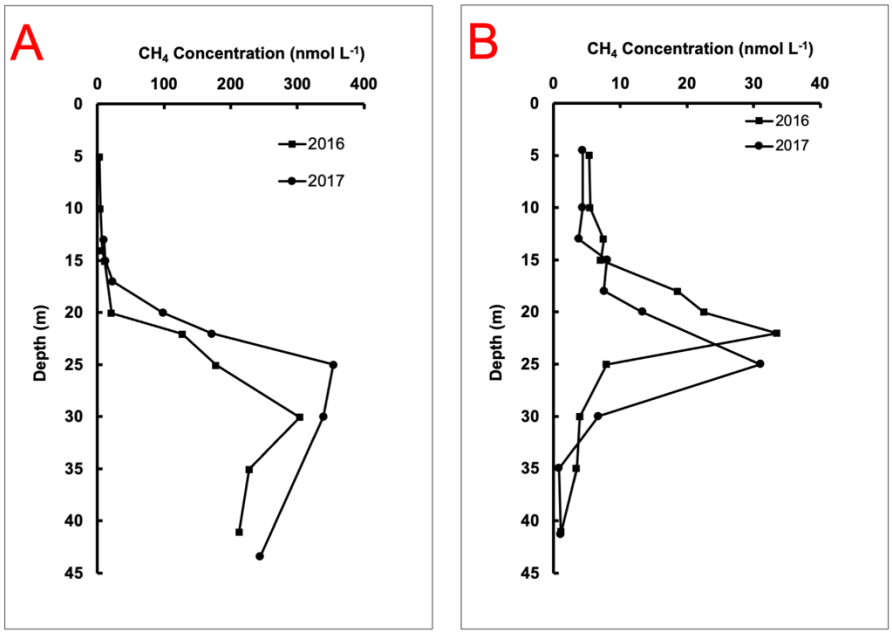


Fig. 3.2 Methane concentration profiles for (A) West Lake Bonney and (B) East Lake Bonney. Data from Li et al. (2020).

Aerobic methanogenesis is likely a major source of the methane in the oxygenated surface waters from 12 to 20m, however, the highest concentrations of methane occur below 20m where the waters are sub-oxic to anoxic (Li et al., 2020), hypersaline and cold (-2 to -4ºC) (Lawrence et al., 2020), which could suggest microbial methanogenesis. However, no evidence for biological methanogenesis has been found in these sub-oxic bottom waters despite sampling and multiple analyses for this metabolic process (Glatz et al., 2006; Tang et al., 2013; Kwon et al., 2017; Li et al., 2020). Therefore, an abiotic source for the methane below the chemocline in WLB seems most likely.

The peak methane concentration in WLB at ~25m depth occurs just below the inflow of brine from Taylor Glacier (TG) (Spigel et al., 2018; Li et al., 2020), suggesting that this brine input could be a potential methane source either directly, or through chemical reactions as the brine input and associated fine grained sediment mixes with lake water, generating methane. The

melting of TG basal ice across the glacier/lake water interface likely supplies fine grained sediments to WLB. TG subglacial sediments contain Fe-minerals schwertmannite, ferrihydrite, and goethite (Raiswell et al., 2009). Concentrations of dimethyl sulfide (DMS) and dimethyl sulfoxide (DMSO) in LB are among the highest recorded in a natural system (Lee et al., 2004). Ferrihydrite and goethite have been shown to catalyze a reaction that leads to methane production through the oxidation of the organosulfur compounds DMS and DMSO in laboratory studies under aerobic (21% O_2), ambient conditions (1,000 mbar and 22°C) (Althoff et al., 2014). Therefore, it is possible that these organosulfur compound-mineral reactions are generating methane in WLB.

The objective of this study was to investigate potential sources of methane in the water column of Lake Bonney below the chemocline. The research had two components; 1) measurement of the concentration and isotopic composition of the water column methane at four locations across Lake Bonney (Fig. 1) and 2) laboratory experiments using the natural source materials: sediment rich basal ice from TG and water from the lake to determine the magnitude and isotopic composition of methane produced from abiotic processes using these materials.

Methods

Field Site

The McMurdo Dry Valleys (MDVs) are a polar desert in East Antarctica that comprise the largest ice-free region on the continent (Levy et al., 2013; Cross et al., 2022). Most surfaces in the valleys consist of sandy, gravely soils and bedrock outcrops, but the valley sides and floor contain glaciers and perennially ice-covered, closed-basin lakes (Lawrence et al., 2020; Cross et al., 2022). Taylor Valley, the southernmost of the MDVs, has been a study site for the McMurdo

Dry Valleys Long-Term Ecological Research (MCM LTER) program since 1993 and thus has an array of data available for the valley and lake systems.

Lake Bonney, the westernmost lake in Taylor Valley, is perennially ice-covered and consists of two steep-sided basins: West Lake Bonney (WLB) and East Lake Bonney (ELB). A contraction and a sill at a depth of about 16m separates the basins (Spigel and Priscu, 1998; Lyons et al., 2000; Fig. 3.1). The ice layer is 3-4m thick, but surface ice around the lake periphery melts during the austral summer, allowing for some gas exchange with the atmosphere and inflow from subaerial streams (Welch et al., 2010). Sunlight penetration during the summer months allows for photosynthetic activity (Kong et al., 2014) and the waters are oxygenated down to about 20m in WLB and 25m in ELB (Li et al., 2020; Fig. 3.3).

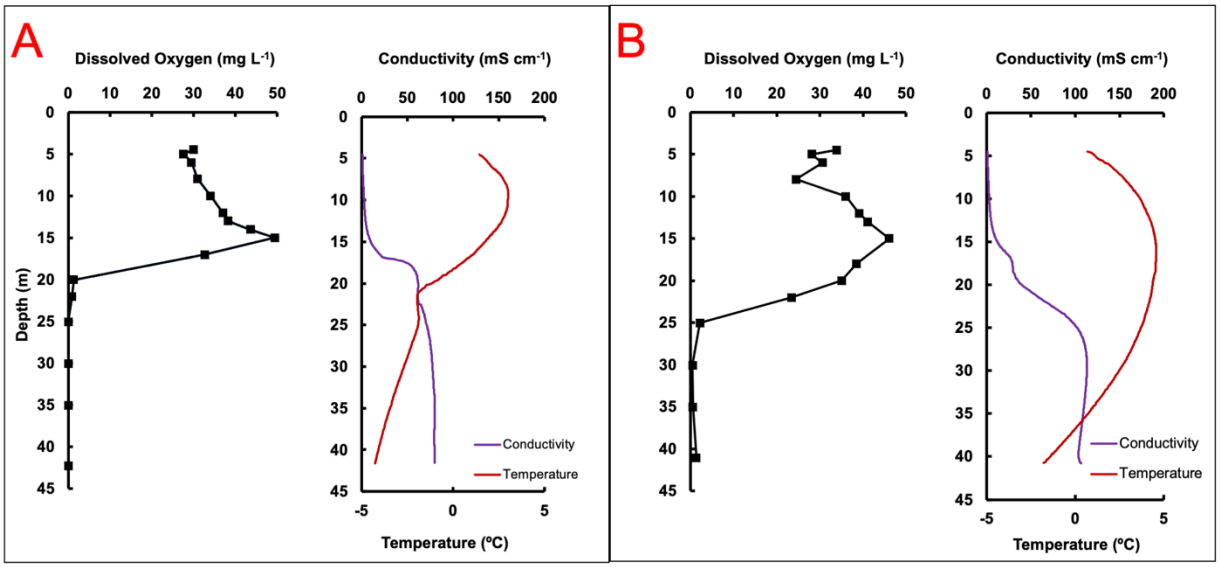


Fig. 3.3 Dissolved oxygen, conductivity, and temperature profiles for (A) West Lake Bonney and (B) East Lake Bonney. Measurements conducted by the MCM LTER project at Locations B and D (Fig. 1) in 2017 (Priscu, 2023). Conductivity and temperature were measured with a SBE 25 Sealogger CTD probe. Dissolved oxygen was determined on discrete samples using a Winkler Titration (limit of detection = 0.09 mg O_2 L^{-1}).

The water column in WLB is increasingly saline with depth, with the deepest waters having a conductivity of ~80 mS cm^{-1} and a salinity 3 times higher than seawater at ~120 g salt kg $solution^{-1}$ (Spigel and Priscu, 1996, Li et al., 2020; Fig. 3.3). ELB is more saline than WLB, with conductivity values more than 100 mS cm^{-1} and a salinity of ~160 g salt kg $solution^{-1}$ near the sediment-water (brine) interface (Spigel and Priscu, 1996; Fig. 3.3). The increasing salinity with depth creates a chemocline around 17m in WLB and 20m in ELB, resulting in highly stratified water columns that have remained stable for decades (Spigel and Priscu, 1998; Lawrence et al., 2020; Fig. 3.4).

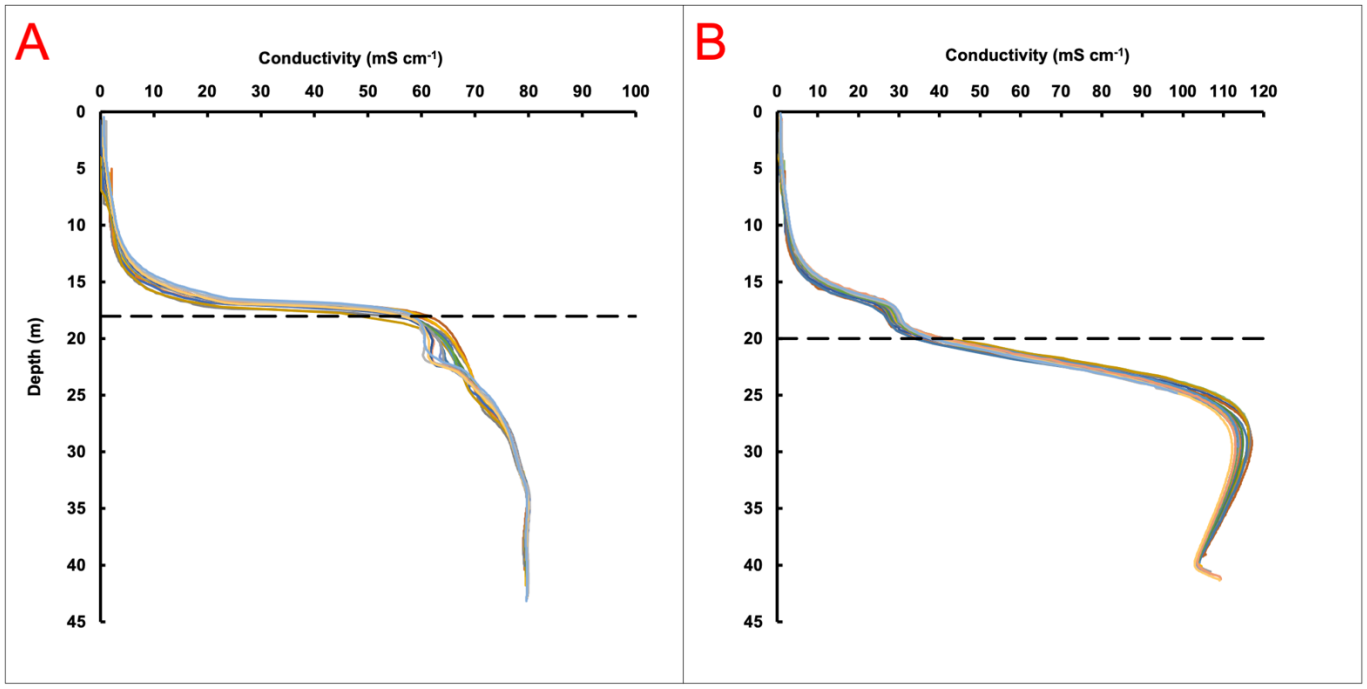


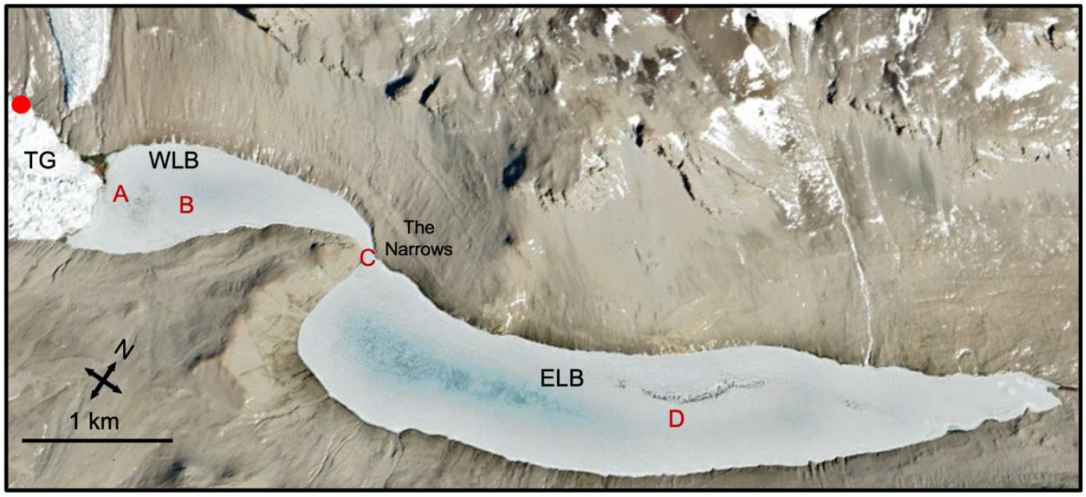
Fig. 3.4 Annual conductivity profile data from 1998-2922 for (A) West Lake Bonney water column and (B) East Lake Bonney water column. Dotted line indicates the depth of the chemocline in each lobe. Profile data are from November each year: 1998-2022 (Priscu, 2023).

Water generally flows from the west lobe to the east lobe, although there is evidence of hydrologic transport above the chemocline in both directions across the sill (Doran et al., 2014). There is no outflow from the lake basin, with most water lost through ice ablation and evaporation from peripheral moats during the melt season (Dugan et al., 2013). Subglacial inflow from Taylor Glacier (TG) enters WLB at a depth of ~21m, as evidenced by anomalies in the annual conductivity and temperature profiles at that depth (Fig. 3.3A, Fig. 3.4A), which do not occur in the ELB conductivity profiles below the chemocline (an increase in conductivity occurs ~16m in ELB, due to WLB water flows across the sill (3.3B, Fig. 3.4B). Additional subglacial inflow from Blood Falls (an iron-rich brine beneath TG) at the western end of the lake (Spigel and Priscu, 1998: Spigel et al., 2018) enters WLB above the chemocline. Seasonal glacial

meltwater streams flowing into the lake's peripheral moats provide the bulk of fluvial inputs to WLB annually (Lyons et al., 2005; Welch et al., 2010; Lawrence et al., 2020).

Sample Collection

Water samples were collected from a depth profile of the WLB water column in four locations (A through D) to determine methane concentration and its isotopic composition. (Fig. 3.5).



Location	Methane Concentration	Methane Isotopes	Conductivity and Temperature	Dissolved Oxygen	DMS and DMSO
A	X	X			
B	X	X	X	X	X
C	X	X			
D	X	X	X		X

Fig. 3.5 (TOP) Sampling sites at Lake Bonney, Taylor Valley, East Antarctica. Red letters indicate borehole locations for lake water sampling. Red dot indicates location of Taylor Glacier basal ice sampling (Montross et al., 2014). TG = Taylor Glacier. WLB = West Lake Bonney. ELB = East Lake Bonney. "The Narrows" is the contraction and bedrock sill that divides the two lobes. (BOTTOM) Table of analytes determined at each sampling location. Conductivity, temperature, and dissolved oxygen are determined annually by the McMurdo Dry Valleys Long Term Environmental Research (MCM LTER) project at Locations B and D (https://mcm.lternet.edu/limnological-data). Concentration profiles for dimethyl sulfide (DMS) and dimethyl sulfoxide (DMSO) were measured by Lee et al. (2004).

Location A was also a sampling site for the autonomous underwater vehicle *Endurance* in 2009 (Spigel et al., 2018: Fig. 2, Site "E3"). It was inferred by Spigel et al. (2018) to be an area of the water column impacted by subglacial outflow, so it was selected for sampling in 2017 as a near-glacier site. Samples at Location B and D were collected in 2016 and 2017 by the MCM LTER Limnological Survey Team at their perennial sampling locations (-77.72007, 162.29724 for WLB; -77.713335, 162.4474 for ELB) in conjunction with their ongoing sampling and measurement campaign for the MCM LTER at a range of sample depths. Location C is the ~16m deep water column over the bedrock sill dividing the two lobes, referred to as "The Narrows." Water sampling depth(s) for methane at Locations B and D corresponded with the annual sampling depths for the MCM LTER and previous sampling depths for methane measurements in 2016. Only 5 depths were sampled at Location A: 6, 10, 15, 24m, and 30m. Location C was sampled for methane at four depths from just below the ice to just above the sill at ~16m.

All water samples were collected through ~35cm diameter boreholes in the lake ice cover using a 5L Niskin bottle (General Oceanics). Two 200ml samples from each depth were transferred through a teflon hose to autoclaved serum vials, which were overflowed, fixed by addition of 2ml of 10N NaOH, and then sealed without headspace. These samples were used for analysis of methane concentration (as reported in Li et al., 2020) and methane stable isotope composition ($\delta^{13}C–CH_4$) for the 2016 samples and ($\delta^{2}H$- and $\delta^{13}C–CH_4$) for the 2017 samples. The ratio of methane to ethane was also determined for the 2017 WLB lake water samples from 20m, 25m, 30m, and 35m, using gas chromatography.

Additional 200ml samples were collected at 20m and 25m in 2017 but with no addition of NaOH. These unamended water samples were used in the TG sediment addition experiments

described below. All samples were stored at 4ºC in the dark from when they were collected, through shipping, and during storage at Montana State University (MSU). At MSU, a 20ml headspace was added to each bottle using ultra-high purity (UHP) N_2 gas, then shaken to equilibrate headspace and liquid gas concentrations (as described in Li et al., 2020).

Basal ice blocks were collected from a tunnel into Taylor Glacier approximately 1.5 km upvalley from the glacier terminus in 2007 (Montross et al., 2014; Fig. 3.5). The basal ice was transported and stored at -20℃.

Water Column Methane Isotopic Analyses

The $\delta^{13}C$-CH_4 values for 2016 and 2017 lake waters were determined using a Picarro G2201-*i* cavity ring-down spectrometer (CRDS) fitted with a Picarro Small Sample Introduction Module 2 (SSIM2). Each vial containing lake water was pressurized with 20ml of ultra-high purity N_2 gas, then 20ml of the headspace was extracted via gas-tight syringe and injected into the SSIM2. The factory calibration of the CRDS was used and a tank of compressed ambient air was used as reference sample between injections to detect any instrument drift. The $\delta^{2}H$-CH_4 values for the 2017 lake water samples were determined by the University of California - Davis Stable Isotope Facility following the methods in Yarnes (2013).

Concentration and Isotopic Composition of Methane
Released from TG Basal Ice

The block of TG basal ice selected for the experiments was from the base of the 4m sequence (380-400cm) sampled in a vertical shaft at the end of a 15m tunnel cut into the glacier in 2007, (Fig. 3.5; Montross et al, 2014). The basal ice cryofacies description following Hubbard et al., (2009) is solid; comprising 0.1 – 5 m thick layers of frozen debris of no preferred texture,

sediment concentrations of > 1000g/L and containing low concentrations of bubbles of no preferred size. The ice block was approximately 22 x 22 x 15cm and weighed 3.6kg.

The approximately 7,200 cm^3 block of sediment-rich basal ice was sealed in a large gas-tight chamber (typically used for maintaining media plates under anaerobic conditions) in a -10°C freezer. The gas-tight chamber was then flushed with Ultra-High Purity (UHP) N_2 gas. The chamber was then moved to a room temperature environment and the block was allowed to melt completely. A sample of the chamber headspace was taken to measure the methane released from the melted basal ice, as follows: 10ml of UHP N_2 was added to the chamber using a gas-tight syringe and then a 10ml sample was extracted and its methane concentration analyzed using an SRI 8610C Gas Chromatograph, following Li et al., (2020).

The melted ice sample consisted of a sediment-rich slurry contained within the gas tight chamber. The chamber was transferred to a glovebox flushed with UHP N_2. Subsamples of wet sediment were taken for-a series of low temperature laboratory experiments as follows: sediment comminution (90g), reaction with DMS/DMSO (50g), and reaction with WLB water samples (20g) described below.

Glacial Sediment Comminution Simulation

The TG basal ice sediments were crushed in the laboratory under an inert headspace to simulate glacial comminution and quantify the amount and isotopic composition of methane that could be released per gram of sediment. The wet TG sediment was dried at 130°C for 48h. Approximately 30g of dried sediment was added to a gas-tight tungsten carbide milling bowl with four grinding balls and the headspace was purged with UHP N_2. The sediment was milled using a Fritsch Pulverisette 6 ball mill at 450 rpm for 10 min to simulate glacial

grinding/crushing. The milling bowl was then pressurized with 25ml UHP N_2 and a 25ml sample of the headspace was extracted for measurement of its methane concentration and isotopic composition ($\delta^{13}C$-CH_4 and $\delta^{2}H$-CH_4).

Grain size analysis of the un-crushed TG sediments was conducted using a 5g subsample of the dried TG sediment. The dried sediment was sieved to remove the >2mm size fraction, then 1g of the sieved portion was added to 30ml of 3.5g L^{-1} sodium hexametaphosphate in a 50ml plastic centrifuge tube, which then was placed on a shaker table for 2h. The grain size distribution of the resulting slurry was analyzed using a Malvern Mastersizer 3000 following Sperazza et al. (2004).

Experiments with TG Sediments and WLB Natural Waters and Organosulfur Compounds

A series of laboratory experiments were initiated to evaluate methane production when TG dried and milled sediments (< 63µm) were added to (i) WLB lake waters from 20m and 25m depth and (ii) DMS and DMSO solutions with concentrations similar to those measured in WLB (Lee et al., 2004) The carbon isotopic composition of the methane ($\delta^{13}C$-CH_4) produced in the experiments with WLB waters was measured as described above. No measurements of $\delta^{2}H$-CH_4 were made.

To evaluate methane production from the interaction of WLB water and TG sediments, triplicate vials were prepared for each WLB water depth (20m and 25m) and for 0.2µm-filtered ultrapure water controls. Water samples were collected as described in Li et al., 2020. Samples were stored upside down in gas-tight 200ml serum vials, then uncapped in a glove box containing UHP N_2 gas to decant the sample into 30ml serum vials. Five grams of dried and milled TG sediment was added to 28 mL of WLB water or 0.2µm-filtered ultrapure water (18.2

MΩ cm^{-1}), in the glove box and capped under a UHP N_2 headspace. All vials were incubated at 5˚C for 72h in the dark. Headspace gases were sampled from two replicate vials for each lake water depth (20m and 25m). The CH_4 concentration was determined at 0, 12, 24, and 72h for each vial, with an HP 5890 gas chromatograph (Hewlett Packard, CA) equipped with a flame ionization detector and 1ml sampling loop as described in Li et al. (2020). The methane to ethane ratio in the headspace of the 20m + TG sediment incubation and 25m + TG sediment incubation was determined 4.5 years after the experiment was initiated using gas chromatography (following Michaud et al., 2017). Ethane produced in the WLB water plus TG sediment incubations was also determined following Michaud et al. (2017) and Li et al. (2020). Additional peaks for C2 hydrocarbons were integrated: C2H4 at 4.92 min and C2H6 at 6.40 min. The standard used for C2 hydrocarbons was a Scotty certified calibration mixture: "Carbon monoxide, carbon dioxide, methane, ethane, ethylene & acetylene each at 1% in nitrogen." The solubility of C_2H_4 and C_2H_6 were assumed to be 3.36 and 1.29 times that of CH_4 in the brine, respectively, as are their approximate proportions in pure water (Sander, 2015)

To evaluate methane production from the interaction of organosulfur compounds and TG sediments, 5g of milled TG sediments were aliquoted into 28 ml autoclaved serum vials. The vials were capped with chlorobutyl stoppers and the headspace in each vial was purged with 0.2 µm filtered UHP N_2 gas. 20 ml of either DMS, DMSO (200 nM in 0.2µm-filtered ultrapure water) or filtered ultrapure water (the control) was added. Each treatment was conducted in triplicate. The vials were incubated at 5˚C upside down for 48h in the dark. Methane concentration was measured at the end of the experiment at 48h as described above.

Results

The water depth values for all relevant figures have been referenced to the 2017 lake level (in meters above sea level) to account for lake level rise over the past two decades (Doran and Gooseff, 2022; Fig. 3.6).

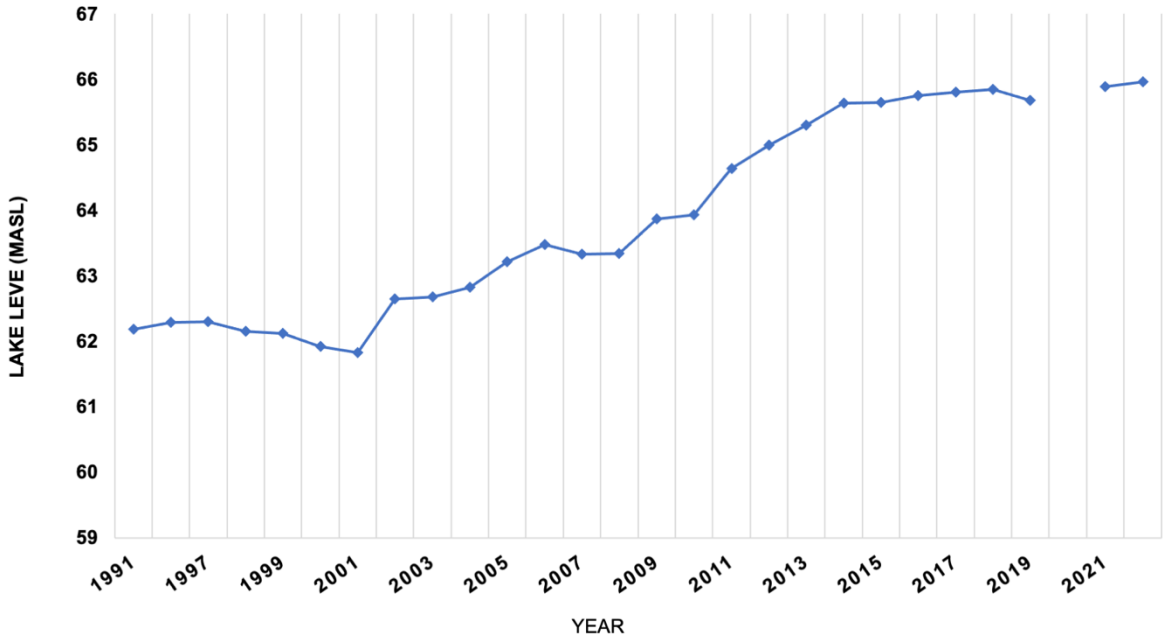


Fig. 3.6 Annual Lake Bonney water column height from 1991-2022 measured in meters above sea level (MASL). Measurements conducted by the MCM LTER (Doran and Gooseff, 2023).

CH_4 Concentration and Isotope Profiles in WLB and ELB

A 2017 methane concentration profile comparison for sampling locations A-D (Fig. 3.5) across the lake is shown in Fig. 3.7. Depth profiles of methane concentration and isotopic composition are presented in Fig. 3.8 for WLB and Fig. 3.9 for ELB (Locations B and D, respectively, in Fig. 3.7). The methane concentration at 25m for Location B was higher than at Location A, closer to Taylor Glacier. Overall, the methane concentrations below the chemocline

in WLB at Locations A and B were an order of magnitude higher than those measured in The Narrows and below the chemocline in ELB.

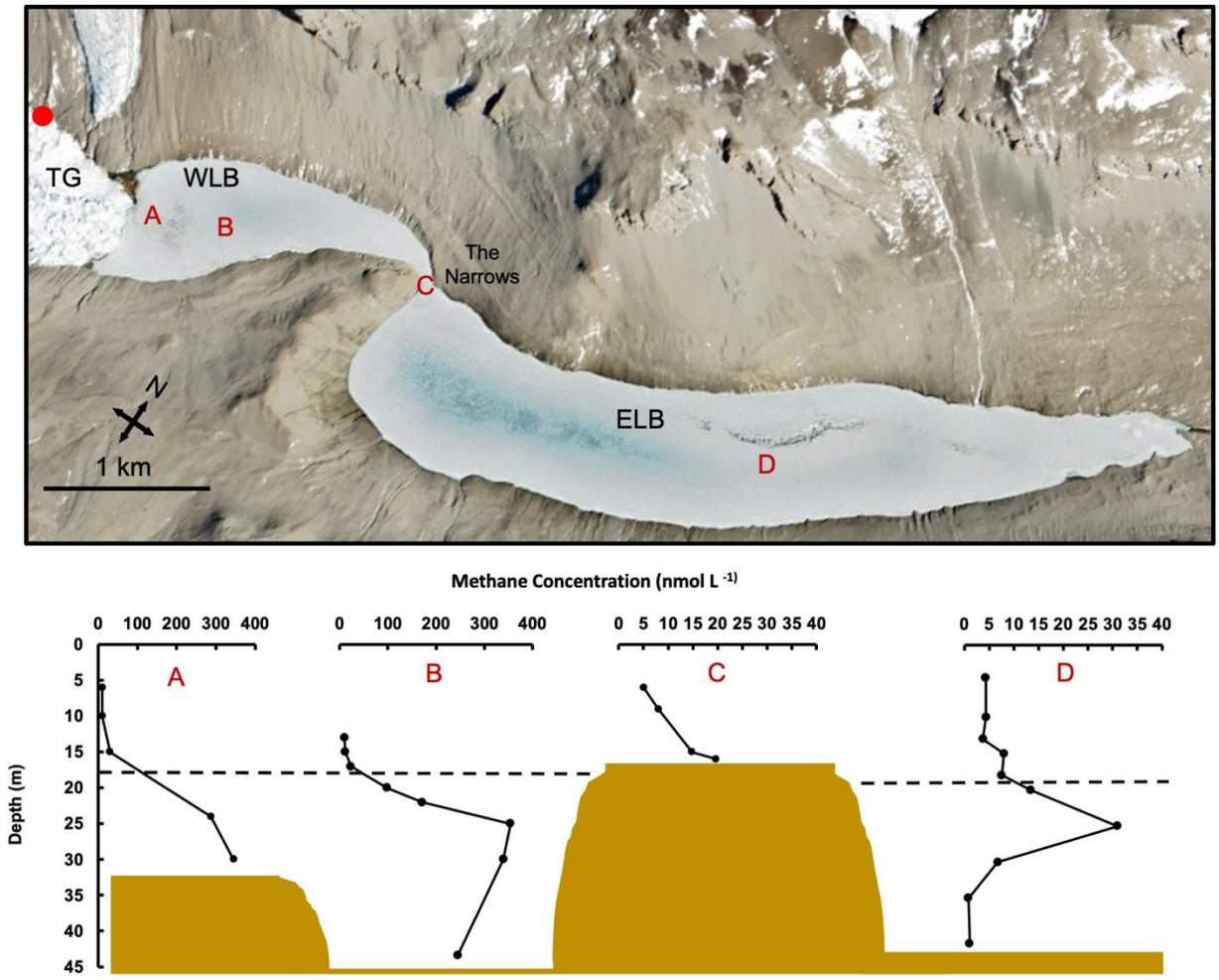


Fig. 3.7 (TOP) Lake water sampling locations at Lake Bonney. (BOTTOM) Methane concentration profiles at each sampling location in 2017. Methane concentrations determined with a gas chromatograph (limit of detection = 3nM). Note the order of magnitude change in methane concentration for the x-axis between locations A/B and locations C/D. Brown shapes indicate the lake bottom depth at each sampling location but do not represent precise bathymetry.

The concentrations and isotopic values for the methane at select depths for Locations A through D are presented in Table 3.1. The $\delta^{13}C\text{-}CH_4$ value measured in 2017 at 24m, around the methane concentration peak in WLB, Location A, was -31.0 ± 1.9 ‰ (Table 3.1). This is similar

to the δ^{13}C-CH_4 values measured at Location B, which were -29.8 ± 2.7 and -27.5 ± 2.8 at 20m and 25m, respectively (Fig. 3.8, Table 3.1).

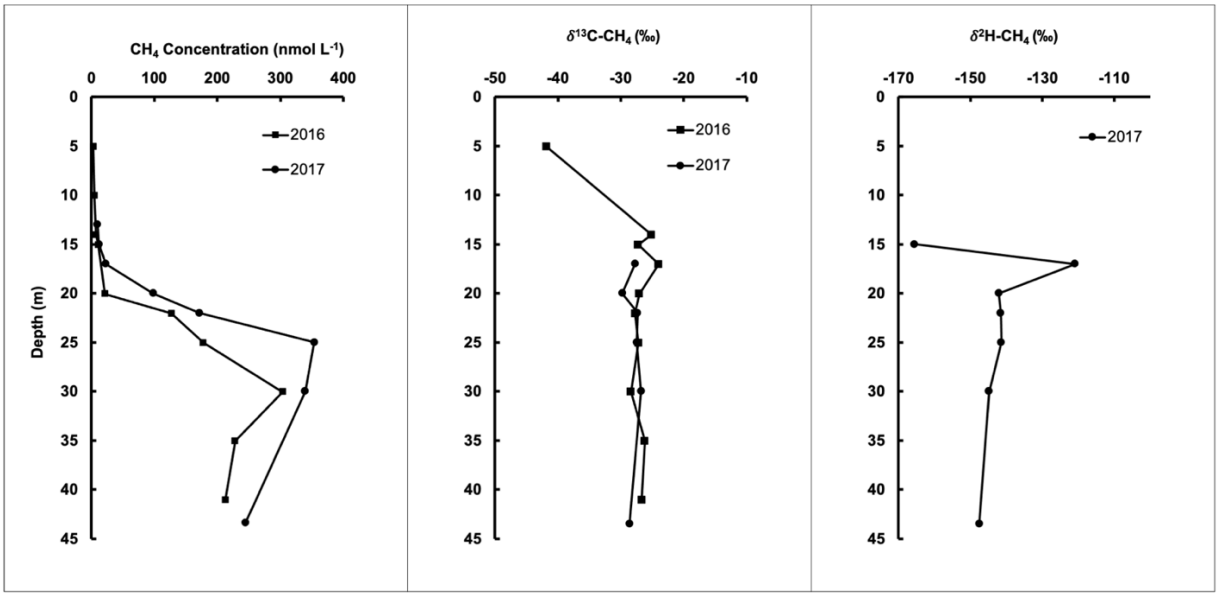


Fig. 3.8 Methane concentration, δ^{13}C–CH_4 and δ^{2}H-CH_4 values in depth profiles for West Lake Bonney at Location B (Fig. 3.5). Methane concentrations determined with a gas chromatograph (limit of detection = 3nM). Gas isotope values measured with a Cavity Ring-Down Spectrometer.

The δ^{13}C-CH_4 values measured in ELB in 2017 were also similar to the methane at Locations A and B in WLB: -29.3 ± 1.9 ‰ and -29.6 ± 3.2 ‰ (Fig. 3.9, Table 3.1).

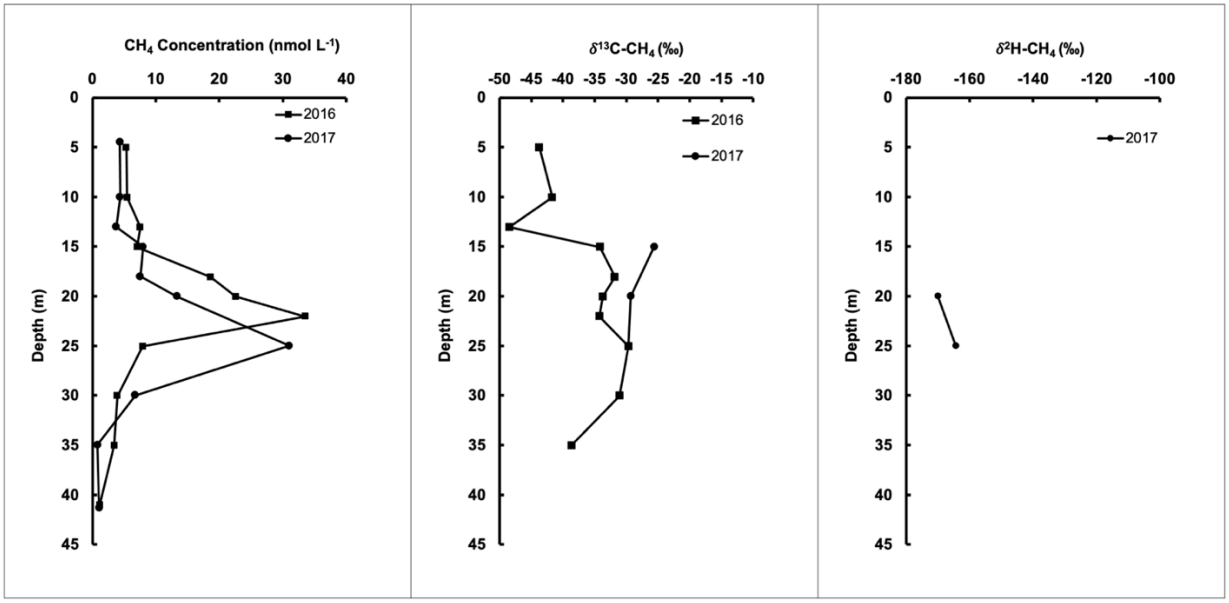


Fig. 3.9 Methane concentration, $\delta^{13}C–CH_4$ and $\delta^{2}H\text{-}CH_4$ values in depth profiles for East Lake Bonney at Location D (Fig. 3.5). Methane concentrations determined with a gas chromatograph (limit of detection = 3nM). Gas isotope values measured with a Cavity Ring-Down Spectrometer.

The $\delta^{2}H\text{-}CH_4$ value measured at 24m for Location A was -141.0 ± 0.1, which was similar to $\delta^{2}H\text{-}CH_4$ values at Location B, which were -142.2 ± 0.1 and -141.5 ± 0.1 for 20 and 25m, respectively. The methane at Location D in ELB had different $\delta^{2}H\text{-}CH_4$ signatures relative to the same depths in WLB, of -169.9 ± 0.1 and -164.3 ± 0.1 for 20m and 25m, respectively (Fig. 3.9, Table 3.1).

Table 3.1. Summary of concentrations and isotopic signatures of methane from lake water measurements and lab experiments to determine potential sources. West Lake Bonney (WLB), The Narrows, and East Lake Bonney (WLB) water measurements are from samples collected from the listed depths in 2017. Location designation references Fig. 3.5. TG = Taylor Glacier. DMS = dimethyl sulfide. DMSO = dimethyl sulfoxide. ND = not determined. Methane concentrations determined with a gas chromatograph (limit of detection = 3nM). Gas isotope values measured with a Cavity Ring-Down Spectrometer.

Source	CH_4 Concentration (nM for water samples / nmol CH_4 g^{-1} substrate for ice and sediment)	^{13}C-CH_4 (‰)	^{2}H-CH_4 (‰)
WLB 24m – Location A	287.3	-31.0 ± 1.9	-141.0 ± 0.1
WLB 30m – Location A	345.0	ND	ND
WLB 20m – Location B	98.2	-29.8 ± 2.7	-142.2 ± 0.6
WLB 25m – Location B	354.1	-27.5 ± 2.8	-141.5 ± 0.7
The Narrows 16m – Location C	19.7	-29.4 ± 3.94	-167.3 ± 0.6
ELB 20m – Location D	13.3	-29.3 ± 1.9	-169.9 ± 0.7
ELB 25m – Location D	31.0	-29.63 ± 3.2	164.3 ± 0.7
TG Basal Ice Melt	0.14 ± 0.01	-27.8 ± 6.8	ND
TG Basal Sediment Comminution	0.33 ± 0.09	-32.4 ± 2.7	-212.3 ± 4.5
DMS + TG Sediment	0.15 ± 0.001	ND	ND
DMSO + TG Sediment	0.20 ± 0.008	ND	ND
WLB 20m + TG Sediment	0.51 ± 0.03	-30.5 ± 0.1	ND
WLB 25m + TG Sediment	1.09 ± 0.02	-28.0 ± 1.1	ND

Direct Methane Sources from Taylor Glacier

The basal ice melt released 0.14 ± 0.01 nmol CH_4 g ice^{-1} with a $\delta^{13}C$-CH_4 value of -27.7‰ ± 6.8 (Table 3.1). The grain size distribution for TG sediments *in situ* is reported in Table 3.2. Milling TG sediments to simulate glacial comminution released an average of 0.33 ± 0.09 nmol CH_4 g^{-1} with a mean $\delta^{13}C$-CH_4 value of -32.4‰ ± 2.7 and $\delta^{2}H$-CH_4 value of -212.3‰ ± 4.5 (Table 3.1).

Table 3.2. Grain size distribution for Taylor Glacier basal ice sediment.

Fraction	Volume %
Clay (<2um)	4.5
Silt (2 - 50um)	18.6
Very fine sand (50-100um)	13.9
Fine sand (100-250um)	33.5
Medium sand (250-500um)	25.4
Coarse sand (500-1000um)	3.9
Very coarse sand (1000-2000um)	0
Total sand (50-2000um)	76.8

Incubations of WLB Water DMS and DMSO, with TG Sediments

WLB water with 5g TG sediment added and incubated at 5˚C for 72h produced 0.51 ± 0.21 nmol CH_4 g sediment^{-1} and 1.09 ± 0.21 nmol CH_4 g sediment^{-1} for 20m and 25m water depth samples, respectively, while no methane was produced in the ultrapure water control (Fig. 3.10). The $\delta^{13}C$-CH_4 values were -30.0‰ ± 0.1 and -28.0‰ ± 1.1 for 20m and 25m, respectively (Table 3.1)

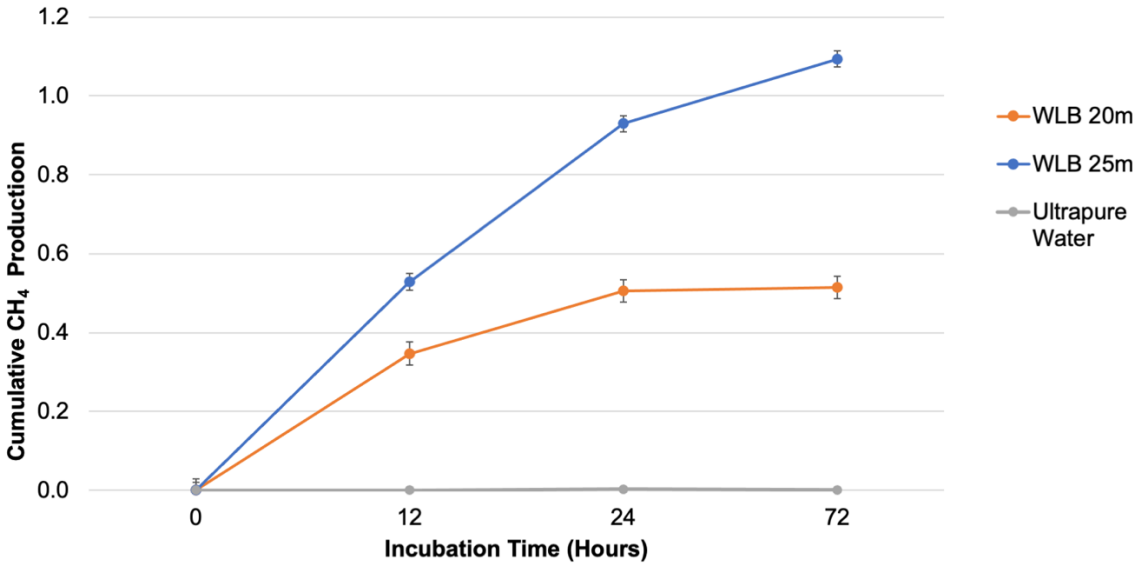


Fig. 3.10 Methane produced over 72h when 5g of dried, milled (<63 µm) of Taylor Glacier (TG) basal sediments were added to 28ml of West Lake Bonney (WLB) water from 20m and 25m from Location B (see Fig. 6) and incubated in the dark for 72h at 5ºC. Methane concentrations at each time point represent cumulative values per gram of sediment. TG sediments added to ultrapure water acted as the control. Error bars indicated standard deviation from the mean (n=3).

The 200 nM DMS solution with 5g TG sediment added produced 0.15 ± 0.001 nmol methane g sediment^{-1} after 48h of incubation at 5°C. The 200 nM DMSO solution with added TG sediment produced 0.20 ± 0.008 nmol methane g sediment^{-1} after 48h hours of incubation at 5°C (Fig. 3.11, Table 3.1).

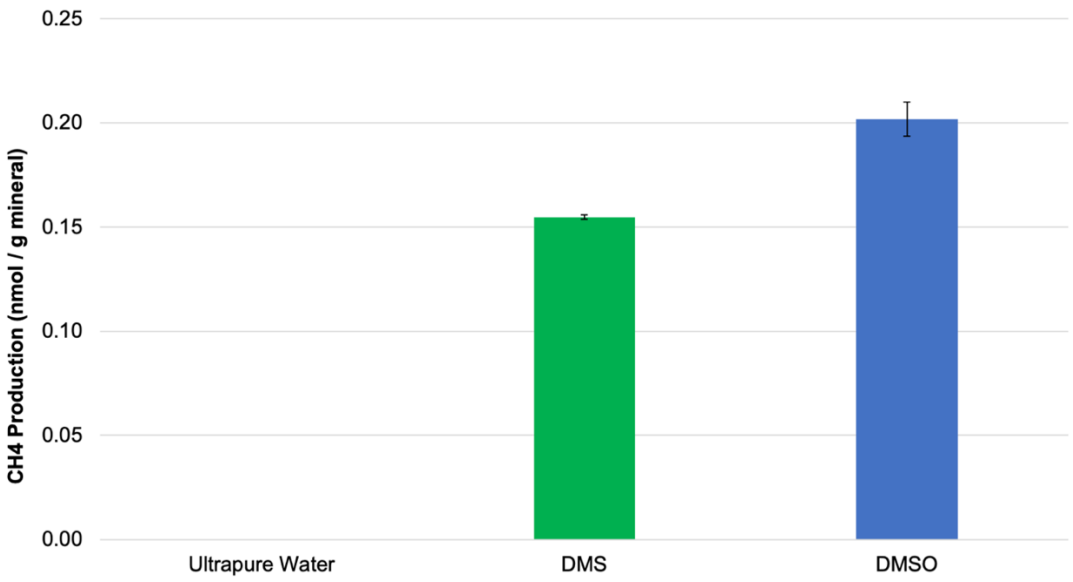


Fig. 3.11 Methane produced when 5g of dried, milled (<63 µm) Taylor Glacier (TG) basal sediments were added to 28ml of 200nM solutions of either dimethyl sulfide (DMS) or dimethyl sulfoxide (DMSO) then incubated in the dark for 48h at 5ºC. TG sediments (5g) in ultrapure water served as the control. Error bars indicated standard deviation from the mean (n=3).

Discussion

Potential Direct Sources of Methane to the WLB Water Column

Methane is supersaturated, relative to the atmosphere, below 20m in West Lake Bonney (WLB), with the highest concentrations occurring between 20 and 25m (Fig. 3.8). The concentration of methane is ~244nM at 43m close the sediment/water interface, peaks at 354nM at 25m, then declines in shallower layers (Fig. 3.8). This profile is not consistent with a simple diffusion gradient of methane sourced from the sediments. Further, there is no evidence for methanogens in sediment cores from WLB (Tang et al., 2013). Therefore, the methane appears to come from an abiotic source or sources in the lake's more recent history, perhaps in the time since the current hydrological configuration became stable ~200 years ago (Poreda et al., 2004).

The isotopic composition of the methane in WLB has a $\delta^{13}C\text{-}CH_4$ value of -29.8‰ ± 2.7 and a $\delta^{2}H\text{-}CH_4$ of -142.2‰ ± 0.7, at 20m, and a $\delta^{13}C\text{-}CH_4$ of -27.5‰ ± 2.8 and $\delta^{2}H\text{-}CH_4$ of -141.5‰ ± 0.7 at 25m (Fig. 3.8, Table 3.1). These values suggest source(s) that are abiotic or thermogenic (Tazaz et al., 2013; Milkov and Etiope, 2018; Fig. 3.12) and/or a methane pool that has been enriched in ^{13}C through methane oxidation (Tazaz et al., 2013).

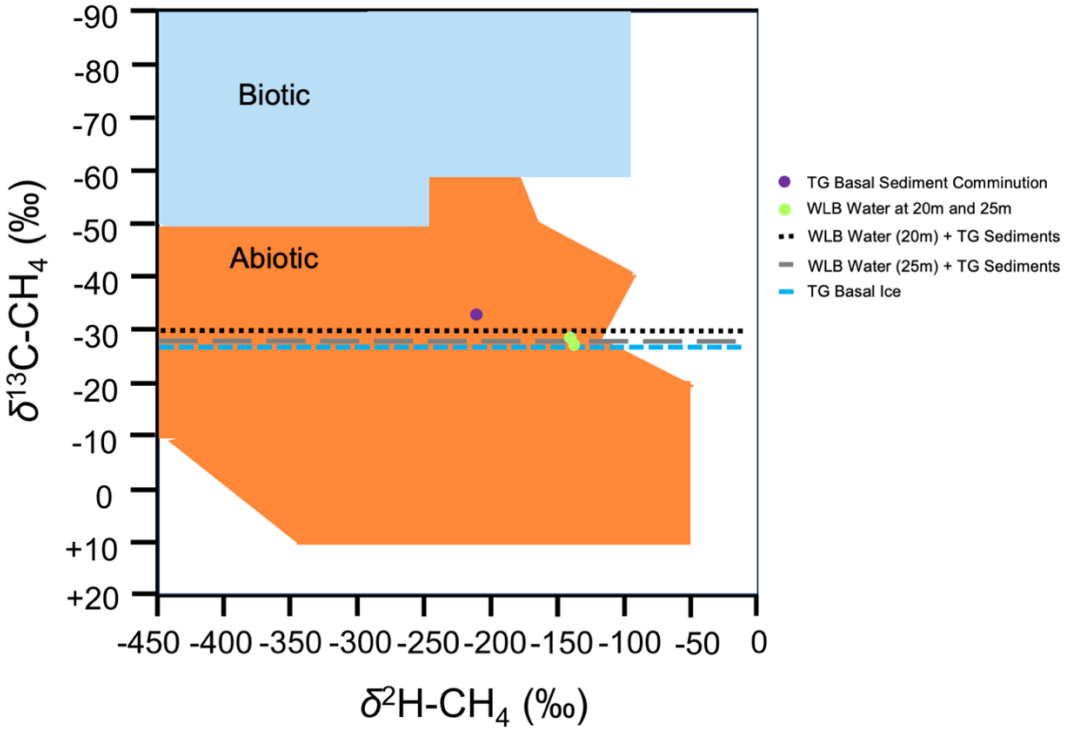


Fig. 3.12 Isotopic composition methane produced from comminution of Taylor Glacier (TG) sediment and methane released from melting TG basal ice, compared to the isotopic composition of methane in the West Lake Bonney (WLB) water column. Dotted lines indicate only $\delta^{13}C\text{–}CH_4$ measurements are available. Base figure adapted from Milkov & Etiope (2018).

Methylotrophic Methanogenesis

The water at 20m and 25m in WLB and ELB contains DMS and DMSO in appreciable concentrations (Lee et al., 2004; Fig. 3.13), so methylotrophic methanogenesis using these dimethyl sulfur compounds as the substrate was considered as a potential process.

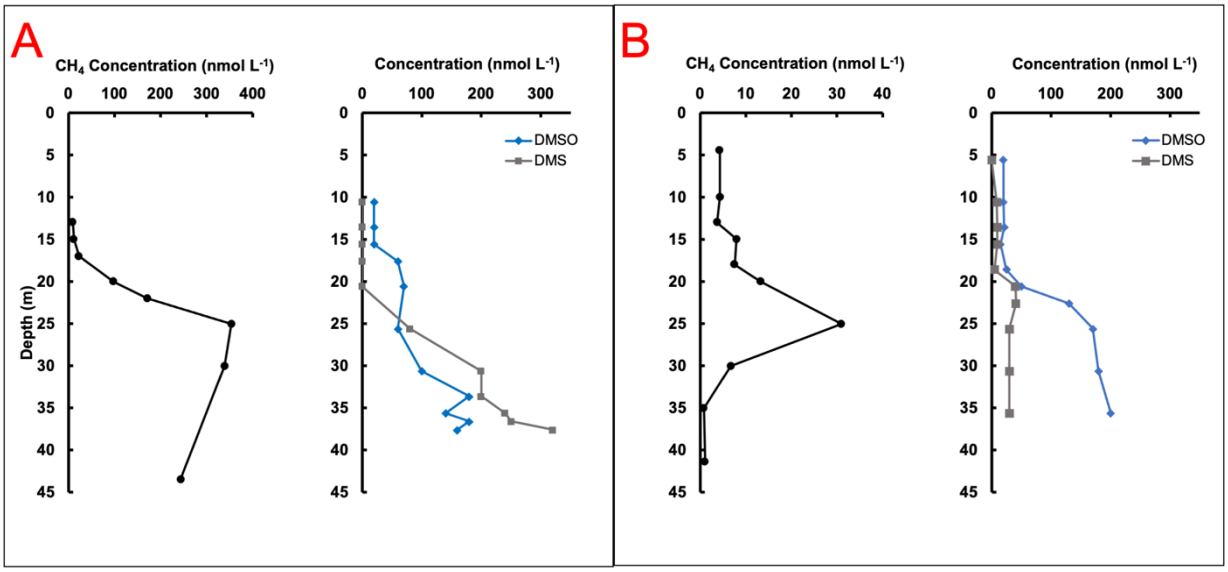


Fig. 3.13 Methane, dimethyl sulfide (DMS), and dimethyl sulfoxide (DMSO) concentrations in (A) West Lake Bonney and (B) East Lake Bonney. Methane samples were collected in 2017 from Locations B and D (Fig. 1). Samples for DMS and DMSO quantification were collected in 1999 from Locations B and D (Fig. 1) as reported in Lee et al. (2004). Note the order of magnitude change in methane concentration for the x-axis in panels (A) and (B). Methane concentrations determined with a gas chromatograph (limit of detection = 3nM)

All methanogens require coenzyme-M for the final steps of CH_4 formation, which is encoded by the methyl CoM reductase subunit A (*mcrA*) gene (Boyd et al., 2010). However, no mcrA gene sequences were detected in the metagenomic analysis of samples from water depths 5-30m in both WLB and ELB (Li et al., 2020), precluding methylotrophic methanogenesis as an active process. Further, in marine systems where microbially-driven methylotrophic methanogenesis using DMS and DMSO as substrates has been observed, $\delta^{13}C$-CH_4 values lower than -40‰ were

measured (Damm et al., 2008; Florez-Leiva et al., 2013), which are significantly different from the values measured in WLB at 20m and lower depths.

Methane produced by non-archaeal methanogens (i.e. eukaryotes and prokaryotes) extends the traditional range of biogenic methane $\delta^{13}C\text{-}CH_4$ up to -5.4 ‰ (Klintzsch et al., 2023). Biological pathways that generate isotopically heavier methane involve phytoplankton in aerobic surface waters utilizing substrates such as methylphosphonate (MPn), dimethyl sulfide (DMS), and dimethylsulfooxide (DMSO) (Florez-Leiva et al., 2013; Klintzsch et al., 2023). These pathways, in combination with methane oxidation, lead to overall $^{13}C\text{-}CH_4$ enrichment in the dissolved methane pool. Li et al. (2020) found only fragments of major methane oxidation genes in Lake Bonney and they were only identified in the shallow waters, well above the methane concentration peak in WLB, which occurs in anaerobic waters. Methane oxidation is, therefore, an unlikely influence on the isotopic character of the WLB methane pool below the chemocline. Lake Bonney water incubations amended with MPn showed a significant increase in methane from water at 15m, but methane in amended water from 20m and 25m was very low to not detected (Li et al., 2020). This suggests that while some methanogenesis via MPn utilization may be occurring below the chemocline, it would not be a major contributor to the methane pool at those depths. Methanogenesis from DMS and DMSO is also possible in Lake Bonney, but unlikely. Lee et al. (2004) found that DMS and DMSO concentrations in both lobes were among the highest ever observed in a natural system. The reduction potential of ELB waters below the chemocline is not conducive to DMSO reduction, but the process could be energetically favorable in WLB (Lee et al., 2004). However, Lee et al. (2004) added a caveat that because there is a significant amount of DMS and DMSO below 22m in WLB, any microbial utilization

would have to be occurring at a very low rate, if at all. Further, unamended incubations of WLB and ELB water from 20m and 25m did not generate methane over 30-70 days (Li et al., 2020), suggesting any microbial methanogenesis would be occurring at a low rate, if it is even present. Previous genetic analyses of the Lake Bonney waters and sediments looked for DNA sequences related to known methanogens (e.g. those using acetoclastic or hydrogenotrophic pathways) or genetic markers for traditional anaerobic methanogenesis, such as *mcrA* (Tang et al., 2013; Kwon et al., 2017; Li et al., 2020; Li et al., 2023). While these genetic analyses would not necessarily identify the non-traditional methanogens, the geochemical evidence discussed above suggests biological methanogenesis is unlikely in any form below the chemocline.

Taylor Glacier Basal Ice Melt and Comminuted Basal Ice Sediments

Taylor Glacier was considered a potential contributory source to the deep methane pool in WLB as the peak concentration in methane occurs just below the inferred depth of subglacial brine inflow to WLB (Fig. 3.2A, Fig. 3.4A). WLB receives brine outflow from the terminus of Taylor Glacier (Spigel et al., 2018; Lawrence et al., 2020) at a depth of 20-25m, as indicated by changes in conductivity, density, and water temperature (Spigel et al., 2018; Fig. 3.3A). It is possible, then, that this glacial brine outflow contains methane, which then accumulates below the chemocline in WLB. Unfortunately, the detailed geochemical measurements of the englacial brine that is the source for Blood Falls on Taylor Glacier do not include dissolved gas measurements (Lyons et al., 2019). Therefore, the methane concentration in the brine remains unknown.

Methane from melting basal ice or glacial grinding of basal sediments could also contribute to WLB. Our laboratory simulations of these processes demonstrated methane release

from both sources. The δ^{13}C-CH4 values of the methane released from melting basal ice (-27.8‰ ± 6.8) are similar to the δ^{13}C of the methane in the WLB water at 20m and 25m (Table 3.1), suggesting this could be a contributing source. However, without δ^{2}H-CH_4 data from the melting basal ice it is not possible to accurately assess its contribution to the methane pool in WLB. Despite the lack of δ^{2}H-CH_4 data, other observations suggest this is unlikely to be a major methane source to WLB. The concentration of CH_4 in the ice is relatively low (0.14 ± 0.01 nmol g^{-1}) and the amount of glacial ice directly melting into Lake Bonney annually is also low, as Taylor Glacier advances only 2-5 m yr^{-1} (Pettit et al., 2014; Spigel et al., 2018) and only about half of the total exposed glacier face in WLB is below the chemocline (Spigel et al., 2018), where the methane concentrations are highest. The meltwater contribution from direct ice melt TG to the lake, therefore, is relatively minor (Spigel et al., 2018), and the amount of melting terminus ice at the depth of the methane peak is even less so. Further, this is consistent with the work of Welch et al., (2010) that attributed the majority of water input to WLB to proglacial valley streams.

Crushed TG sediments, simulating rock comminution at the bed of the glacier also yielded methane, and at higher concentration than for the melted basal ice; 0.33 ± 0.09 nmol g^{-1}, The methane from this source had a δ^{13}C-CH_4 value of -32.4 ‰ ± 2.7 which was within the range of the lake water δ^{13}C-CH_4 values at 20 and 25m, but the δ^{2}H-CH_4 value of -212.3 ‰ ± 4.5 was significantly different (-70 ‰) from the lake water δ^{2}H-CH_4 values at 20 and 25m (Fig. 3.8) suggesting this is unlikely to be a major source for the WLB methane pool. The deposition of these fine-grained sediments into WLB, however, may catalyze abiotic reactions with organosulfur compounds that produces methane, discussed below.

Methanogenesis from Organosulfur Compound-Mineral Reactions

Methane can be produced abiotically when ferrous minerals react with DMS and DMSO (Althoff et al., 2014). The deep waters of WLB have higher concentrations of DMS and DMSO than are commonly found in natural systems (Lee et al., 2004; Fig. 3.13). These compounds are likely produced by phytoplankton in the photic zone as an osmoregulator, then cells and organic particulates sink to deeper layers where cell death or membrane permeation releases the methylated sulfur compounds into the water column (Lee et al., 2004). Heterotrophic activity is limited below the chemocline due to rapidly increasing salinity (Ward et al., 2003), which may explain the sudden increase in methylated sulfur compounds in the hypolimnion as cells and organic particulates are less likely to be scavenged at these depths. The highest concentrations of DMS and DMSO occur below 20m (Lee et al., 2004) where the methane concentration peaks (Li et al., 2020; Fig. 3.2A). We hypothesized that reactions between the iron-bearing minerals in TG basal sediments (Raiswell et al., 2009) and the organosulfur compounds in the lake could produce methane. Basal sediments from TG were added to solutions of DMS and DMSO, and to unamended water from WLB at 20 and 25m to test our hypothesis.

When milled TG basal sediments were added to 200nM solutions of DMS and DMSO and incubated at 5˚C, 0.15 ± 0.001 and 0.20 ± 0.008 nmol g sediment^{-1}, respectively, of methane were produced over 48h (Fig. 3.11). This experiment demonstrates that methane is produced when only these chemicals and basal sediments are present. When TG sediments were added to WLB water from depths encompassing the observed methane peak, methane was produced. Over a period of 72h, mixtures of TG sediments and WLB water, incubated at 5˚C, produced 0.51 ± 0.03 and 1.09 ± 0.02 nmol CH_4 g sediment^{-1} when mixed with 20m and 25m water samples,

respectively (Fig. 3.10). The water-sediment interaction experiments produced methane with $\delta^{13}C\text{-}CH_4$ values of -30.5‰ ± 0.1 and -28.0‰ ± 1.1 with 20m and 25m WLB water, respectively. At 20m and 25m in WLB, the methane had $\delta^{13}C\text{-}CH_4$ signatures of -29.8‰ ± 2.7 and -27.5‰ ± 2.8, respectively, in 2017, suggesting that the proposed organosulfur-mineral reactions may be occurring in WLB.

Previous demonstrations of methane production through reactions between DMS/DMSO and iron-bearing minerals, in the presence of hydrogen peroxide (H_2O_2), occurred at ~22ºC under aerobic and anaerobic conditions (Althoff et al., 2010; Althoff et al., 2014). The general reactions proposed by these studies require hydroxyl radicals to react with the methylated sulfur compounds, cleaving the methyl group, which subsequently reacts with H_2O_2 to produce methane. The oxidation of DMSO by hydroxyl radicals to produced methyl radicals has previously been demonstrated (Steiner and Babbs, 1990; Urbanski et al., 1998; Herscu-Kluska et al., 2008). The generation of H_2O_2 and hydroxyl radicals can occur during water/mineral interactions and mineral comminution at 0ºC and 4ºC (Gill-Olivas et al., 2021; Gill-Olivas et al., 2023), indicating that some of the reactions proposed by Althoff et al. 2010 could be possible under *in situ* conditions in WLB. Additionally, the work by Gill-Olivas et al. shows that iron-bearing minerals can be a source of both H_2O_2 and hydroxyl radicals, and TG basal sediments contain iron minerals (Raiswell et al., 2009). Therefore, all reactants necessary for abiotic methanogenesis are present below 20m in WLB. A series of reactions for the potential abiotic generation of methane in WLB are presented below:

1. Generation of hydrogen peroxide and hydroxyl radicals through water/mineral interactions (Gill-Olivas et al., 2023, Reaction 1,2)

2. Generation of additional hydroxyl radicals through Fenton's Reaction (Herscu-Kluska et al., 2008, Reaction 3).
3. Reaction between hydroxyl radicals and DMSO (Herscu-Kluska et al., 2008, Reaction 4)
4. Reaction between methyl radicals and hydrogen peroxide (Herscu-Kluska et al., 2008; Althoff et al., 2014, Reaction 5)

Reaction 1: $Fe_3^{+}{}_{surface} + H_2O \rightarrow Fe_2^{+}{}_{surface} + \cdot OH + H^+$

Reaction 2: $\cdot OH + \cdot OH \rightarrow H_2O_2$

Reaction 3: $Fe^{2+} + H_2O_2 \rightarrow Fe^{3+} + \cdot OH + OH^-$

Reaction 4: $\cdot OH + CH_3SOCH_3$ (DMSO) $\rightarrow \cdot CH_3 + CH_3SOOH$

Reaction 5: $\cdot CH_3 + H_2O_2 \rightarrow CH_4 + \cdot HOO$

This series of reactions could occur in LB as follows. Fine-grained sediments deposited into the lake sink to deeper layers and water reactions with ferric iron on the mineral surface produces hydroxyl radicals and hydrogen peroxide. The fine grain particles will descend at lower velocities below the chemocline, given the increase in fluid density. The hydroxyl radicals then react with DMS and DMSO at depths below 20m, where the concentration of these compounds begins to increase, leading to the formation of methyl radicals. The methyl radicals react with hydrogen peroxide produced from the mineral/water interactions to form methane at depths below 20m.

Laboratory experiments show the formation of methane from organosulfur-mineral reactions could be possible in Lake Bonney but the contribution of this process to the WLB methane pool appears to be limited, based on the methane hydrogen isotopic data as described below.

Estimating the Magnitude of Organosulfur Compound-Mineral Reactions as a Contributor to the WLB Methane Pool. No δ^2H-CH_4 measurements were made from the experiments with WLB waters and TG crushed sediment. Therefore, it is not possible to accurately assess the potential contribution of this abiotic source to the methane pool in WLB using an isotope mass balance approach. However, we can use an isotope mass balance model to estimate what the δ^2H of the DMSO would be if it was the source of the methyl group in the water column methane at 20m and 25m. Reactions 4 and 5 above indicate that three of the hydrogen atoms in the methane molecule would come from the methyl group of DMSO. The fourth hydrogen would come from the lake water, according to Reaction 1. The δ^2H-H_2O at 30m in LB, near where one might predict Reaction 1 would occur, is -330.0 ‰ (Lyons et al., 2019) and the average δ^2H-CH_4 value for WLB waters between 20m and 25m is -141.6 ‰ (Table 3.1). The δ^2H of the methyl group from DMSO is calculated according to Whiticar (1999):

$\delta^2H\text{-}CH_4 = 0.75(\delta^2H\text{-}CH_3) + 0.25\ (\delta^2H\text{-}H_2O)$

$\delta^2H\text{-}CH_3 = [\delta^2H\text{-}CH_4 - (0.25\ \delta^2H\text{-}H_2O)]/0.75]$

$\delta^2H\text{-}CH_3 = [-141.6‰ - (0.25 \times -330)]/0.75]$

$\delta^2H\text{-}CH_3 = -79.0‰$

The methyl group in DMSO used in Reaction 3 would therefore have a δ^2H of -79‰ for this reaction to be considered a viable precursor to the methane measured in the lake water. Lee et al. (2004) suggest the DMSO is of microbial origin, sourced from phytoplankton above the chemocline, but there are multiple possible formation pathways involving abiotic and biotic transformations that could cause isotopic fractionation. However, the hydrogen isotopic

fractionation that would be required to account for the δ^2H values of the methane measured in WLB are not realistic. δ^2H-H_2O values for 4-12m depth in the WLB water column range from -305 to -320 ‰ (Gooseff et al., 2006). Therefore, there would need to be a consistent positive isotopic fractionation effect in creation of DMSO/DMS with lake water as the H source for the organic molecules, of the order of 226 to 241‰ to generate δ^2H-CH_3 values of -79.0‰. Biological isotopic fractionation processes favor the lighter isotope (Whiticar, 1999; Madigan et al., 2018). Therefore, a highly unusual (and unprecedented) biologic process would be required to produce methyl compounds with such positive δ^2H values. Thus, although all the reactants for this process are present in the WLB waters below 20m it seems highly unlikely that this would be a major source for the methane pool.

The methane to ethane ratio in the TG sediment plus WLB water experiments differ greatly from those measured in the water column, further suggesting that the organosulfur-mineral reactions are not a significant methane source in the western part of WLB. The C_1:C_2 ratios in the WLB waters were 26, 46, 57, and 54 at 20m, 25m, 30m, and 35m, respectively compared to the C_1:C_2 ratios in the TG sediment plus WLB water experiments were 3 and 5 for 20m and 25m water, respectively. The origin of methane can be inferred from a binary diagram, often termed a "Bernard" plot, where $\delta^{13}C$-CH_4 versus the concentration ratio [$C_1/(C_2 + C_3)$] of methane (C_1), ethane (C_2) and propane (C_3) are plotted (Whiticar, 1999; Milkov and Etiope, 2018). Propane was not measured, but plotting the $\delta^{13}C$-CH_4 versus the gas ratio [$C_1/(C_2)$] on a Bernard plot, places the samples in the thermogenic/abiotic source region (Fig. 7C in Milkov and Etiope, 2018). Together, the δ^2H-CH_4 mixing model and methane/ethane ratio results indicate that if organosulfur-mineral reactions are occurring in WLB, they are producing low, (single digit

nM) concentrations of CH_4, i.e. that would have a minimal impact on the isotopic signature of the methane in WLB. Therefore, a larger thermogenic/abiotic source is likely the most significant contributor to the methane pool, discussed below.

Legacy Methane

The $\delta^{13}C$-CH_4 and $\delta^{2}H$-CH_4 values in WLB (Fig. 3.8) indicate an abiotic source that is likely thermogenic (Milkov and Etiope, 2018). Methane has been observed in other McMurdo Dry Valley Lakes, including Lake Vanda in Wright Valley and Lake Fryxell in Taylor Valley, but in both lakes the source is active biological methanogenesis (Saxton et al., 2016; Saxton et al., 2021). While legacy thermogenic methane may also be present in Lakes Vanda and Fryxell, the $\delta^{13}C$-CH_4 signature shows biotic processes are dominant in these systems (Saxton et al., 2021). In WLB, 16S rRNA gene-based pyrosequencing found no evidence for methanogens in the water column or sediments (Tang et al., 2013; Kwon et al., 2017; Lee et al., 2023) and the methanogenesis marker gene *mcrA* was absent in waters below the chemocline (Li et al., 2020). This is therefore consistent with an abiotic methane signature. However, the methane concentration profile is atypical. If legacy thermogenic methane was seeping from the lake sediments without any additional (biologic) modification, the concentration profile should follow a diffusional profile from deeper to shallower waters below the chemocline, given the stratified nature of the lake water The bow-shaped concentration profile, with a peak at the depth of brine inflow, suggests the influence of an input from TG.

The organosulfur-mineral reactions, basal ice melt and sediment comminution sources described above do not appear to be significant contributors to the WLB methane pool. The methane released from TG basal ice had a $\delta^{13}C$-CH_4 similar to the lake water methane, but the

concentration per gram of ice was relatively low (Table 3.1), suggesting this was not a significant source. However, the basal ice is likely not homogenous across the glacier, nor are the basal sediments beneath the glacier. Therefore, the ice block used in this study, from the peripheral of the glacier tongue, ~1.5km north of the terminus (Fig. 3.5) may not be representative of the subglacial environment across the terminus. Thus, it is possible that TG basal ice may contain higher concentrations of methane than measured in this work. Even so, direct melting of TG basal ice into WLB at the terminus is still unlikely to be the main methane source as annual ice melt into the lake is limited. The subglacial environment is likely still a source of methane to WLB, considering the concentration peak at the depth of subglacial brine inflow, pointing to the methane being dissolved within the brine.

Legacy Biological Methane

Methane seep from ancient marine sediments and/or brine beneath TG could carry a biogenic signature if methanogens were present and active in the Taylor Valley fjords. In anaerobic marine sediments, methanogenesis is typically acetoclastic and/or hydrogenotrophic (Ferry and Lessner, 2008), with some methyl-type fermentation when sulfate reduction dominates (Mitterer et al., 2010; Bueno de Mesquita et al., 2023). Acetoclastic methanogenesis has been identified as the dominant biologic methane source in deep Antarctic marine sediments off the coast of East Antarctica, near the Ross Sea region (Carr et al., 2018). Microbial methane from marine sediments can have a dD-CH_4 values as high as -101‰ (Milkov and Etiope, 2018), which overlaps with the dD-CH_4 values measured in the Lake Bonney water column (Fig. 3.8, Fig. 3.9). However, the associated $\delta^{13}C$-CH_4 from these marine sediment methanogenesis pathways is <-50‰ (Milkov and Etiope, 2018), which is more negative than the $\delta^{13}C$-CH_4 of the

WLB methane pool below the chemocline, so relict biological methane from the marine sediments beneath TG is unlikely a source to the lake water. However, alternative methanogenic pathways exist for marine organisms that produce isotopically heavier methane.

The dissolved methane pool in ocean surface waters is enriched in $\delta^{13}C\text{-}CH_4$ due to a combination of methane oxidation and phytoplankton-driven methanogenesis using unconventional substrates, such as methylphosphonate and dimethyl sulfide, producing gas more enriched in ^{13}C than methane from traditional, anerobic pathways (Florez-Leiva et al., 2013; Klintzsch et al., 2023). If the fjords that filled Taylor Valley had active aerobic methanogenesis and methane oxidation in their surface waters, then there may have been a dissolved methane pools more enriched in ^{13}C, which became trapped beneath Taylor Glacier during its advance. This marine-derived methane could then still exist in the brine currently beneath the glacier and be carried into WLB. However, the $\delta^{13}C\text{-}CH_4$ of dissolved methane in the upper ocean waters (~0-50m) generally ranges from about -53 to -45‰ (Florez-Leiva et al., 2013; Yoshikawa et al., 2014; Taenzer et al., 2020) with some values at 100m depth reaching -33‰ (Sasakawa et al., 2008), which are all more negative than the $\delta^{13}C\text{-}CH_4$ values of the WLB methane pool below the chemocline, suggesting legacy marine methane is unlikely a major source.

Legacy Thermogenic Methane

The isotopic signature of the methane in WLB suggests the gas is thermogenic in origin (Milkov and Etiope, 2018). There are two primary crustal sources of abiotic methane emanating from beneath glaciers and ice sheets, thermogenic methane related to hydrocarbon production in sedimentary basins and Fischer-Tropsch type inorganic reactions in geothermal systems (Etiope and Klusman, 2002; Wadham et al., 2012; Burns et al., 2018). This crustally-derived methane is

supplied to the subglacial environment via gas permeable faults and fractured rocks and is trapped by the overlying ice, rather than being released directly to the atmosphere. The Beacon Sandstone formation underlying Taylor Glacier could be a crustal source of abiotic methane.

The Beacon Sandstone Formation was first described by Ferrar (1905) as an approximately 600m-thick sandstone exposure in the Royal Society Mountain Range (Beacon Heights, near Taylor Glacier), overlying a granite layer and capped with basalt. A survey by Hamilton and Hayes (1963) described the Beacon Sandstone as a prominent mountain outcrop feature throughout the Ross Sea coast of East Antarctica, with an estimated 1,200m-thick, cliff-forming sandstone layer, intruded with Mesozoic Ferrar Dolerites and overlain with carbonaceous shale strata containing fossilized flora. The sandstone layers are the dominant sequence of the Beacon Supergroup, a 2.5-3km thick Triassic to Devonian-age clastic succession that is roughly continuous along the west coast of the Ross Sea between Mackay Glacier (~80km north of Taylor Valley) and Beardmore Glacier (~700km to the South) (Isbell, 1999; Cox et al., 2012).

The Beacon Supergroup consists of the Devonian-age Taylor Group, underlying the Permian and Triassic-age Victoria group. The basement rocks are Precambrian marble, amphibolite, schist, gneiss and Neoproterozoic greywacke, shale, and metasedimentary rock (Isbell, 1999) that are separated from the Beacon Supergroup by the Kukri Erosion Surface, a near-horizontal unconformity separating late-Cambrian to early Devonian granitoids from the Devonian sandstone above (Isbell, 1999; Cox et al., 2012). Overlying the Kukri Erosion Surface is the ~1400m-thick Taylor Group, consisting of sedimentary sequence composed of alternating beds of fine-grained, pale sandstone and darker siltstone (Isbell, 1999; Cox et al., 2012). The

siltstones contain evidence for deposition in a lacustrine or lagoon setting, including trace fossils (e.g. bivalves, trilobites, fish), ripple marks, and mud cracks (Hamilton and Hayes, 1963; Isbell, 1999; Cox et al., 2012). Between the geologically similar Taylor and Victoria groups is the Maya Erosion Surface which represents a time gap of 86 to 109 million years, equivalent to at least the Carboniferous Period (Cox et al., 2012).

The Victoria Group is the upper member of the Beacon Supergroup and is a Gondwanan sequence of basal glacial beds overlain with sandstones and coal beds dating from early Permian to late Triassic with a preserved thickness of ~1000 m (Isbell, 1999; Cox et al., 2012). The majority of the Victoria Group sections are incomplete, since they are capped by Jurassic dolerite sills, lavas, or the East Antarctica Ice Sheet (Cox et al., 2012). Substantial erosion in some parts of the Transantarctic Mountains make it difficult to determine the precise burial depth of the Beacon Sandstone, but Vavra et al., (1979) estimate a burial depth of 600-2000m (Bernet and Gaupp, 2005). Diagenesis of the Beacon Sandstone occurred in three phases: shallow burial diagenesis, contact diagenesis, and post-contact diagenesis (Bernet and Gaupp, 2005). Heating from shallow burial (burial diagenesis) would be limited, but heating from magmatic intrusions (contact diagenesis) was estimated to reach 200-300°C (Bernet and Gaupp, 2005). There is also evidence for additional hydrothermal heating of the Beacon Sandstone (post-contact diagenesis) linked to the rifting of New Zealand and Australia from Antarctica (Bernet and Gaupp, 2005). Thermogenic methane can form between 157 and 300°C (Horita and Berndt, 1999; Etiope and Lollar, 2013; Stolper et al., 2014). The magmatic intrusions that formed the dolerite strata in the Beacon Sandstone could have heated the organic matter in the Taylor and Victoria groups, generating methane.

The dolerite intrusions of the Beacon Supergroup, referred to as the Ferrar Group, have an igneous origin in the early Jurassic (Cox et al., 2012), the result of magmatism during the continental breakup of Gondwana (Riley and Knight, 2001). The sills are on average 100–200m thick and locally can exceed 700 m, with individual sills having a significant aerial extent, up to 60,000 km^2 (Elliot and Fleming 2004). The Ferrar Group is composed of plagioclase, pyroxene, and oxide minerals, including high concentrations of MgO (Faure et al., 2011). The Ferrar Dolerite formed when deep crustal rifts breached the subcrustal mantle, allowing magma with subducted oceanic sediment to enter the rifts and undergo decompression melting (Faure et al., 2011). Certain igneous rocks can contain methane with a thermogenic signature (Milkov and Etiope, 2018) and in an exploration study for mantle-derived methane, $\delta^{13}C\text{-}CH_4$ measurements from deep drilling fluids associated with dolerites intruding into granite ranged between -19 and -27‰ (Jeffrey and Kaplan, 1988). The lower of these $\delta^{13}C\text{-}CH_4$ values are similar to those measured in the LB water column (Table 3.1). Jeffrey and Kaplan (1988) note that the origin of the methane may be from the deep upper-mantle or alternatively from abiogenic synthesis in crustal rocks, for example via hydrolysis of mafic rocks or the reduction of CO_2 via Fischer-Tropsch reactions. Therefore, it is possible that the Ferrar Dolerites could contain thermogenic methane, but this would need to be verified through direct rock sampling.

The presence of spherulitic structures in Beacon Sandstone blocks encased within Ferrar dolerite intrusions indicate localized melting, followed by slow cooling (Ballance and Waiters, 2002). The thermal alteration of Beacon sandstone is also apparent with the abundant calcite in pore spaces of the sandstone near dolerite intrusions (Ballance and Waiters, 2002). Calcite authigenesis would require a significant source of calcium, which could have been sourced from

plagioclase in the dolerite (Ballance and Waiters, 2002). Thermal heating of the coals within the Beacon Sandstone would release CO_2 and CH_4, raising the pH and precipitating the calcite (Ballance and Waiters, 2002). An abrupt increase in atmospheric CO_2 ~183 mya (early Jurassic) is attributed to the rapid oxidation of thermogenic methane released from magma-intruded organic-rich rocks, such as Triassic-aged coals and carbonaceous shales, during the break-up of Gondwana (McElwain et al., 2005). The dolerite sills of the Ferrar Group are remnants of the magmatic flows that caused the thermal metamorphism of organic-rich Triassic strata such as the Victoria Group of the Beacon Supergroup (Isbell et al., 1999) releasing methane with $\delta^{13}C\text{-}CH_4$ values as low as -35‰ (McElwain et al., 2005).

The most likely source of methane beneath Taylor Glacier today is the prevalent carbonaceous shale deposits within the Beacon Sandstone described by Hamilton and Hayes (1963). In an alpine glacial setting at Robertson Glacier, Canadian Rockies, glacial grinding of bedrock shales is an abiotic subglacial source of methane, releasing an estimated 0.004 t km^{-2} yr^{-1} (MacDonald et al., 2018). While contemporary glacial comminution is likely limited beneath TG for the reasons discussed above, past advances of the East Antarctic Ice sheet (including Taylor Glacier) have eroded ~1.5-2 km of the upper Beacon Supergroup (Cox et al., 2012), which could have release methane that remained trapped beneath the glacier. Diffusion of methane from fractured rocks is also possible and subglacial gas concentrations could build up beneath the glacier given its current cold-based thermal regime.

The Dry Valleys encompass a block of the Transantarctic Mountains, with large bounding transform faults beneath Mackay Glacier, north of McKelvey Valley, and beneath Ferrar Glacier, south of Taylor Valley, which have caused the valleys to act as a single block since the early

Tertiary (Prentice et al., 1998; Sugden et al., 1995). Sugden et al. (1995) found evidence for downfaulting beneath Mount Newall in the Asgard range, which is part of a fault zone that cuts south across Taylor Valley ~ 20 km down valley from the present-day terminus. The faulting likely occurred before and during a period of valley downcutting by rivers and glaciers, which ended ~15 mya and was followed by subsidence and marine incursion, leading to the development of a fjord system (Elston and Bressler, 1981; Sugden et al., 1995). Continued faulting likely did not occur following subsidence, based on the continuity of slopes across mountain fronts in Taylor Valley (Sugden et al., 1995). Uplift during the Quaternary has been modest at ~ 300m (Sugden et al., 1995).

Taylor Glacier has likely been stable at its current margins since ~ 12.8 ka. Between 70 and 130 ka there is evidence for an advance of Taylor Glacier at least 10km down valley, associated with increasing ice thickness (Higgins et al., 2000; Kavanaugh et al., 2009). Higgins et al., (2000) describe Taylor Glacier and smaller alpine glaciers in the region expanding during interglacial periods over at least the past ~ 400ka and retreating during the coldest phases of the glacial periods. This repeated pattern of advance and retreat would lead to erosion beneath Taylor Glacier with the potential for fracturing of the underlying bedrock to shallow depths (Benn and Evans, 2010).

The subglacial environment beneath TG has no direct contact with the atmosphere, nor does the brine, except where it is forced to the surface at Blood Falls (Lyons et al., 2019). No englacial conduits, such as moulins, connect the glacier surface to the bed, even during the summer melt season (Lewis et al., 1998), so the subglacial environment is completely isolated from the atmosphere. Therefore, methane could have been accumulating in the brine-saturated

sediments and/or being incorporated into the basal ice of TG and subglacial brine flows could then carry the stored methane into WLB.

Deposition of Legacy Methane into WLB

The timing and amount of methane released from brines flowing beneath TG and into WLB would be dependent on glacial dynamics, subglacial hydrology and the hydrologic history of the lake. WLB has been ice-covered for a long period of time, perhaps on the order of 100,000 years (Poreda et al., 2004). It is not known when TG retreated to its current position, but it is estimated that an increased inflow event into WLB occurred about 3,000 years ago that raised the lake level to the height of the sill (Poreda et al., 2004). The most recent filling/spillover from WLB in ELB occurred ~250 years ago during a re-advance of TG (Hendy et al., 1977) that resulted in a permanent ice cover and stratified ELB ~200 years ago (Poreda et al., 2004). The highly stratified hydrological configuration of Lake Bonney formed ~200 years ago has persisted to this day (Poreda et al., 2004; Doran et al., 2014; Warrier et al., 2015), although a regional warming trend has altered aspects of the lake hydrology in the last few decades.

A subglacial/englacial hydrologic system exists beneath TG that supplies brine input into WLB at the terminus of the glacier (Badgeley et al., 2017; Lawrence et al., 2020; Fig. 3.14B). Approximately 20% of inputs to WLB are directly from TG (Doran et al., 2014). Proglacial streams Lawson and Lyons (Fig. 3.14A) contribute about 60-78% of inflow to WLB (Fountain et al., 1999; Doran et al., 2014).

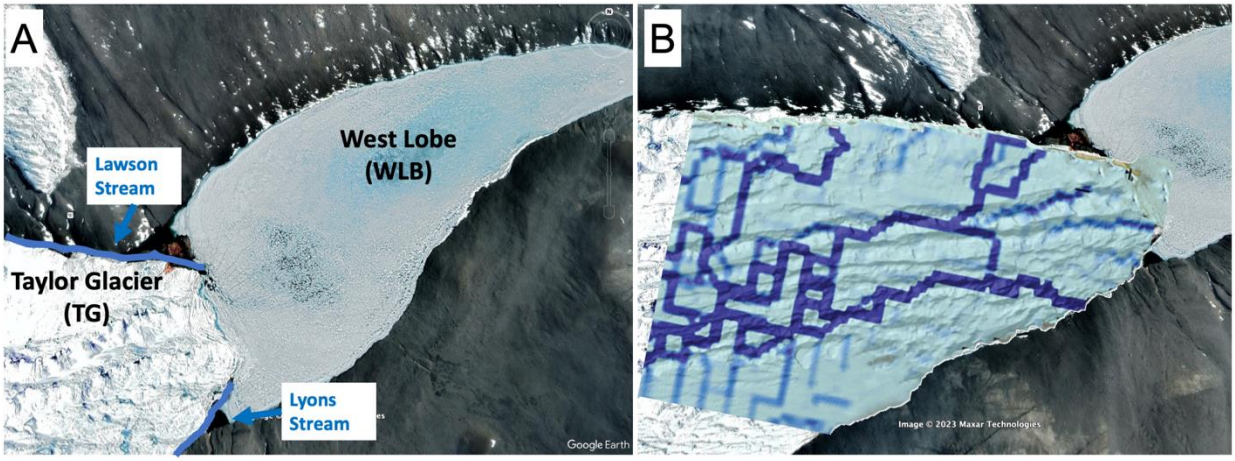


Fig. 3.14 Major fluvial inputs to West Lake Bonney (WLB). A) Seasonal, subaerial proglacial streams that flow into the peripheral moats that form on WLB during the summer melt season (Welch et al., 2010). B) Modelled Taylor Glacier englacial and subglacial flow paths for brine delivery into WLB (adapted from Lawrence et al., 2020). Satellite images from Google Earth.

Between 1969 and 2001, changing cloud cover patterns coupled with a gradual warming trend increased solar radiation and air temperatures in the Bonney Basin, leading to greater meltwater generation (Bomblies et al., 2001) and the level of Lake Bonney had risen ~5m by 1990, primarily adding increased depth to the freshwater layer above the chemocline (Spigel and Priscu, 1996). Taylor Valley underwent a subsequent cooling period from 1993-2002, during which there was relatively little glacier melt and low stream flows (McKnight et al., 1999). This led to a decline in lake levels by ~0.006 to 0.08 m yr^{-1} (Doran et al., 2008). The cooler period ended dramatically during the 2001-02 austral summer, which was the warmest on record for the MDV (Lyons et al., 2005; Doran et al., 2008). The lake level has continued to rise annually since then, adding over 3m of water to the epilimnion since 2002 (Fig. 3.6). Subglacial inflow to WLB would not be affected by increased surface temperatures (Badgeley et al., 2017; Lawrence et al., 2020), but changes to the glacier terminus position and depth could alter subglacial drainage patterns.

The density stratification in LB is primarily controlled by salinity because there is a wide range of salinities creating the vertical gradient, while temperature variations in the water are relatively small (Spigel et al., 2018). Since temperature profiles in the lake closely follow density profiles, small changes in temperature can be used as a passive tracer for water movements (Spigel and Priscu, 1998; Spigel et al., 2018). The depth of subglacial brine inflow to WLB is identified by a "temperature anomaly" within 100m of the glacier where temperatures at ~21m are 3-4ºC colder than in waters above, below, or >100m eastward (Spigel et al., 2018). The temperature of the subglacial brine is about -7ºC (Badgeley et al., 2017) and WLB water at 21m (>100m from the TG terminus), is about -1 to -2ºC (Spigel et al., 2018). The WLB water temperature at 21m near the glacier is -3 to -4.5ºC, which is consistent with colder brine inflows mixing with lake's ambient water temperature (Lawrence et al., 2020). Temperature profiles from 1991 show a similar temperature anomaly, but which occurs around 26m (Spigel et al., 2018). The authors attribute the change in depth to a restructuring of subglacial inflow to WLB, possibly coinciding with a calving event. Aerial photographs of TG show that portions of the terminus calved into the lake sometime between 1998 and 2006, which could explain the change in subglacial brine inflow depth from 26m to 21m, as indicated by the change in depth of the temperature anomaly (Spigel et al., 2018).

The long-term conductivity data for WLB show a change that could further constrain the timing of the TG subglacial reconfiguration. Water conductivity will decrease with decreasing temperature for a given salinity (Smith, 1962), so where the subglacial brine enters at 21m, the water conductivity is ~5 mS cm^{-1} lower than it is at 22-23m, creating a bow-shape in the profile

for WLB (Fig. 3.4A) This profile inversion seems to only have been present at its current depth since 2013 (Fig. 3.1).

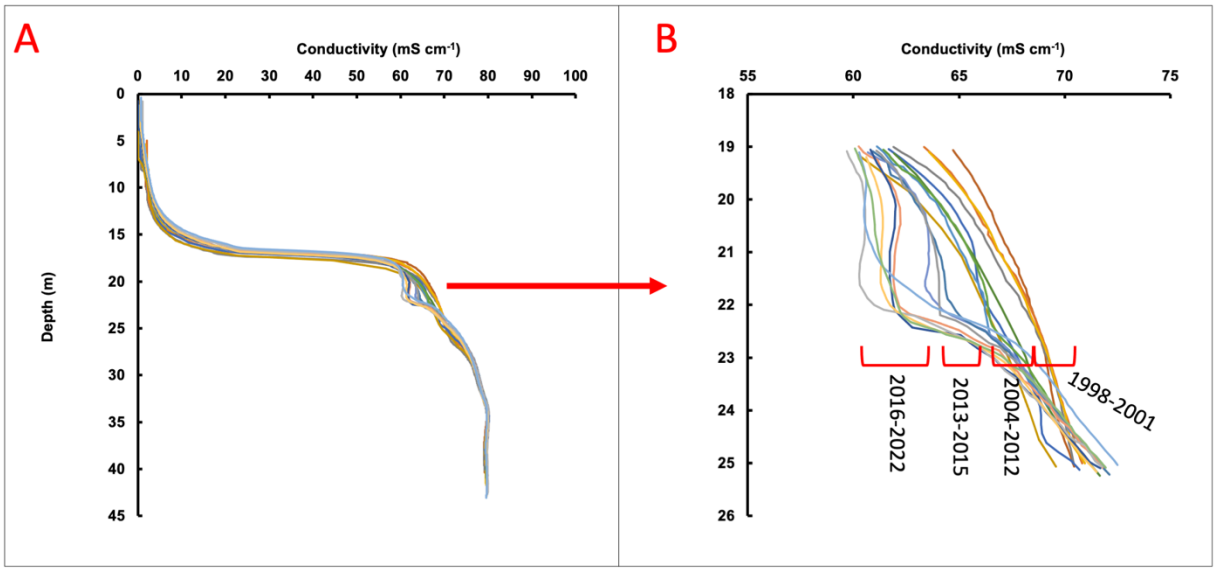


Fig. 3.15 Annual conductivity data for the West Lake Bonney water column at the MCM LTER sampling site (~600m east of Taylor Glacier terminus). A) Complete conductivity profiles from November of each year. All depth values are adjusted to the 2017 lake level. B) Enlargement of the anomalous section of the conductivity profile with brackets indicating the range of years in each cluster. Data from Priscu, 2023.

Profiles from 1998 to 2011 show the conductivity inversion moving upwards from ~26m, where the temperature anomaly was also measured in 1991 (Spigel et al., 2018), to ~23m in 2011 (Fig. 3.16).

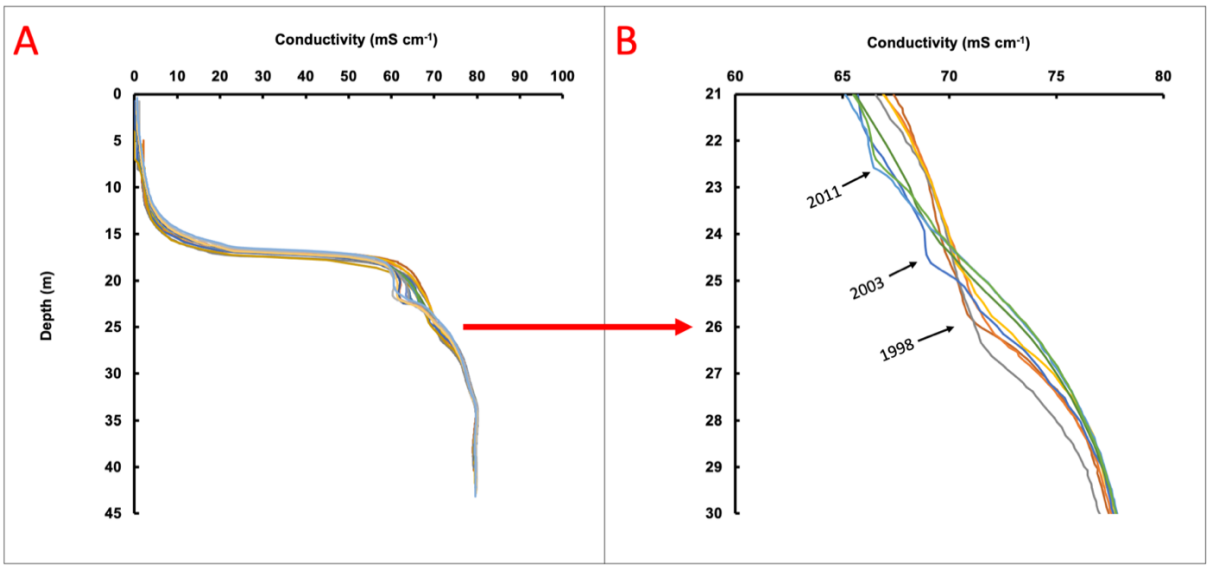


Fig. 3.16 Annual conductivity data for the West Lake Bonney water column at Location B (Fig. 3.7). (A) Complete conductivity profiles from November of each year. All depth values are referenced to the 2017 lake level. (B) Enlargement of the 21-30m section of the profile with the migrating anomaly labeled for select years. Data from Priscu, 2023.

Together these data suggest that the subglacial flow structure for TG changed starting around 1998, possibly due to the TG calving event observed by Spigel et al. (2018), until the depth of brine inflow stabilized around 2013 at 21m. The methane profiles in WLB in 2016 and 2017 (Fig. 3.8) have similar concentrations to a methane profile measured in 2012 (John Priscu, personal correspondence), indicating that the concentration for most of the gas profile changed little over five years. The methane concentrations at 25m and 30m in 2017 are 354 and 339 nmol L^{-1}, respectively, while the concentration at 22m, just below the current depth of subglacial inflow, is ~171 nmol L^{-1} (Fig. 3.8). The concentration difference could suggest that earlier methane inputs from beneath TG occurred at 30m, but a changing subglacial hydrology shifted the depth of brine inflow to WLB upwards, leading to the higher concentration at 25m, until another glacial change shifted the inflow depth to 21m. The brine inflow has occurred at 21m for

maybe only 5 years, possibly explaining the lower methane concentration there, compared to the 26m inflow depth in 1991 (Spigel et al., 2018).

The concentration of methane at 25m nearly doubled from November 2016 to November 2017, while the concentration at 30m increased by a comparatively small amount over that same timeframe (Fig. 3.8), suggesting the increased methane was associated with brine inflow. Lawrence et al. (2020) measured 24-48h periods of 1-2ºC water temperature decreases around 19m in WLB that coincided with katabatic wind events during the austral winters (May – August) of 2015 and 2016. Lawrence et al. (2020) interpreted the sudden water temperature decrease as the result of a subglacial brine "pulse" into WLB. The exact mechanistic connection between the high wind events and subglacial outflow is not known but Lawrence et al. (2020) suggest that high winds generate enough pressure on the lake surface ice to cause internal waves in the water column, possibly leading to a pressure reduction at the glacier front, triggering brine release from the TG subglacial environment (Lawrence et al., 2020).

The concentration of methane in WLB increases laterally eastward at the depth of glacial inflow (Fig. 3.7), which would seem contradictory if the glacier is the primary source at those depths. Diffusion and water flow would carry methane outward from the glacier, but higher concentrations would most likely occur at Location A (Fig. 3.7), near the source of the methane, dissipating in waters further away (e.g. Location B, Fig. 3.7). Spigel et al. (2018) observed a pattern of "layering" with the temperature anomalies that they associated with melting glacier ice and subglacial brine intrusions into a heavily stratified water column at depths of neutral buoyancy. Temperature and conductivity measurements from ~19m to near the lake bottom were recorded by an autonomous underwater vehicle (AUV) at multiple sampling points within 100m

of the glacier front in 2009 (Spigel et al., 2018). The AUV recorded Temperature decreases of 3-4ºC and density inversions of ~1-1.5 kg m^3 around 21m for multiple sampling locations (Spigel et al., 2018). Annual sampling at the MCM LTER location has also demonstrated abnormally cold temperatures around 21m (adjusted depth) since 2013 (Fig. 3.17; Li et al., 2020; Lawrence et al., 2020).

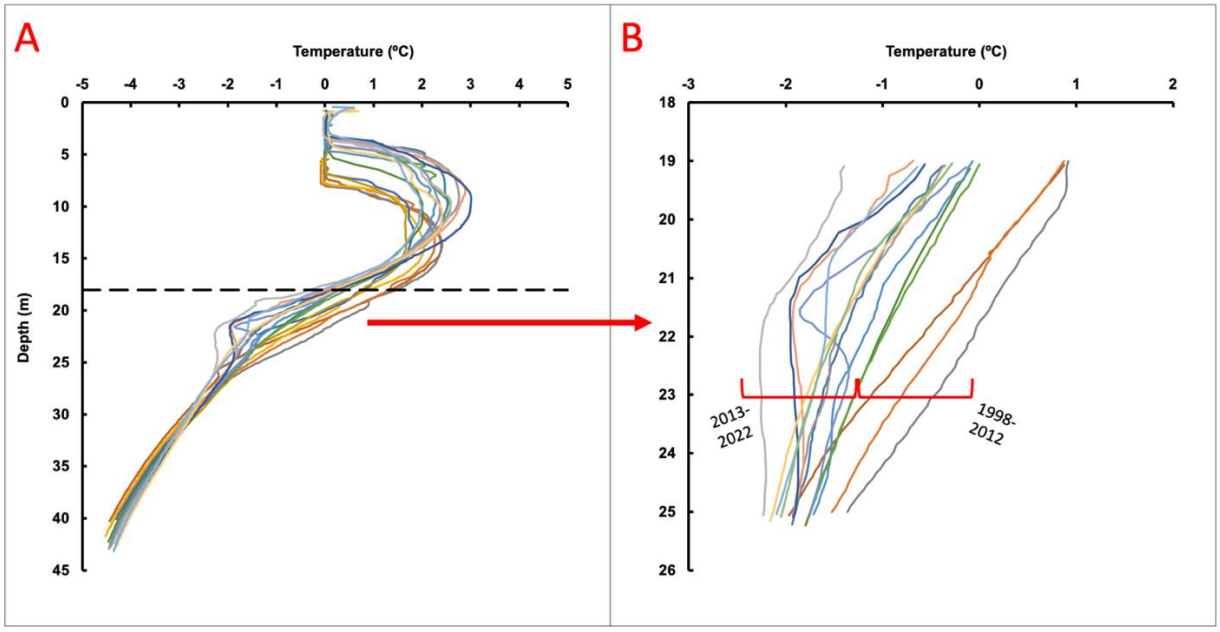


Fig. 3.17 (A) Annual temperature profile data for 1998-2022 for the West Lake Bonney water column Location B, Fig.3.7, measured in November each year. (Priscu, 2023). All depth values are referenced to the 2017 lake level. Dotted line indicates the depth of the chemocline (B) Enlargement of the 19 – 25m depth of the conductivity profile immediately below the chemocline with brackets indicating the range of years in each cluster.

Lawrence et al. (2020) suggest abnormally lower temperatures in the profiles that consistently appear between 20.3 and 21.7 m at multiple sampling sites from the glacier front, eastward into the lake, are evidence for horizontal brine flows. Lawrence et al. (2020) suggest that the brine intrusions travel laterally, cooling the water above and below until thermal equilibrium is reached. The lake water density between 18 and 23m (controlled predominantly by salinity) is

similar to that of the subglacial brine (1100 kg m^{-3}), so the cooler temperature of the brine creates a miniature thermal stratification, separating the brine intrusion from the slightly warmer waters above and below, leading to a lateral brine flow outward from the glacier (Lawrence et al., 2020). Heat transfer occurs between the brine layer and the warmer lake water above and below until thermal equilibrium is reached. Since the lower temperature anomaly has appeared at 21m at Location B consistently since ~2013 (Fig. 3.17), the brine flows may be travelling that far into WLB. If the brine contains dissolved methane, the temperature stratification could limit gas diffusion from the lateral brine flow until thermal equilibrium is reached. The retention of methane gas within the brine until the point of thermal equilibrium could explain the higher concentration of methane at Location B, (354nM at 25m depth) relative to Location A, nearest the glacier, (287 nM at 24m depth) (Fig. 3.7).

Potential Impact of Organosulfur-Mineral Reactions on ELB Methane Pool

Lateral transport of glacially-derived methane likely does not extend to ELB, as most water exchange across the narrows occurs above the chemoclines of both lobes (Spigel and Priscu, 1998; Spigel et al., 2018). The methane concentration peak in ELB below the chemocline (Fig. 3.7), may represent methane supplied to ELB during a prior spillover event from WLB into ELB ~250 years ago (Hendy et al., 1977). The $\delta^{13}C$-CH_4 value at 25m in ELB (-29‰) is more similar to the sub-chemocline $\delta^{13}C$-CH_4 values in WLB (-29‰ to -26‰) than those in the shallower depths of ELB (-43 to -50‰) (Fig. 3.9), consistent with spillover from WLB as the source. This is supported by dissolved inorganic carbon (DIC) measurements in ELB. The apparent age of DIC increases with depth in WLB, but in ELB the oldest DIC is found immediately below the chemocline (~20-25m), with younger DIC below 25m (Doran et al.,

2014). Likely older, more saline water from WLB passed over the sill and sank to a depth of equal density in ELB as the basin was filling (Spigel and Priscu, 1998; Doran et al., 2014), possibly carrying methane as well. The $\delta^{2}H\text{-}CH_4$ values, however, are -169‰ and -164‰ at 20 and 25m, respectively, in ELB, which differs from the WLB values at the concentration peak, which range from -144‰ to -141‰ (Fig. 3.8, Fig. 3.9). This potentially indicates an additional methane source in ELB with a $\delta^{13}C\text{-}CH_4$ value similar to the spillover methane input but with a more negative $^{2}H\text{-}CH_4$, perhaps from the organosulfur-mineral reactions proposed in reactions 1-5 in section 4.2 above.

The reactants necessary for methane generation from organosulfur-mineral reactions are also present in ELB, without requiring direct inputs from TG. Waters at the depths of the methane peak contain DMSO (Fig. 3.13B; Lee et al., 2004) and fine-grained sediment particles deposited on the ice surface can be transported through the ice via melting to the ELB water column (Fritsen and Priscu, 1999; Vick-Majors et al., 2014) and across the sill from WLB (Spigel et al., 2018). As in WLB, the concentration of DMSO is relatively low above the chemocline, so reactions with sinking particles would be limited until 20-25m, which is coincident with the methane peak (Fig. 3.13B). If this reaction is occurring below the chemocline, the methane generated could potentially have a greater impact on the bulk $\delta^{2}H\text{-}CH_4$ in ELB because the overall concentration of methane is an order of magnitude lower than in WLB. Calculations for this scenario are presented in Table 3.3, where hypothetical proportions of each methane source and their respective $\delta^{2}H\text{-}CH_4$ are considered in an isotope mixing model.

Table 3.3 Calculations for hypothetical WLB/ELB methane mixing model

	A	B	C	D	E	F	G
	Mean δ^2H-CH_4 values in WLB	δ^2H-H_2O of ELB Water	Hypothetical Proportion of CH_4 sourced from WLB	Proportion of CH_4 derived from DMSO	Calculated δ^2H-CH_4 of Mixture	CH_4 Concentrations in Narrows and ELB (nM)	Calculated concentration of DMSO-generated CH_4 based on Column D proportions (nM)
	-141.6	-320	0.856	0.144	-167.3	Narrows: 19.7	2.8
	-141.6	-320	0.841	0.159	-170.0	ELB 20m: 13.3	2.1
	-141.6	-320	0.873	0.127	-164.3	ELB 25m: 31.0	3.9
Calculations (Letters indicate column values)	Measured in lake water (this study)	Measured in lake water (Gooseff et al., 2006)	Hypothetical	1-C	(A*C)+(B*D)	Measured in lake (this study)	(D*F)

The first model assumption is that the three hydrogens in DMSO and the fourth hydrogen in the subsequently formed methane via reactions 1-5 (above section: "Methanogenesis from Organosulfur Compound-Mineral Reactions"), are all sourced from the lake water, without any isotopic fractionation. Therefore, the δ^2H-CH_4 from organosulfur-mineral reactions would be -320 ‰ (Table 3.3, Column B). The second model assumption is that relict methane from the WLB spillover event has a δ^2H-CH_4 of -141.6 ‰, (Table 3.3, Column C) the average value for the sub-chemocline waters in WLB (Table 3.1, Fig. 3.8). We assume these two end members are the only sources and model the proportions of each required to achieve the measured δ^2H-CH_4 values for sub-chemocline ELB waters and those in the base of The Narrows. The model shows that 12 – 16% of the total methane in ELB could be from DMSO generated methane (Table 3.3, Column D). From the isotope mixing model proportions one can calculate that the concentration of DMSO-derived methane needed to shift the δ^2H-CH_4 signature from the WLB-measured value to that observed in ELB, is 2.1– 3.9 nM (Table 3.3, Column G). Thus, methane input from the

organosulfur-mineral reactions provide a potential explanation for the measured differences in $\delta^{2}H\text{-}CH_4$ between the sub-chemocline waters in WLB and ELB.

Conclusions

Potential abiotic methane sources for the methane pool in WLB below the chemocline were investigated: melting TG basal ice, crushed TG basal sediments, and crushed TG sediment-organosulfur compound reactions from WLB. The isotopic composition of the methane from each of these sources was measured and compared with the isotopic composition of the WLB waters. All three processes generated methane with $\delta^{13}C\text{-}CH_4$ values similar to those in the lake waters below the chemocline (20m depth) in WLB. Methane from crushed basal sediments had $\delta^{2}H\text{-}CH_4$ values that were significantly different (-70‰) than the lake water $\delta^{2}H\text{-}CH_4$ values at 20 and 25m depth, suggesting this is unlikely to be a major source for the WLB methane pool. Melting basal ice yielded $\delta^{13}C\text{-}CH_4$ values similar to those of crushed basal sediments plus sediment-organosulfur compound reactions from WLB waters. No $\delta^{2}H\text{-}CH_4$ measurements were made from the experiments with WLB waters and TG crushed sediment or from the melting basal ice so it was not possible to use an isotope mass balance approach to assess their relative potential contributions to the WLB methane pool. However, other analysis showed that neither process would likely be significant contributors to the methane pool. One caveat to this finding is that it is possible that the $\delta^{2}H\text{-}CH_4$ values from melting basal could be similar to the deep methane pool and if so, further work assessing both the variability in methane concentration in the ice and the flux of ice into the lake would be warranted. Future research should focus on $\delta^{2}H\text{-}CH_4$ measurements of the potential contributory processes.

Methane derived from DMSO reactions with iron-bearing minerals in sinking sediment particles may be a proportionately more significant process in ELB. Methane concentrations below the chemocline are an order of magnitude lower in ELB than WLB, but the $\delta^{13}C\text{-}CH_4$ values suggest it has a similar source as WLB. Most of the methane in ELB was likely supplied during a spillover event from WLB ~250 years ago. The $\delta^{2}H\text{-}CH_4$ values for ELB were different from WLB, potentially indicating an additional methane source in ELB with a $\delta^{13}C\text{-}CH_4$ value similar to the spillover methane input from WLB but with a more negative $^{2}H\text{-}CH_4$, likely from the organosulfur compound-mineral reactions. This is, to the author's knowledge, the first data set that is consistent with organosulfur compound-mineral reactions producing methane in a natural system.

References

Althoff, F., Jugold, A., & Keppler, F. (2010). Methane formation by oxidation of ascorbic acid using iron minerals and hydrogen peroxide. Chemosphere, 80(3), 286-292.

Althoff, F., Benzing, K., Comba, P., McRoberts, C., Boyd, D. R., Greiner, S., & Keppler, F. (2014). Abiotic methanogenesis from organosulphur compounds under ambient conditions. Nature Communications, 5(1), 4205.

Badgeley, J. A., Pettit, E. C., Carr, C. G., Tulaczyk, S., Mikucki, J. A., Lyons, W. B., & MIDGE Science Team. (2017). An englacial hydrologic system of brine within a cold glacier: Blood Falls, McMurdo Dry Valleys, Antarctica. Journal of Glaciology, 63(239), 387-400.

Ballance, P. F., & Waiters, W. A. (2002). Hydrothermal alteration, contact metamorphism, and authigenesis in Ferrar Supergroup and Beacon Supergroup rocks, Carapace Nunatak, Allan Hills, and Coombs Hills, Victoria Land, Antarctica. *New Zealand Journal of Geology and Geophysics*, *45*(1), 71-84.

Benn, D., & Evans, D. J. (2010). Glaciers and glaciation. Routledge.

Bernet, M., & Gaupp, R. (2005). Diagenetic history of Triassic sandstone from the Beacon Supergroup in central Victoria Land, Antarctica. *New Zealand Journal of Geology and Geophysics*, *48*(3), 447-458.

Bomblies, A., McKnight, D. M., & Andrews, E. D. (2001). Retrospective simulation of lake-level rise in Lake Bonney based on recent 21-year record: indication of recent climate change in the McMurdo Dry Valleys, Antarctica. Journal of Paleolimnology, 25, 477-492.

Bueno de Mesquita, C. P., Wu, D., & Tringe, S. G. (2023). Methyl-based methanogenesis: an ecological and genomic review. *Microbiology and Molecular Biology Reviews*, *87*(1), e00024-22.

Burns, R., Wynn, P. M., Barker, P., McNamara, N., Oakley, S., Ostle, N., Stott, A.W., Tuffen, H., Zhou, Z., Tweed F.S., & Stuart, M. (2018). Direct isotopic evidence of biogenic methane production and efflux from beneath a temperate glacier. Scientific reports, 8(1), 17118.

Boyd, E. S., Skidmore, M., Mitchell, A. C., Bakermans, C., & Peters, J. W. (2010). Methanogenesis in subglacial sediments. Environmental microbiology reports, 2(5), 685-692.

Carr, S. A., Schubotz, F., Dunbar, R. B., Mills, C. T., Dias, R., Summons, R. E., & Mandernack, K. W. (2018). Acetoclastic Methanosaeta are dominant methanogens in organic-rich Antarctic marine sediments. *The ISME Journal*, *12*(2), 330-342.

Coolen, M. J., Hopmans, E. C., Rijpstra, W. I. C., Muyzer, G., Schouten, S., Volkman, J. K., & Damsté, J. S. S. (2004). Evolution of the methane cycle in Ace Lake (Antarctica) during the Holocene: response of methanogens and methanotrophs to environmental change. Organic Geochemistry, 35(10), 1151-1167.

Cox, S., Turnbull, I. M., Isaac, M. J., Townsend, D., & Lyttle, B. S. (2012). Geology of southern Victoria land Antarctica. Institute of Geological & Nuclear Sciences 1:250 000 Geological Map 22, 1-140.

Cragg, B. A., Parkes, R. J., Fry, J. C., Herbert, R. A., Wimpenny, J. W., & Getliff, J. M. (1990). Bacterial biomass and activity profiles within deep sediment layers. In Proceedings of the Ocean Drilling Program Scientific Results (Vol. 112, pp. 607-619). Ocean Drilling Program.

Cross, J. M., Fountain, A. G., Hoffman, M. J., & Obryk, M. K. (2022). Physical Controls on the Hydrology of Perennially Ice-Covered Lakes, Taylor Valley, Antarctica (1996-2013). Journal of Geophysical Research: Earth Surface, e2022JF006833.

Damm, E., Kiene, R. P., Schwarz, J., Falck, E., & Dieckmann, G. (2008). Methane cycling in Arctic shelf water and its relationship with phytoplankton biomass and DMSP. Marine Chemistry, 109(1-2), 45-59.

Dieser, M., Broemsen, E. L., Cameron, K. A., King, G. M., Achberger, A., Choquette, K., Hagedorn, B., Sletten, R., Junge, K., & Christner, B. C. (2014). Molecular and biogeochemical evidence for methane cycling beneath the western margin of the Greenland Ice Sheet. The ISME journal, 8(11), 2305-2316.

Doran, P. T., McKay, C. P., Fountain, A. G., Nylen, T., McKnight, D. M., Jaros, C., & Barrett, J. E. (2008). Hydrologic response to extreme warm and cold summers in the McMurdo Dry Valleys, East Antarctica. Antarctic Science, 20(5), 499-509.

Doran, P. T., Kenig, F., Knoepfle, J. L., Mikucki, J. A., & Lyons, W. B. (2014). Radiocarbon distribution and the effect of legacy in lakes of the McMurdo Dry Valleys, Antarctica. Limnology and oceanography, 59(3), 811-826.

Doran, P.T. & Gooseff, M.N. (2023). Lake level surveys in the McMurdo Dry Valleys, Antarctica (1991-2023, ongoing). Environmental Data Initiative. DOI: 10.6073/pasta/927439563d37c9461011e0060a5c1a87

Dugan, H. A., Obryk, M. K., & Doran, P. T. (2013). Lake ice ablation rates from permanently ice-covered Antarctic lakes. Journal of Glaciology, 59(215), 491-498.

Elston, D. P., & Bressler, S. L. (1981). Magneto-stratigraphic studies in neogene deposits of Taylor Valley and McMurdo Sound, Antarctica. Journal of the Royal Society of New Zealand, 11(4), 481-486.

Elliot, D. H., & Fleming, T. H. (2004). Occurrence and dispersal of magmas in the Jurassic Ferrar large igneous province, Antarctica. *Gondwana Research*, *7*(1), 223-237.

Etiope, G., & Klusman, R. W. (2002). Geologic emissions of methane to the atmosphere. Chemosphere, 49(8), 777-789.

Etiope, G., Oehler, D. Z., & Allen, C. C. (2011). Methane emissions from Earth's degassing: Implications for Mars. Planetary and Space Science, 59(2-3), 182-195.

Etiope, G., & Sherwood Lollar, B. (2013). Abiotic methane on Earth. Reviews of Geophysics, 51(2), 276-299.

Faure, G., Mensing, T. M., Faure, G., & Mensing, T. M. (2011). Ferrar Group: Dolerite Sills and the Dufek Intrusion. *The Transantarctic Mountains: Rocks, Ice, Meteorites and Water*, 415-469.

Ferrar, H. T. (1905). Notes on the physical geography of the Antarctic. *The Geographical Journal*, *25*(4), 373-382.

Ferry, J. G., & Lessner, D. J. (2008). Methanogenesis in marine sediments. *Annals of the New York Academy of Sciences*, *1125*(1), 147-157.

Florez-Leiva, L., Damm, E., & Farías, L. (2013). Methane production induced by dimethylsulfide in surface water of an upwelling ecosystem. Progress in oceanography, 112, 38-48.

Fountain, A. G., Lyons, W. B., Burkins, M. B., Dana, G. L., Doran, P. T., Lewis, K. J., McKnight, D.M., Moorehead, D.L., Parsons, A.N., Priscu, J.C., & Wall, D.H. (1999). Physical controls on the Taylor Valley ecosystem, Antarctica. Bioscience, 49(12), 961-971.

Fritsen, C. H., & Priscu, J. C. (1999). Seasonal change in the optical properties of the permanent ice cover on Lake Bonney, Antarctica: consequences for lake productivity and phytoplankton dynamics. Limnology and Oceanography, 44(2), 447-454.

Garcia, J. L. (1990). Taxonomy and ecology of methanogens. FEMS Microbiology Letters, 87(3-4), 297-308.

Gill-Olivas, B., Telling, J., Tranter, M., Skidmore, M., Christner, B., O'Doherty, S., & Priscu, J. (2021). Subglacial erosion has the potential to sustain microbial processes in Subglacial Lake Whillans, Antarctica. Communications Earth & Environment, 2(1), 134.

Gill-Olivas, B., Telling, J., Skidmore, M., & Tranter, M. (2023). Abrasion of sedimentary rocks as a source of hydrogen peroxide and nutrients to subglacial ecosystems. Biogeosciences, 20(5), 929-943.

Glatz, R. E., Lepp, P. W., Ward, B. B., & Francis, C. A. (2006). Planktonic microbial community composition across steep physical/chemical gradients in permanently ice-covered Lake Bonney, Antarctica. Geobiology, 4(1), 53-67.

Gooseff, M. N., Lyons, W. B., McKnight, D. M., Vaughn, B. H., Fountain, A. G., & Dowling, C. (2006). A stable isotopic investigation of a polar desert hydrologic system, McMurdo Dry Valleys, Antarctica. Arctic, Antarctic, and Alpine Research, 38(1), 60-71.

Hall, B. L., & Denton, G. H. (2000). Radiocarbon chronology of Ross Sea drift, eastern Taylor Valley, Antarctica: Evidence for a grounded ice sheet in the Ross Sea at the last glacial maximum. Geografiska Annaler: Series A, Physical Geography, 82(2-3), 305-336.

Hamilton, W., & Hayes, P. T. (1963). *Type section of the Beacon Sandstone of Antarctica* (No. 456-A).

Hendy, C. H., Wilson, A. T., Popplewell, K. B., & House, D. A. (1977). Dating of geochemical events in Lake Bonney, Antarctica, and their relation to glacial and climate changes. New Zealand Journal of Geology and Geophysics, 20(6), 1103-1122.

Herscu-Kluska, R., Masarwa, A., Saphier, M., Cohen, H., & Meyerstein, D. (2008). Mechanism of the reaction of radicals with peroxides and dimethyl sulfoxide in aqueous solution. Chemistry–A European Journal, 14(19), 5880-5889.

Higgins, S. M., Hendy, C. H., & Denton, G. H. (2000). Geochronology of Bonney drift, Taylor Valley, Antarctica: evidence for interglacial expansions of Taylor Glacier. Geografiska Annaler: Series A, Physical Geography, 82(2-3), 391-409.

Horita, J., & Berndt, M. E. (1999). Abiogenic methane formation and isotopic fractionation under hydrothermal conditions. *Science*, *285*(5430), 1055-1057.

Hubbard, B., Cook, S., & Coulson, H. (2009). Basal ice facies: a review and unifying approach. Quaternary Science Reviews, 28(19-20), 1956-1969.

Isbell, J. L. (1999). The Kukri Erosion Surface; a reassessment of its relationship to rocks of the Beacon Supergroup in the central Transantarctic Mountains, Antarctica. *Antarctic Science*, *11*(2), 228-238.

Jeffrey, A. W. A., & Kaplan, I. R. (1988). Hydrocarbons and inorganic gases in the Gravberg-1 well, Siljan Ring, Sweden. Chemical Geology, 71(1-3), 237-255.

Kavanaugh, J. L., Cuffey, K. M., Morse, D. L., Bliss, A. K., & Aciego, S. M. (2009). Dynamics and mass balance of Taylor Glacier, Antarctica: 3. State of mass balance. Journal of Geophysical Research: Earth Surface, 114(F4).

Karr, E. A., Ng, J. M., Belchik, S. M., Sattley, W. M., Madigan, M. T., & Achenbach, L. A. (2006). Biodiversity of methanogenic and other Archaea in the permanently frozen Lake Fryxell, Antarctica. Applied and Environmental Microbiology, 72(2), 1663-1666.

Klintzsch, T., Geisinger, H., Wieland, A., Langer, G., Nehrke, G., Bizic, M., Greule, M., Lenhart, K., Borsch, C., Schroll, M., & Keppler, F. (2023). Stable carbon isotope signature of

methane released from phytoplankton. *Geophysical research letters*, *50*(12), e2023GL103317.

Kong, W., Li, W., Romancova, I., Prášil, O., & Morgan-Kiss, R. M. (2014). An integrated study of photochemical function and expression of a key photochemical gene (psbA) in photosynthetic communities of Lake Bonney (McMurdo Dry Valleys, Antarctica). FEMS Microbiology Ecology, 89(2), 293-302.

Kwon, M., Kim, M., Takacs-Vesbach, C., Lee, J., Hong, S. G., Kim, S. J., Priscu, J.C. & Kim, O. S. (2017). Niche specialization of bacteria in permanently ice-covered lakes of the M cMurdo Dry Valleys, Antarctica. Environmental microbiology, 19(6), 2258-2271.

Lawrence, J. P., Doran, P. T., Winslow, L. A., & Priscu, J. C. (2020). Subglacial brine flow and wind-induced internal waves in Lake Bonney, Antarctica. Antarctic Science, 32(3), 223-237.

Lawson Knoepfle, J., Doran, P. T., Kenig, F., Lyons, W. B., & Galchenko, V. F. (2009). Particulate organic and dissolved inorganic carbon stable isotopic compositions in Taylor Valley lakes, Antarctica: the effect of legacy. Hydrobiologia, 632, 139-156.

Lee, P. A., Priscu, J. C., DiTullio, G. R., Riseman, S. F., Tursich, N., & de Mora, S. J. (2004). Elevated levels of dimethylated-sulfur compounds in Lake Bonney, a poorly ventilated Antarctic lake. Limnology and oceanography, 49(4), 1044-1055.

Lee, H., Hwang, K., Cho, A., Kim, S., Kim, M., Morgan-Kiss, R., Priscu, J.C., Kim, K.M., & Kim, O. S. (2023). Microbial assemblages and associated biogeochemical processes in Lake Bonney, a permanently ice-covered lake in the McMurdo Dry Valleys, Antarctica.

Levy, J. (2013). How big are the McMurdo Dry Valleys? Estimating ice-free area using Landsat image data. Antarctic Science, 25(1), 119-120.

Lewis, K. J., Fountain, A. G., & Dana, G. L. (1998). Surface energy balance and meltwater production for a Dry Valley glacier, Taylor Valley, Antarctica. Annals of Glaciology, 27, 603-609.

Li, W., Dore, J. E., Steigmeyer, A. J., Cho, Y. J., Kim, O. S., Liu, Y., Morgan-Kiss, R.M., Skidmore, M., & Priscu, J. C. (2020). Methane production in the oxygenated water column of a perennially ice-covered Antarctic lake. Limnology and Oceanography, 65(1), 143-156.

Lyons, W., Fountain R., Priscu, J. C., Neumann, K, & Welch, K. A. (2000). Importance of landscape position and legacy: the evolution of the lakes in Taylor Valley, Antarctica. Freshwater Biology, 43(3), 355-367.

Lyons, W. B., Welch, K. A., Snyder, G., Olesik, J., Graham, E. Y., Marion, G. M., & Poreda, R. J. (2005). Halogen geochemistry of the McMurdo Dry Valleys lakes, Antarctica: clues to the origin of solutes and lake evolution. Geochimica et Cosmochimica Acta, 69(2), 305-323.

Lyons, W. B., Mikucki, J. A., German, L. A., Welch, K. A., Welch, S. A., Gardner, C. B., Tulaczyk, S.M; Pettit, E.C., Kowalski, J., & Dachwald, B. (2019). The geochemistry of englacial brine from Taylor Glacier, Antarctica. Journal of Geophysical Research: Biogeosciences, 124(3), 633-648.

Madigan, M. T., Bender, K. S., Buckley, D. H., Sattley, W. M., & Stahl, D. A. (2018). Brock biology of microorganisms. 15th Global Edition. Boston, US: Benjamin Cummins, 1, 1391-1407.

McElwain, J. C., Wade-Murphy, J., & Hesselbo, S. P. (2005). Changes in carbon dioxide during an oceanic anoxic event linked to intrusion into Gondwana coals. Nature, 435(7041), 479-482.

McKnight, D. M., Niyogi, D. K., Alger, A. S., Bomblies, A., Conovitz, P. A., & Tate, C. M. (1999). Dry valley streams in Antarctica: ecosystems waiting for water. Bioscience, 49(12), 985-995.

Michaud, A. B., Dore, J. E., Achberger, A. M., Christner, B. C., Mitchell, A. C., Skidmore, M. L., Vick-Majors, T., & Priscu, J. C. (2017). Microbial oxidation as a methane sink beneath the West Antarctic Ice Sheet. Nature Geoscience, 10(8), 582-586.

Milkov, A. V., & Etiope, G. (2018). Revised genetic diagrams for natural gases based on a global dataset of> 20,000 samples. Organic geochemistry, 125, 109-120.

Mitterer, R. M. (2010). Methanogenesis and sulfate reduction in marine sediments: A new model. *Earth and Planetary Science Letters*, *295*(3-4), 358-366.

Montross, S., Skidmore, M., Christner, B., Samyn, D., Tison, J. L., Lorrain, R., Doyle, S. & Fitzsimons, S. (2014). Debris-rich basal ice as a microbial habitat, Taylor Glacier, Antarctica. Geomicrobiology Journal, 31(1), 76-81.

Newberry, C. J., Webster, G., Cragg, B. A., Parkes, R. J., Weightman, A. J., & Fry, J. C. (2004). Diversity of prokaryotes and methanogenesis in deep subsurface sediments from the Nankai Trough, Ocean Drilling Program Leg 190. Environmental Microbiology, 6(3), 274-287.

Penger, J., Conrad, R., & Blaser, M. (2012). Stable carbon isotope fractionation by methylotrophic methanogenic archaea. Applied and environmental microbiology, 78(21), 7596-7602.

Pettit, E. C., Whorton, E. N., Waddington, E. D., & Sletten, R. S. (2014). Influence of debris-rich basal ice on flow of a polar glacier. Journal of Glaciology, 60(223), 989-1006.

Poreda, R. J., Hunt, A. G., Lyons, W. B., & Welch, K. A. (2004). The helium isotopic chemistry of Lake Bonney, Taylor Valley, Antarctica: Timing of late Holocene climate change in Antarctica. Aquatic Geochemistry, 10, 353-371.

Prentice, M. L., Kleman, J. L., & Stroeven, A. P. (1998). The composite glacial erosional landscape of the northern McMurdo Dry Valleys: Implications for Antarctic Tertiary glacial history. *Ecosystem Dynamics in a Polar Desert: the Mcmurdo Dry Valleys, Antarctica, 72*, 1-38.

Priscu, J.C. 2023. Conductivity, temperature, and depth (CTD) vertical profiles collected from lakes in the McMurdo Dry Valleys, Antarctica (1993-2023, ongoing). Environmental Data Initiative. DOI: 10.6073/pasta/650871571843bde5e0db6fb52cf549a4. Dataset accessed 1 April 2024.

Raiswell, R., Benning, L. G., Davidson, L., Tranter, M., & Tulaczyk, S. (2009). Schwertmannite in wet, acid, and oxic microenvironments beneath polar and polythermal glaciers. Geology, 37(5), 431-434.

Repeta, D. J., Ferrón, S., Sosa, O. A., Johnson, C. G., Repeta, L. D., Acker, M., DeLong, E., & Karl, D. M. (2016). Marine methane paradox explained by bacterial degradation of dissolved organic matter. Nature Geoscience, 9(12), 884-887.

Riley, T. R., & Knight, K. B. (2001). Age of pre-break-up Gondwana magmatism. *Antarctic Science, 13*(2), 99-110.

Rivkina, E., Shcherbakova, V., Laurinavichius, K., Petrovskaya, L., Krivushin, K., Kraev, G., Pecheritsina, S.; & Gilichinsky, D. (2007). Biogeochemistry of methane and methanogenic archaea in permafrost. FEMS microbiology ecology, 61(1), 1-15.

Sander, R. (2015). Compilation of Henry's law constants (version 4.0) for water as solvent. Atmospheric Chemistry and Physics, 15(8), 4399-4981.

Sasakawa, M., Tsunogai, U., Kameyama, S., Nakagawa, F., Nojiri, Y., & Tsuda, A. (2008). Carbon isotopic characterization for the origin of excess methane in subsurface seawater. *Journal of Geophysical Research: Oceans*, *113*(C3).

Saxton, M. A., Samarkin, V. A., Schutte, C. A., Bowles, M. W., Madigan, M. T., Cadieux, S. B., Pratt, L.M. & Joye, S. B. (2016). Biogeochemical and 16S rRNA gene sequence evidence supports a novel mode of anaerobic methanotrophy in permanently ice-covered Lake Fryxell, Antarctica. Limnology and Oceanography, 61(S1), S119-S130.

Saxton, M. A., Samarkin, V. A., Madigan, M. T., Bowles, M. W., Sattley, W. M., Schutte, C. A., & Joye, S. B. (2021). Sulfate reduction and methanogenesis in the hypersaline deep waters and sediments of a perennially ice-covered lake. Limnology and Oceanography, 66(5), 1804-1818.

Schoell, M. (1980). The hydrogen and carbon isotopic composition of methane from natural gases of various origins. Geochimica et cosmochimica ACTA, 44(5), 649-661.

Sebacher, D. I., Harriss, R. C., Bartlett, K. B., Sebacher, S. M., & Grice, S. S. (1986). Atmospheric methane sources: Alaskan tundra bogs, an alpine fen, and a subarctic boreal marsh. Tellus B, 38(1), 1-10.

Smith, S. H. (1962). Temperature correction in conductivity measurements 1. Limnology and Oceanography, 7(3), 330-334.

Sosa, O. A., Repeta, D. J., Ferrón, S., Bryant, J. A., Mende, D. R., Karl, D. M., & DeLong, E. F. (2017). Isolation and characterization of bacteria that degrade phosphonates in marine dissolved organic matter. Frontiers in microbiology, 8, 1786.

Sperazza, M., Moore, J. N., & Hendrix, M. S. (2004). High-resolution particle size analysis of naturally occurring very fine-grained sediment through laser diffractometry. Journal of Sedimentary Research, 74(5), 736-743.

Spigel, R. H., & Priscu, J. C. (1996). Evolution of temperature and salt structure of Lake Bonney, a chemically stratified Antarctic lake. Hydrobiologia, 321, 177-190.

Spigel, R. H., & Priscu, J. C. (1998). Physical limnology of the McMurdo Dry Valleys lakes. Ecosystem dynamics in a polar desert: the McMurdo Dry Valleys, Antarctica, 72, 153-187.

Spigel, R. H., Priscu, J. C., Obryk, M. K., Stone, W., & Doran, P. T. (2018). The physical limnology of a permanently ice-covered and chemically stratified Antarctic lake using

high resolution spatial data from an autonomous underwater vehicle. Limnology and Oceanography, 63(3), 1234-1252.

Steiner, M. G., & Babbs, C. F. (1990). Quantitation of the hydroxyl radical by reaction with dimethyl sulfoxide. Archives of biochemistry and biophysics, 278(2), 478-481.

Stibal, M., Wadham, J. L., Lis, G. P., Telling, J., Pancost, R. D., Dubnick, A., Sharp, M., Lawson, E., Butler, C., Hasan, F., Tranter, M., & Anesio, A. M. (2012). Methanogenic potential of Arctic and Antarctic subglacial environments with contrasting organic carbon sources. Global Change Biology, 18(11), 3332-3345.

Stolper, D. A., Lawson, M., Davis, C. L., Ferreira, A. A., Neto, E. S., Ellis, G. S., Lewan, M.D., Martini, A.M., Tang, Y., Schoell, M., Sessions, A.L., & Eiler, J. M. (2014). Formation temperatures of thermogenic and biogenic methane. *Science*, *344*(6191), 1500-1503.

Sugden, D. E., Denton, G. H., & Marchant, D. R. (1995). Landscape evolution of the Dry Valleys, Transantarctic Mountains: tectonic implications. Journal of Geophysical Research: Solid Earth, 100(B6), 9949-9967.

Taenzer, L., Carini, P. C., Masterson, A. M., Bourque, B., Gaube, J. H., & Leavitt, W. D. (2020). Microbial methane from methylphosphonate isotopically records source. *Geophysical Research Letters*, *47*(1), e2019GL085872.

Tang, C., Madigan, M. T., & Lanoil, B. (2013). Bacterial and archaeal diversity in sediments of west Lake Bonney, McMurdo Dry Valleys, Antarctica. Applied and environmental microbiology, 79(3), 1034-1038.

Tazaz, A. M., Bebout, B. M., Kelley, C. A., Poole, J., & Chanton, J. P. (2013). Redefining the isotopic boundaries of biogenic methane: Methane from endoevaporites. Icarus, 224(2), 268-275.

Urbanski, S. P., Stickel, R. E., & Wine, P. H. (1998). Mechanistic and kinetic study of the gas-phase reaction of hydroxyl radical with dimethyl sulfoxide. The Journal of Physical Chemistry A, 102(51), 10522-10529.

Vavra, C. L., KD, S., & JW, C. (1979). Sedimentary petrology of the Triassic Fremouw Formation, central Transantarctic Mountains.

Vick-Majors, T. J., Priscu, J. C., & Amaral-Zettler, L. A. (2014). Modular community structure suggests metabolic plasticity during the transition to polar night in ice-covered Antarctic lakes. The ISME journal, 8(4), 778-789.

Wadham, J. L., Tranter, M., Tulaczyk, S., & Sharp, M. (2008). Subglacial methanogenesis: a potential climatic amplifier?. Global Biogeochemical Cycles, 22(2).

Wadham, J. L., Arndt, S., Tulaczyk, S., Stibal, M., Tranter, M., Telling, J., Lis, G.P., Lawson, E., Ridgwell, A., Dubnick, A., Sharp, M.J., Anesio, A.M., & Butler, C. E. H. (2012). Potential methane reservoirs beneath Antarctica. Nature, 488(7413), 633-637.

Wang, Q., Dore, J. E., & McDermott, T. R. (2017). Methylphosphonate metabolism by Pseudomonas sp. populations contributes to the methane oversaturation paradox in an oxic freshwater lake. Environmental Microbiology, 19(6), 2366-2378.

Wang, Q., Alowaifeer, A., Kerner, P., Balasubramanian, N., Patterson, A., Christian, W., Tarver, A., Dore, J., Hatzenpichler, R., Boothner, B., & McDermott, T. R. (2021). Aerobic bacterial methane synthesis. Proceedings of the National Academy of Sciences, 118(27), e2019229118.

Ward, B. B., Granger, J., Maldonado, M. T., & Wells, M. L. (2003). What limits bacterial production in the suboxic region of permanently ice-covered Lake Bonney, Antarctica?. Aquatic microbial ecology, 31(1), 33-47.

Warrier, R. B., Castro, M. C., Hall, C. M., Kenig, F., & Doran, P. T. (2015). Reconstructing the evolution of Lake Bonney, Antarctica using dissolved noble gases. Applied Geochemistry, 58, 46-61.

Welch, K. A., Lyons, W. B., Whisner, C., Gardner, C. B., Gooseff, M. N., McKnight, D. M., & Priscu, J. C. (2010). Spatial variations in the geochemistry of glacial meltwater streams in the Taylor Valley, Antarctica. Antarctic Science, 22(6), 662-672.

Whiticar, M. J. (1999). Carbon and hydrogen isotope systematics of bacterial formation and oxidation of methane. Chemical Geology, 161(1-3), 291-314.

Yarnes, C. (2013). δ13C and δ2H measurement of methane from ecological and geological sources by gas chromatography/combustion/pyrolysis isotope-ratio mass spectrometry. Rapid Communications in Mass Spectrometry, 27(9), 1036-1044.

Yoshikawa, C., Hayashi, E., Yamada, K., Yoshida, O., Toyoda, S., & Yoshida, N. (2014). Methane sources and sinks in the subtropical South Pacific along 17 S as traced by stable isotope ratios. *Chemical Geology*, *382*, 24-31.

CHAPTER FOUR

THEME 2 INTRODUCTION

Sulfur Oxidizing Organisms in Subglacial Systems

Subglacial Environments as Microbial Biomes

Ice-covered environments, such as those beneath ice sheets and glaciers, are biogeochemically and hydrologically dynamic systems, producing trace elements, nutrients, organic compounds, and greenhouse gases that can have a significant impact on downstream ecosystems and potentially impact the global carbon cycle (Wadham et al. 2012; Michaud et al., 2017; Hawkings et al., 2020). Early research on weathering processes in sub-ice systems interpreted the chemical composition of subglacial outflow waters as solely the result of abiotic mineral weathering (e.g. Raiswell and Thomas, 1984; Tranter et al., 1993). However, two decades ago, the role of microbes in impacting subglacial mineral weathering processes and elemental cycling was recognized (e.g. Sharp et al., 1999; Skidmore et al., 2000; Tranter et al 2002) and has been an important area of research since (Skidmore et al., 2005; Tranter et al., 2005; Wadham et al., 2010; Montross et al., 2013; Nixon et al., 2017).

Subglacial environments have stable temperatures and where liquid water is present, flowing ice comminutes bedrock into fine-grained sediments with fresh reactive mineral surfaces (Telling et al., 2015). Water beneath glaciers and ice sheets will often saturate the sediments, which may promote microbial activity (Tranter et al., 2005). The water acts as a solvent in biochemical reactions, establishes electrochemical gradients (e.g. proton motive force), and transport of nutrients (e.g. C, N, P, Fe) (Achberger et al., 2017). Active microbial communities

have been documented in basal ice, subglacial sediments, subglacial lakes, and subglacial outflows at the ice margin (Mikucki et al., 2004; Skidmore et al., 2005; Boyd et al., 2011; Hamilton et al., 2013; Mitchell et al., 2013; Boyd et al., 2014; Achberger et al., 2017; Davis et al., 2023). The microbial communities in subglacial environments are diverse and adapted to dark, oligotrophic conditions (Hamilton et al., 2013; Boyd et al., 2014). The sediments at the base of a glacier are typically a more stable environment than at the surface or periphery and can have a consistent source of nutrients and energy (Skidmore et al., 2005). The nutrients and energy sources for microbes in subglacial systems are derived from the mineralization of stored organic matter or from glacial processes like bedrock comminution that provide electron donors and acceptors (Achberger et al., 2017). Overlying ice prevents phototrophy in subglacial systems, so primary productivity is conducted by chemoautotrophic organisms that convert inorganic carbon into organic compounds using inorganic electron donors. However, surface melt waters which are dilute, may reach the bed of temperate and polythermal ice masses supplying dissolved gases and organic carbon (Tranter et al., 2005; Telling et al., 2015; Achberger, 2017).

Chemolithoautotrophic metabolisms in subglacial environments are supported primarily by two factors: the comminution of underlying bedrock and water-rock interactions (Mitchell et al., 2013; Telling et al., 2015; Achberger 2017). Glacier ice grinds bedrock and sediments at the ice-bed interface, producing mechanically weathered rock with a high surface area to volume ratio (Tranter et al., 2005). These fresh surfaces provide redox-active elements for microbial metabolisms (Achberger et al., 2017). Concurrently, basal frictional heating can produce liquid water, which can solubilize microbially-essential ions from mineral surfaces, including redox-

active elements like sulfur, iron, manganese, and H_2, (Tranter et al., 2005; Telling et al., 2015) that can be used as electron donors or acceptors, depending on the redox state of the subglacial environment (Achberger et al., 2017). Primary production in these systems commonly utilizes iron, sulfur, and nitrogen compounds (Boyd et al., 2011; Mitchell et al., 2013; Purcell et al., 2014; Harrold et al., 2016; Nixon et al., 2017; Davis et al., 2023).

The availability of oxygen in subglacial environments is mostly controlled by water transport from supraglacial to subglacial environments (Tranter et al., 2005; Achberger et al., 2017). In temperate and polythermal glaciers, dissolved oxygen is typically near saturation when the water enters the bed (Achberger et al., 2017). The temporal and spatial distribution of oxygen at the bed is controlled by the hydrologic structure (Tranter et al., 2005). Channelized systems provide efficient paths for oxygenated water and air-filled channels when water is not present, favoring aerobic microorganisms (Tranter et al., 2005). Conversely, in distributed systems the water moves slower, has longer water-rock reaction times and retention times, leading to depletion of oxygen without regular and significant renewal, thus providing a redox gradient and habitat for anaerobic organisms (Tranter et al., 2005).

The dominant microbial metabolism in a subglacial system can change temporally as the system is driven from oxic to anoxic conditions. Under oxic conditions, sulfide oxidation and decomposition of organic matter are possible (Tranter et al., 2005; Boyd et al., 2014). Once the system becomes anoxic, sulfide oxidation can continue, using Fe(III) as the oxidant (Tranter et al., 2003), but nitrate, iron and sulfate reduction, and methanogenesis may also be present (Tranter et al., 2005; Boyd et al., 2011; Purcell et al., 2014; Nixon et al., 2017).

Microbial Influence on Subglacial Geochemistry

Microorganisms can influence the geochemistry of subglacial outflow waters directly with metabolic products or indirectly through enhanced mineral weathering from metabolic end products (Achberger et al., 2017). Iron and sulfur-oxidizing bacteria have been proposed as primary producers in subglacial systems, providing fixed carbon to the environment (Foght et al., 2004; Skidmore et al., 2005; Mitchell et al., 2013; Boyd et al., 2014). Subglacial sulfur oxidizers that convert thiosulfate to sulfate (Harrold et al., 2016) have been inferred as a major source of elevated sulfate concentrations in subglacial outflow (Wadham et al., 2010; Boyd et al., 2014; Stevenson et al., 2017). The proposed mechanism of subglacial microbial sulfur oxidation would result in the production of protons, which could, in term, enhance mineral weathering (Harrold et al., 2016). The sediments of Whillans Subglacial Lake show a peak in Si concentration that coincides with a peak in the abundance of 16S rRNA gene sequences closely related to species of known sulfur and/or iron oxidizers *Thiobacillus* and *Sideroxydans* (Achberger et al., 2016; Michaud et al., 2016) implying that there may be a link between these components. Microcosm experiments have shown that cation release from minerals is accelerated up to 8-fold in the presence of subglacial microorganisms, compared to abiotic rates, possibly due to the liberation of acidity through microbial oxidation of pyrite and/or mineral dissolution by carbonic acid that forms from heterotrophically-produced CO_2 (Montross et al., 2013; Boyd et al., 2014).

Heterotrophic activity in subglacial systems will likely be limited by the availability of organic substrates and low concentrations of nitrogen, relative to carbon and phosphorous (Boyd et al., 2011; Christner et al., 2014; Vick-Majors et al., 2016). Organic matter sources are from chemolithotrophic primary production, relict deposits in sediments overridden by the glacier, and/or from supraglacial inflow (Bhatia et al., 2010; Boyd et al., 2014; Willis et al., 2015).

Heterotrophic activity has been inferred in numerous subglacial systems through radiotracer and/or nutrient amendment of subglacial waters and sediments with low temperature incubation (e.g. Skidmore et al., 2000; Foght et al., 2004; Mikucki et al., 2004; Lanoil et al., 2009). Low rates of heterotrophic activity were measured in SLW, and it was inferred that carbon was primarily apportioned to respiration rather than biomass production in this system (Vick-Majors et al., 2016).

Environmental Influence on Microbial Biomass, Activity, and Community Structure

It has been argued that the two primary influences on subglacial microbial community structure are physical factors and chemical factors (Skidmore et al., 2005). The physical factors (no light, stable cold temperatures) are common to these environments so communities influenced by them will likely have cosmopolitan distribution. The chemical factors (hydrology bedrock lithology, solute sources, carbon sources, electron acceptors) will be unique to each system, so microbial diversity influenced primarily by these factors could be endemic to specific locations (Skidmore et al., 2005). A comparison of taxa from 24 geographically and physically distinct glacial systems showed that physical variables such as latitude, glacier area, and elevation were a major influence on the taxa present, suggesting a correspondence between physical habitat types and niche and taxonomic diversity (Kohler et al., 2020). Similarly, Cl^-, SO_4^{2-}, and DOC also showed an influence on taxa, possibly reflecting differences in the presence of certain solutes/resources necessary for particular taxa (Kohler et al., 2020). However, Kohler et al. (2020) also found correlations between taxa and environmental factors that were mixed or counterintuitive. One example was OTUs associated with autotrophic sulfur oxidizers *Thiobacillus* sp. and *Sulfuricurvum* sp., which had a positive correlation with DOC, but had no

relationship with SO_4^{2-}. However, the authors noted that caution should be exercised in drawing conclusions from the inferred metabolisms of clustered OTUs, since phylogenetic similarity alone does not confirm similarity in physiological process. Kohler et al., (2020) also note that the prevalence of certain OTUs, seemingly in contradiction with the physiochemical nature of the system, may then highlight the heterogeneity of these environments. Further the OTU distribution may then identify the presence of microhabitats that support organisms which have a significant impact on subglacial processes, but which may be limited in their distribution through the environment (Kohler et al., 2020).

The oxygen levels at the bed of a glacier are a major influence on the active microbial processes and, subsequently, weathering processes and resulting geochemistry of outflow waters. When the subglacial environment is oxic, carbonate hydrolysis, carbonate dissolutions, and sulfide oxidation are the most common, resulting in a high ratio of sulfate: sulfate+bicarbonate (sulfate mass fraction-SMF) in outflow waters (Tranter et al., 2002). Generally, if the SMF value is low (<0.4) this indicates that sulfide minerals are less abundant or the environment is anoxic (Wadham et al., 2004). However, a low SMF value despite a relatively high concentration of sulfate in the system was observed in the outflow waters of Finsterwalderbreen Glacier, Svalbard. Wadham et al. (2004) suggested this indicated that the processes of sulfide oxidation and sulfate reduction were both present beneath the glacier, as bacterial sulfate reduction both decreases sulfate and increases bicarbonate (Wadham et al., 2004).

Sulfur oxidizers may be a significant factor in subglacial biogeochemical cycling (Skidmore et al., 2005; Lanoil et al., 2009; Harrold et al., 2016; Davis et al., 2023), especially in subglacial sediments containing iron-sulfide minerals (Mitchell et al., 2013; Harrold et al., 2016).

For example, Boyd et al., (2014) demonstrate the coupling of carbon fixation with iron and/or sulfur oxidation. At Haut Glacier d'Arolla, sulfate concentrations in outflow waters were higher than could be achieved with O_2-saturated waters, suggesting another oxidizing agent and potentially microbial influence (Tranter et al., 2002). Tranter et al., (2002) suggested that microbes in the subglacial sediments were driving sulfide weathering either by catalyzing it directly or by oxidizing organic carbon, which lowers the pO_2 of the system and drives further weathering of sulfides with other oxidants, such as Fe^{3+}.

Influence of Substrates on Subglacial Microbial Diversity

Basal ice results from glaciologic processes at the base of a glacier, including accretion of material from the bed, freezing subglacial water, and entrainment of debris (Knight et al., 1997). The basal ice has a significantly higher concentration of solutes and sediments than (meteoric) glacier ice that forms from the snowpack through the intermediate firnification process (Foght et al., 2004). The cell count in basal ice from Lower Wright Glacier (LWG), Antarctica (~8 $x10^6$ cells per gram sediment) is an order of magnitude higher than cell counts in subglacial sediments from Russell Glacier (RG), Greenland (~9 x 10^5 cells per gram sediment) (Stibal et al., 2012). LWG sediments are lake sediments that were overridden by the glacier within the last 200-300 years, while RG sediments are composed mainly of Holocene soil (~11,000 – 12000 years old) (Stibal et al., 2012). Stibal et al., (2012) suggest the difference in microbial abundance could be attributed to the differing substrates of the sites, with the younger sediments potentially having more abundant labile organic matter, leading to a microbial community with a higher biomass. The mineralogy of subglacial sediments may also influence microbial community structure (Skidmore et al., 2005). A study comparing two systems with different bedrock, Bench Glacier

(BG), Alaska and John Evans Glacier (JEG), Ellesmere Island, Nunavut, Canada, demonstrated different provenances for the sulfate in the subglacial water. The sulfate measured in a subglacial stream at BG was produced by the oxidation of pyrite while the sulfate at JEG was produced by the dissolution of gypsum (Skidmore et al., 2005). Abundant 16S rRNA gene sequences from BG sediments were closely related to known iron and/or sulfur oxidizers, while such sequences were sparse or not detected in JEG sediments. This indicated that microbial community composition was likely influenced by catchment mineralogy and, in turn, appeared to influence the water chemistry of the two sites. Similarities in both the water chemistry and bedrock minerology between BG and Haut Glacier d'Arolla, Switzerland, suggested that local mineral substrates may directly influence microbial community composition in these two geographically distinct systems (Skidmore et al., 2005).

Influence of Pyrite on Subglacial Microbial Diversity

The presence of pyrite the subglacial system at Robertson Glacier, Alberta, Canada has been shown to be the dominant mineralogical control on bacterial community structure and function (Mitchell et al., 2013). Even though pyrite is present in this system in only trace amounts (0.56 wt% in the rock and 1.2 wt% in the sediment), 53.4% of phylotypes associated with the RG sediment microbial community colonized pyrite minerals incubated in the subglacial outflowing waters (Mitchell et al., 2013). The majority of the 16S rRNA genes recovered from the RG sediments were closely related to the genera *Thiobacillus*, *Acidithibacillus*, and *Sideroxydans*, which have been shown to catalyze the oxidation of ferrous iron and sulfur in pure cultures (Hallberg et al., 2010; Harrold et al., 2016) Additionally, there was a correlation between microbial biomass associated with specific minerals incubated in the glacial waters and each

mineral's iron content, inferring that the organisms were using iron in the minerals for metabolism.

Subglacial Sulfur Oxidation

Previous studies on subglacial environments have focused on metabolisms involving nitrogen (Boyd et al., 2011; Montross et al., 2013; Vick-Majors et al., 2016), sulfur (Skidmore et al., 2000; Boyd et al., 2014, Purcell et al., 2014; Harrold et al., 2016), methane (Boyd et al., 2010, Michaud et al., 2017), and iron compounds (Mitchell et al., 2013; Nixon et al., 2017). however, an integrated model that links multiple microbial metabolisms for the microbial community in subglacial sediments has not been established. Pyrite oxidation is a dominant geochemical process in subglacial environments (Tranter et al., 2002). Sulfate, a product of pyrite oxidation, is the second-most dominant anion after bicarbonate in most proglacial and subglacial meltwaters from alpine, Arctic, and Antarctic environments (Brown, 2002), and it is always enriched in proglacial waters relative to input waters, suggesting a lithogenic source (Mitchell et al., 2013). The oxidation of pyrite is microbially mediated (Montross et al., 2013, Skidmore et al., 2005, Wadham et al., 2004), but the mechanisms involved, and the magnitude of the microbial contribution are not well understood.

The presence of iron-bearing minerals in sub-ice environments may be a key factor in supporting microbial activity and microbially-mediated weathering processes. Pyrite has also been considered as an important source for generating protons in subglacial systems, through oxidative weathering. (e.g. Tranter et al., 2002; Skidmore et al., 2005; Tranter et al., 2005; Montross et al., 2013), and thiosulfate under circumneutral pH conditions, which can be used as an electron donor to support chemolithoautotrophic metabolism (Harrold et al., 2016). The ferric

oxide mineral hematite has also been shown to be an electron acceptor for chemolithoautotrophic metabolism in glacial enrichment cultures, from Iceland, with hydrogen as the electron donor (Dunham et al., 2021).

Iron export from glacial systems as nanoparticulate phases exceeds those from major world rivers (e.g. Hawkings et al., 2020) and microbial activity may be a major contributor to the subglacial iron mineral weathering (Harrold et al., 2016). Several mechanisms have been proposed for microbial pyrite oxidation (e.g. Moses and Herman, 1991; Percak-Dennett et al., 2017) that could accelerate mineral weathering either through direct contact with pyrite or through indirect abiotic weathering with metabolic products. The pH of subglacial waters is typically circumneutral (Skidmore et al., 2005; Wadham et al., 2010, Boyd et al., 2014, Christner et al., 2014; Hawkings et al., 2020), so previously identified microbial mechanisms for iron-mineral oxidation under acidic conditions (Percak-Dennett et al., 2017) would only be favored in sub-ice environments at the micron scale. At a neutral pH, a solid-phase Fe-based mechanism could lead to microbial acceleration of pyrite oxidation, if the organisms are in direct contact with the mineral (Moses and Herman, 1991; Percak-Dennett et al., 2017). Percak-Dennett et al., (2017) document the generation of Fe^{2+} (Reaction 1) in an initial abiotic reaction between oxygenated water and pyrite:

Reaction 1: $FeS_2 + 1.5O_2 \rightarrow S_2O_3^{2-} + Fe^{2+}$

The Fe^{2+} adsorbs to the mineral surface and is oxidized by dissolved oxygen in the water, resulting in surface associated Fe(III). The surface Fe(III) then acts as an oxidant, accepting electrons from underlying reduced S in the pyrite (FeS_2), leading to adsorbed Fe(II) (Reaction 2):

Reaction 2: $FeS_2 + Fe^{2+} \rightarrow FeS_2 \equiv Fe(II)_{adsorbed}$

Oxygen molecules are then transferred from the hydration sphere of the adsorbed Fe(II) to the pyrite sulfur in succession until a stable sulfur species (sulfate) disassociates from the mineral surface. Percak-Dennett et al., 2017 suggest that bacterial cells on the mineral surface could facilitate the reaction of adsorbed Fe(II) with oxygen, thus accelerating this reaction and pyrite weathering. Organisms capable of solid-associated Fe(II) oxidation have previously been isolated from temperate, terrestrial subsoil where Fe redox cycling occurs (Shelobolina et al., 2012)

The abiotic oxidation of pyrite (reaction 1) could also support microbial activity that indirectly enhances mineral weathering. The abiotic oxidation of pyrite (FeS_2) can produce thiosulfate at circumneutral pH, (7.5-8.5) (Moses et. al., 1987; Moses and Herman, 1991) as demonstrated in laboratory experiments, making this a viable process in most subglacial systems. Sulfur oxidizers may be a significant factor in subglacial biogeochemical cycling (Skidmore et al., 2005; Lanoil et al., 2009; Harrold et al., 2016; Davis et al., 2023), especially in subglacial sediments containing iron-sulfide minerals (Mitchell et al., 2013; Harrold et al., 2016). Pyrite has also been considered as an important source for generating protons in subglacial systems, through oxidative weathering. (e.g. Tranter et al., 2002; Skidmore et al., 2005; Tranter et al., 2005; Montross et al., 2013), and thiosulfate under circumneutral pH conditions, which can be used as an electron donor to support chemolithoautotrophic metabolism (Harrold et al., 2016). However, thiosulfate is rarely quantifiable in subglacial waters, and when measured only exists in low concentrations (<1 μM; Harrold et al., 2016). In contrast, sulfate is often a dominant anion

in subglacial waters (Tranter et al., 2002), suggesting a previously unquantified oxidative step in these subglacial environments.

Boyd et al., (2014) demonstrate the coupling of carbon fixation with iron and/or sulfur oxidation, but to date only one organism that oxidizes sulfur compounds has been isolated from subglacial sediments (Harrold et al., 2016). This sulfur-oxidizing organism *Thiobacillus* sp. (RG5) was isolated from thawed basal sediments from Robertson Glacier (RG), an alpine glacier in the Canadian Rockies. The isolate utilized thiosulfate ($S_2O_3^{2-}$) as an electron donor and nitrate, nitrite, or oxygen as the electron acceptor (Harrold et al., 2016). Harrold et al. (2016) propose that in RG sediments, thiosulfate can be oxidized to sulfate (SO_4) by organisms like *Thiobacillus,* with oxygen (the preferred electron donor), or nitrite/nitrate if oxygen is depleted. Although abiotic pyrite oxidation was suggested the putative source of thiosulfate for *Thiobacillus* in a subglacial system, the microbial utilization of thiosulfate derived from pyrite was not demonstrated by Harrold et al. (2016) as their enrichment and growth experiments utilized a sodium-thiosulfate salt.

The importance of pyrite on microbial community structure and activity and influence on biogeochemical processes in the subglacial environment for Robertson Glacier, Canadian Rockies is well documented (Mitchell et al., 2013; Hamilton et al., 2013; Boyd et al., 2014, Harrold et al., 2016). The Robertson Glacier catchment is underlain by a carbonate/clastic sequence including shale interbeds and visible pyrite (Harrold et al., 2016). Similarly, mineralogical, geochemical, and genetic evidence indicate the presence of pyrite and putative sulfur oxidizers in the subglacial sediments of Bench Glacier, Alaska and that these influence subglacial biogeochemical processes (Skidmore et al., 2005). The Bench Glacier catchment is

underlain by metasedimentary rocks (Winkler et al., 1981), a contrasting lithology to the Robertson Glacier, lacking in carbonate, but also with visible pyrite. The aim of my research was to investigate the presence of sulfur-oxidizing microbes in the subglacial sediments of Bench Glacier, isolate a sulfur oxidizing organism and determine if the sulfur oxidizer isolate can utilize thiosulfate sourced solely from the abiotic oxidation of pyrite.

Bench Glacier, Alaska

Bench Glacier (BG) is a 7.5km^2 (7km long, 1km wide) temperate valley glacier in the Chugach Range of Alaska, ranging in elevation from 950 to 1,600m (Fig. 4.1; MacGregor et al., 2005). The cross section is roughly parabolic, with ice thickness of 150-200m over most of the glacier length (Bradford et al., 2009). It is located approximately 30km east of the town of Valdez and 50km northeast of Prince William Sound (MacGregor et al., 2005). It flows to the north-northwest, down elevation, with an average equilibrium line altitude (ELA) of ~1,500m and has no tributaries (MacGregor et al., 2005; Bradford et al., 2009).

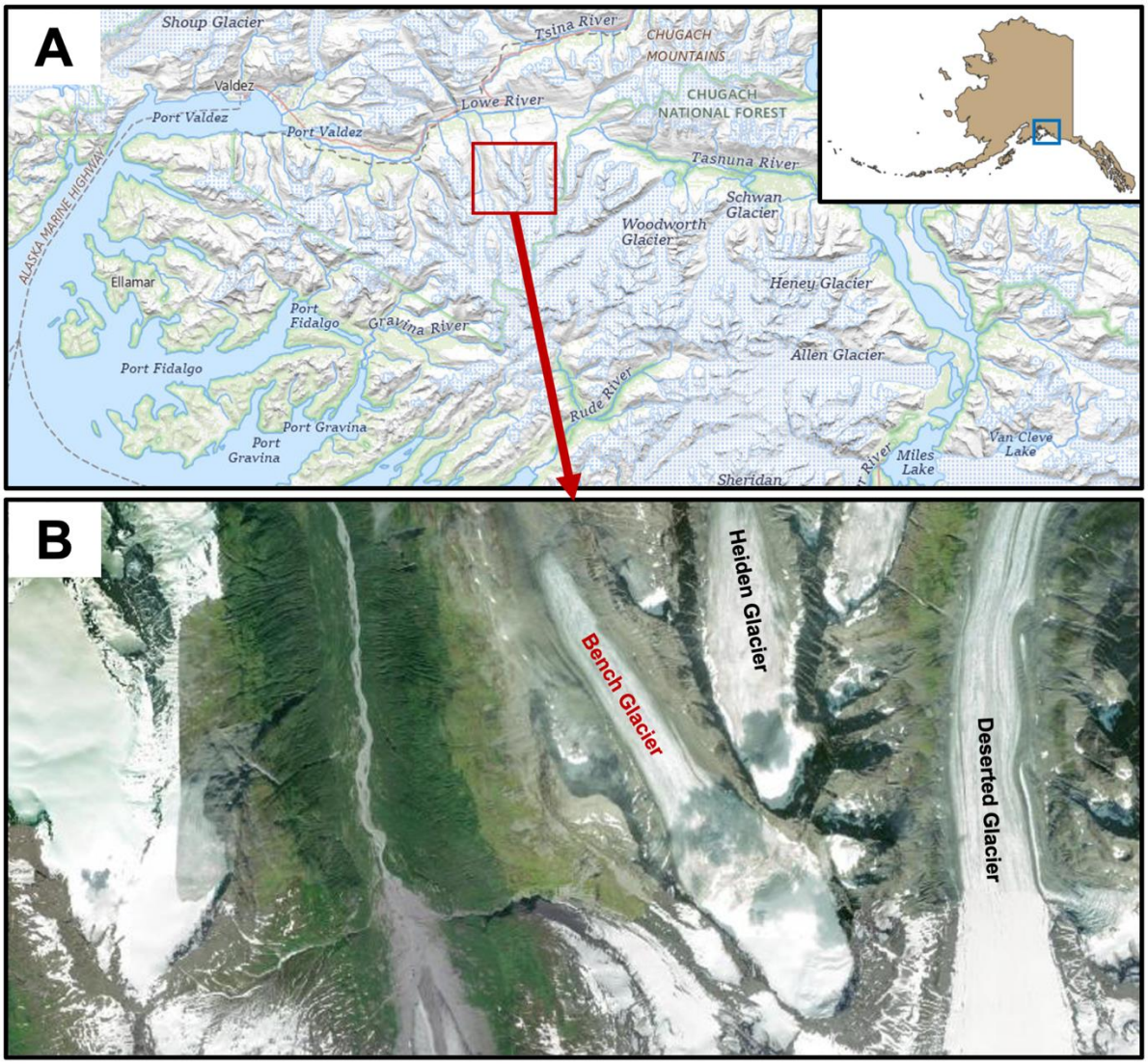


Fig. 4.1 (A) Map of Chugach Mountain Range, AK. Blue square on inset shows location of this region in Alaska. Red Box indicates location of Bench Glacier. (B) Satellite image of Bench Glacier (61.0252° N, 145.6751° W). Alaska inset map from U.S. State Department (https://2017-2021.state.gov/states/Alaska). Map images in Panels A and B from USGS (https://edits.nationalmap.gov/apps/gaz-domestic/public/summary/1398862).

Thin, discontinuous till and supraglacial debris lines most of the lower valley walls, but ice-penetrating radar and borehole video suggest till cover at the bed is thin and disperse (MacGregor et al., 2005; Bradford et al., 2009). Proglacial outflow forms the Bench River, which flows ~6km from the terminus to the Lowe River, which empties into Port Valdez/Prince William

Sound (Fig. 4.1; Anderson et al., 2000). Much of the drainage basin below the glacier consists of sediments from BG, with the outermost moraine at 2.8km from the terminus (Anderson et al., 2000). Some of the sediments in this basin were deposited during the Last Glacial Maximum, so weathering time of these sediments ranges from 1 to 10k years (Anderson et al., 2000).

Glacial Hydrology

Glacier motion in the winter is primarily driven by ice deformation, with little water discharge or storage recorded during this season (MacGregor et al., 2005). Conduits with a 2m radius would likely be closed during the winter season, except for the one located under thin ice at the terminus (MacGregor et al., 2005). A propagating speed-up event occurs in late spring/early summer, coinciding with maximum water storage that pressurizes a poorly-connected linked-cavity system, leading to enhanced basal sliding. The rapid basal motion then increases local connections between cavities, leading to enhanced subglacial hydraulic connectivity as the primary conduit extends headward up-glacier. Once the speed-up event ends, surface motion slows significantly within a week. The recorded slower basal motion after this point was attributed to regelation (MacGregor et al., 2005). Basal water storage does not decline though, for 20-30 days after the end of the speed-up event, highlighting the long timescale over which water stored in the subglacial linked-cavity network and the englacial system flows into the conduit system. Radar data suggests a high water content within englacial voids in the glacier, especially in areas of extensional strain or decreased compression (Bradford et al., 2009), which could explain this period of slow drainage. The slow decline in storage could also indicate that there is low interconnectivity within the remaining subglacial cavity system and/or that the cavity system is well isolated from the conduits.

The glacier surface melt rate increases in mid-summer as the snowpack thins, but this does not trigger rapid basal motion, indicating the development of an efficient conduit system that prevents water pressure increases (MacGregor et al., 2005). Diurnal changes in borehole water levels in boreholes drilled to the glacier bed emerges during this period (around July 1), further supporting the model of an early-season, relatively uniform distributed system that evolves into a more channelized system by mid-summer, likely one with limited cross-glacier connectivity but long down-glacier flow paths (Fudge et al., 2008).

Bedrock Composition and Subglacial Sediments

The BG basin is underlain with late-Cretaceous age (~60 mya) meta-sedimentary rocks, weakly to strongly foliated marine argillite, siltstone, sandstone and conglomerate sandstone (Winkler et al., 1981). Although Bench Glacier is small, it significantly modifies its landscape by lowering its bed by 1-2 mm/yr, despite sliding only 1-2 m/yr (Riihimaki et al., 2005). There are multiple lines of evidence to suggest the subglacial environment is sediment-poor. Ice-penetrating radar and borehole video suggest till cover at the bed is thin and disperse (MacGregor et al., 2005; Bradford et al., 2009). The transient vertical motion of the glacier ice is consistent with a glacier moving over a hard bed (Anderson et al., 2004) and is too large to be the result of basal sediment dilation (Riihimaki et al., 2005). Additionally, exposed basal ice is relatively sediment-free, suggesting that the base is sediment-poor as much of it would have been incorporated into the ice through regelation. Therefore, most of the sediment discharged to the glacial foreland likely comes from the bedrock itself and is likely formed during the melt season (Riihimaki et al., 2005). The ratio of quarrying to abrasion rates is roughly 2:1, based on the amount of coarse to fine grains in proglacial discharge (Riihimaki et al., 2005). The sediment

discharge does not peak until later in the season when a conduit system is established, allowing water and sediments produced from basal sliding to be flushed from the subglacial system (Riihimaki et al., 2005).

It has been suggested that the subglacial hydrological system is capable of essentially sweeping the ablation area bed clean on annual timescales, as indicated by a high sediment "pulse" at the ending of the speed-up period and limited sediment discharge after (Riihimaki et al., 2005). However, others suggest the glacier may maintain a thin, discontinuous sediment layer throughout the year (Bradford et al., 2008; Babcock and Bradford, 2014). The highest measured sediment concentration discharged from the glacier came following a flood event in September 1999, which Riihimaki et al., 2005 suggest could have been triggered by enhanced basal sliding (though there are no measurements to constrain this) or the expansion of conduits into areas of the bed with stored sediments. It may be that regions of sediment, perhaps channel marginal zones, do exist perennially, though their distribution at the bed is sparse and heterogeneous.

Pyrite Content

There is visible pyrite and rusting in the catchment rocks (Anderson et al., 2000; Skidmore et al., 2005). Sulfate in the subglacial waters at BG is derived from pyrite through sulfide oxidation (Skidmore et al., 2005), suggesting the presence of active sulfide and sulfur oxidizers. This is supported by 16S rRNA gene sequence data for the microbial community in BG sediments demonstrating abundant sequences related to *Gallionella ferruginea* or the genus *Thiobacillus,* known iron and/or sulfur oxidizers in culture (Skidmore et al., 2005). Sulfate was the dominant anion in outflow waters at Bench, with δ^{34}S-SO4 analysis indicating it is derived from pyrite via sulfide oxidation (Skidmore et al., 2005).

References

Achberger, A. M., Christner, B. C., Michaud, A. B., Priscu, J. C., Skidmore, M. L., Vick-Majors, T. J., & WISSARD Science Team. (2016). Microbial community structure of subglacial lake Whillans, West Antarctica. Frontiers in Microbiology, 7, 212607.

Achberger, A. M., Michaud, A. B., Vick-Majors, T. J., Christner, B. C., Skidmore, M. L., Priscu, J. C., & Tranter, M. (2017). Microbiology of subglacial environments. Psychrophiles: from Biodiversity to Biotechnology, 83-110.

Anderson, S. P., Drever, J. I., Frost, C. D., & Holden, P. (2000). Chemical weathering in the foreland of a retreating glacier. Geochimica et Cosmochimica Acta, 64(7), 1173-1189.

Anderson, R. S., Anderson, S. P., MacGregor, K. R., Waddington, E. D., O'Neel, S., Riihimaki, C. A., & Loso, M. G. (2004). Strong feedbacks between hydrology and sliding of a small alpine glacier. Journal of Geophysical Research: Earth Surface, 109(F3).

Babcock, E., & Bradford, J. (2014). Quantifying the basal conditions of a mountain glacier using a targeted full-waveform inversion: Bench Glacier, Alaska, USA. Journal of Glaciology, 60(224), 1221-1231.

Bhatia, M. P., Das, S. B., Longnecker, K., Charette, M. A., & Kujawinski, E. B. (2010). Molecular characterization of dissolved organic matter associated with the Greenland ice sheet. Geochimica et Cosmochimica Acta, 74(13), 3768-3784.

Boyd, E. S., Lange, R. K., Mitchell, A. C., Havig, J. R., Hamilton, T. L., Lafrenière, M. J., Shock, E.L., Peters, J.W., & Skidmore, M. (2011). Diversity, abundance, and potential activity of nitrifying and nitrate-reducing microbial assemblages in a subglacial ecosystem. Applied and Environmental Microbiology, 77(14), 4778-4787.

Boyd, E. S., Hamilton, T. L., Havig, J. R., Skidmore, M. L., & Shock, E. L. (2014). Chemolithotrophic primary production in a subglacial ecosystem. Applied and Environmental Microbiology, 80(19), 6146-6153.

Bradford, J. H., Nichols, J., Mikesell, T. D., & Harper, J. T. (2009). Continuous profiles of electromagnetic wave velocity and water content in glaciers: an example from Bench Glacier, Alaska, USA. Annals of Glaciology, 50(51), 1-9.

Christner, B. C., Priscu, J. C., Achberger, A. M., Barbante, C., Carter, S. P., Christianson, K., Michaud, A.B., Mikucki, J.A., Mitchell, J.A., & Vick-Majors, T. J. (2014). A microbial ecosystem beneath the West Antarctic ice sheet. Nature, 512(7514), 310-313.

Davis, C. L., Venturelli, R. A., Michaud, A. B., Hawkings, J. R., Achberger, A. M., Vick-Majors, T. J., Rosenheim, B.E., Dore, J.E., Steigmeyer, A.J., Skidmoore, M.L, Barker, J.D.,

Benning, L.G., Siegfried, M.R., Priscu, J.C., Christner, B. C., & the SALSA Science Team (2023). Biogeochemical and historical drivers of microbial community composition and structure in sediments from Mercer Subglacial Lake, West Antarctica. ISME Communications, 3(1), 8.

Dunham, E. C., Dore, J. E., Skidmore, M. L., Roden, E. E., & Boyd, E. S. (2021). Lithogenic hydrogen supports microbial primary production in subglacial and proglacial environments. Proceedings of the National Academy of Sciences, 118(2), e2007051117.

Foght, J., Aislabie, J., Turner, S., Brown, C. E., Ryburn, J., Saul, D. J., & Lawson, W. J. M. E. (2004). Culturable bacteria in subglacial sediments and ice from two southern hemisphere glaciers. Microbial Ecology, 47, 329-340.

Fudge, T. J., Humphrey, N. F., Harper, J. T., & Pfeffer, W. T. (2008). Diurnal fluctuations in borehole water levels: configuration of the drainage system beneath Bench Glacier, Alaska, USA. Journal of Glaciology, 54(185), 297-306.

Hallberg, K. B., González-Toril, E., & Johnson, D. B. (2010). Acidithiobacillus ferrivorans, sp. nov.; facultatively anaerobic, psychrotolerant iron-, and sulfur-oxidizing acidophiles isolated from metal mine-impacted environments. Extremophiles, 14, 9-19.

Hamilton, T. L., Peters, J. W., Skidmore, M. L., & Boyd, E. S. (2013). Molecular evidence for an active endogenous microbiome beneath glacial ice. The ISME Journal, 7(7), 1402-1412.

Harrold, Z.R., Skidmore, M.L., Hamilton, T.L., Desch, L., Amada, K., Van Gelder, W., Glover, K., Roden, E.E., & Boyd, E.S. (2016). Aerobic and anaerobic thiosulfate oxidation by a cold-adapted, subglacial chemoautotroph. Applied and Environmental Microbiology, 82(5), 1486-1495.

Hawkings, J. R., Skidmore, M. L., Wadham, J. L., Priscu, J. C., Morton, P. L., Hatton, J. E., Gardner, C.B., Kohler, T.J., Stibal, M., Bagshaw, E.A., Steigmeyer, A.J., Barker, J., Dore, J.E., Lyons, W.B., Tranter, M., Specer, R.G., & the SALSA Science Team. (2020). Enhanced trace element mobilization by Earth's ice sheets. Proceedings of the National Academy of Sciences, 117(50), 31648-31659.

Knight, P. G. (1997). The basal ice layer of glaciers and ice sheets. Quaternary Science Reviews, 16(9), 975-993.

Kohler, T. J., Vinšová, P., Falteisek, L., Žárský, J. D., Yde, J. C., Hatton, J. E., Hawkings, J.R., Lamarche-Gagnon, G., Hood, E., Cameronn K.A. & Stibal, M. (2020). Patterns in microbial assemblages exported from the meltwater of Arctic and Sub-Arctic glaciers. Frontiers in Microbiology, 11, 669.

Lanoil, B., Skidmore, M., Priscu, J. C., Han, S., Foo, W., Vogel, S. W., Tulaczyk, S. & Engelhardt, H. (2009). Bacteria beneath the West Antarctic ice sheet. Environmental Microbiology, 11(3), 609-615.

Macgregor, K. R., Riihimaki, C. A., & Anderson, R. S. (2005). Spatial and temporal evolution of rapid basal sliding on Bench Glacier, Alaska, USA. Journal of Glaciology, 51(172), 49-63.

Michaud, A. B., Skidmore, M. L., Mitchell, A. C., Vick-Majors, T. J., Barbante, C., Turetta, C., vanGelder, W. & Priscu, J. C. (2016). Solute sources and geochemical processes in subglacial lake Whillans, west Antarctica. Geology, 44(5), 347-350.

Michaud, A. B., Dore, J. E., Achberger, A. M., Christner, B. C., Mitchell, A. C., Skidmore, M. L., Vick-Majors, T., & Priscu, J. C. (2017). Microbial oxidation as a methane sink beneath the West Antarctic Ice Sheet. Nature Geoscience, 10(8), 582-586.

Mikucki, J. A., Foreman, C. M., Sattler, B., Berry Lyons, W., & Priscu, J. C. (2004). Geomicrobiology of Blood Falls: an iron-rich saline discharge at the terminus of the Taylor Glacier, Antarctica. Aquatic Geochemistry, 10, 199-220.

Mitchell, A. C., Lafrenière, M. J., Skidmore, M. L., & Boyd, E. S. (2013). Influence of bedrock mineral composition on microbial diversity in a subglacial environment. Geology, 41(8), 855-858.

Montross, S. N., Skidmore, M., Tranter, M., Kivimäki, A. L., & Parkes, R. J. (2013). A microbial driver of chemical weathering in glaciated systems. Geology, 41(2), 215-218.

Moses, C. O., Nordstrom, D. K., Herman, J. S., & Mills, A. L. (1987). Aqueous pyrite oxidation by dissolved oxygen and by ferric iron. Geochimica et Cosmochimica Acta, 51(6), 1561-1571.

Moses, C. O., & Herman, J. S. (1991). Pyrite oxidation at circumneutral pH. Geochimica et Cosmochimica Acta, 55(2), 471-482.

Nixon, S. L., Telling, J. P., Wadham, J. L., & Cockell, C. S. (2017). Viable cold-tolerant iron-reducing microorganisms in geographically diverse subglacial environments. Biogeosciences, 14(6), 1445-1455.

Percak-Dennett, E., He, S., Converse, B., Konishi, H., Xu, H., Corcoran, A., Nooguera, D., Chann, C., Bhayyacharyya, A., Borch, T., Boyd, E., & Roden, E. E. (2017). Microbial acceleration of aerobic pyrite oxidation at circumneutral pH. Geobiology, 15(5), 690-703.

Purcell, A. M., Mikucki, J. A., Achberger, A. M., Alekhina, I. A., Barbante, C., Christner, B. C., Ghosh, D., Michaud, A.B., Mitchell, A.C., Priscu, J.C., Scherer, R., Skidmore, M.L., Vic-

Majors, T.J., & Wissard Science Team. (2014). Microbial sulfur transformations in sediments from Subglacial Lake Whillans. Frontiers in Microbiology, 5, 594.

Raiswell, R., & Thomas, A. G. (1984). Solute acquisition in glacial melt waters. I. Fjallsjökull (south-east Iceland): bulk melt waters with closed-system characteristics. Journal of Glaciology, 30(104), 35-43.

Raiswell, R., Benning, L. G., Davidson, L., Tranter, M., & Tulaczyk, S. (2009). Schwertmannite in wet, acid, and oxic microenvironments beneath polar and polythermal glaciers. Geology, 37(5), 431-434.

Riihimaki, C. A., MacGregor, K. R., Anderson, R. S., Anderson, S. P., & Loso, M. G. (2005). Sediment evacuation and glacial erosion rates at a small alpine glacier. Journal of Geophysical Research: Earth Surface, 110(F3).

Shelobolina, E., Konishi, H., Xu, H., Benzine, J., Xiong, M. Y., Wu, T., Blothe, M.,& Roden, E. (2012). Isolation of phyllosilicate–iron redox cycling microorganisms from an illite–smectite rich hydromorphic soil. Frontiers in microbiology, 3, 134.

Skidmore, M. L., Foght, J. M., & Sharp, M. J. (2000). Microbial life beneath a high Arctic glacier. Applied and Environmental Microbiology, 66(8), 3214-3220.

Skidmore, M., Anderson, S. P., Sharp, M., Foght, J., & Lanoil, B. D. (2005). Comparison of microbial community compositions of two subglacial environments reveals a possible role for microbes in chemical weathering processes. Applied and Environmental Microbiology, 71(11), 6986-6997.

Stevenson, E. I., Fantle, M. S., Das, S. B., Williams, H. M., & Aciego, S. M. (2017). The iron isotopic composition of subglacial streams draining the Greenland ice sheet. Geochimica et Cosmochimica Acta, 213, 237-254.

Stibal, M., Wadham, J. L., Lis, G. P., Telling, J., Pancost, R. D., Dubnick, A., Sharp, M.J., Lawson, E.C., Butler, C.E.H., Hasan, F., Tranter, M. & Anesio, A. M. (2012). Methanogenic potential of Arctic and Antarctic subglacial environments with contrasting organic carbon sources. Global Change Biology, 18(11), 3332-3345.

Telling, J., Boyd, E. S., Bone, N., Jones, E. L., Tranter, M., MacFarlane, J. W., Martin, P.G., Wadham, J.L., Lamarche-Gagnon, G., Skidmore, M.L., Hamilton, T.L., Hill, E., Jackson, M., & Hodgson, D. A. (2015). Rock comminution as a source of hydrogen for subglacial ecosystems. Nature Geoscience, 8(11), 851-855.

Tranter, M., Brown, G., Raiswell, R., Sharp, M., & Gurnell, A. (1993). A conceptual model of solute acquisition by Alpine glacial meltwaters. Journal of Glaciology, 39(133), 573-581.

Tranter, M., Sharp, M. J., Lamb, H. R., Brown, G. H., Hubbard, B. P., & Willis, I. C. (2002). Geochemical weathering at the bed of Haut Glacier d'Arolla, Switzerland—a new model. Hydrological Processes, 16(5), 959-993.

Tranter, M. (2003). Geochemical weathering in glacial and proglacial environments. Treatise on geochemistry, 5, 605.

Tranter, M., Skidmore, M., & Wadham, J. (2005). Hydrological controls on microbial communities in subglacial environments. Hydrological Processes, 19(4), 995-998.

Vick-Majors, T. J., Mitchell, A. C., Achberger, A. M., Christner, B. C., Dore, J. E., Michaud, A. B., Mikucki, J.A., Purcell, A.M., Skidmore, M.L., Priscu, J.C., & WISSARD Science Team. (2016). Physiological ecology of microorganisms in Subglacial Lake Whillans. Frontiers in microbiology, 7, 216269.

Wadham, J. L., Hodgkins, R., Cooper, R. J., & Tranter, M. (2001). Evidence for seasonal subglacial outburst events at a polythermal glacier, Finsterwalderbreen, Svalbard. Hydrological Processes, 15(12), 2259-2280.

Wadham, J. L., Bottrell, S., Tranter, M., & Raiswell, R. (2004). Stable isotope evidence for microbial sulphate reduction at the bed of a polythermal high Arctic glacier. Earth and Planetary Science Letters, 219(3-4), 341-355.

Wadham, J. L., Tranter, M., Skidmore, M., Hodson, A. J., Priscu, J., Lyons, W. B., Sharp, M., Wynn, P., & Jackson, M. (2010). Biogeochemical weathering under ice: Size matters. Global Biogeochemical Cycles, 24(3).

Weiss, J. V., Rentz, J. A., Plaia, T., Neubauer, S. C., Merrill-Floyd, M., Lilburn, T., Bradburne, C.; Megonigal, J.P., & Emerson, D. (2007). Characterization of neutrophilic Fe (II)-oxidizing bacteria isolated from the rhizosphere of wetland plants and description of Ferritrophicum radicicola gen. nov. sp. nov., and Sideroxydans paludicola sp. nov. Geomicrobiology Journal, 24(7-8), 559-570.

Willis, M. J., Herried, B. G., Bevis, M. G., & Bell, R. E. (2015). Recharge of a subglacial lake by surface meltwater in northeast Greenland. Nature, 518(7538), 223-227.

Winkler, G. R., Silberman, M. L., Grantz, A., Miller, R. J., & MacKevett Jr, E. M. (1980). Geologic map and summary geochronology of the Valdez quadrangle, southern Alaska (No. 80-892-A).

CHAPTER FIVE

SULFUR OXIDATION BY A SUBGLACIAL BACTERIUM

Introduction

Overlying ice prevents phototrophy in subglacial systems, so primary productivity is conducted by chemoautotrophic organisms that convert inorganic carbon into organic compounds using inorganic electron donors (Skidmore et al., 2000; Boyd et al., 2014; Christner et al., 2014; Davis et al., 2023). Subglacial environments have relatively stable temperatures and, where liquid water is present, the flowing ice generates fine grained sediments from abrasion and crushing of the bedrock (Tranter et al., 2002; Wadham et al., 2010). Water/rock interactions on freshly exposed reactive mineral surfaces can be a source of redox compounds that organisms can use in chemoautotrophy (Montross et al., 2013; Boyd et al., 2014; Telling et al., 2015). Specifically, subglacial water interactions with pyrite could provide metabolites for microbial sulfur oxidation (Mitchell et al., 2013; Montross et al., 2013; Gill-Olivas et al., 2021).

Pyrite is a mineral commonly found in a range of rock types and has a widespread distribution globally (e.g. Brown et al., 1996; Raiswell et al. 2009; Michaud et al., 2016; Harrold et al., 2016). It has also been measured in subglacial sediments from several environments (e.g. Brown et al., 1996; Raiswell et al. 2009; Michaud et al., 2016; Harrold et al., 2016). The abiotic oxidation of pyrite (FeS_2) as demonstrated in laboratory experiments at circumneutral pH (7.5-8.5) can produce thiosulfate (Moses et. al., 1987; Moses and Herman, 1991). Circumneutral pH values are common in subglacial waters (e.g. Skidmore et al., 2005; Wadham et al., 2010, Boyd et al., 2014, Christner et al., 2014; Hawkings et al., 2020) and subglacial pyrite oxidation has

been inferred from geochemical data (Tranter et al., 2002; Skidmore et al., 2005, Boyd et al., 2014). Thiosulfate, therefore, would likely be found in outflows from subglacial environments where pyrite is present. However, this compound has not commonly been reported in chemical analyses of subglacial waters (Tranter et al., 2002; Fortner et al., 2005; Michaud et al., 2016; Hawkings et al., 2020; Davis et al., 2023). Only one study has reported thiosulfate concentrations from outflowing glacial waters and the measured concentration was low (< 1 uM; Harrold et al., 2016). This implies that thiosulfate concentrations from outflowing glacial waters are likely below detection by standard analytical techniques (e.g. ion chromatography). In contrast, sulfate is often a dominant anion in subglacial waters and in certain glacial systems, $\delta^{34}S$ values indicate sulfides are the primary source (Tranter, 2003; Wadham et al., 2004; Mitchell et al., 2013). Sulfide minerals are oxidized at a circumneutral pH, but thiosulfate concentrations are below detection limits, which suggests a sink for thiosulfate. Microbial sulfur oxidation could serve as that sink, explaining the low concentrations of thiosulfate in subglacial systems.

Thiosulfate is used as an electron donor to support chemoautotrophic metabolism in sulfur oxidizing microorganisms (Schreiber and Pavlostathis, 1998; Mohapatra et al., 2008; Harrold et al., 2016; Wang et al., 2019). Genetic and geochemical data suggest microbial sulfur oxidation may be widespread in subglacial systems. concentrations of sulfate measured in glacial outflow waters are commonly higher than could be achieved through the abiotic oxidation of sulfide minerals (Tranter et al., 2002; Skidmore et al., 2005; Wadham et al., 2010). Stable isotopic data indicate the sulfate in several glacial systems (e.g. Bench Glacier, AK; Robertson Glacier, Canada) is sourced from sulfide mineral oxidation (Skidmore et al., 2005; Wadham et al., 2010; Mitchell et al., 2013). The sulfide mineral pyrite has been shown to be the dominant

mineral influencing subglacial community structure and diversity for a glacial catchment in the Canadian Rockies (Mitchell et al., 2013). Genetic evidence from microbial communities in multiple glacial systems across the world (e.g. Bench Glacier, AK; Kamb Ice Stream, Antarctica; Whillans Subglacial Lake, Antarctica; Robertson Glacier, Canada) suggests the presence of organisms closely related to known sulfur and/or iron oxidizers (Lanoil et al., 2009; Hamilton et al., 2013; Christner et al., 2014; Achberger et al., 2017). To date, though, only one organism capable of thiosulfate oxidation at close to in situ temperatures (5°C) for the subglacial environment has previously been isolated from a subglacial system (Harrold et al., 2016).

The sulfur-oxidizing organism *Thiobacillus* sp. (RG5) was isolated from subglacial sediments at Robertson Glacier (RG), Canadian Rockies (Harrold et al., 2016). The isolate utilized thiosulfate ($S_2O_3^{2-}$) from sodium thiosulfate ($Na_2S_2O_3$) as an electron donor and nitrate, nitrite, or oxygen as the electron acceptor (Harrold et al., 2016). Harrold et al. (2016) proposed that in RG sediments, thiosulfate can be oxidized to sulfate (SO_4) by organisms like *Thiobacillus* sp. (RG5), with oxygen (the preferred electron donor), or nitrite/nitrate if oxygen is depleted. Harrold et al. (2016) suggested abiotic pyrite oxidation as the source of thiosulfate for *Thiobacillus* sp. (RG5) *in situ* beneath Robertson Glacier but did not show the organism's ability to metabolize thiosulfate sourced from sulfide minerals. Demonstrating a connection between abiotic pyrite oxidation and microbial thiosulfate oxidation is key to determining the viability of this metabolism in subglacial environments.

The objective of this research was to investigate the presence of sulfur-oxidizing microbes in subglacial sediments at a glacier geographically and lithologically distinct from Robertson Glacier, Canadian Rockies. Bench Glacier (BG) in the Chugach Range, Alaska is

underlain with late-Cretaceous age, ~60-million-year-old (mya) meta-sediments (Winkler et al., 1981) that contain visible pyrite (Anderson et al., 2000). Sulfate in the subglacial waters at BG is derived from pyrite through sulfide oxidation, suggesting the presence of active sulfide and sulfur oxidizers (Skidmore et al., 2005). 16S rRNA gene sequence data for the microbial community in BG sediments demonstrates the presence of phylotypes related to known iron and/or sulfur oxidizers (Skidmore et al., 2005), supporting a microbial role in sulfide oxidation. Therefore, subglacial sediments from BG were used in a targeted-enrichment culturing strategy, with the aim of isolating thiosulfate-oxidizing organisms, characterizing them genetically, and testing their ability to utilize pyrite as the sole sulfur source at close to *in situ* subglacial temperatures.

Methods

Study Site and Sample Collection

Bench Glacier (BG) is a 7.5km^2 (7km long, 1km wide) temperate valley glacier in the Chugach Range of Alaska, ranging in elevation from 940 to 1,600m above sea level (masl) (MacGregor et al., 2005). Ice thickness is ~30m at the headwall and at the terminus, with thickness ranging from ~100-150m along the glacier length, with a maximum thickness of 185m occurring 3.5km upglacier from the terminus (Bradford et al., 2009; MacGregor et al., 2005). The glacier is located approximately 30km east of Valdez and 50km northeast of Prince William Sound (MacGregor et al., 2005). It flows to the north-northwest, down elevation, with an average equilibrium line altitude (ELA) of ~1,500m and has no tributaries (MacGregor et al., 2005; Bradford et al., 2009). Proglacial outflow forms the Bench River, which flows ~6km from the terminus to the Lowe River, which empties into Port Valdez/Prince William Sound (Anderson et

al., 2000). The BG catchment is underlain with late-Cretaceous age (~60 mya) meta-sediments, dominated by quartz and feldspars (Winkler et al., 1981). Much of the drainage basin below the glacier consists of sediments from BG, with the outermost moraine at 2.8km from the terminus (Anderson et al., 2000).

Although Bench Glacier is small, it significantly modifies its landscape by lowering its bed by 1-2 mm/yr, despite sliding only 1-2 m/yr (Riihimaki et al., 2005). Thin, discontinuous till and supraglacial debris lines most of the lower valley walls, but there are multiple lines of evidence to suggest the subglacial environment is sediment-poor. Ice-penetrating radar and borehole video suggest till cover at the bed is thin and disperse (MacGregor et al., 2005; Bradford et al., 2009). The transient vertical motion of the glacier ice is consistent with a glacier moving over a hard bed (Anderson et al., 2004) and is too large to be the result of basal sediment dilation (Riihimaki et al., 2005). Additionally, exposed basal ice at the terminus is relatively sediment-free, further suggesting a sediment-poor base (Riihimaki et al., 2005). Therefore, most of the sediment discharged to the glacial foreland likely comes from the bedrock itself and is likely formed during the melt season (Riihimaki et al., 2005).

The subglacial sediment samples used in this research were collected in October 2004 by Mark Skidmore from sediments at the ice/sediment interface, inside a natural cave at the glacier terminus of BG, where the outflowing subglacial stream was located (Fig. 5.1). The sediments were kept frozen until used.

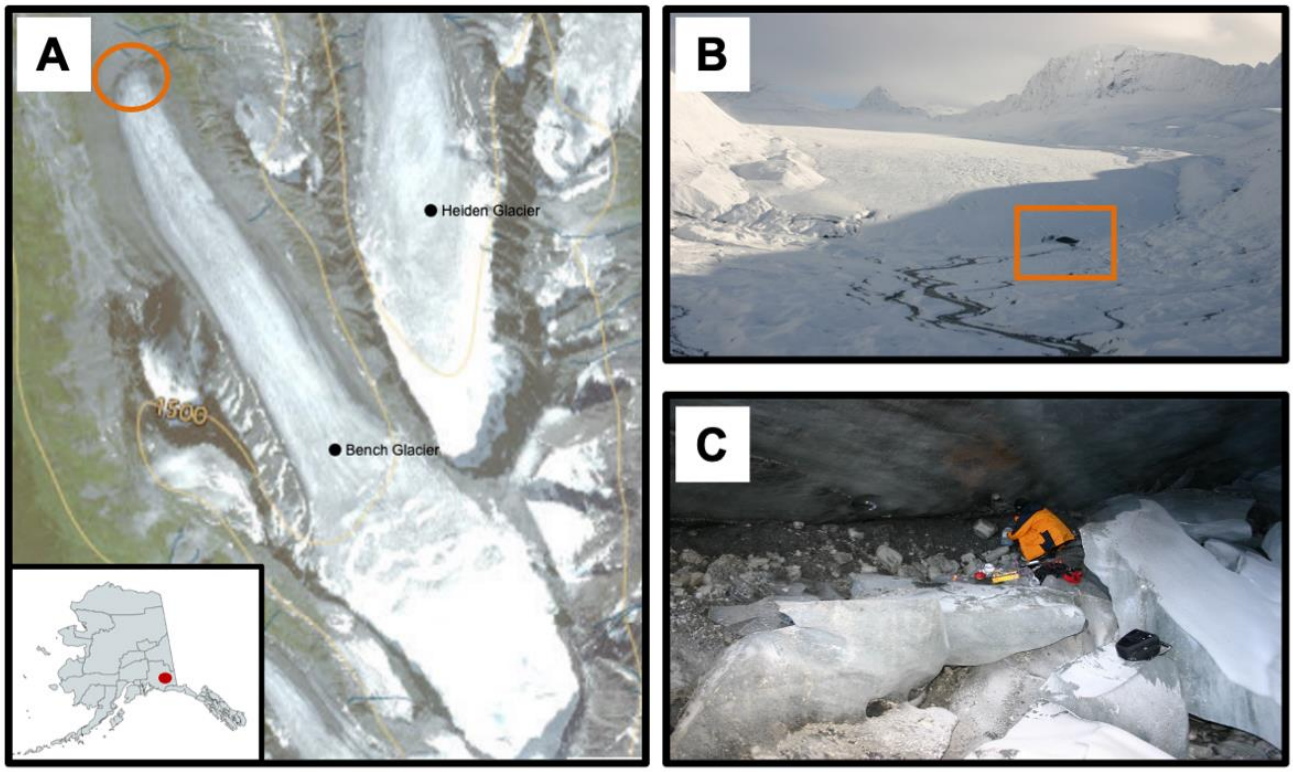


Fig. 5.1 A) Bench Glacier, AK and sediment sampling site (image from USGS – https://edits.nationalmap.gov/apps/gaz-domestic/public/summary/1398862). Red dot on inset indicates location of Bench Glacier in Alaska. Orange circle highlights the terminus region sampled. B) Orange square indicates sampling point at glacier terminus. C) Collecting subglacial sediments at the ice/sediment interface, inside a natural cave at the glacier terminus, where the outflowing subglacial stream exits the glacier. Photos for B and C, courtesy Mark Skidmore.

Sulfur Oxidizers Enrichment Cultures and Dilution Series

Previous studies enriching for sediment chemoautotrophs used liquid growth media consisting of base salts (typically potassium, phosphate, ammonium, and magnesium complexes), vitamins, and other trace elements (Widdel and Pfennig, 1981; Sorokin et al., 2007; Jung et al., 2010; Harrold et al., 2016; Nixon et al., 2017). These studies each adjusted the growth media to simulate the *in situ* conditions of their focus environments with regards to salinity and pH, which were commonly modified with NaCl and carbonate or HCl, respectively (Widdel and Pfennig, 1981; Sorokin et al., 2007; Jung et al., 2010; Harrold et al., 2016; Nixon et

al., 2017). When sodium bicarbonate was used to adjust pH, it also provided a pH buffer and a carbon source for the target organisms (Sorokin et al., 2007; Jung et al., 2010; Harrold et al., 2016). Successful enrichments (e.g. Sorokin et al., 2007; Jung et al., 2010; Harrold et al., 2016) also supplemented their media with vitamin and trace element solutions containing micronutrients that have been shown to improve cell growth in culture (e.g. Wolin and Wolfe; 1963; Widdel and Pfennig, 1981; Widdel et al., 1983; Fennell et al., 2004). Environmental sediments were added to growth media, amended with solutions containing electron donor and acceptor compounds to encourage specific chemoautotrophic processes, such as sulfur oxidation (e.g. Sorokin et al., 2007; Jung et al., 2010; Harrold et al., 2016). Harrold et al. (2016) was the only previous study to enrich for and isolate a sulfur-oxidizing organism from subglacial sediments, so their specific culturing approach was used as the basis for the present study.

Growth media for the Bench Glacier sulfur oxidizer enrichment cultures consisted of the base salts, vitamins, and trace elements solutions used by Harrold et al. (2016). Thiosulfate was added to the live enrichments to encourage sulfur oxidation. The base salts solution (Table 5.1) was prepared according to Harrold et al. (2016), following Sorokin et al. (2007). The Wolfe's vitamins solution (Wolin and Wolfe, 1963) was prepared in a 10x concentration (Table 5.1). The trace elements solution (Table 5.1) was a 10x SL 10, originally described in Widdel and Pfennig (1981) and Widdel et al., (1983). The thiosulfate solution was produced with sodium thiosulfate salt to a concentration of 20mM. Each solution was prepared aseptically using 0.2um-filtered ultrapure water. The base salts solution was verified to be at a pH ~8, then transferred to a capped bottle, autoclaved, and sealed with Parafilm. The vitamins, trace elements, and thiosulfate solutions were filtered (0.2µm) into furnaced serum vials, which were stoppered and crimp-

sealed, then flushed with UHP N_2. All solutions were stored at 4°C until enrichment culture preparation.

Table 5.1. Media composition for Bench Glacier enrichment cultures, dilution series, and pyrite experiments

Base Salts Solution
(Sorokin et al., 2007; Harrold et al., 2016)

Compound	Concentration (mM)
NH_4Cl	5.1
K_2HPO_4	10.0
$MgCl_2$	0.3
NaCl	5.0
$NaHCO_3$	20.0

Trace Elements (10x)
(Widdel and Pfennig, 1981; Widdel et al., 1983)

Compound	Concentration (mM)
HCl (25%)	0.03
$MnCl_2$	7.9
$CoCl_2$	14.6
$ZnCl_2$	5.1
$CuCl_2$	1.2
$H3BO_3$	10.0
$NaMoO_4$	1.7
$NiCl_2$	0.3
$FeCl_2$	1.1

Wolfe's Vitamins Solution (10x)
(Wolin and Wolfe; 1963)

Compound	Concentration (mM)
Biotin (vitamin B)	0.08
Folic Acid	0.04
pyridoxine-HCL (vit. B12)	0.59
riboflavin (vit. B2)	0.13
Thiamine HCl (vit. B1)	0.18
nicotinic acid	0.40
Calcium DL - pantothenate	0.10
Vitamin B-12	0.007
p-aminobenzoic acid	0.36
thioctic acid (Lipoic Acid)	0.24

Six initial enrichment cultures were prepared, with three containing sediments from Bench Glacier in growth media and 5mM thiosulfate, and three uninoculated controls containing only growth media and thiosulfate. Culture work was conducted in a laminar flow hood that was cleaned with 70% ethanol then exposed to ultraviolet light for 3 hours. Six, 70ml serum vials were furnaced, then pre-chilled at 4ºC and kept on ice during work in the laminar flow hood. The three control vials were prepared first, without any sediment present in the hood to prevent contamination. Each control vial contained 18.6 ml of base salts, 0.2 ml each of the vitamins and

trace elements solutions (0.1% concentration, following Harrold et al., 2016) and 1 ml of the sodium thiosulfate solution to a final media concentration of 1 mM thiosulfate. The final media volume in each vial was 20ml and the pH was ~8. The control vials were then stoppered and crimp-sealed.

A slurry was created from the thawed Bench subglacial sediment sample by adding 100 ml of ultrapure (18.2 MΩ cm^{-1}), autoclaved water to 200 g of sediment and mixing with sterilized stir bar and stir plate. Harrold et al. (2016) used a 1:2 sediment to water ratio for their slurry and a 1:10 slurry to media ratio (vol/vol) in their enrichment cultures. This study used a higher sediment:water ratio in the slurry (2:1) and a higher slurry:media ratio (1:7, vol/vol) to increase chances for sulfur oxidizer growth. The three live incubations were initiated by adding 3ml of the sediment slurry to 70ml serum vials containing 15.6 ml of base salts, 0.2 ml each of vitamins and trace elements (0.1% concentration) and 1ml of 20mM sodium thiosulfate (1mM concentration). The pH of the final culture media was confirmed to ~8, then the vials were stoppered and crimp-sealed. All vials were stored at 4ºC in the dark for ~3 months before growth monitoring began.

Active sulfur oxidation in the incubations was identified as a decrease in the concentration of thiosulfate with a concurrent increase in sulfate for the live controls, with no changes to either analyte in the control treatments. Population growth was identified as an increase in the number of cells over time. The concentrations of major dissolved ions including thiosulfate were determined using a Metrohm 930 Compact IC Flex ion chromatograph with an A Supp 5 anion column and a Metrosep C4 cation column. Vials that showed a decrease in the concentration of thiosulfate over time were considered active cultures, with no such decrease in

the parallel controls. Cell counts were conducted by vacuum filtering a 200 µl media subsample onto 0.2 µm polycarbonate membrane filters (Isopore). The filters were stained with SYBR Gold nucleic acid gel stain (Invitrogen) and mounted to a glass microscope slide. Cells were counted using epifluorescence microscopy, taking the average number of cells from 20 fields of view. The active enrichments were passaged in a dilution series (10^{-1} through 10^{-4} of the original culture) into fresh media to dilute out non-target organisms. The media only controls were also diluted in series. The highest dilution treatments (10^{-4}) in the "live" series continued to show thiosulfate consumption, and cell counts of the culture showed an increase in the abundance of cells over time from 10^5 to 10^6 cells ml^{-1} over a 60-day period, while no cells were observed in the control treatments. The 10^{-4} dilution treatments were then subjected to a second serial dilution series (10^{-1} through 10^{-6}) to increase the probability of achieving a pure culture. The highest dilution in the second series (10^{-6}) were actively consuming thiosulfate, and cells from the culture observed with epifluorescence microscopy appeared phenotypically similar. Thus, these dilutions were presumed to be pure cultures and were passaged into a larger volume of media containing additional thiosulfate to increase cell abundance (10^6 cells ml^{-1}) for DNA extraction and the pyrite utilization experiment.

The 10^{-6} dilution cultures were passaged into three 200ml flasks to increase cell abundance for DNA extraction. Each of the new culture flasks contained 20ml of media from the 10^{-6} dilution series vials, 1 ml each of trace elements and vitamins solutions, and sodium thiosulfate to a final concentration of 1mM. The base salts solution comprised the remainder of the media, which had a final volume of 100ml in each flask. The cultures were incubated at 4ºC for 3 months and sampled every two weeks to determine ion concentrations and cell abundance,

as described above. When thiosulfate concentrations decreased to less than 100uM, the cultures were passaged into 100ml of new media as described above. After ~90 days, the cell concentration in the media, determined with epifluorescence microscopy, was 10^8 cells ml^{-1}, which was considered sufficient for DNA extraction.

Genetic Characterization of the Isolate

Seventy ml of active culture media containing 10^8 cells ml^{-1} was filtered onto a 0.2 μm polycarbonate filter, and DNA was extracted from the filter using a FastDNA Spin Kit for Soil (MP Biomedicals, Irvine, CA). Extracted genomic DNA was quantified using Qubit Fluorometric Quantification (Thermo Fisher Scientific, Waltham, MA). DNA Library preparation was performed by the Microbial Genome Sequencing Center (Pittsburgh, PA) with sequencing conducted on the Illumina NextSeq 2000 platform (2x151 bp reads) to a depth of 200Mbp. The isolate was identified by performing a Basic Local Alignment Search Tool (BLAST) (Altschul et al., 1990), using the DNA-directed RNA polymerase subunit beta (rpoB) gene. Functional annotation of genes from the isolate was conducted through the KEGG Automatic Annotation Server (KAAS) by using the bi-directional best hit (BBH) method to assign orthologs to protein sequences (Overbeek et al., 1999). A BLAST was performed with the identified protein sequences for *soxB* and *cbbl*, genes which code for the Sox complex for sulfur oxidation and the ribulose-1,5-bisphoosphate carboxylase/oxygenase (RubisCO) protein in the Calvin-Benson cycle, respectively. The similarity of these genes in the Bench Glacier isolate were compared to those of other isolates in the NCBI database.

Isolate Activity with Pyrite as Sole Source of Thiosulfate

Experiments were set up at 4°C, using pyrite as the sole sulfur source to determine if the BG isolate could utilize thiosulfate produced by the abiotic oxidation of pyrite. Pyrite was obtained from Hausen Rock Treasure Wholesale Inc. (Product # 10691, "Golden Pyrite Sand/Granules"). The pyrite was prepared using a procedure modified from Moses et al. (1987). The pyrite was crushed in a Fritsch Pulverisette 6 ball mill at 350 rpm for 5 minutes. The crushed pyrite was sieved though a 63-250 μm sieve stack on a shaker for two hours and approximately 30g of the 125-250 μm size fraction was collected and divided between two 50ml polypropylene tubes for washing.

The pyrite was washed to remove fine-grained particles and oxidation products from the mineral surface. 15ml of 100% acetone was added to each polypropylene tube and the tubes were vortexed for 10 seconds, then centrifuged at 5,000g for 5 min. The supernatant was removed, and fresh acetone was added. This process was repeated until the supernatant appeared clear, and the sedimented pyrite changed color from black to gold. The washing procedure was repeated three more times with 10% HCl to remove oxidation products from the mineral surface, then three times with concentrated acetone to remove remaining HCl. Approximately 3g of washed pyrite were stored for grain size, microscopic, and XRD analyses. The remaining mineral was transferred wet to two furnaced 70 ml serum vials, crimp sealed, and dried under a flow of ultra-high-purity N_2 gas and then retained in the sealed vials under a N_2 headspace.

The chemical composition of the pyrite was determined with x-ray diffraction (XRD). A grain-size analysis of the sieved and washed pyrite was conducted using a Mastersizer 3000 (Malvern Panalytical). The surface features of pyrite grains were observed with a scanning

electron microscope (SEM) for comparison with pyrite grains following the water/pyrite interaction during the incubation experiment.

Pyrite was added to dialysis tubing for the experiments to allow water/pyrite interactions to occur while preventing direct organism/mineral contact (Fig. 5.2). Approximately 15cm strips of Spectrum Spectra/Pr 1 RC dialysis membrane tubing (molecular weight cutoff 6-8 kD) were soaked in a 70% ethanol solution overnight. The tubing was then rinsed with ultrapure water (18.2 MΩ cm^{-1}) and stored in a furnaced beaker containing ultrapure water. Approximately 2g of the washed pyrite was weighed out into each of three furnaced beakers. One end of the dialysis tubing was folded over multiple times and tied shut with fishing line. Ultrapure water was added to the pyrite, which was then transferred with a pipette to the open end of the dialysis tubing. The open end of the tubing was tied shut once the ~2 g of pyrite was transferred. Both ends of the tubing were tied together and the outside of the tubing was rinsed with ultrapure water to remove any pyrite. The dialysis bag was then suspended from a rubber stopper with fishing line (Fig. 5.2). This process was repeated to prepare six dialysis bags, each with 2g of washed pyrite.

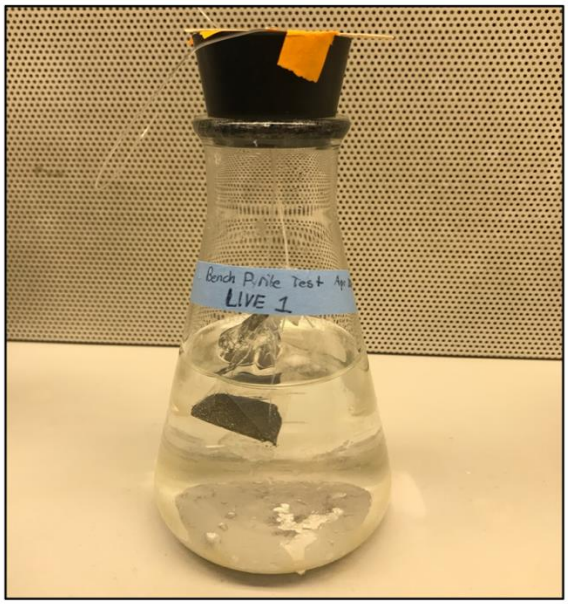


Fig. 5.2 Example of pyrite experimental flask setup with pyrite-filled dialysis bag suspended in media.

Three live (inoculated) and three control (uninoculated) flasks were prepared to determine if the Bench Glacier isolate could utilize thiosulfate produced by water/pyrite interactions. All incubations were prepared in a laminar flow hood, which was cleaned with 70% ethanol and subjected to UV radiation for 60 minutes prior to experiment preparation. Control flasks were prepared and sampled in the laminar flow hood first so that no live cultures would be present in the hood during work with the control treatments. Growth media was prepared as described above and added to furnaced, pre-chilled flasks. The media consisted of 176 ml of base salts, 2 ml of the vitamins solution, and 2 ml of the trace elements solution. Cell abundance in the isolate culture was determined through epifluorescence microscopy (as described above) to be 10^8 cells ml^{-1}. The live flasks were amended with 20ml of the Bench isolate culture (to a final concentration of 10^7 cells ml^{-1}, while the control flasks were amended with an additional 20ml of base salts media (Table 5.1). The final media volume was 200ml. The flasks were stored at 4°C

while the pyrite was added to dialysis tubing as described above. The experiment was initiated by fitting a stopper with the suspended pyrite dialysis bag to each flask. The pyrite in the dialysis bags remained fully submerged in media throughout the experiment.

The flasks were stored at 4°C in the dark and media was sampled at 0, 3, 7, 14, 21, and 28 days for determination of total dissolved ion concentrations (5ml from each experiment), and cell numbers (1ml from each experiment). The pH of the media was also determined at each timepoint with a pH meter that was cleaned with 70% ethanol and rinsed with ultrapure water between incubation measurements. “Time 0” sampling in the experiments was immediately prior to the addition of pyrite, and thus simply a measure of the media composition.

After 28 days, 50ml of media from each of the live treatments was filtered onto gold-coated polycarbonate membrane filters, for SEM analysis to determine if pyrite grains were present in the incubation media outside of the dialysis bag. If particles were observed, their elemental composition was determined with energy dispersive spectroscopy (EDS). Pyrite grains from live and control dialysis bags were also collected after 28 days for comparison of surface features with washed, unincubated pyrite grains.

Results

Genetic Characterization of a Thiosulfate Oxidizing Organism

An enrichment culture containing subglacial sediments from Bench Glacier and 1 mM thiosulfate showed a decrease in thiosulfate concentrations over time, indicating microbial thiosulfate utilization and likely growth of thiosulfate oxidizing organisms. A serial dilution of this culture also showed a decrease in thiosulfate concentrations over time and concurrent

increase in sulfate concentrations (Fig. 5.3). The sulfate produced in the incubations was in a nearly 2:1 concentration ratio with the decrease in thiosulfate.

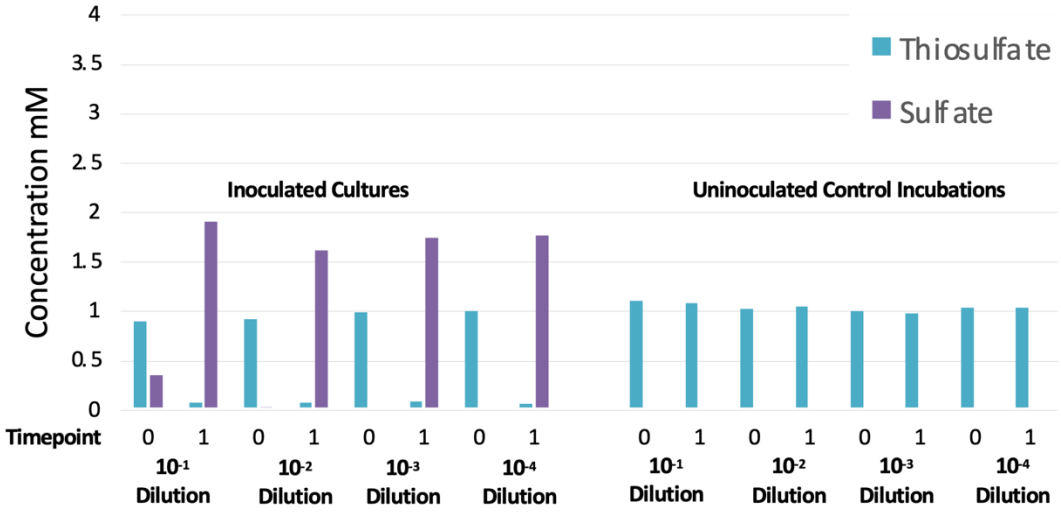


Fig. 5.3 Dilution series from active thiosulfate oxidizer enrichment culture containing sediments from Bench Glacier (BG). A subsample from the BG enrichment culture was passaged into new media in a serial dilution (10^{-1} to 10^{-4}). The uninoculated control incubations were also diluted in series. Media was incubated at 4°C in the dark, with an aerobic headspace. Timepoint 0 was the start of the incubation and timepoint 1 was one month after the start. Thiosulfate and sulfate concentrations determined with ion chromatography (limit of detection: 1µM).

The Bench Glacier isolate was identified as a *Polaromonas sp.* via BLAST, using the DNA-directed RNA polymerase subunit beta (rpoB) gene. Details on the isolate genome are presented in Table 5.2.

Table 5.2. Statistics associated with the assembly of the Bench Glacier *Polaromonas sp.* isolate

Genome Feature	Value
Total number of base pairs[1]	3,902,691
Number of contigs[1]	31
%GC Content[2]	62

1. Determined with PROKKA
2. Determined with CheckM

Functional annotation of genes using KAAS identified the presence of all functional genes necessary for the sulfur oxidation (SOX) pathway and inorganic carbon fixation (Fig. 5.4). Most functional genes associated with the reductive pentose phosphate cycle (Calvin-Benson) for carbon fixation were present in the *Polaromonas sp.* genome.

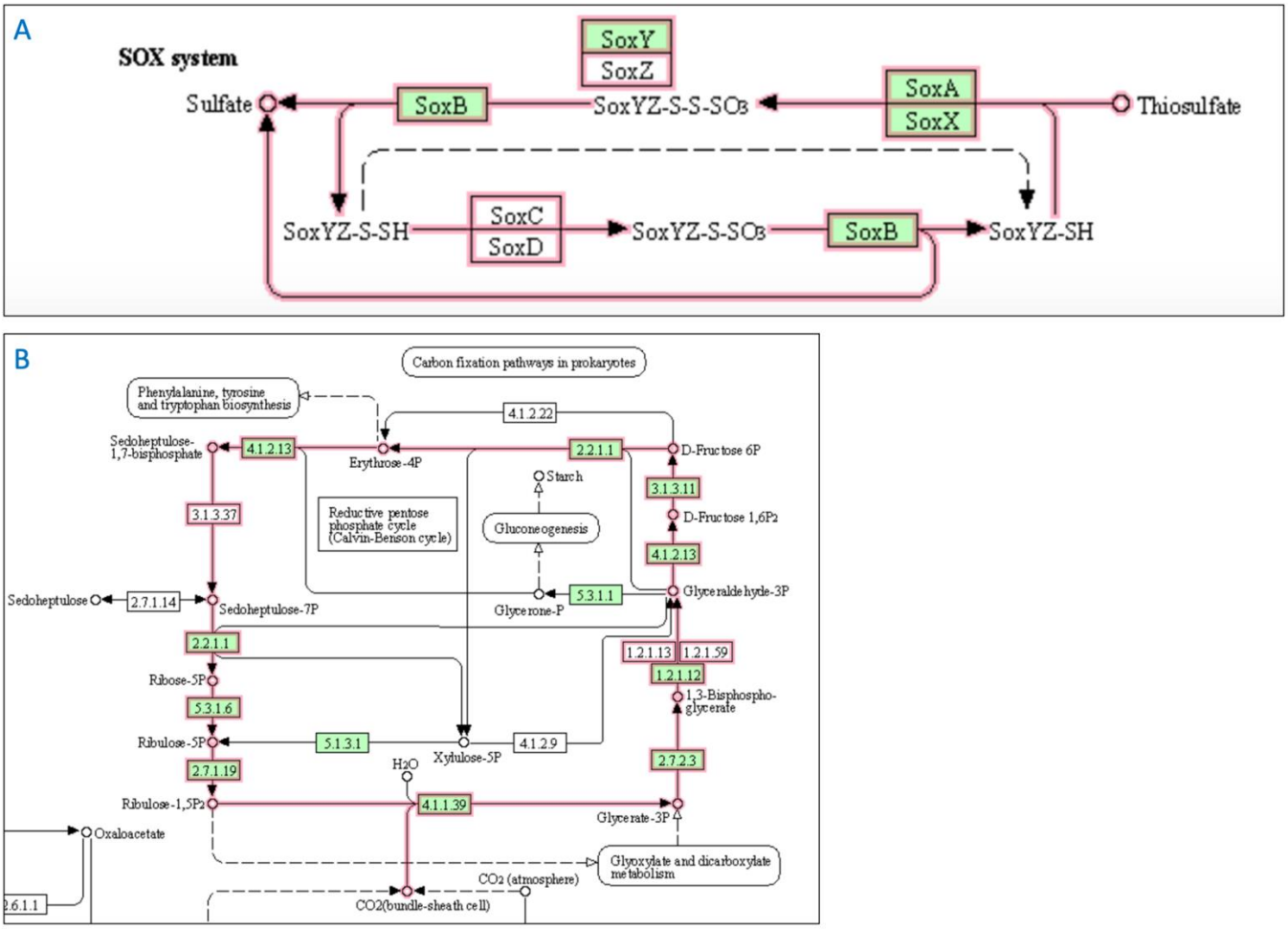


Fig. 5.4 KEGG pathway mapping of A) sulfur oxidation (Sox) pathway and B) carbon fixation pathway (Calvin Cycle) for Polaromonas isolate from Bench Glacier sediments. Green-filled boxes indicate that a gene is present in isolate genome.

A protein BLAST was conducted to compare the similarity of *soxB* and *cbbl* genes in the Bench Glacier isolate to other *Polaromonas* isolates in the NCBI database. These results are presented in Table 5.3.

Table 5.3. Percent similarity in sequence identity of select genes (*soxB* and *cbbl*) in the Bench Glacier isolate when compared to *Polaromonas* isolates in NCBI Genome Database. *soxB* is a key gene in the sulfur oxidation pathway and *cbbl* is a key gene in the Calvin Cycle.

Species	Isolate Source	Sulfur Oxidation (SoxB)	Calvin Cycle (cbbl)
P. eurypsychrophilia[1]	Glacial ice core (Tibet)	69.2 %	26.9 %
P. glacialis[2]	Glacial foreland soil (Svalbard)	Not Detected	Not Detected
P. jejuensis[3]	Mountain soil (S. Korea)	70.8 %	Not Detected
P. naphthalenivorans[4]	Coal-tar-contaminated sediment (New York)	Not Detected	32.3%
P. vacuolata[5]	Beneath sea ice (Antarctica Coast)	Not Detected	Not Detected

References: [1]Xing et al., 2016., [2]Wang et al., 2014., [3]Weon et al., 2008., [4]Jeon et al., 2004., [5]Hwang et al., 2021.

The Bench isolate genome also contained the NarGHI genes coding for the dissimilatory nitrate reduction pathway to nitrite. Marker gene narG in the Bench isolate shared greater sequence similarity to narG in *Polaromonas* isolates *P. eurypsychrophilia* (86% similarity) from Tibetan glacial ice cores (Xing et al., 2016) and *P. glacialis* (85% similarity) from a high Arctic glacial foreland soil in the Svalbard Archipelago, Norway (Wang et al., 2014), than in *P. jejuensis* (31% similarity) from mountain soil in South Korea (Weon et al., 2008).

Genes encoding the entire glycolysis pathway, associated with heterotrophy, were present in the Bench glacier isolate. The 2,3-bisphosphoglycerate-dependent phosphoglycerate mutase (PGM) sequence in the isolate shared 87% similarity to the PGM gene in an isolate of *P. jejuensis* from mountain soil in South Korea, and 91% similarity to the PGM gene in *P. glacialis* from a high Arctic glacial foreland soil in the Svalbard Archipelago, Norway (Wang et al., 2014). The PGM gene was not present in the *P. eurypsychrophilia* genome (Xing et al., 2016).

Pyrite Analyses

Approximately 82% of the pyrite grains used in the pyrite utilization experiments were in the target size fraction between 125 and 250 µM in size (Table 5.4). The remaining grains were between 76 and 125 µM (~11.3%) or between 250 and 310 µM (~7%). X-Ray diffraction analysis (XRD) determined that the pyrite used in the experiments was 100 Wt% FeS_2 (46.6% Fe, 53.4% S).

Table 5.4. Grain size distribution of pyrite used in Bench Glacier isolate pyrite utilization experiments.

Size (µm)	Volume %
76	0.12
86.4	1.06
98.1	3.33
111	6.83
127	10.86
144	14.4
163	16.4
186	16.21
211	13.82
240	9.92
272	5.65
310	1.4

Pyrite grains used in the live incubations were visually compared to the control incubation pyrite grains using SEM and there was no apparent difference in the surface characteristics between grains in the two treatments (Fig. 5.5).

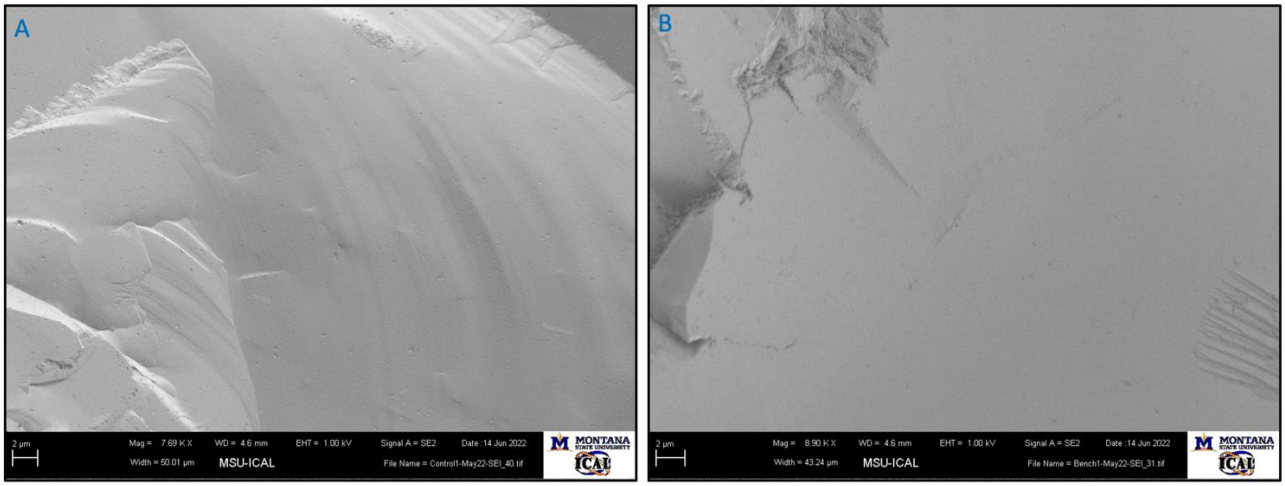


Fig. 5.5 Pyrite grain surfaces from control incubation dialysis bag (A), and live incubation dialysis bag (B). Images captured with Scanning Electron Microscopy (SEM).

Particulates were observed on filters after vacuum filtering 50ml of the growth media incubated with a submerged dialysis bag of pyrite in both the live and control flasks. EDS analysis identified the particulates as precipitates containing potassium, magnesium, zinc, manganese, cobalt, calcium, and iron, but none contained sulfur (Fig. 5.6). This indicated that pyrite grains were not present in the media and remained entirely in the dialysis bag during the incubation experiment for both live and control treatments.

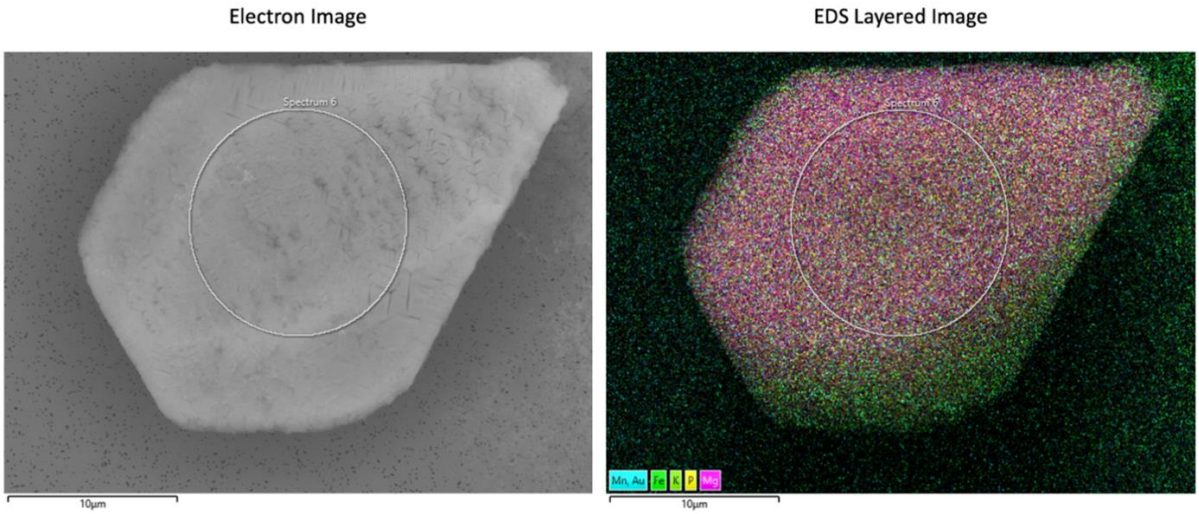


Fig. 5.6 Example of "crystalline" precipitate from incubation media observed at 301,740 X magnification with Electron Microscopy (Left) and with Energy-Dispersive X-Ray Spectroscopy (EDS) (Right). Legend for elements in the EDS image is shown bottom left of right panel. "Spectrum 6" circle is a targeting display icon for the electron microscope.

Bench Glacier Isolate Utilization of Thiosulfate Sourced from Pyrite

Uninoculated control treatments showed the production of thiosulfate and sulfate over the 28-day experiment, while inoculated cultures had no measurable thiosulfate at any point during the experiment (Fig. 5.7A) and concentrations of sulfate that were higher than the control (Fig. 5.7B).

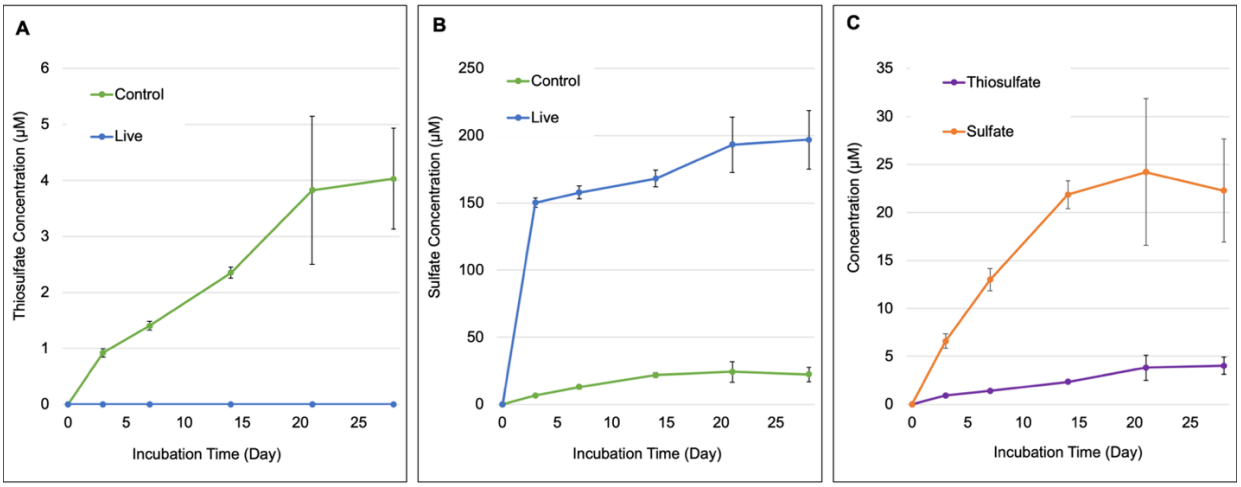


Fig. 5.7 Mean thiosulfate (A) and sulfate (B) concentrations in incubation media containing pyrite in a dialysis bag submerged in the media. "Control" treatments were uninoculated. "Live" treatments were inoculated with the Bench Glacier Polaromonas sp. isolate. C) Thiosulfate and sulfate in control treatments. Error bars represent standard deviation between the three replicate incubations. Concentrations are cumulative. Sulfate concentrations in live incubations are corrected for T=0 due to sulfate being present in the isolate cultures used for inoculation. Thiosulfate and sulfate concentrations determined with ion chromatography (limit of detection: 1µM).

The number of cells in the media did not appear to change significantly in the first three days (Fig. 5.8), even though the largest increase in the concentration of sulfate occurred during this time.

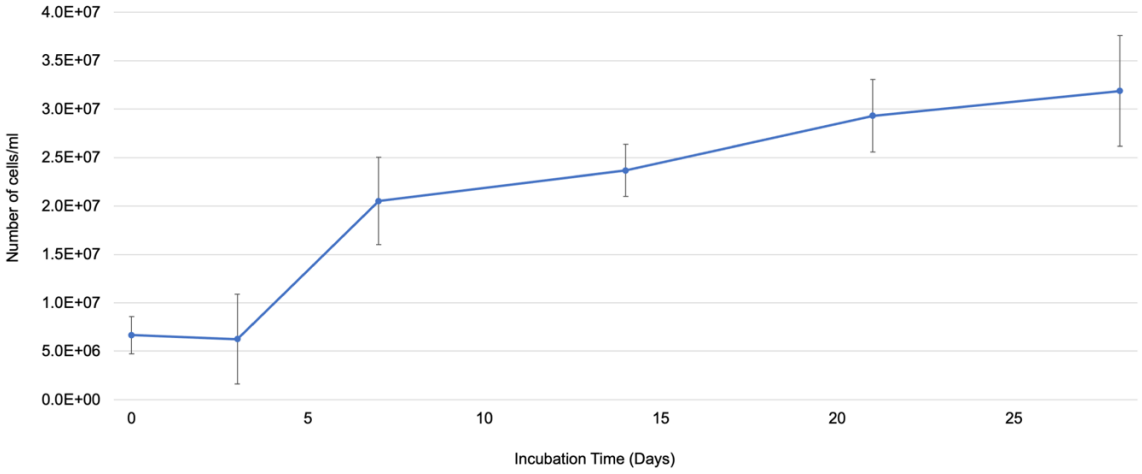


Fig. 5.8 Cell counts in the aqueous phase for "live" incubations in the pyrite utilization experiment. Error bars represent standard deviation between the three replicate incubations.

However, precipitates were observed in the media and filtering and staining the precipitates for epifluorescence microscopy (as described above) revealed many cells were associated with this precipitate that formed during the incubation (Fig. 5.9). These cells were not counted, and therefore there are no measurements of the total biomass and its change through time in the experiment. The average temperature in the incubator was 3.9 ± 0.3 °C throughout the experiment. The pH in all flasks increased slightly over the 28 days of incubation, from 8.3 ± 0.0 to 8.8 ± 0.1 in the controls and from 8.3 ± 0.0 to 8.8 ± 0.1 in the live incubations.

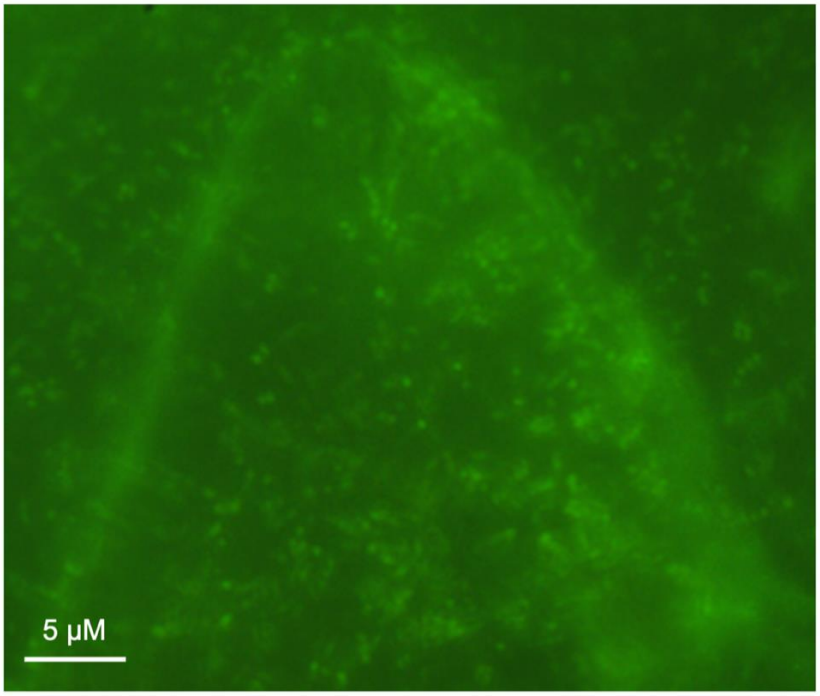


Fig. 5.9 Cells associated with precipitate formed in pyrite utilization experiment media inoculated with Polaromonas sp. The cells were stained with SYBR Gold nucleic acid gel stain (Invitrogen) and appear bright green when imaged with epifluorescence microscopy.

Discussion

Identification and Isolation of a Thiosulfate-Oxidizing Organism

The only sulfur oxidizing organism previously isolated and identified from a subglacial system was a strain of *Thiobacillus* sp. from Robertson Glacier, Canadian Rockies (Harrold et al., 2016). The *Polaromonas* sp. isolated in this present study represents the second. The utilization of thiosulfate and production of sulfate was in a 1:2 ratio for the enrichment cultures and dilution series that used an aqueous solution of NaS_2O_3 (Fig. 3), see equation 1

Equation 1: $S_2O_3^{2-} + 2O_2 + H_2O \rightarrow 2SO_4^{2-} + 2H^+$ (biotic)

Harrold et al. (2016) proposed an *in situ* model for sustaining sulfur oxidizing organisms in a subglacial system via the abiotic oxidation of sulfide minerals such as pyrite. Interactions between oxygenated water and pyrite result in the production of aqueous thiosulfate at a circumneutral pH (Moses et al., 1987; Moses and Herman, 1991). Harrold et al. (2016) suggested this abiotic process (Reaction 1) could provide a source of thiosulfate, which could then be oxidized by microorganisms (Reaction 2).

Reaction 1: $2FeS_2 + 3O_2 + 6H_2O \rightarrow 2S_2O_3^{2-} + 2Fe(OH)_{3(s)}$ (abiotic)

Reaction 2: $S_2O_3^{2-} + 2O_2 + H_2O \rightarrow 2SO_4^{2-} + 2H^+$ (biotic)

The ability of *Thiobacillus* sp. (RG5) to utilize thiosulfate generated from mineral/water reactions, however, was not determined in Harrold et al. (2016). The proposed pyrite/sulfur oxidizer relationship was tested in this study using the Bench Glacier isolate.

The *Polaromonas* isolate was added to growth media with pyrite as the sole sulfur source (Fig. 5.2). Thiosulfate concentrations increased in the control (uninoculated) treatments but remained below the detection limit in the live treatments (Fig. 5.7A). These results indicate the isolate utilized the thiosulfate as it was produced from the water/mineral reactions. However, the stoichiometric relationship between thiosulfate utilization and sulfate production in the live pyrite incubations does not appear to follow Reaction 2, the results from Harrold et al. (2016), or my enrichment cultures. If the organism were converting 1 mole of thiosulfate to 2 moles of sulfate (Reaction 1), then the concentration of sulfate in the live treatments should be double the amount of thiosulfate measured in the control incubations. The cumulative thiosulfate produced in the controls over 28 days of incubation was ~ 4uM (Fig. 5.7C). If a similar amount of

thiosulfate was produced by water/mineral reactions in the live treatments, we would expect sulfate concentrations in those treatments to be 8uM after 28 days. The sulfate concentrations measured in the live treatments, however, were 50 times higher than the thiosulfate concentration in the control incubations (Fig. 5.7B). Oxidation of thiosulfate with dissolved oxygen in the media (i.e. an abiotic version of Reaction 2) is likely minimal. Multiple studies measuring microbial sulfur oxidation have included uninoculated/sterilized control treatments containing $Na_2S_2O_3$, which were monitored for sulfate production. Two studies with aerobic control treatments at circumneutral pH, incubated in seawater at temperatures 0-4ºC, showed no changes to thiosulfate or sulfate concentrations over 12 hours (Houghton et al., 2016) or 200 days (Tuttle and Jannasch, 1976). Abiotic controls in Harrold et al. (2016) containing 6mM $Na_2S_2O_3$ showed less than 0.1mM sulfate production in aerobic, pH 8.3 solutions at 5.1ºC and 14.4ºCover 50 days, indicating thiosulfate oxidation with dissolved oxygen in the media was minimal (1.7% of the starting concentration).

The rate of sulfate production in the first three days of my biotic pyrite incubation experiments was more than 20 times greater than the rate in the subsequent 25 days of incubation (Table 5.5).

Table 5.5 Comparison of sulfate production rates during aqueous pyrite oxidation. “Biotic” incubation indicates sulfur-oxidizing organisms were present in aqueous media with pyrite. “Abiotic” incubations contained no organisms, only pyrite. All three studies were conducted in aerobic media. The media in the present study had a pH ~8, while the other two studies had media pH of ~7.

	Present Study		Percak-Dennett et al. (2017)	Moses & Herman (1991)
	Days 0-3 moles $SO_4/m^2/sec$	Days 3-28 moles $SO_4/m^2/sec$	moles $SO_4/m^2/sec$	moles $SO_4/m^2/sec$
Biotic Incubation	3.2×10^{-9}	1.2×10^{-10}	1.9×10^{-9}	N/A
Abiotic Incubation	1.4×10^{-10}	4.0×10^{-11}	3.2×10^{-10}	6.7×10^{-10}

Sulfate production rates in the first three days for both abiotic and biotic incubations were within the same order of magnitude as previous studies where aqueous pyrite oxidation was observed under aerobic conditions at a circumneutral pH (Table 5.5). The sulfate production rate in my abiotic pyrite experiment between days 0 and 3 days (1.4×10^{-10} mol $SO_4/m^2/sec$) was slightly lower than the abiotic aqueous pyrite oxidation experiments by Percak-Dennett et al. (2017) at 3.2×10^{-10} mol $SO_4/m^2/sec$ and Moses and Herman (1991) at 6.7×10^{-10} mol $SO_4/m^2/sec$, but within the same order of magnitude. The reason for the abrupt 20-fold rate decrease in sulfate production in the biotic experiments over days 4-28 is unclear. I was unable to obtain accurate cell counts for the biotic incubation experiments as a cell flocculation was associated with a precipitate that formed at the bottom of the incubation flask. Further experiments would be required to determine if the order-of-magnitude higher sulfate production rate in the first three days incubation is also associated with an increase in cell number.

Three possible scenarios that could account for the additional sulfate in the live incubations are 1) sulfate is also produced abiotically from pyrite-water reactions and/or 2) the microbial oxidation of thiosulfate drives additional abiotic thiosulfate production, which leads to further microbial oxidation of thiosulfate to sulfate and/or 3) sulfate production from pyrite occurs via an as yet unidentified mechanism. Previous studies have demonstrated that pyrite oxidation by dissolved oxygen in an aqueous solution produces sulfate at pH 7-9 (Moses et al., 1987; Xu and Schoonen, 1995; Rimstidt and Vaughan, 2003), and this was observed in our abiotic pyrite incubations (Fig. 5.7C). The amount of sulfate produced abiotically from pyrite/water interactions was 6-9 times higher than the total thiosulfate produced at each timepoint (Fig. 5.7C). The abiotic control experiments generated ~20 μM sulfate after 28 days, while sulfate in the live treatments was far greater, reaching nearly 200 μM (Fig. 5.7B). Therefore, abiotic reactions alone cannot explain the sulfate concentration in the inoculated experiments, indicating a microbial influence.

The presence of microorganisms in a system enhances mineral weathering (e.g. Mitchell et al., 2013; Montross et al., 2013; Boyd et al., 2014; Percak-Dennett et al., 2017). Microbial activity increases the rate at which elements are dissociated from the mineral as the biological reactions involved are generally faster than abiotic reactions, and previous studies have demonstrated this when microbes are in direct contact with the mineral (e.g. Montross et al., 2013; Boyd et al., 2014, Percak-Dennett et al., 2017). For example, microcosm experiments have shown that cation release from minerals are accelerated up to 8-fold in the presence of subglacial microorganisms, compared to abiotic rates, possibly due to mineral dissolution by carbonic acid that forms from heterotrophically-produced CO_2 and/or microbial oxidation of pyrite (Montross

et al., 2013; Boyd et al., 2014). Additionally, iron and sulfur-oxidizing species of *Rhizobiales* and *Ralstonia* were shown to enhance pyrite weathering at ~23ºC and circumneutral pH, with nearly all cells directly associated with the mineral surface (Percak-Dennett et al., 2017). The authors of the latter study proposed two mechanisms by which their *Rhizobiales* and *Ralstonia* isolates were enhancing pyrite weathering, both of which resulted in the production of sulfate.

Percak-Dennett et al., (2017) proposed a "polythionate intermediate model" for pyrite oxidation:

Reaction 3: $FeS_2 + 1.5O_2 \rightarrow S_2O_3^{2-} + Fe^{2+}$ (abiotic surface reaction)

Reaction 4: $S_2O_3^{2-} + 2O_2 + H_2O \rightarrow 2SO_4^{2-} + 2H^+$ (biotic)

Reaction 5: $Fe^{2+} + 0.25O_2 + 2.5H_2O \rightarrow Fe(OH)_3 + 4H^+$ (abiotic)

Under fully aerobic conditions, the Fe(II) in Reaction 3 will be rapidly oxidized to the Fe(III) hydroxide in Reaction 5 (Percak-Dennett et al., 2017), which was also suggested by Harrold et al. (2016) in Reaction 1 above. Percak-Dennett observed the formation of $Fe(OH)_3$ on the surface of the pyrite associated with microbial cells, while none formed in uninoculated treatments, suggesting microbial influence on its formation, despite the reactions for its formation being described as abiotic. The experimental system is not in equilibrium and therefore microbial oxidation of thiosulfate (Reaction 4) would not affect Reaction 3, thus having no effect of the concentration of Fe^{2+} available for Reaction 5. Further, microbial oxidation of thiosulfate (Reaction 4) would also not influence the production of additional thiosulfate via Reaction 3. Therefore, the additional sulfate in the Bench isolate experiments is not due to accelerating

Reaction 3. Instead, we must infer that sulfate production from pyrite occurs via an as yet unidentified mechanism.

There was no significant difference between total polythionate concentrations in the biotic and abiotic pyrite incubations conducted by Percak-Dennett et al. (2017), as would be expected if Reaction 4 were driving thiosulfate consumption in the inoculated media. They suggest that while this does not preclude the polythionate intermediate model as an active process, it indicates there is a more dominant mechanism in the live incubations driving the formation of $Fe(OH)_3$ and the higher production of sulfate.

The second pyrite weathering mechanism suggested by Percak-Dennett et al. (2017) is "sorbed Fe redox cycling," wherein cyclic oxidation/reduction of iron on the pyrite surface serves as a transport for electrons from pyrite-S to dissolved oxygen in the water until a stable sulfoxy species, such as sulfate, disassociates from the mineral surface (following Moses and Herman, 1991; Reactions 6-11 below). The Fe^{2+} formed during pyrite-water interactions (Reaction 3 above) adsorbs to the mineral surface (Reaction 6). The Fe(II) then donates electrons to O_2, leading to the formation of Fe(III) on the mineral surface (Reaction 7), which then accepts electrons from pyrite-S and is reduced to an adsorbed Fe(II) (Reaction 8). As more dissolved oxygen is added, the adsorbed Fe(II) is oxidized again (Reaction 9). The resulting Fe(III) then again accepts electrons from the reduced S in the underlying pyrite, leading to a transfer of the oxygen from the hydration sphere of the iron to the pyrite-S (Reaction 10). This multi-step electron transfer from pyrite-S to dissolved oxygen continues until a stable sulfate is formed and disassociates from the mineral into the media (Reaction 11).

Reactions 6-11

6: $FeS_2 + Fe^{2+} \rightarrow FeS_2{\equiv}Fe(II)_{ads}$ (abiotic surface reaction)

7: $FeS_2{\equiv}Fe(II)_{ads} + 0.25O_2 \rightarrow FeS_2{\equiv}Fe(III)_{ads}$ (biotic)

8: $FeS_2{\equiv}Fe(III)_{ads} \rightarrow FeSSOH{\equiv}Fe(II)_{ads}$ (abiotic e^- transfer from pyrite to $Fe(III)_{ads}$)

9: $FeSSOH{\equiv}Fe(II)_{ads} + 0.25O_2 \rightarrow FeSSOH{\equiv}Fe(III)_{ads}$ (biotic)

10: $FeSSOH{\equiv}Fe(III)_{ads} \rightarrow FeSSO_2H{\equiv}Fe(II)_{ads}$ (abiotic, e^- transfer from pyrite to $Fe(III)_{ads}$)

11: [multiple e^- transfer steps] $\rightarrow Fe(OH)_3 + 2SO_4^{2-}$ (abiotic)

Moses and Herman (1991) suggested the "sorbed Fe redox cycling" model is the rate-limiting process for pyrite oxidation at circumneutral pH, and the results from Percak-Dennett et al. (2017) indicate microbial activity accelerates this process. As a result, sulfate concentrations in the live incubations were higher than in the controls for the Percak-Dennett et al. (2017) study. This may not be the primary source of sulfate in the Bench isolate pyrite incubations, however. The majority of *Rhizobiales* and *Ralstonia* isolate cells observed via cryoSEM in Percak-Dennett et al. (2017) were in close association with the pyrite, which led the authors to argue that mineral-cell contact was likely necessary for reactions 6-11 (above) to occur. However, Percak-Dennett et al. (2017) did not conduct a parallel set of incubations with dialysis tubing preventing cell-mineral contact, so this remains an open question. The Bench Glacier isolate incubations used dialysis tubing to prevent cell-mineral contact, and increased sulfate production was observed in the live pyrite utilization experiments (Fig. 5.7B). Percak-Dennett et al. (2017) suggest Reactions 7 and 9 are promoted by enzymatic activity during cell-mineral contact, which could not occur in our study. Thus, if Percak-Dennett et al. (2017) are correct that microbial

acceleration of sorbed Fe redox cycling requires direct contact with the pyrite, then the "sorbed redox cycling" model is not a source of sulfate in the Bench Glacier isolate experiments.

Genetic Characterization of the Bench Isolate

The sulfur oxidizer isolated from the sediments of Bench Glacier is a strain of *Polaromonas sp.* which, to the author's knowledge, is a genus not previously identified as capable of sulfur oxidation and, furthermore, has traditionally been considered heterotrophic (e.g. Foght et al., 2004; Yagi et al., 2009; Giddings et al., 2010; Segawa et al., 2014) There are three pathways that have traditionally been considered the genetic mechanisms for microbial thiosulfate oxidation (Ghosh and Dam, 2009; Houghton et al., 2016; Zhang et al., 2020). The Sox pathway is commonly utilized by phototrophic and chemotrophic bacteria alphaproteobacteria (Friedrich et al., 2001; Houghton et al., 2016). The pathway consists of seven enzymes, SoxAXYZBCD, which catalyze the oxidation of 1 mol of thiosulfate to 2 mols of sulfate. Five Sox proteins, SoxAX, SoxYZ, and SoxB have been suggested as essential to sulfur oxidation as they were present in all available sulfur-oxidizing bacterial genomes studied by Friedrich et al. (2001). These five proteins catalyze the conversion of half of the thiosulfate to generate one mole of sulfate (Friedrich et al., 2001; Houghton et al., 2016; Fig. 5.4A), while a second mole of sulfate can be formed through the activity of proteins SoxB and SoxCD (Friedrich et al., 2001; Houghton et al., 2016; Fig. 5.4A). The genome of the *Polaromonas* isolate in this study contained homologues for four of the five enzymes required in the first pathway (Fig. 5.4A), but SoxZ was not identified. Friedrich et al. (2001) suggest that SoxZ's N-terminal amino acid sequence is homologous to SoxA in the sulfur-oxidizing chemolithoautotroph *P. pantotrophus*, so SoxA may be functionally identical to SoxYZ, making

SoxZ unnecessary for thiosulfate oxidation to sulfate in *P. pantotrophus* (Friedrich et al., 2001; Dambe et al., 2005).

The isolate is possibly coupling sulfur oxidation with carbon fixation through the Calvin cycle, as most of the functional genes associated with this process are present in the isolate's genome (Fig 5.4B), and limited organic carbon substrates were present in the enrichment culture or experimental media (21 μM of dissolved organic carbon from the vitamins solution). The cbbl gene, which codes for ribulose-1,5-bisphoosphate carboxylase/oxygenase (RubisCO) protein in the Calvin-Benson cycle, was identified in the Bench Glacier *Polaromonas* isolate (Table 5.3). This gene has been associated with bicarbonate uptake in arctic bacteria (Alonso-Sáez et al., 2010) and was previously used to identify autotrophs in subglacial sediments (Boyd et al., 2014). Together, these results suggest the Bench Glacier *Polaromonas* sp. could be capable of autotrophy. Autotrophic metabolism in this genus has, to this author's knowledge, only been identified once previously, in a *Polaromonas* strain isolated from seasonally frozen forest soils near Fairbanks, AK (Sizova and Panikov, 2007). *Polaromonas hydrogenivorans* cells were able to grow chemolithotrophically with H_2 and CO_2 or organotrophically with various organic acids, sugars, and alcohols (Sizova and Panikov, 2007). The *Polaromonas* species isolated from the sediments beneath Bench Glacier represents the first example of a member of this genus to be shown capable of thiosulfate oxidation. *Polaromonas* is widespread in glacial environments, (e.g. Darcy et al., 2011; Franzetti et al., 2013; Kohler et al., 2020), with one study identifying the genus in 24 glacial systems including those in the Canadian Arctic, Greenland, Iceland, and Norway (Kohler et al., 2020). Therefore, it is possible that *Polaromonas* sp. may be involved in sulfur oxidation in subglacial environments. Furthermore, a review of the genomes for

previously isolated species of *Polaromonas* reveals two strains with soxB genes (Table 5.3); *Polaromonas eurypsychrophilia*, which was isolated from an ice core in the Muztagh Glacier on the Tibetan Plateau (Xing et al., 2016) (NCBI Reference Sequence: NZ_BMIG00000000.1) and *Polaramonas jejuensis* sp. (NCBI Reference Sequence: GCF_001598235.1), isolated from mountain soil in South Korea (Weon et al., 2008). However, neither of these studies examined whether the isolates could use sulfur oxidation as an energy source, only aerobic heterotrophic growth was explored (Xing et al., 2016; Weon et al., 2008).

The genome of the Bench isolate contains functional genes coding for glycolysis, suggesting this species of *Polaromonas* is also capable of heterotrophy, which could be its preferred metabolism if organic carbon sources are available. However, the presence of genes encoding sulfur oxidation and the experimental demonstration of sulfur oxidation in the absence of significant organic carbon sources in the growth media indicate chemoautotrophy is a viable metabolic process for this isolate and its ability to utilize thiosulfate sourced from pyrite suggests a potential, but previously unconsidered role for *Polaromonas* in subglacial biogeochemical cycling.

The sulfur oxidizer *Thiobacillus RG5* was capable of sulfur oxidation under anaerobic conditions by using nitrate as an electron acceptor (Harrold et al., 2016). The genome from the Bench Glacier *Polaromonas* isolate contains genes coding for the Dissimilatory Nitrate Reduction pathway to nitrite. This suggests that the Bench isolate may be capable of anerobic thiosulfate oxidation. Subglacial sediments can become anaerobic for all, or part of the year (Benn and Evans, 2010), so the ability to use alternate oxidants could be an important survival mechanism for sediment microorganisms. The rate of thiosulfate oxidation was much slower

when nitrate was the oxidant, compared to oxygen, for the *Thiobacillus* from Robertson Glacier and less energy was produced from the anerobic metabolism (Harrold et al., 2016). Coupling thiosulfate oxidation with nitrate reduction would not be as energetically favorable as the aerobic pathway, but it could provide metabolic diversity to support the *Polaromonas* population in the Bench Glacier sediments when oxygen is unavailable.

Global Distribution and Adaptability of *Polaromonas*

The wide habitat range of *Polaromonas* includes temperate environments such as the forest soils of Alaska (Sizova and Panikov, 2007) and groundwater in New York and Germany (Jeon et al., 2004; Taubert et al., 2022). *Polaromonas* sp. are common and abundant in a range of frozen, glacial, and recently deglaciated environments (e.g. Foght et al., 2004; Liu et al., 2007; Nemergut et al., 2007; Darcy et al., 2011; Franzetti et al., 2013; Wang et al., 2014; Kohler et al. 2020) possibly due to a combination of features that give the genus selective advantages over others in colonizing new systems and adapting to strenuous conditions (Franzetti et al., 2013). *Polaromonas* phylotypes are more widely dispersed globally than other microbial clades found in glacial environments (Darcy et al., 2011, Nemergut et al., 2011; Kohler et al., 2020). *Polaromonas* has been found on six continents, with one study identifying the genus in 24 glacial systems from the Canadian Arctic to Greenland (Kohler et al., 2020). *Polaromonas* have been identified in ice core and snowpack samples from multiple glaciers on the Tibetan Plateau at elevations greater than 6,000 masl (Liu et al., 2009; Zhang et al., 2010; Xing et al., 2016), and in glacial snow and meltwater on Mount Everest at >6,000 masl (Liu et al., 2006 Liu et al., 2007). Darcy et al. (2011) suggest the prevalence of *Polaromonas* in higher elevation environments could indicate global atmospheric dispersal.

The aerobiological dispersal concept is supported by the presence of the *hipA* gene in some *Polaromonas* genomes (Darcy et al., 2011). The *hipA* gene is associated with the formation of metabolically dormant cells (Black et al., 1994) and was present in the metagenome sequenced from glacial ice of the Northern Schneeferner, Germany, suggesting the gene provides a survival mechanism during long-term transport and dormancy under frozen conditions (Simon et al. 2009; Darcy et al., 2011). The *Polaromonas* phylotypes observed in frozen forest soils in Alaska can also metabolize a diverse range of organic compounds to gain energy (Sizova and Panikov, 2007; Nemergut et al., 2011). The metabolic diversity of this genus may be the result of horizontal gene transfer, suggesting *Polaromonas* is a "opportunitroph" (Nemergut et al., 2011). Together, these characteristics demonstrate that *Polaromonas* is widespread globally, metabolically diverse, and adaptable to extreme conditions. The Bench Glacier isolate represents the first example of an autotrophic, thiosulfate-oxidizing species of *Polaromonas* in subglacial environments.

Conclusions

The *Polaromonas* species isolated from Bench Glacier sediments represents the first demonstration of thiosulfate-oxidizing activity in this genus and is only the second sulfur-oxidizer isolated from a subglacial environment. The Bench Glacier isolate was capable of oxidizing thiosulfate that was generated abiotically from pyrite at 4^{o}C, circumneutral pH, and without direct cell-mineral contact. *Polaromonas* sp. are common phylotypes in over 30 subglacial systems throughout the world and since pyrite is common in subglacial environments, as are circumneutral pH conditions, organisms capable of using thiosulfate as an electron donor may be widespread beneath glaciers/ice masses on Earth today and in the geologic past. The

Bench Glacier isolate demonstrates the potential metabolic versatility of *Polaromonas* organisms, with traits perhaps acquired through horizontal gene transfer that allow them to adapt to new environments and changing conditions.

References

Achberger, A. M., Michaud, A. B., Vick-Majors, T. J., Christner, B. C., Skidmore, M. L., Priscu, J. C., & Tranter, M. (2017). Microbiology of subglacial environments. Psychrophiles: from biodiversity to biotechnology, 83-110.

Alonso-Sáez, L., Galand, P. E., Casamayor, E. O., Pedros-Alio, C., & Bertilsson, S. (2010). High bicarbonate assimilation in the dark by Arctic bacteria. The ISME journal, 4(12), 1581-1590

Altschul, S. F., Gish, W., Miller, W., Myers, E. W., & Lipman, D. J. (1990). Basic local alignment search tool. Journal of Molecular Biology, 215(3), 403-410.

Anderson, S. P., Drever, J. I., Frost, C. D., & Holden, P. (2000). Chemical weathering in the foreland of a retreating glacier. Geochimica et Cosmochimica Acta, 64(7), 1173-1189.

Benn, D., & Evans, D. J. (2010). Glaciers and glaciation. Routledge.

Black, D. S., Irwin, B., & Moyed, H. S. (1994). Autoregulation of hip, an operon that affects lethality due to inhibition of peptidoglycan or DNA synthesis. Journal of Bacteriology, 176(13), 4081-4091.

Boyd, E. S., Hamilton, T. L., Havig, J. R., Skidmore, M. L., & Shock, E. L. (2014). Chemolithotrophic primary production in a subglacial ecosystem. Applied and Environmental Microbiology, 80(19), 6146-6153.

Bradford, J. H., Nichols, J., Mikesell, T. D., & Harper, J. T. (2009). Continuous profiles of electromagnetic wave velocity and water content in glaciers: an example from Bench Glacier, Alaska, USA. Annals of Glaciology, 50(51), 1-9.

Brown, G. H., Sharp, M., & Tranter, M. (1996). Subglacial chemical erosion: seasonal variations in solute provenance, Haut Glacier d'Arolla, Valais, Switzerland. Annals of Glaciology, 22, 25-31.

Christner, B. C., Priscu, J. C., Achberger, A. M., Barbante, C., Carter, S. P., Christianson, K., Michaud, A.B., Mikucki, J.A., Mitchell, A.C., Skidmore, M.L., & Vick-Majors, T. J.

(2014). A microbial ecosystem beneath the West Antarctic ice sheet. Nature, 512(7514), 310-313.

Dambe, T., Quentmeier, A., Rother, D., Friedrich, C., & Scheidig, A. J. (2005). Structure of the cytochrome complex SoxXA of Paracoccus pantotrophus, a heme enzyme initiating chemotrophic sulfur oxidation. Journal of structural biology, 152(3), 229-234.

Darcy, J. L., Lynch, R. C., King, A. J., Robeson, M. S., & Schmidt, S. K. (2011). Global distribution of Polaromonas phylotypes-evidence for a highly successful dispersal capacity. PLoS One, 6(8), e23742.

Davis, C. L., Venturelli, R. A., Michaud, A. B., Hawkings, J. R., Achberger, A. M., Vick-Majors, T. J., Rosenheim, B.E., Dore, J.E.; Steigmeyer, A.J., Skidmore, M.L., Barker, J.D., Benning, L.G., Siegfried, M.R., Priscu, J.C., & Christner, B. C. (2023). Biogeochemical and historical drivers of microbial community composition and structure in sediments from Mercer Subglacial Lake, West Antarctica. ISME communications, 3(1), 8.

Fennell, D. E., Rhee, S. K., Ahn, Y. B., Häggblom, M. M., & Kerkhof, L. J. (2004). Detection and characterization of a dehalogenating microorganism by terminal restriction fragment length polymorphism fingerprinting of 16S rRNA in a sulfidogenic, 2-bromophenol-utilizing enrichment. Applied and environmental microbiology, 70(2), 1169-1175.

Foght, J., Aislabie, J., Turner, S., Brown, C. E., Ryburn, J., Saul, D. J., & Lawson, W. J. M. E. (2004). Culturable bacteria in subglacial sediments and ice from two southern hemisphere glaciers. Microbial Ecology, 47, 329-340.

Fortner, S. K., Tranter, M., Fountain, A., Lyons, W. B., & Welch, K. A. (2005). The geochemistry of supraglacial streams of Canada Glacier, Taylor Valley (Antarctica), and their evolution into proglacial waters. Aquatic Geochemistry, 11, 391-412.

Franzetti, A., Tatangelo, V., Gandolfi, I., Bertolini, V., Bestetti, G., Diolaiuti, G., D'agata, C., Mihalcea, C., Smiraglia, C., & Ambrosini, R. (2013). Bacterial community structure on two alpine debris-covered glaciers and biogeography of Polaromonas phylotypes. The ISME journal, 7(8), 1483-1492.

Friedrich, C. G., Rother, D., Bardischewsky, F., Quentmeier, A., & Fischer, J. (2001). Oxidation of reduced inorganic sulfur compounds by bacteria: emergence of a common mechanism?. Applied and environmental microbiology, 67(7), 2873-2882.

Ghosh, W., & Dam, B. (2009). Biochemistry and molecular biology of lithotrophic sulfur oxidation by taxonomically and ecologically diverse bacteria and archaea. FEMS microbiology reviews, 33(6), 999-1043.

Giddings, C. G., Jennings, L. K., & Gossett, J. M. (2010). Microcosm Assessment of a DNA Probe Applied to Aerobic Degradation of cis-1, 2-Dichloroethene by Polaromonas sp. Strain JS666. Groundwater Monitoring & Remediation, 30(2), 97-105.

Gill-Olivas, B., Telling, J., Tranter, M., Skidmore, M., Christner, B., O'Doherty, S., & Priscu, J. (2021). Subglacial erosion has the potential to sustain microbial processes in Subglacial Lake Whillans, Antarctica. Communications Earth & Environment, 2(1), 134.

Hamilton, T. L., Peters, J. W., Skidmore, M. L., & Boyd, E. S. (2013). Molecular evidence for an active endogenous microbiome beneath glacial ice. The ISME journal, 7(7), 1402-1412.

Harrold, Z. R., Skidmore, M. L., Hamilton, T. L., Desch, L., Amada, K., Van Gelder, W., Glover, K., Roden, E.E., & Boyd, E. S. (2016). Aerobic and anaerobic thiosulfate oxidation by a cold-adapted, subglacial chemoautotroph. Applied and environmental microbiology, 82(5), 1486-1495.

Hawkings, J. R., Skidmore, M. L., Wadham, J. L., Priscu, J. C., Morton, P. L., Hatton, J. E., Gardner, C.B., Kohler, T.J., Stibal, M., Bagshaw, E.A., Steigmeyer, A.J., Barker, J., Dore, J.E., Lyons, W.B., Tranter, M., Specer, R.G., & the SALSA Science Team. (2020). Enhanced trace element mobilization by Earth's ice sheets. Proceedings of the National Academy of Sciences, 117(50), 31648-31659.

Houghton, J. L., Foustoukos, D. I., Flynn, T. M., Vetriani, C., Bradley, A. S., & Fike, D. A. (2016). Thiosulfate oxidation by Thiomicrospira thermophila: metabolic flexibility in response to ambient geochemistry. Environmental microbiology, 18(9), 3057-3072.

Hwang, K., Choe, H., Nasir, A., & Kim, K. M. (2021). Complete genome of Polaromonas vacuolata KCTC 22033T isolated from beneath Antarctic Sea ice. Marine genomics, 55, 100790.

Jeon, C. O., Park, W., Ghiorse, W. C., & Madsen, E. L. (2004). Polaromonas naphthalenivorans sp. nov., a naphthalene-degrading bacterium from naphthalene-contaminated sediment. International journal of systematic and evolutionary microbiology, 54(1), 93-97.

Jung, M. Y., Pham, V., Park, S. J., Kim, S. J., Chae, J. C., Roh, Y., & Rhee, S. K. (2010). Metagenomic assessment of a sulfur-oxidizing enrichment culture derived from marine sediment. The Journal of Microbiology, 48, 739-747.

Kohler, T. J., Vinšová, P., Falteisek, L., Žárský, J. D., Yde, J. C., Hatton, J. E., Hawkings, J.R., Lamarche-Gagnon, G., Hood, E., Cameron, K.A., & Stibal, M. (2020). Patterns in microbial assemblages exported from the meltwater of Arctic and Sub-Arctic glaciers. Frontiers in Microbiology, 11, 669.

Lanoil, B., Skidmore, M., Priscu, J. C., Han, S., Foo, W., Vogel, S. W., Tulaczyk, S., & Engelhardt, H. (2009). Bacteria beneath the West Antarctic ice sheet. Environmental Microbiology, 11(3), 609-615.

Liu, Y., Yao, T., Jiao, N., Kang, S., Zeng, Y., & Huang, S. (2006). Microbial community structure in moraine lakes and glacial meltwaters, Mount Everest. FEMS microbiology letters, 265(1), 98-105.

Liu, Y., Yao, T., Kang, S., Jiao, N., Zeng, Y., Huang, S., & Luo, T. (2007). Microbial community structure in major habitats above 6000 m on Mount Everest. Chinese Science Bulletin, 52(17), 2350-2357.

Liu, Y., Yao, T., Jiao, N., Kang, S., Xu, B., Zeng, Y., Huang, S., & Liu, X. (2009). Bacterial diversity in the snow over Tibetan Plateau Glaciers. Extremophiles, 13, 411-423.

MacGregor, K. R., Riihimaki, C. A., & Anderson, R. S. (2005). Spatial and temporal evolution of rapid basal sliding on Bench Glacier, Alaska, USA. Journal of Glaciology, 51(172), 49-63.

Michaud, A. B., Skidmore, M. L., Mitchell, A. C., Vick-Majors, T. J., Barbante, C., Turetta, C., Vangelder, W., & Priscu, J. C. (2016). Solute sources and geochemical processes in subglacial lake Whillans, west Antarctica. Geology, 44(5), 347-350.

Mitchell, A. C., Lafrenière, M. J., Skidmore, M. L., & Boyd, E. S. (2013). Influence of bedrock mineral composition on microbial diversity in a subglacial environment. Geology, 41(8), 855-858.

Mohapatra, B. R., Gould, W. D., Dinardo, O., & Koren, D. W. (2008). An overview of the biochemical and molecular aspects of microbial oxidation of inorganic sulfur compounds. CLEAN–Soil, Air, Water, 36(10-11), 823-829.

Montross, S. N., Skidmore, M., Tranter, M., Kivimäki, A. L., & Parkes, R. J. (2013). A microbial driver of chemical weathering in glaciated systems. Geology, 41(2), 215-218.

Moses, C. O., Nordstrom, D. K., Herman, J. S., & Mills, A. L. (1987). Aqueous pyrite oxidation by dissolved oxygen and by ferric iron. Geochimica et Cosmochimica Acta, 51(6), 1561-1571.

Moses, C. O., & Herman, J. S. (1991). Pyrite oxidation at circumneutral pH. Geochimica et cosmochimica acta, 55(2), 471-482.

Nemergut, D. R., Anderson, S. P., Cleveland, C. C., Martin, A. P., Miller, A. E., Seimon, A., & Schmidt, S. K. (2007). Microbial community succession in an unvegetated, recently deglaciated soil. Microbial ecology, 53, 110-122.

Nixon, S. L., Telling, J. P., Wadham, J. L., & Cockell, C. S. (2017). Viable cold-tolerant iron-reducing microorganisms in geographically diverse subglacial environments. Biogeosciences, 14(6), 1445-1455.

Overbeek, R., Fonstein, M., D'souza, M., Pusch, G. D., & Maltsev, N. (1999). The use of gene clusters to infer functional coupling. Proceedings of the National Academy of Sciences, 96(6), 2896-2901.

Percak-Dennett, E., He, S., Converse, B., Konishi, H., Xu, H., Corcoran, A., Noguera, D., Chan, C., Bhattacharyya, A., Borch, T., Boyd, E., & Roden, E. (2017). Microbial acceleration of aerobic pyrite oxidation at circumneutral pH. Geobiology, 15(5), 690-703.

Raiswell, R., Benning, L. G., Davidson, L., Tranter, M., & Tulaczyk, S. (2009). Schwertmannite in wet, acid, and oxic microenvironments beneath polar and polythermal glaciers. Geology, 37(5), 431-434.

Riihimaki, C. A., MacGregor, K. R., Anderson, R. S., Anderson, S. P., & Loso, M. G. (2005). Sediment evacuation and glacial erosion rates at a small alpine glacier. Journal of Geophysical Research: Earth Surface, 110(F3).

Rimstidt, J. D., & Vaughan, D. J. (2003). Pyrite oxidation: a state-of-the-art assessment of the reaction mechanism. Geochimica et Cosmochimica acta, 67(5), 873-880.

Segawa, T., Ishii, S., Ohte, N., Akiyoshi, A., Yamada, A., Maruyama, F., Li, Z., Hongoh, Y., & Takeuchi, N. (2014). The nitrogen cycle in cryoconites: naturally occurring nitrification-denitrification granules on a glacier. Environmental microbiology, 16(10), 3250-3262.

Skidmore, M. L., Foght, J. M., & Sharp, M. J. (2000). Microbial life beneath a high Arctic glacier. Applied and environmental microbiology, 66(8), 3214-3220.

Skidmore, M., Anderson, S. P., Sharp, M., Foght, J., & Lanoil, B. D. (2005). Comparison of microbial community compositions of two subglacial environments reveals a possible role for microbes in chemical weathering processes. Applied and environmental microbiology, 71(11), 6986-6997.

Schreiber, D. C., & Pavlostathis, S. G. (1998). Biological oxidation of thiosulfate in mixed heterotrophic/autotrophic cultures. Water Research, 32(5), 1363-1372.

Simon, C., Wiezer, A., Strittmatter, A. W., & Daniel, R. (2009). Phylogenetic diversity and metabolic potential revealed in a glacier ice metagenome. Applied and environmental microbiology, 75(23), 7519-7526.

Sizova, M., & Panikov, N. (2007). Polaromonas hydrogenivorans sp. nov., a psychrotolerant hydrogen-oxidizing bacterium from Alaskan soil. International journal of systematic and evolutionary microbiology, 57(3), 616-619.

Sorokin, D. Y., Tourova, T. P., Braker, G., & Muyzer, G. (2007). Thiohalomonas denitrificans gen. nov., sp. nov. and Thiohalomonas nitratireducens sp. nov., novel obligately chemolithoautotrophic, moderately halophilic, thiodenitrifying Gammaproteobacteria from hypersaline habitats. International journal of systematic and evolutionary microbiology, 57(7), 1582-1589.

Taubert, M., Overholt, W. A., Heinze, B. M., Matanfack, G. A., Houhou, R., Jehmlich, N., voonn Bergen, M., Rosch, P., Popp, J., & Küsel, K. (2022). Bolstering fitness via CO2 fixation and organic carbon uptake: mixotrophs in modern groundwater. The ISME journal, 16(4), 1153-1162.

Telling, J., Boyd, E. S., Bone, N., Jones, E. L., Tranter, M., MacFarlane, J. W., Martin, O.G., Wadham, J.L., Lamarche-Gagnon, G., Skidmore, M.L., Hamilton, T.L., Hill, E., Jackson, M., & Hodgson, D. A. (2015). Rock comminution as a source of hydrogen for subglacial ecosystems. Nature Geoscience, 8(11), 851-855.

Tranter, M., Sharp, M. J., Lamb, H. R., Brown, G. H., Hubbard, B. P., & Willis, I. C. (2002). Geochemical weathering at the bed of Haut Glacier d'Arolla, Switzerland—a new model. Hydrological processes, 16(5), 959-993.

Tranter, M. (2003). Geochemical weathering in glacial and proglacial environments. Treatise on geochemistry, 5, 605.

Tuttle, J. H., & Jannasch, H. W. (1976). Microbial utilization of thiosulfate in the deep sea 1. Limnology and Oceanography, 21(5),

Wadham, J. L., Bottrell, S., Tranter, M., & Raiswell, R. (2004). Stable isotope evidence for microbial sulphate reduction at the bed of a polythermal high Arctic glacier. Earth and Planetary Science Letters, 219(3-4), 341-355.

Wadham, J. L., Tranter, M., Skidmore, M., Hodson, A. J., Priscu, J., Lyons, W. B., Sharp, M., Wynn, P. & Jackson, M. (2010). Biogeochemical weathering under ice: Size matters. Global Biogeochemical Cycles, 24(3).

Wang, Z., Chang, X., Yang, X., Pan, L., & Dai, J. (2014). Draft genome sequence of Polaromonas glacialis strain R3-9, a psychrotolerant bacterium isolated from Arctic glacial foreland. Genome announcements, 2(4), 10-1128.

Wang, R., Lin, J. Q., Liu, X. M., Pang, X., Zhang, C. J., Yang, C. L., Lin, J.Q., & Chen, L. X. (2019). Sulfur oxidation in the acidophilic autotrophic Acidithiobacillus spp. Frontiers in microbiology, 9, 3290.

Weon, H. Y., Yoo, S. H., Hong, S. B., Kwon, S. W., Stackebrandt, E., Go, S. J., & Koo, B. S. (2008). Polaromonas jejuensis sp. nov., isolated from soil in Korea. International journal of systematic and evolutionary microbiology, 58(7), 1525-1528.

Widdel, F., & Pfennig, N. (1981). Studies on dissimilatory sulfate-reducing bacteria that decompose fatty acids: I. Isolation of new sulfate-reducing bacteria enriched with acetate from saline environments. Description of Desulfobacter postgatei gen. nov., sp. nov. Archives of microbiology, 129, 395-400.

Widdel, F., Kohring, G. W., & Mayer, F. (1983). Studies on dissimilatory sulfate-reducing bacteria that decompose fatty acids: III. Characterization of the filamentous gliding Desulfonema limicola gen. nov. sp. nov., and Desulfonema magnum sp. nov. Archives of microbiology, 134, 286-294.

Winkler, G. R., Silberman, M. L., Grantz, A., Miller, R. J., & MacEvitt Jr, E. M. (1981). Geologic map and summary geochronology of the Valdez quadrangle, southern Alaska, 1 sheet, scale 1: 250,000. US Geol. Surv. Open File Rep, 80-892.

Wolin, E. A., Wolin, M., & Wolfe, R. S. (1963). Formation of methane by bacterial extracts. Journal of Biological Chemistry, 238(8), 2882-2886.

Xing, T., Yao, T., Liu, Y., Wang, N., Xu, B., Shen, L., Gu, Z., Gu, B., Liu, H., & Zhou, Y. (2016). Polaromonas eurypsychrophila sp. nov., isolated from an ice core. International Journal of Systematic and Evolutionary Microbiology, 66(7), 2497-2501.

Xu, Y., & Schoonen, M. A. (1995). The stability of thiosulfate in the presence of pyrite in low-temperature aqueous solutions. Geochimica et Cosmochimica Acta, 59(22), 4605-4622.

Yagi, J. M., Sims, D., Brettin, T., Bruce, D., & Madsen, E. L. (2009). The genome of Polaromonas naphthalenivorans strain CJ2, isolated from coal tar-contaminated sediment, reveals physiological and metabolic versatility and evolution through extensive horizontal gene transfer. Environmental microbiology, 11(9), 2253-2270.

Zhang, S., Yang, G., Wang, Y., & Hou, S. (2010). Abundance and community of snow bacteria from three glaciers in the Tibetan Plateau. Journal of Environmental Sciences, 22(9), 1418-1424.

Zhang, J., Liu, R., Xi, S., Cai, R., Zhang, X., & Sun, C. (2020). A novel bacterial thiosulfate oxidation pathway provides a new clue about the formation of zero-valent sulfur in deep sea. The ISME Journal, 14(9), 2261-2274.

CHAPTER SIX

CONCLUSION

Concluding Remarks

The goal of this dissertation was to study the influence of iron and sulfur minerals on sub-ice biogeochemical processes in two glaciated environments. The dissertation had two themes. In Theme 1, I explored the role of iron bearing minerals in an abiotic reaction that produces methane as a possible source to an unexplained methane pool in Lake Bonney, Antarctica. In Theme 2, I examined the influence of iron-sulfide minerals on biological activity in subglacial sediments from Bench Glacier, Alaska. This research has demonstrated that the presence of iron and sulfur minerals potentially drives abiotic and biotic processes in both glaciated systems, though the magnitude of these processes is not fully understood.

Theme 1 had two objectives:

(i) Examine potential direct sources of methane to Lake Bonney associated with subglacial processes at Taylor Glacier.

(ii) Determine whether naturally occurring organosulfur compounds from the lake react with iron-bearing minerals in Taylor Glacier (TG) basal sediments and generate methane.

The 2017 methane concentration profile for West Lobe Lake Bonney (WLB) showed high concentrations, greater than atmospheric saturation below the chemocline at 18m. The methane in these waters had $\delta^{13}C\text{-}CH_4$ values ranging from -27.5 to -31.0 ‰ and $\delta^{2}H\text{-}CH_4$ values ranging from -141.0 to -142.2 ‰. Such values are consistent with an abiotic (thermogenic) origin for the methane rather than through microbial production (e.g. Milkov and Etiope, 2018). Collectively

the results from my experimental work indicate that direct basal ice melt, rock comminution and methane production from sediment organosulfur compounds are not major sources of methane to WLB. This therefore indicates that the primary source of methane in LB is thermogenic. The specific source for the crustally-derived methane supplied to the subglacial environment at TG (e.g. via gas permeable faults and fractured rocks) and trapped by the overlying ice remains unknown. However, potential sources for thermogenic methane are the Beacon Supergroup formation that underlies TG, which contains carbonaceous shale, a typical source rock for methane.

The methane concentration profile in WLB is not consistent with a simple diffusion gradient of methane sourced from the sediments (Li et al., 2020). The concentration profile suggests the sediments may be a methane source, but the highest concentrations are between 20 and 25m depth, in the 40m deep water column, which is the same depth that brine inflows from TG have been inferred from water column measurements (Spigel et al., 2018; Lawrence et al., 2020). My analysis of the methane water column data combined with the temperature and salinity profiles from Spigel et al., (2018) and Lawrence et al., (2020) provides robust evidence for the brine inflows as direct sources of methane to WLB. It is possible that methane is also seeping into the basal waters of the lake through the sediments, in addition to the direct brine inflows. The Blood Falls englacial brine that emanates supraglacially at TG has the same source beneath TG as the subglacial brine inflows (Badgeley et al., 2017). However, despite detailed geochemical data on the Blood Falls brines, no data on its methane concentration have been published (Lyons et al., 2019), thus precluding definitive confirmation of the brine as the methane source.

My work has demonstrated that naturally occurring organosulfur compounds DMS and DMSO from the LB waters will produce methane when reacted with glacial sediments at low (close to in situ) temperature. Previously these reactions had only been demonstrated at 25°C under laboratory conditions using synthetic organosulfur compounds and pure mineral phases (Althoff et al., 2014). Isotope mass balance modelling shows that these organosulfur-mineral reactions may be occurring below the chemocline in LB, but this is only evident in East Lobe Lake Bonney (ELB) where the methane concentrations (≤ 31 nM) are an order of magnitude lower than in WLB, but DMS and DMSO concentrations are comparable to WLB.

The methane in ELB waters had $\delta^{13}C\text{-}CH_4$ values ranging from -29.3 to -29.6 ‰, within the range for WLB, but the $\delta^{2}H\text{-}CH_4$ values ranged from -164.3 to -169.9 ‰. This suggests another methane source to these ELB waters in addition to the thermogenic methane. The additional methane source would have $\delta^{13}C\text{-}CH_4$ values comparable to the thermogenic source (-27.5 to -31.0 ‰) i.e. the WLB water, but with a more negative $\delta^{2}H\text{-}CH_4$ values. Isotopic mass balance modelling shows 12 – 16% (2.1 - 3.9 nM) of the total methane in ELB could be from DMSO generated methane, assuming the $\delta^{2}H\text{-}CH_4$ from organosulfur-mineral reactions is -320 ‰, consistent with the source water $\delta^{2}H\text{-}H_2O$ and $\delta^{2}H\text{-}CH_4$ for the thermogenic methane is -141.6 ‰. Such low (2-4 nM) concentrations would not have a significant impact on the isotopic signature of the methane in WLB, where concentrations are ~ 300nM or higher.

Theme 2 had two objectives:

(i) Investigate the presence of sulfur-oxidizing microbes in the subglacial sediments of Bench Glacier and isolate the organism.

(ii) Determine the sulfur oxidizer isolate can utilize thiosulfate sourced solely from the abiotic oxidation of pyrite.

The *Polaromonas* species I isolated from Bench Glacier sediments represents the first demonstration of thiosulfate-oxidizing activity in this genus and is only the second sulfur-oxidizer isolated from a subglacial environment. The *Polaromonas* species isolated is autotrophic, coupling CO_2 fixation with the oxidation of thiosulfate to sulfate under aerobic conditions at close to *in situ* subglacial temperatures (4°C). My low temperature (4°C) experiments using the isolate physically separated cells from the pyrite in an aqueous setting showing that it can utilize thiosulfate sourced solely from the abiotic oxidation of pyrite. This is the first time a glacial isolate has been shown to exhibit this capability. This implies that in the subglacial environment, direct cellular contact with the mineral pyrite is not required for an organism such as this *Polaromonas* species to be metabolically active.

I found no prior studies in my research that documented the genus *Polaromonas* conducting sulfur oxidation, with only one previous study showing that *Polaromonas* engages in any form of autotrophy (Sizova and Panikov, 2007) and most prior literature considering the genus to be heterotrophic (e.g. Foght et al., 2004; Yagi et al., 2009; Giddings et al., 2010; Segawa et al., 2014). My examination of available genomes from *Polaromonas* isolates found that some contain the genes necessary for sulfur oxidation and inorganic carbon fixation via the Calvin Cycle, but their potential role as primary producers had not been previously considered (Jeon et all., 2004; Xing et al., 2016). *Polaromonas* has been found on six continents, with one study identifying the genus in 24 glacial systems from the Canadian Arctic to Greenland (Kohler et al., 2020). Therefore, the discovery of a *Polaromonas* species with thiosulfate-oxidizing activity, has

broad implications for understanding microbial sulfur oxidizing process beneath ice sheets and glaciers. This research also highlights our understanding of the interplay between abiotic glacial processes and the subglacial biosphere is still limited and these results have opened new prospects for the role of microorganisms in subglacial biogeochemical cycling.

References

Althoff, F., Benzing, K., Comba, P., McRoberts, C., Boyd, D. R., Greiner, S., & Keppler, F. (2014). Abiotic methanogenesis from organosulphur compounds under ambient conditions. Nature Communications, 5(1), 4205.

Badgeley, J. A., Pettit, E. C., Carr, C. G., Tulaczyk, S., Mikucki, J. A., Lyons, W. B., & MIDGE Science Team. (2017). An englacial hydrologic system of brine within a cold glacier: Blood Falls, McMurdo Dry Valleys, Antarctica. Journal of Glaciology, 63(239), 387-400.

Foght, J., Aislabie, J., Turner, S., Brown, C. E., Ryburn, J., Saul, D. J., & Lawson, W. J. M. E. (2004). Culturable bacteria in subglacial sediments and ice from two southern hemisphere glaciers. Microbial Ecology, 47, 329-340.

Giddings, C. G., Jennings, L. K., & Gossett, J. M. (2010). Microcosm Assessment of a DNA Probe Applied to Aerobic Degradation of cis-1, 2-Dichloroethene by Polaromonas sp. Strain JS666. Groundwater Monitoring & Remediation, 30(2), 97-105.

Jeon, C. O., Park, W., Ghiorse, W. C., & Madsen, E. L. (2004). Polaromonas naphthalenivorans sp. nov., a naphthalene-degrading bacterium from naphthalene-contaminated sediment. International journal of systematic and evolutionary microbiology, 54(1), 93-97.

Kohler, T. J., Vinšová, P., Falteisek, L., Žárský, J. D., Yde, J. C., Hatton, J. E., Hawkings, J.R., Lamarche-Gagnon, G., Hood, E., Cameronn K.A. & Stibal, M. (2020). Patterns in microbial assemblages exported from the meltwater of Arctic and Sub-Arctic glaciers. Frontiers in Microbiology, 11, 669.

Lawrence, J. P., Doran, P. T., Winslow, L. A., & Priscu, J. C. (2020). Subglacial brine flow and wind-induced internal waves in Lake Bonney, Antarctica. Antarctic Science, 32(3), 223-237.

Li W., Dore J.E., Steigmeyer, A.J., Cho, Y-J., Kim, O-S., Liu, Y., Morgan-Kiss, R.M., Skidmore, M.L., Priscu, J.C. (2020). Methane production in the oxygenated water column of a perennially ice-covered Antarctic lake. Limnology and Oceanography, 65(1), 143-156.

Lyons, W. B., Mikucki, J. A., German, L. A., Welch, K. A., Welch, S. A., Gardner, C. B., Tulaczyk, S.M; Pettit, E.C., Kowalski, J., & Dachwald, B. (2019). The geochemistry of englacial brine from Taylor Glacier, Antarctica. Journal of Geophysical Research: Biogeosciences, 124(3), 633-648.

Milkov, A. V., & Etiope, G. (2018). Revised genetic diagrams for natural gases based on a global dataset of > 20,000 samples. Organic Geochemistry, 125, 109-120.

Segawa, T., Ishii, S., Ohte, N., Akiyoshi, A., Yamada, A., Maruyama, F., Li, Z., Hongoh, Y., & Takeuchi, N. (2014). The nitrogen cycle in cryoconites: naturally occurring nitrification-denitrification granules on a glacier. Environmental microbiology, 16(10), 3250-3262.

Sizova, M., & Panikov, N. (2007). Polaromonas hydrogenivorans sp. nov., a psychrotolerant hydrogen-oxidizing bacterium from Alaskan soil. International journal of systematic and evolutionary microbiology, 57(3), 616-619.

Spigel, R. H., Priscu, J. C., Obryk, M. K., Stone, W., & Doran, P. T. (2018). The physical limnology of a permanently ice-covered and chemically stratified Antarctic lake using high resolution spatial data from an autonomous underwater vehicle. Limnology and Oceanography, 63(3), 1234-1252.

Xing, T., Yao, T., Liu, Y., Wang, N., Xu, B., Shen, L., Gu, Z., Gu, B., Liu, H., & Zhou, Y. (2016). Polaromonas eurypsychrophila sp. nov., isolated from an ice core. International Journal of Systematic and Evolutionary Microbiology, 66(7), 2497-2501.

Yagi, J. M., Sims, D., Brettin, T., Bruce, D., & Madsen, E. L. (2009). The genome of Polaromonas naphthalenivorans strain CJ2, isolated from coal tar-contaminated sediment, reveals physiological and metabolic versatility and evolution through extensive horizontal gene transfer. Environmental microbiology, 11(9), 2253-2270.

REFERENCES CITED

Achberger, A. M., Christner, B. C., Michaud, A. B., Priscu, J. C., Skidmore, M. L., Vick-Majors, T. J., & WISSARD Science Team. (2016). Microbial community structure of subglacial lake Whillans, West Antarctica. Frontiers in Microbiology, 7, 212607.

Achberger, A. M., Michaud, A. B., Vick-Majors, T. J., Christner, B. C., Skidmore, M. L., Priscu, J. C., & Tranter, M. (2017). Microbiology of subglacial environments. Psychrophiles: from Biodiversity to Biotechnology, 83-110.

Aciego, S. M., Cuffey, K. M., Kavanaugh, J. L., Morse, D. L., & Severinghaus, J. P. (2007). Pleistocene ice and paleo-strain rates at Taylor Glacier, Antarctica. Quaternary Research, 68(3), 303-313.

Adams, E. E., Priscu, J. C., Fritsen, C. H., Smith, S. R., & Brackman, S. L. (1998). Permanent ice covers of the McMurdo Dry Valley Lakes, Antarctica: bubble formation and metamorphism. Ecosystem dynamics in a polar desert: the McMurdo dry valleys, Antarctica, 72, 281-295.

Alonso-Sáez, L., Galand, P. E., Casamayor, E. O., Pedros-Alio, C., & Bertilsson, S. (2010). High bicarbonate assimilation in the dark by Arctic bacteria. The ISME journal, 4(12), 1581-1590

Althoff, F., Jugold, A., & Keppler, F. (2010). Methane formation by oxidation of ascorbic acid using iron minerals and hydrogen peroxide. Chemosphere, 80(3), 286-292.

Althoff, F., Benzing, K., Comba, P., McRoberts, C., Boyd, D. R., Greiner, S., & Keppler, F. (2014). Abiotic methanogenesis from organosulphur compounds under ambient conditions. Nature Communications, 5(1), 4205.

Altschul, S. F., Gish, W., Miller, W., Myers, E. W., & Lipman, D. J. (1990). Basic local alignment search tool. Journal of Molecular Biology, 215(3), 403-410.

Anderson, S. P., Drever, J. I., Frost, C. D., & Holden, P. (2000). Chemical weathering in the foreland of a retreating glacier. Geochimica et Cosmochimica Acta, 64(7), 1173-1189.

Anderson, R. S., Anderson, S. P., MacGregor, K. R., Waddington, E. D., O'Neel, S., Riihimaki, C. A., & Loso, M. G. (2004). Strong feedbacks between hydrology and sliding of a small alpine glacier. Journal of Geophysical Research: Earth Surface, 109(F3).

Anderson, J. B., Conway, H., Bart, P. J., Witus, A. E., Greenwood, S. L., McKay, R. M., Hall, B.L., Ackert, R.P., Licht, K., Jakobsson, M., & Stone, J. O. (2014). Ross Sea paleo-ice sheet drainage and deglacial history during and since the LGM. Quaternary Science Reviews, 100, 31-54.

Anderson, J. T., Wilson, G. S., Fink, D., Lilly, K., Levy, R. H., & Townsend, D. (2017). Reconciling marine and terrestrial evidence for post LGM ice sheet retreat in southern McMurdo Sound, Antarctica. Quaternary Science Reviews, 157, 1-13.

Babcock, E., & Bradford, J. (2014). Quantifying the basal conditions of a mountain glacier using a targeted full-waveform inversion: Bench Glacier, Alaska, USA. Journal of Glaciology, 60(224), 1221-1231.

Badgeley, J. A., Pettit, E. C., Carr, C. G., Tulaczyk, S., Mikucki, J. A., Lyons, W. B., & MIDGE Science Team. (2017). An englacial hydrologic system of brine within a cold glacier: Blood Falls, McMurdo Dry Valleys, Antarctica. Journal of Glaciology, 63(239), 387-400.

Baggenstos, D., Severinghaus, J. P., Mulvaney, R., McConnell, J. R., Sigl, M., Maselli, O., Petit, J., Grente, B., & Steig, E. J. (2018). A horizontal ice core from Taylor Glacier, its implications for Antarctic climate history, and an improved Taylor Dome ice core time scale. Paleoceanography and Paleoclimatology, 33(7), 778-794.

Benn, D., & Evans, D. J. (2010). Glaciers and glaciation. Routledge.

Berger, G. W., Doran, P. T., & Thomsen, K. J. (2013). Micro-hole and multigrain quartz luminescence dating of Paleodeltas at Lake Fryxell, McMurdo Dry Valleys (Antarctica), and relevance for lake history. Quaternary Geochronology, 18, 119-134.

Bhatia, M. P., Das, S. B., Longnecker, K., Charette, M. A., & Kujawinski, E. B. (2010). Molecular characterization of dissolved organic matter associated with the Greenland ice sheet. Geochimica et Cosmochimica Acta, 74(13), 3768-3784.

Bindschadler, R. (2006). The environment and evolution of the West Antarctic ice sheet: setting the stage. Philosophical Transactions of the Royal Society A: Mathematical, Physical and Engineering Sciences, 364(1844), 1583-1605.

Bižić-Ionescu, M., Ionescu, D., Günthel, M., Tang, K. W., & Grossart, H. P. (2018). Oxic methane cycling: New evidence for methane formation in oxic lake water. Biogenesis of hydrocarbons, 1-22.

Black, D. S., Irwin, B., & Moyed, H. S. (1994). Autoregulation of hip, an operon that affects lethality due to inhibition of peptidoglycan or DNA synthesis. Journal of Bacteriology, 176(13), 4081-4091.

Bockheim, J. G., Campbell, I. B., & McLeod, M. (2007). Permafrost distribution and active-layer depths in the McMurdo Dry Valleys, Antarctica. Permafrost and periglacial processes, 18(3), 217-227.

Bogard, M. J., Del Giorgio, P. A., Boutet, L., Chaves, M. C. G., Prairie, Y. T., Merante, A., & Derry, A. M. (2014). Oxic water column methanogenesis as a major component of aquatic CH4 fluxes. Nature communications, 5(1), 5350.

Bomblies, A., McKnight, D. M., & Andrews, E. D. (2001). Retrospective simulation of lake-level rise in Lake Bonney based on recent 21-year record: indication of recent climate change in the McMurdo Dry Valleys, Antarctica. Journal of Paleolimnology, 25, 477-492.

Boyd, E. S., Skidmore, M., Mitchell, A. C., Bakermans, C., & Peters, J. W. (2010). Methanogenesis in subglacial sediments. Environmental microbiology reports, 2(5), 685-692.

Boyd, E. S., Lange, R. K., Mitchell, A. C., Havig, J. R., Hamilton, T. L., Lafrenière, M. J., Shock, E.L., Peters, J.W., & Skidmore, M. (2011). Diversity, abundance, and potential activity of nitrifying and nitrate-reducing microbial assemblages in a subglacial ecosystem. Applied and Environmental Microbiology, 77(14), 4778-4787.

Boyd, E. S., Hamilton, T. L., Havig, J. R., Skidmore, M. L., & Shock, E. L. (2014). Chemolithotrophic primary production in a subglacial ecosystem. Applied and environmental microbiology, 80(19), 6146-6153.

Bradford, J. H., Nichols, J., Mikesell, T. D., & Harper, J. T. (2009). Continuous profiles of electromagnetic wave velocity and water content in glaciers: an example from Bench Glacier, Alaska, USA. Annals of Glaciology, 50(51), 1-9.

Brown, G. H., Sharp, M., & Tranter, M. (1996). Subglacial chemical erosion: seasonal variations in solute provenance, Haut Glacier d'Arolla, Valais, Switzerland. Annals of Glaciology, 22, 25-31.

Burns, R., Wynn, P. M., Barker, P., McNamara, N., Oakley, S., Ostle, N., Stott, A.W., Tuffen, H., Zhou, Z., Tweed. F.S., Chesler, A., & Stuart, M. (2018). Direct isotopic evidence of biogenic methane production and efflux from beneath a temperate glacier. Scientific reports, 8(1), 17118.

Castendyk, D. N., Obryk, M. K., Leidman, S. Z., Gooseff, M., & Hawes, I. (2016). Lake Vanda: A sentinel for climate change in the McMurdo Sound Region of Antarctica. Global and Planetary Change, 144, 213-227.Castendyk, D. N., Obryk, M. K., Leidman, S. Z., Gooseff, M., & Hawes, I. (2016). Lake Vanda: A sentinel for climate change in the McMurdo Sound Region of Antarctica. Global and Planetary Change, 144, 213-227. Castendyk, D. N., Obryk, M. K., Leidman, S. Z., Gooseff, M., & Hawes, I. (2016). Lake Vanda: A sentinel for climate change in the McMurdo Sound Region of Antarctica. Global and Planetary Change, 144, 213-227.

Chapman-Smith, M. (1975). Geologic log of DVDP 12. Lake Leon, Taylor Valley: Dry Valley Drilling Project Bulletin, (5), 61-70.

Chinn, T. J. (1993). Physical hydrology of the dry valley lakes. Physical and biogeochemical processes in Antarctic lakes, 59, 1-51.

Christiansen, J. R., & Jørgensen, C. J. (2018). First observation of direct methane emission to the atmosphere from the subglacial domain of the Greenland Ice Sheet. Scientific reports, 8(1), 16623.

Christner, B. C., Priscu, J. C., Achberger, A. M., Barbante, C., Carter, S. P., Christianson, K., .Michaud, A.B., Mikucki, J.A., Mitchell, J.A., & Vick-Majors, T. J. (2014). A microbial ecosystem beneath the West Antarctic ice sheet. Nature, 512(7514), 310-313.

Clow, G. D., McKay, C. P., Simmons Jr, G. M., & Wharton Jr, R. A. (1988). Climatological observations and predicted sublimation rates at Lake Hoare, Antarctica. Journal of Climate, 1(7), 715-728.

Coolen, M. J., Hopmans, E. C., Rijpstra, W. I. C., Muyzer, G., Schouten, S., Volkman, J. K., & Damsté, J. S. S. (2004). Evolution of the methane cycle in Ace Lake (Antarctica) during the Holocene: response of methanogens and methanotrophs to environmental change. Organic Geochemistry, 35(10), 1151-1167.

Cox, S., Turnbull, I. M., Isaac, M. J., Townsend, D., & Lyttle, B. S. (2012). Geology of southern Victoria land Antarctica. Institute of Geological & Nuclear Sciences 1:250 000 Geological Map 22, 1-140.

Cragg, B. A., Parkes, R. J., Fry, J. C., Herbert, R. A., Wimpenny, J. W., & Getliff, J. M. (1990). Bacterial biomass and activity profiles within deep sediment layers. In Proceedings of the Ocean Drilling Program Scientific Results (Vol. 112, pp. 607-619). Ocean Drilling Program.

Cross, J. M., Fountain, A. G., Hoffman, M. J., & Obryk, M. K. (2022). Physical Controls on the Hydrology of Perennially Ice-Covered Lakes, Taylor Valley, Antarctica (1996–2013). Journal of Geophysical Research: Earth Surface, 127(12), e2022JF006833.

Cunningham, W. L., Leventer, A., Andrews, J. T., Jennings, A. E., & Licht, K. J. (1999). Late Pleistocene-Holocene marine conditions in the Ross Sea, Antarctica: evidence from the diatom record. The Holocene, 9(2), 129-139.

Dambe, T., Quentmeier, A., Rother, D., Friedrich, C., & Scheidig, A. J. (2005). Structure of the cytochrome complex SoxXA of Paracoccus pantotrophus, a heme enzyme initiating chemotrophic sulfur oxidation. Journal of structural biology, 152(3), 229-234.

Damm, E., Kiene, R. P., Schwarz, J., Falck, E., & Dieckmann, G. (2008). Methane cycling in Arctic shelf water and its relationship with phytoplankton biomass and DMSP. Marine Chemistry, 109(1-2), 45-59.

Damm, E., Helmke, E., Thoms, S., Schauer, U., Nöthig, E., Bakker, K., & Kiene, R. P. (2010). Methane production in aerobic oligotrophic surface water in the central Arctic Ocean. Biogeosciences, 7(3), 1099-1108.

Darcy, J. L., Lynch, R. C., King, A. J., Robeson, M. S., & Schmidt, S. K. (2011). Global distribution of Polaromonas phylotypes-evidence for a highly successful dispersal capacity. PLoS One, 6(8), e23742.

Davis, C. L., Venturelli, R. A., Michaud, A. B., Hawkings, J. R., Achberger, A. M., Vick-Majors, T. J., Rosenheim, B.E., Dore, J.E., Steigmeyer, A.J., Skidmoore, M.L, Barker, J.D., Benning, L.G., Siegfried, M.R., Priscu, J.C., Christner, B. C., & the SALSA Science Team (2023). Biogeochemical and historical drivers of microbial community composition and structure in sediments from Mercer Subglacial Lake, West Antarctica. ISME Communications, 3(1), 8.

Denton, G. H., & Marchant, D. R. (2000). The geologic basis for a reconstruction of a grounded ice sheet in McMurdo Sound, Antarctica, at the last glacial maximum. Geografiska Annaler: Series A, Physical Geography, 82(2-3), 167-211.

Dieser, M., Broemsen, E. L., Cameron, K. A., King, G. M., Achberger, A., Choquette, K., Hagedorn, B., Sletten, R., Junge, K., & Christner, B. C. (2014). Molecular and biogeochemical evidence for methane cycling beneath the western margin of the Greenland Ice Sheet. The ISME Journal, 8(11), 2305-2316.

Dieser, M., Broemsen, E. L., Cameron, K. A., King, G. M., Achberger, A., Choquette, K., Hagedorn, B., Sletten, R., Junge, K., & Christner, B. C. (2014). Molecular and biogeochemical evidence for methane cycling beneath the western margin of the Greenland Ice Sheet. The ISME journal, 8(11), 2305-2316.

Doran, P. T., McKay, C. P., Clow, G. D., Dana, G. L., Fountain, A. G., Nylen, T., & Lyons, W. B. (2002). Valley floor climate observations from the McMurdo Dry Valleys, Antarctica, 1986–2000. Journal of Geophysical Research: Atmospheres, 107(D24), ACL-13.

Doran, P. T., McKay, C. P., Fountain, A. G., Nylen, T., McKnight, D. M., Jaros, C., & Barrett, J. E. (2008). Hydrologic response to extreme warm and cold summers in the McMurdo Dry Valleys, East Antarctica. Antarctic Science, 20(5), 499-509.

Doran, P. T., Kenig, F., Knoepfle, J. L., Mikucki, J. A., & Lyons, W. B. (2014). Radiocarbon distribution and the effect of legacy in lakes of the McMurdo Dry Valleys, Antarctica. Limnology and Oceanography, 59(3), 811-826.

Doran, P.T. & Gooseff, M.N. (2023). Lake level surveys in the McMurdo Dry Valleys, Antarctica (1991-2023, ongoing). Environmental Data Initiative. DOI: 10.6073/pasta/927439563d37c9461011e0060a5c1a87

Doyle, S. M., & Christner, B. C. (2022). Variation in bacterial composition, diversity, and activity across different subglacial basal ice types. The Cryosphere, 16(10), 4033-4051.

Dugan, H. A., Obryk, M. K., & Doran, P. T. (2013). Lake ice ablation rates from permanently ice-covered Antarctic lakes. Journal of Glaciology, 59(215), 491-498.

Dunham, E. C., Dore, J. E., Skidmore, M. L., Roden, E. E., & Boyd, E. S. (2021). Lithogenic hydrogen supports microbial primary production in subglacial and proglacial environments. Proceedings of the National Academy of Sciences, 118(2), e2007051117.

Dziadek, R., Gohl, K., Diehl, A., & Kaul, N. (2017). Geothermal heat flux in the Amundsen Sea sector of West Antarctica: New insights from temperature measurements, depth to the bottom of the magnetic source estimation, and thermal modeling. Geochemistry, Geophysics, Geosystems, 18(7), 2657-2672.

Eberhardt, M. K., & Colina, R. (1988). The reaction of OH radicals with dimethyl sulfoxide. A comparative study of Fenton's reagent and the radiolysis of aqueous dimethyl sulfoxide solutions. The Journal of Organic Chemistry, 53(5), 1071-1074.

Elliot, D. H. (2013). The geological and tectonic evolution of the Transantarctic Mountains: a review. Geological Society, London, Special Publications, 381(1), 7-35.

Elston, D. P., & Bressler, S. L. (1981). Magneto-stratigraphic studies in neogene deposits of Taylor Valley and McMurdo Sound, Antarctica. Journal of the Royal Society of New Zealand, 11(4), 481-486.

Etiope, G., & Klusman, R. W. (2002). Geologic emissions of methane to the atmosphere. Chemosphere, 49(8), 777-789.

Etiope, G., Oehler, D. Z., & Allen, C. C. (2011). Methane emissions from Earth’s degassing: Implications for Mars. Planetary and Space Science, 59(2-3), 182-195.

Etiope, G., & Sherwood Lollar, B. (2013). Abiotic methane on Earth. Reviews of Geophysics, 51(2), 276-299.

Fennell, D. E., Rhee, S. K., Ahn, Y. B., Häggblom, M. M., & Kerkhof, L. J. (2004). Detection and characterization of a dehalogenating microorganism by terminal restriction fragment length polymorphism fingerprinting of 16S rRNA in a sulfidogenic, 2-bromophenol-utilizing enrichment. Applied and environmental microbiology, 70(2), 1169-1175.

Ferry, J. G. (2010). The chemical biology of methanogenesis. Planetary and Space Science, 58(14-15), 1775-1783.

Fisher, A. T., Mankoff, K. D., Tulaczyk, S. M., Tyler, S. W., Foley, N., & WISSARD Science Team. (2015). High geothermal heat flux measured below the West Antarctic Ice Sheet. Science Advances, 1(6), e1500093.

Florez-Leiva, L., Damm, E., & Farías, L. (2013). Methane production induced by dimethylsulfide in surface water of an upwelling ecosystem. Progress in oceanography, 112, 38-48.

Foght, J., Aislabie, J., Turner, S., Brown, C. E., Ryburn, J., Saul, D. J., & Lawson, W. J. M. E. (2004). Culturable bacteria in subglacial sediments and ice from two southern hemisphere glaciers. Microbial Ecology, 47, 329-340.

Foley, N., Tulaczyk, S., Auken, E., Schamper, C., Dugan, H., Mikucki, J., Virginia, R., & Doran, P. (2016). Helicopter-borne transient electromagnetics in high-latitude environments: An application in the McMurdo Dry Valleys, Antarctica. Geophysics, 81(1), WA87-WA99.

Foreman, C. M., Wolf, C. F., & Priscu, J. C. (2004). Impact of episodic warming events. Aquatic Geochemistry, 10, 239-268.

Fortner, S. K., Tranter, M., Fountain, A., Lyons, W. B., & Welch, K. A. (2005). The geochemistry of supraglacial streams of Canada Glacier, Taylor Valley (Antarctica), and their evolution into proglacial waters. Aquatic Geochemistry, 11, 391-412.

Fountain, A. G., Dana, G. L., Lewis, K. J., Vaughn, B. H., & Mcknight, D. H. (1998). Glaciers of the McMurdo Dry Valleys, Southern Victoria Land, Antarctica. Ecosystem Dynamics in a Polar Desert: The McMurdo Dry Valleys, Antarctica, 72, 65-75.

Fountain, A. G., Lyons, W. B., Burkins, M. B., Dana, G. L., Doran, P. T., Lewis, K. J., McKnight, D.M, Moorhead, D.L., Parsons, A.N, Priscu, J.C., Wall, D.H., Wharton, R.A., & Virginia, R. A. (1999). Physical controls on the Taylor Valley ecosystem, Antarctica. Bioscience, 49(12), 961-971.

Fountain, A. G., Levy, J. S., Gooseff, M. N., & Van Horn, D. (2014). The McMurdo Dry Valleys: a landscape on the threshold of change. Geomorphology, 225, 25-35.

Fountain, A. G., Neumann, T. A., Glenn, P. L., & Chinn, T. (2004). Can climate warming induce glacier advance in Taylor Valley, Antarctica?. Journal of Glaciology, 50(171), 556-564.

Fountain, A. G., Nylen, T. H., Monaghan, A., Basagic, H. J., & Bromwich, D. (2010). Snow in the McMurdo dry valleys, Antarctica. International Journal of Climatology: A Journal of the Royal Meteorological Society, 30(5), 633-642.

Franzetti, A., Tatangelo, V., Gandolfi, I., Bertolini, V., Bestetti, G., Diolaiuti, G., D'agata, C., Mihalcea, C., Smiraglia, C., & Ambrosini, R. (2013). Bacterial community structure on two alpine debris-covered glaciers and biogeography of Polaromonas phylotypes. The ISME journal, 7(8), 1483-1492.

Fretwell, P., Pritchard, H. D., Vaughan, D. G., Bamber, J. L., Barrand, N. E., Bell, R., Bianchi,C., Bingham,R.G., Blankenship, D.D., Casassa, G., Catania, G., Callens,D., Conway, H., Cook,A.J., Corr, H.F.J., Damaske, D., Damm,V., Ferraccioli, F., Forsberg,R., Fujita,S., Gim,Y., Gogineni,P., Griggs,J.A., Hindmarsh,R.C.A., Holmlund,P., Holt,J.W., Jacobel,R.W., Jenkins,A., Jokat,W., Jordan,T., King,E.C., Kohler,J., Krabill,W., Riger-Kusk,M., Langley,K.A., Leitchenkov,G., Leuschen,C., Luyendyk, B.P., Matsuoka,K., Mouginot,J., Nitsche,F.O., Nogi,Y., Nost,O.A., Popov,S.V., Rignot,E., Rippin,D.M., Rivera,A., Roberts,J., Ross,N., Siegert,M.J., Smith,A.M., Steinhage,D., Studinger,M., Sun,B., Tinto,B.K., Welch,B.C., Wilson,D., Young,D.A., Xiangbin,C., & Zirizzotti, A. (2013). Bedmap2: improved ice bed, surface and thickness datasets for Antarctica. The cryosphere, 7(1), 375-393.

Friedrich, C. G., Rother, D., Bardischewsky, F., Quentmeier, A., & Fischer, J. (2001). Oxidation of reduced inorganic sulfur compounds by bacteria: emergence of a common mechanism?. Applied and environmental microbiology, 67(7), 2873-2882.

Fritsen, C. H., & Priscu, J. C. (1999). Seasonal change in the optical properties of the permanent ice cover on Lake Bonney, Antarctica: consequences for lake productivity and phytoplankton dynamics. Limnology and Oceanography, 44(2), 447-454.

Fudge, T. J., Humphrey, N. F., Harper, J. T., & Pfeffer, W. T. (2008). Diurnal fluctuations in borehole water levels: configuration of the drainage system beneath Bench Glacier, Alaska, USA. Journal of Glaciology, 54(185), 297-306.

Garcia, J. L. (1990). Taxonomy and ecology of methanogens. FEMS Microbiology Letters, 87(3-4), 297-308.

Ghosh, W., & Dam, B. (2009). Biochemistry and molecular biology of lithotrophic sulfur oxidation by taxonomically and ecologically diverse bacteria and archaea. FEMS microbiology reviews, 33(6), 999-1043.

Giddings, C. G., Jennings, L. K., & Gossett, J. M. (2010). Microcosm Assessment of a DNA Probe Applied to Aerobic Degradation of cis-1, 2-Dichloroethene by Polaromonas sp. Strain JS666. Groundwater Monitoring & Remediation, 30(2), 97-105.

Gill-Olivas, B., Telling, J., Tranter, M., Skidmore, M., Christner, B., O'Doherty, S., & Priscu, J. (2021). Subglacial erosion has the potential to sustain microbial processes in Subglacial Lake Whillans, Antarctica. Communications Earth & Environment, 2(1), 134.

Gill-Olivas, B., Telling, J., Skidmore, M., & Tranter, M. (2023). Abrasion of sedimentary rocks as a source of hydrogen peroxide and nutrients to subglacial ecosystems. Biogeosciences, 20(5), 929-943.

Glatz, R. E., Lepp, P. W., Ward, B. B., & Francis, C. A. (2006). Planktonic microbial community composition across steep physical/chemical gradients in permanently ice-covered Lake Bonney, Antarctica. Geobiology, 4(1), 53-67.

Glen, J. W. (1958). The flow law of ice: A discussion of the assumptions made in glacier theory, their experimental foundations and consequences. IASH Publications, 47(171), e183.

Goodge, J. W. (2020). Geological and tectonic evolution of the Transantarctic Mountains, from ancient craton to recent enigma. Gondwana Research, 80, 50-122.

Goordial, J., Davila, A., Lacelle, D., Pollard, W., Marinova, M. M., Greer, C. W., DiRuggiero, J., McKay, C.P., & Whyte, L. G. (2016). Nearing the cold-arid limits of microbial life in permafrost of an upper dry valley, Antarctica. The ISME journal, 10(7), 1613-1624.

Gooseff, M. N., Lyons, W. B., McKnight, D. M., Vaughn, B. H., Fountain, A. G., & Dowling, C. (2006). A stable isotopic investigation of a polar desert hydrologic system, McMurdo Dry Valleys, Antarctica. Arctic, Antarctic, and Alpine Research, 38(1), 60-71.

Gooseff, M. N., McKnight, D. M., Doran, P., Fountain, A. G., & Lyons, W. B. (2011). Hydrological connectivity of the landscape of the McMurdo Dry Valleys, Antarctica. Geography Compass, 5(9), 666-681.

Hall, B. L., & Denton, G. H. (2000). Radiocarbon chronology of Ross Sea drift, eastern Taylor Valley, Antarctica: Evidence for a grounded ice sheet in the Ross Sea at the last glacial maximum. Geografiska Annaler: Series A, Physical Geography, 82(2-3), 305-336.

Hall, B. L., Hendy, C. H., & Denton, G. H. (2006). Lake-ice conveyor deposits: geomorphology, sedimentology, and importance in reconstructing the glacial history of the Dry Valleys. Geomorphology, 75(1-2), 143-156.

Hall, B. L., Denton, G. H., Stone, J. O., & Conway, H. (2013). History of the grounded ice sheet in the Ross Sea sector of Antarctica during the Last Glacial Maximum and the last termination. Geological Society, London, Special Publications, 381(1), 167-181.

Hall, B. L., Denton, G. H., Heath, S. L., Jackson, M. S., & Koffman, T. N. (2015). Accumulation and marine forcing of ice dynamics in the western Ross Sea during the last deglaciation. Nature Geoscience, 8(8), 625-628.

Hall, C. M., Castro, M. C., Kenig, F., & Doran, P. T. (2017). Constraining the recent history of the perennially ice-covered Lake Bonney, East Antarctica using He, Kr and Xe concentrations. Geochimica et Cosmochimica Acta, 209, 233-253.

Hallberg, K. B., González-Toril, E., & Johnson, D. B. (2010). Acidithiobacillus ferrivorans, sp. nov.; facultatively anaerobic, psychrotolerant iron-, and sulfur-oxidizing acidophiles isolated from metal mine-impacted environments. Extremophiles, 14, 9-19.

Hamilton, W., & Hayes, P. T. (1963). Type Section of the Beacon Sandstone of Antarctica. Geological Survey Professional Paper (No. 456-A).

Hamilton, T. L., Peters, J. W., Skidmore, M. L., & Boyd, E. S. (2013). Molecular evidence for an active endogenous microbiome beneath glacial ice. The ISME Journal, 7(7), 1402-1412.

Harrold, Z. R., Skidmore, M. L., Hamilton, T. L., Desch, L., Amada, K., Van Gelder, W., Glover, K., Roden, E.E., & Boyd, E. S. (2016). Aerobic and anaerobic thiosulfate oxidation by a cold-adapted, subglacial chemoautotroph. Applied and environmental microbiology, 82(5), 1486-1495.

Hawkings, J. R., Skidmore, M. L., Wadham, J. L., Priscu, J. C., Morton, P. L., Hatton, J. E., Gardner, C.B., Kohler, T.J., Stibal, M., Bagshaw, E.A., Steigmeyer, A.J., Barker, J., Dore, J.E., Lyons, W.B., Tranter, M., Specer, R.G., & the SALSA Science Team. (2020). Enhanced trace element mobilization by Earth's ice sheets. Proceedings of the National Academy of Sciences, 117(50), 31648-31659.

Hendy, C. H., Wilson, A. T., Popplewell, K. B., & House, D. A. (1977). Dating of geochemical events in Lake Bonney, Antarctica, and their relation to glacial and climate changes. New Zealand Journal of Geology and Geophysics, 20(6), 1103-1122.

Herscu-Kluska, R., Masarwa, A., Saphier, M., Cohen, H., & Meyerstein, D. (2008). Mechanism of the reaction of radicals with peroxides and dimethyl sulfoxide in aqueous solution. Chemistry–A European Journal, 14(19), 5880-5889.

Higgins, S. M., Hendy, C. H., & Denton, G. H. (2000). Geochronology of Bonney drift, Taylor Valley, Antarctica: evidence for interglacial expansions of Taylor Glacier. Geografiska Annaler: Series A, Physical Geography, 82(2-3), 391-409.

Houghton, J. L., Foustoukos, D. I., Flynn, T. M., Vetriani, C., Bradley, A. S., & Fike, D. A. (2016). Thiosulfate oxidation by Thiomicrospira thermophila: metabolic flexibility in response to ambient geochemistry. Environmental microbiology, 18(9), 3057-3072.

Hubbard, A., Lawson, W., Anderson, B., Hubbard, B., & Blatter, H. (2004). Evidence for subglacial ponding across Taylor Glacier, Dry Valleys, Antarctica. Annals of Glaciology, 39, 79-84.

Hubbard, B., Cook, S., & Coulson, H. (2009). Basal ice facies: a review and unifying approach. Quaternary Science Reviews, 28(19-20), 1956-1969.

Hwang, K., Choe, H., Nasir, A., & Kim, K. M. (2021). Complete genome of Polaromonas vacuolata KCTC 22033T isolated from beneath Antarctic Sea ice. Marine genomics, 55, 100790.

Jeffrey, A. W. A., & Kaplan, I. R. (1988). Hydrocarbons and inorganic gases in the Gravberg-1 well, Siljan Ring, Sweden. Chemical Geology, 71(1-3), 237-255.

Jennings-Mays, S.E., & Wharton, J.R. (1996). McMurdo Dry Valleys Long-Term Ecological Research (LTER): An overview of 1994-1995 research activities. Antarctic Journal of the United States, 30, 275-275.

Jeon, C. O., Park, W., Ghiorse, W. C., & Madsen, E. L. (2004). Polaromonas naphthalenivorans sp. nov., a naphthalene-degrading bacterium from naphthalene-contaminated sediment. International journal of systematic and evolutionary microbiology, 54(1), 93-97.

Jung, M. Y., Pham, V., Park, S. J., Kim, S. J., Chae, J. C., Roh, Y., & Rhee, S. K. (2010). Metagenomic assessment of a sulfur-oxidizing enrichment culture derived from marine sediment. The Journal of Microbiology, 48, 739-747.

Karl, D. M., Beversdorf, L., Björkman, K. M., Church, M. J., Martinez, A., & Delong, E. F. (2008). Aerobic production of methane in the sea. Nature Geoscience, 1(7), 473-478.

Karr, E. A., Ng, J. M., Belchik, S. M., Sattley, W. M., Madigan, M. T., & Achenbach, L. A. (2006). Biodiversity of methanogenic and other Archaea in the permanently frozen Lake Fryxell, Antarctica. Applied and Environmental Microbiology, 72(2), 1663-1666.

Kavanaugh, J. L., Cuffey, K. M., Morse, D. L., Bliss, A. K., & Aciego, S. M. (2009). Dynamics and mass balance of Taylor Glacier, Antarctica: 3. State of mass balance. Journal of Geophysical Research: Earth Surface, 114(F4).

Keys, J. R. (1979). Saline discharge at the terminus of Taylor Glacier. Antarctic Journal of the US, 14, 82–85.

Knight, P. G. (1997). The basal ice layer of glaciers and ice sheets. Quaternary Science Reviews, 16(9), 975-993.

Kohler, T. J., Vinšová, P., Falteisek, L., Žárský, J. D., Yde, J. C., Hatton, J. E., Hawkings, J.R., Lamarche-Gagnon, G., Hood, E., Cameronn K.A. & Stibal, M. (2020). Patterns in microbial assemblages exported from the meltwater of Arctic and Sub-Arctic glaciers. Frontiers in Microbiology, 11, 669.

Kong, W., Li, W., Romancova, I., Prášil, O., & Morgan-Kiss, R. M. (2014). An integrated study of photochemical function and expression of a key photochemical gene (psbA) in photosynthetic communities of Lake Bonney (McMurdo Dry Valleys, Antarctica). FEMS Microbiology Ecology, 89(2), 293-302.

Kwon, M., Kim, M., Takacs-Vesbach, C., Lee, J., Hong, S. G., Kim, S. J., Priscu, J.C., & Kim, O. S. (2017). Niche specialization of bacteria in permanently ice-covered lakes of the McMurdo Dry Valleys, Antarctica. Environmental microbiology, 19(6), 2258-2271.

Lamarche-Gagnon, G., Wadham, J. L., Sherwood Lollar, B., Arndt, S., Fietzek, P., Beaton, A. D., Tedstone, A.J., Telling, J., Bagshaw, E., Hawkings, J.R., Kohler, T.J., Zarsky, J.D., Moowlem, M.C., Anesio, A.M., & Stibal, M. (2019). Greenland melt drives continuous export of methane from the ice-sheet bed. Nature, 565(7737), 73-77.

Lanoil, B., Skidmore, M., Priscu, J. C., Han, S., Foo, W., Vogel, S. W., Tulaczyk, S., & Engelhardt, H. (2009). Bacteria beneath the West Antarctic ice sheet. Environmental Microbiology, 11(3), 609-615.

Lawrence, J. P., Doran, P. T., Winslow, L. A., & Priscu, J. C. (2020). Subglacial brine flow and wind-induced internal waves in Lake Bonney, Antarctica. Antarctic Science, 32(3), 223-237.

Lawson Knoepfle, J., Doran, P. T., Kenig, F., Lyons, W. B., & Galchenko, V. F. (2009). Particulate organic and dissolved inorganic carbon stable isotopic compositions in Taylor Valley lakes, Antarctica: the effect of legacy. Hydrobiologia, 632, 139-156.

Lee, P. A., Priscu, J. C., DiTullio, G. R., Riseman, S. F., Tursich, N., & de Mora, S. J. (2004). Elevated levels of dimethylated-sulfur compounds in Lake Bonney, a poorly ventilated Antarctic lake. Limnology and Oceanography, 49(4), 1044-1055.

Lee, P. G., Park, C., Moon, C. H., Park, M. O., & Gwon, K. Y. (2001). Biomass and species composition of phytoplankton and zooplankton along the salinity gradients in the Seomjin River Estuary. The Sea: Journal of the Korean Society of Oceanography, 6(2), 93-102.

Lee, H., Hwang, K., Cho, A., Kim, S., Kim, M., Morgan-Kiss, R., Priscu, J.C., Kim, K.M., & Kim, O. S. (2023). Microbial assemblages and associated biogeochemical processes in Lake Bonney, a permanently ice-covered lake in the McMurdo Dry Valleys, Antarctica.

Levy, J. (2013). How big are the McMurdo Dry Valleys? Estimating ice-free area using Landsat image data. Antarctic Science, 25(1), 119-120.

Levy, J. S., Fountain, A. G., O'Connor, J. E., Welch, K. A., & Lyons, W. B. (2013). Garwood valley, Antarctica: a new record of last glacial maximum to Holocene glaciofluvial processes in the McMurdo dry valleys. Bulletin, 125(9-10), 1484-1502.

Lewis, K. J., Fountain, A. G., & Dana, G. L. (1998). Surface energy balance and meltwater production for a Dry Valley glacier, Taylor Valley, Antarctica. Annals of Glaciology, 27, 603-609.

Li W., Dore J.E., Steigmeyer, A.J., Cho, Y-J., Kim, O-S., Liu, Y., Morgan-Kiss, R.M., Skidmore, M.L., Priscu, J.C. (2020). Methane production in the oxygenated water column of a perennially ice-covered Antarctic lake. Limnology and Oceanography, 65(1), 143-156.

Li, W., Chiuchiolo, A., Lawrence, J., Takacs-Vesbach, C., Morgan-Kiss, R., & Priscu, J.C. (In Preparation). Flux of particulate organic matter to the sediments of Lak Bonney, a permanently ice-covered Antarctic lake.

Liu, Y., Yao, T., Jiao, N., Kang, S., Zeng, Y., & Huang, S. (2006). Microbial community structure in moraine lakes and glacial meltwaters, Mount Everest. FEMS microbiology letters, 265(1), 98-105.

Liu, Y., Yao, T., Kang, S., Jiao, N., Zeng, Y., Huang, S., & Luo, T. (2007). Microbial community structure in major habitats above 6000 m on Mount Everest. Chinese Science Bulletin, 52(17), 2350-2357.

Liu, Y., Yao, T., Jiao, N., Kang, S., Xu, B., Zeng, Y., Huang, S., & Liu, X. (2009). Bacterial diversity in the snow over Tibetan Plateau Glaciers. Extremophiles, 13, 411-423.

Lizotte, M. P., Sharp, T. R., & Priscu, J. C. (1996). Phytoplankton dynamics in the stratified water column of Lake Bonney, Antarctica: I. Biomass and productivity during the winter-spring transition. Polar Biology, 16, 155-162.

Lovley, D. R., & Phillips, E. J. (1987). Competitive mechanisms for inhibition of sulfate reduction and methane production in the zone of ferric iron reduction in sediments. Applied and Environmental Microbiology, 53(11), 2636-2641.

Lyons, W., Fountain R., Priscu, J. C., Neumann, K, & Welch, K. A. (2000). Importance of landscape position and legacy: the evolution of the lakes in Taylor Valley, Antarctica. Freshwater Biology, 43(3), 355-367.

Lyons, W. B., Welch, K. A., Priscu, J. C., Laybourn-Parry, J., Moorhead, D., McKnight, D. M., Doran, P.T., & Tranter, M. (2001). The Mcmurdo Dry Valleys Long-Term Ecological Research Program: New understanding of the biogeochemistry of the Dry Valley Lakes: A review. Polar Geography, 25(3), 202-217.

Lyons, W. B., Welch, K. A., Snyder, G., Olesik, J., Graham, E. Y., Marion, G. M., & Poreda, R. J. (2005). Halogen geochemistry of the McMurdo Dry Valleys lakes, Antarctica: clues to the origin of solutes and lake evolution. Geochimica et Cosmochimica Acta, 69(2), 305-323.

Lyons, W. B., Mikucki, J. A., German, L. A., Welch, K. A., Welch, S. A., Gardner, C. B., Tulaczyk, S.M; Pettit, E.C., Kowalski, J., & Dachwald, B. (2019). The geochemistry of englacial brine from Taylor Glacier, Antarctica. Journal of Geophysical Research: Biogeosciences, 124(3), 633-648.

Macdonald, M. L., Wadham, J. L., Telling, J., & Skidmore, M. L. (2018). Glacial erosion liberates lithologic energy sources for microbes and acidity for chemical weathering beneath glaciers and ice sheets. *Frontiers in Earth Science*, *6*, 416476.

Macgregor, K. R., Riihimaki, C. A., & Anderson, R. S. (2005). Spatial and temporal evolution of rapid basal sliding on Bench Glacier, Alaska, USA. Journal of Glaciology, 51(172), 49-63.

Madigan, M. T., Bender, K. S., Buckley, D. H., Sattley, W. M., & Stahl, D. A. (2018). Brock biology of microorganisms. 15th Global Edition. Boston, US: Benjamin Cummins, 1, 1391-1407.

McElwain, J. C., Wade-Murphy, J., & Hesselbo, S. P. (2005). Changes in carbon dioxide during an oceanic anoxic event linked to intrusion into Gondwana coals. Nature, 435(7041), 479-482.

McKnight, D. M., Niyogi, D. K., Alger, A. S., Bomblies, A., Conovitz, P. A., & Tate, C. M. (1999). Dry valley streams in Antarctica: ecosystems waiting for water. Bioscience, 49(12), 985-995.

Metcalf, W. W., Griffin, B. M., Cicchillo, R. M., Gao, J., Janga, S. C., Cooke, H. A., Circelloo, B.T., Evans, B.S., Martens-Habbena, W.Stahl, D.A., & Van Der Donk, W. A. (2012). Synthesis of methylphosphonic acid by marine microbes: a source for methane in the aerobic ocean. Science, 337(6098), 1104-1107.

Michaud, A. B., Skidmore, M. L., Mitchell, A. C., Vick-Majors, T. J., Barbante, C., Turetta, C., vanGelder, W. & Priscu, J. C. (2016). Solute sources and geochemical processes in subglacial lake Whillans, west Antarctica. Geology, 44(5), 347-350.

Michaud, A. B., Dore, J. E., Achberger, A. M., Christner, B. C., Mitchell, A. C., Skidmore, M. L., Vick-Majors, T., & Priscu, J. C. (2017). Microbial oxidation as a methane sink beneath the West Antarctic Ice Sheet. Nature Geoscience, 10(8), 582-586.

Mikucki, J. A., Foreman, C. M., Sattler, B., Berry Lyons, W., & Priscu, J. C. (2004). Geomicrobiology of Blood Falls: an iron-rich saline discharge at the terminus of the Taylor Glacier, Antarctica. Aquatic Geochemistry, 10, 199-220.

Mikucki, J. A., & Priscu, J. C. (2007). Bacterial diversity associated with Blood Falls, a subglacial outflow from the Taylor Glacier, Antarctica. Applied and Environmental Microbiology, 73(12), 4029-4039.

Mikucki, J. A., Pearson, A., Johnston, D. T., Turchyn, A. V., Farquhar, J., Schrag, D. P., Anbar, A.D., Priscu, J.C., & Lee, P. A. (2009). A contemporary microbially maintained subglacial ferrous" ocean". Science, 324(5925), 397-400.

Mikucki, J. A., Auken, E., Tulaczyk, S., Virginia, R. A., Schamper, C., Sørensen, K. I., Doran, P.T., Dugan, H., & Foley, N. (2015). Deep groundwater and potential subsurface habitats beneath an Antarctic dry valley. Nature Communications, 6(1), 6831.

Milkov, A. V., & Etiope, G. (2018). Revised genetic diagrams for natural gases based on a global dataset of > 20,000 samples. Organic Geochemistry, 125, 109-120.

Mitchell, A. C., Lafrenière, M. J., Skidmore, M. L., & Boyd, E. S. (2013). Influence of bedrock mineral composition on microbial diversity in a subglacial environment. Geology, 41(8), 855-858.

Mitterer, R. M. (2010). Methanogenesis and sulfate reduction in marine sediments: A new model. Earth and Planetary Science Letters, 295(3-4), 358-366.

Mohapatra, B. R., Gould, W. D., Dinardo, O., & Koren, D. W. (2008). An overview of the biochemical and molecular aspects of microbial oxidation of inorganic sulfur compounds. CLEAN–Soil, Air, Water, 36(10-11), 823-829.

Monaghan, A. J., Bromwich, D. H., Powers, J. G., & Manning, K. W. (2005). The climate of the McMurdo, Antarctica, region as represented by one year of forecasts from the Antarctic Mesoscale Prediction System. Journal of Climate, 18(8), 1174-1189.

Montross, S. N., Skidmore, M., Tranter, M., Kivimäki, A. L., & Parkes, R. J. (2013). A microbial driver of chemical weathering in glaciated systems. Geology, 41(2), 215-218.

Montross, S., Skidmore, M., Christner, B., Samyn, D., Tison, J. L., Lorrain, R., Doyle, S. & Fitzsimons, S. (2014). Debris-rich basal ice as a microbial habitat, Taylor Glacier, Antarctica. Geomicrobiology Journal, 31(1), 76-81.

Moses, C. O., Nordstrom, D. K., Herman, J. S., & Mills, A. L. (1987). Aqueous pyrite oxidation by dissolved oxygen and by ferric iron. Geochimica et Cosmochimica Acta, 51(6), 1561-1571.

Moses, C. O., & Herman, J. S. (1991). Pyrite oxidation at circumneutral pH. Geochimica et Cosmochimica Acta, 55(2), 471-482.

Murray, A. E., Kenig, F., Fritsen, C. H., McKay, C. P., Cawley, K. M., Edwards, R., Kuhn, E., McKnnight, D.M., Ostrom, N.E., Peng, V., Ponce, A., Priscu, J.C., Samarkin, V., Townsend, A.T., Wagh, P., Young, S.A., Yung, P.T., & Doran, P. T. (2012). Microbial life at− 13 C in the brine of an ice-sealed Antarctic lake. Proceedings of the National Academy of Sciences, 109(50), 20626-20631.

Myers, M. E., Doran, P. T., & Myers, K. F. (2020). Summer valley-floor snowfall in Taylor Valley, Antarctica from 1995–2017. The Cryosphere Discussions, 2020, 1-24.

Myers, K. F., Doran, P. T., Tulaczyk, S. M., Foley, N. T., Bording, T. S., Auken, E., Dugan, H.A., Mikucki, J.A., Foged, N., Grombacher, D. & Virginia, R. A. (2021). Thermal legacy of a large paleolake in Taylor Valley, East Antarctica, as evidenced by an airborne electromagnetic survey. The Cryosphere, 15(8), 3577-3593.

Nemergut, D. R., Anderson, S. P., Cleveland, C. C., Martin, A. P., Miller, A. E., Seimon, A., & Schmidt, S. K. (2007). Microbial community succession in an unvegetated, recently deglaciated soil. Microbial ecology, 53, 110-122.

Nesbitt, H. W., Bancroft, G. M., Pratt, A. R., & Scaini, M. J. (1998). Sulfur and iron surface states on fractured pyrite surfaces. American Mineralogist, 83(9-10), 1067-1076.

Newberry, C. J., Webster, G., Cragg, B. A., Parkes, R. J., Weightman, A. J., & Fry, J. C. (2004). Diversity of prokaryotes and methanogenesis in deep subsurface sediments from the Nankai Trough, Ocean Drilling Program Leg 190. Environmental Microbiology, 6(3), 274-287.

Nixon, S. L., Telling, J. P., Wadham, J. L., & Cockell, C. S. (2017). Viable cold-tolerant iron-reducing microorganisms in geographically diverse subglacial environments. Biogeosciences, 14(6), 1445-1455.

Nylen, T. H., Fountain, A. G., & Doran, P. T. (2004). Climatology of katabatic winds in the McMurdo dry valleys, southern Victoria Land, Antarctica. Journal of Geophysical Research: Atmospheres, 109(D3).

Obryk, M. K., Doran, P. T., Hicks, J. A., McKay, C. P., & Priscu, J. C. (2016). Modeling the thickness of perennial ice covers on stratified lakes of the Taylor Valley, Antarctica. Journal of Glaciology, 62(235), 825-834.

Offre, P., Spang, A., & Schleper, C. (2013). Archaea in biogeochemical cycles. Annual Review of Microbiology, 67, 437-457.

Oremland, R. S., & Polcin, S. (1982). Methanogenesis and sulfate reduction: competitive and noncompetitive substrates in estuarine sediments. Applied and Environmental Microbiology, 44(6), 1270-1276.

Overbeek, R., Fonstein, M., D'souza, M., Pusch, G. D., & Maltsev, N. (1999). The use of gene clusters to infer functional coupling. Proceedings of the National Academy of Sciences, 96(6), 2896-2901.

Patriarche, J. D., Priscu, J. C., Takacs-Vesbach, C., Winslow, L., Myers, K. F., Buelow, H., Morgan-Kiss, R.M, & Doran, P. T. (2021). Year-round and long-term phytoplankton dynamics in Lake Bonney, a permanently ice-covered Antarctic lake. Journal of Geophysical Research: Biogeosciences, 126(4), e2020JG005925.

Penger, J., Conrad, R., & Blaser, M. (2012). Stable carbon isotope fractionation by methylotrophic methanogenic archaea. Applied and environmental microbiology, 78(21), 7596-7602.

Percak-Dennett, E., He, S., Converse, B., Konishi, H., Xu, H., Corcoran, A., Nooguera, D., Chann, C., Bhayyacharyya, A., Borch, T., Boyd, E., & Roden, E. E. (2017). Microbial acceleration of aerobic pyrite oxidation at circumneutral pH. Geobiology, 15(5), 690-703.

Petit, J. R., Jouzel, J., Raynaud, D., Barkov, N. I., Barnola, J. M., Basile, I., Bender, M., Chappellaz, J., Davis, M., Delaygue, G., Delmotte, M., Kotylakov, V.M., Legrand, M., Lipenkov, V.Y., Lorius, C., Pepin, L., Ritz, C., Saltzman, E., & Stievenard, M. (1999). Climate and atmospheric history of the past 420,000 years from the Vostok ice core, Antarctica. Nature, 399(6735), 429-436.

Pettit, E. C., Whorton, E. N., Waddington, E. D., & Sletten, R. S. (2014). Influence of debris-rich basal ice on flow of a polar glacier. Journal of Glaciology, 60(223), 989-1006.

Poreda, R. J., Hunt, A. G., Lyons, W. B., & Welch, K. A. (2004). The helium isotopic chemistry of Lake Bonney, Taylor Valley, Antarctica: Timing of late Holocene climate change in Antarctica. Aquatic Geochemistry, 10, 353-371.

Potter, J., & Konnerup-Madsen, J. (2003). A review of the occurrence and origin of abiogenic hydrocarbons in igneous rocks. Geological Society, London, Special Publications, 214(1), 151-173.

Powell, R. D. (1981). Sedimentation conditions in Taylor Valley, Antarctica, inferred from textural analysis of DVDP cores. Dry Valley Drilling Project, 33, 331-349.

Priscu, J. 2016. McMurdo Dry Valleys Depths, Areas, Volumes Measured by Jeffrey Schmok ver 5. Environmental Data Initiative. https://doi.org/10.6073/pasta/631a5c32f27e37a8094e2e18e4dec63c (Accessed 2024-05-02).

Priscu, J.C. 2023. Conductivity, temperature, and depth (CTD) vertical profiles collected from lakes in the McMurdo Dry Valleys, Antarctica (1993-2023, ongoing). Environmental Data Initiative. DOI: 10.6073/pasta/650871571843bde5e0db6fb52cf549a4. Dataset accessed 1 April 2024.

Purcell, A. M., Mikucki, J. A., Achberger, A. M., Alekhina, I. A., Barbante, C., Christner, B. C., Ghosh, D., Michaud, A.B., Mitchell, A.C., Priscu, J.C., Scherer, R., Skidmore, M.L., Vic-Majors, T.J., & Wissard Science Team. (2014). Microbial sulfur transformations in sediments from Subglacial Lake Whillans. Frontiers in Microbiology, 5, 594.

Raiswell, R., & Thomas, A. G. (1984). Solute acquisition in glacial melt waters. I. Fjallsjökull (south-east Iceland): bulk melt waters with closed-system characteristics. Journal of Glaciology, 30(104), 35-43.

Raiswell, R., Benning, L. G., Davidson, L., Tranter, M., & Tulaczyk, S. (2009). Schwertmannite in wet, acid, and oxic microenvironments beneath polar and polythermal glaciers. Geology, 37(5), 431-434.

Repeta, D. J., Ferrón, S., Sosa, O. A., Johnson, C. G., Repeta, L. D., Acker, M., DeLong, E., & Karl, D. M. (2016). Marine methane paradox explained by bacterial degradation of dissolved organic matter. Nature Geoscience, 9(12), 884-887.

Riihimaki, C. A., MacGregor, K. R., Anderson, R. S., Anderson, S. P., & Loso, M. G. (2005). Sediment evacuation and glacial erosion rates at a small alpine glacier. Journal of Geophysical Research: Earth Surface, 110(F3).

Rimstidt, J. D., & Vaughan, D. J. (2003). Pyrite oxidation: a state-of-the-art assessment of the reaction mechanism. Geochimica et Cosmochimica acta, 67(5), 873-880.

Rivkina, E., Shcherbakova, V., Laurinavichius, K., Petrovskaya, L., Krivushin, K., Kraev, G., Pecheritsina, S.; & Gilichinsky, D. (2007). Biogeochemistry of methane and methanogenic archaea in permafrost. FEMS microbiology ecology, 61(1), 1-15.

Šabacká, M., Priscu, J. C., Basagic, H. J., Fountain, A. G., Wall, D. H., Virginia, R. A., & Greenwood, M. C. (2012). Aeolian flux of biotic and abiotic material in Taylor Valley, Antarctica. Geomorphology, 155, 102-111.

Sander, R. (2015). Compilation of Henry's law constants (version 4.0) for water as solvent. Atmospheric Chemistry and Physics, 15(8), 4399-4981.

Sapper, S. E., Jørgensen, C. J., Schroll, M., Keppler, F., & Christiansen, J. R. (2023). Methane emissions from subglacial meltwater of three alpine glaciers in Yukon, Canada. Arctic, Antarctic, and Alpine Research, 55(1), 2284456.

Saxton, M. A., Samarkin, V. A., Schutte, C. A., Bowles, M. W., Madigan, M. T., Cadieux, S. B., Pratt, L.M., & Joye, S. B. (2016). Biogeochemical and 16S rRNA gene sequence evidence supports a novel mode of anaerobic methanotrophy in permanently ice-covered Lake Fryxell, Antarctica. Limnology and Oceanography, 61(S1), S119-S130.

Saxton, M. A., Samarkin, V. A., Madigan, M. T., Bowles, M. W., Sattley, W. M., Schutte, C. A., & Joye, S. B. (2021). Sulfate reduction and methanogenesis in the hypersaline deep waters and sediments of a perennially ice-covered lake. Limnology and Oceanography, 66(5), 1804-1818.

Schoell, M. (1980). The hydrogen and carbon isotopic composition of methane from natural gases of various origins. Geochimica et cosmochimica ACTA, 44(5), 649-661.

Schönheit, P., Kristjansson, J. K., & Thauer, R. K. (1982). Kinetic mechanism for the ability of sulfate reducers to out-compete methanogens for acetate. Archives of Microbiology, 132, 285-288.

Schreiber, D. C., & Pavlostathis, S. G. (1998). Biological oxidation of thiosulfate in mixed heterotrophic/autotrophic cultures. Water Research, 32(5), 1363-1372.

Sebacher, D. I., Harriss, R. C., Bartlett, K. B., Sebacher, S. M., & Grice, S. S. (1986). Atmospheric methane sources: Alaskan tundra bogs, an alpine fen, and a subarctic boreal marsh. Tellus B, 38(1), 1-10.

Segawa, T., Ishii, S., Ohte, N., Akiyoshi, A., Yamada, A., Maruyama, F., Li, Z., Hongoh, Y., & Takeuchi, N. (2014). The nitrogen cycle in cryoconites: naturally occurring nitrification-denitrification granules on a glacier. Environmental microbiology, 16(10), 3250-3262.

Shelobolina, E., Konishi, H., Xu, H., Benzine, J., Xiong, M. Y., Wu, T., Blothe, M.,& Roden, E. (2012). Isolation of phyllosilicate–iron redox cycling microorganisms from an illite–smectite rich hydromorphic soil. Frontiers in microbiology, 3, 134.

Siegert, M. J. (2008). Antarctic subglacial topography and ice-sheet evolution. Earth Surface Processes and Landforms: The Journal of the British Geomorphological Research Group, 33(4), 646-660.

Simon, C., Wiezer, A., Strittmatter, A. W., & Daniel, R. (2009). Phylogenetic diversity and metabolic potential revealed in a glacier ice metagenome. Applied and environmental microbiology, 75(23), 7519-7526.

Sizova, M., & Panikov, N. (2007). Polaromonas hydrogenivorans sp. nov., a psychrotolerant hydrogen-oxidizing bacterium from Alaskan soil. International journal of systematic and evolutionary microbiology, 57(3), 616-619.

Skidmore, M. L., Foght, J. M., & Sharp, M. J. (2000). Microbial life beneath a high Arctic glacier. Applied and Environmental Microbiology, 66(8), 3214-3220.

Skidmore, M., Anderson, S. P., Sharp, M., Foght, J., & Lanoil, B. D. (2005). Comparison of microbial community compositions of two subglacial environments reveals a possible role for microbes in chemical weathering processes. Applied and Environmental Microbiology, 71(11), 6986-6997.

Smith, R. L., Miller, L. G., & Howes, B. L. (1993). The geochemistry of methane in Lake Fryxell, an amictic, permanently ice-covered, Antarctic lake. Biogeochemistry, 21, 95-115.

Smith, S. H. (1962). Temperature correction in conductivity measurements 1. Limnology and Oceanography, 7(3), 330-334.

Sorokin, D. Y., Tourova, T. P., Braker, G., & Muyzer, G. (2007). Thiohalomonas denitrificans gen. nov., sp. nov. and Thiohalomonas nitratireducens sp. nov., novel obligately chemolithoautotrophic, moderately halophilic, thiodenitrifying Gammaproteobacteria from hypersaline habitats. International journal of systematic and evolutionary microbiology, 57(7), 1582-1589.

Sosa, O. A., Repeta, D. J., Ferrón, S., Bryant, J. A., Mende, D. R., Karl, D. M., & DeLong, E. F. (2017). Isolation and characterization of bacteria that degrade phosphonates in marine dissolved organic matter. Frontiers in microbiology, 8, 1786.

Sperazza, M., Moore, J. N., & Hendrix, M. S. (2004). High-resolution particle size analysis of naturally occurring very fine-grained sediment through laser diffractometry. Journal of Sedimentary Research, 74(5), 736-743.

Spigel, R. H., & Priscu, J. C. (1996). Evolution of temperature and salt structure of Lake Bonney, a chemically stratified Antarctic lake. Hydrobiologia, 321, 177-190.

Spigel, R. H., & Priscu, J. C. (1996). Evolution of temperature and salt structure of Lake Bonney, a chemically stratified Antarctic lake. Hydrobiologia, 321, 177-190.

Spigel, R. H., & Priscu, J. C. (1998). Physical limnology of the McMurdo Dry Valleys lakes. Ecosystem Dynamics in Polar Desert: the McMurdo Dry Valleys, Antarctica, 72, 153-187.

Spigel, R. H., Priscu, J. C., Obryk, M. K., Stone, W., & Doran, P. T. (2018). The physical limnology of a permanently ice-covered and chemically stratified Antarctic lake using high resolution spatial data from an autonomous underwater vehicle. Limnology and Oceanography, 63(3), 1234-1252.

Steig, E. J., Morse, D. L., Waddington, E. D., Stuiver, M., Grootes, P. M., Mayewski, P. A., Twickler, M.S., & Whitlow, S. I. (2000). Wisconsinan and Holocene climate history from an ice core at Taylor Dome, western Ross Embayment, Antarctica. Geografiska Annaler: Series A, Physical Geography, 82(2-3), 213-235.

Steiner, M. G., & Babbs, C. F. (1990). Quantitation of the hydroxyl radical by reaction with dimethyl sulfoxide. Archives of biochemistry and biophysics, 278(2), 478-481.

Stevenson, E. I., Fantle, M. S., Das, S. B., Williams, H. M., & Aciego, S. M. (2017). The iron isotopic composition of subglacial streams draining the Greenland ice sheet. Geochimica et Cosmochimica Acta, 213, 237-254.

Stibal, M., Wadham, J. L., Lis, G. P., Telling, J., Pancost, R. D., Dubnick, A., Sharp, M., Lawson, E., Butler, C., Hasan, F., Tranter, M., & Anesio, A. M. (2012). Methanogenic potential of Arctic and Antarctic subglacial environments with contrasting organic carbon sources. Global Change Biology, 18(11), 3332-3345.

Sugden, D. E., Denton, G. H., & Marchant, D. R. (1995). Landscape evolution of the Dry Valleys, Transantarctic Mountains: tectonic implications. Journal of Geophysical Research: Solid Earth, 100(B6), 9949-9967.

Swanger, K. M., Marchant, D. R., Kowalewski, D. E., & Head III, J. W. (2010). Viscous flow lobes in central Taylor Valley, Antarctica: origin as remnant buried glacial ice. Geomorphology, 120(3-4), 174-185.

Tamppari, L. K., Anderson, R. M., Archer, P. D., Douglas, S., Kounaves, S. P., McKay, C. P., Ming, D.W., Moore, Q., Quinn, J.E., Smith, P.H., Stroble, S., & Zent, A. P. (2012). Effects of extreme cold and aridity on soils and habitability: McMurdo Dry Valleys as an analogue for the Mars Phoenix landing site. Antarctic Science, 24(3), 211-228.

Tang, C., Madigan, M. T., & Lanoil, B. (2013). Bacterial and archaeal diversity in sediments of west Lake Bonney, McMurdo Dry Valleys, Antarctica. Applied and Environmental Microbiology, 79(3), 1034-1038.

Taubert, M., Overholt, W. A., Heinze, B. M., Matanfack, G. A., Houhou, R., Jehmlich, N., voonn Bergen, M., Rosch, P., Popp, J., & Küsel, K. (2022). Bolstering fitness via CO2 fixation and organic carbon uptake: mixotrophs in modern groundwater. The ISME journal, 16(4), 1153-1162.

Tazaz, A. M., Bebout, B. M., Kelley, C. A., Poole, J., & Chanton, J. P. (2013). Redefining the isotopic boundaries of biogenic methane: Methane from endoevaporites. Icarus, 224(2), 268-275.

Telling, J., Boyd, E. S., Bone, N., Jones, E. L., Tranter, M., MacFarlane, J. W., Martin, P.G., Wadham, J.L., Lamarche-Gagnon, G., Skidmore, M.L., Hamilton, T.L., Hill, E., Jackson, M., & Hodgson, D. A. (2015). Rock comminution as a source of hydrogen for subglacial ecosystems. Nature Geoscience, 8(11), 851-855.

Tranter, M., Brown, G., Raiswell, R., Sharp, M., & Gurnell, A. (1993). A conceptual model of solute acquisition by Alpine glacial meltwaters. Journal of Glaciology, 39(133), 573-581.

Tranter, M., Sharp, M. J., Lamb, H. R., Brown, G. H., Hubbard, B. P., & Willis, I. C. (2002). Geochemical weathering at the bed of Haut Glacier d'Arolla, Switzerland—a new model. Hydrological Processes, 16(5), 959-993.

Tranter, M. (2003). Geochemical weathering in glacial and proglacial environments. Treatise on geochemistry, 5, 605.

Tranter, M., Skidmore, M., & Wadham, J. (2005). Hydrological controls on microbial communities in subglacial environments. Hydrological Processes, 19(4), 995-998.

Tuttle, J. H., & Jannasch, H. W. (1976). Microbial utilization of thiosulfate in the deep sea 1. Limnology and Oceanography, 21(5)

Urbanski, S. P., Stickel, R. E., & Wine, P. H. (1998). Mechanistic and kinetic study of the gas-phase reaction of hydroxyl radical with dimethyl sulfoxide. The Journal of Physical Chemistry A, 102(51), 10522-10529.

Vick-Majors, T. J., Priscu, J. C., & Amaral-Zettler, L. A. (2014). Modular community structure suggests metabolic plasticity during the transition to polar night in ice-covered Antarctic lakes. The ISME Journal, 8(4), 778-789.

Vick-Majors, T. J., Mitchell, A. C., Achberger, A. M., Christner, B. C., Dore, J. E., Michaud, A. B., Mikucki, J.A., Purcell, A.M., Skidmore, M.L., Priscu, J.C., & WISSARD Science Team. (2016). Physiological ecology of microorganisms in Subglacial Lake Whillans. Frontiers in microbiology, 7, 216269.

Wadham, J. L., Hodgkins, R., Cooper, R. J., & Tranter, M. (2001). Evidence for seasonal subglacial outburst events at a polythermal glacier, Finsterwalderbreen, Svalbard. Hydrological Processes, 15(12), 2259-2280.

Wadham, J. L., Bottrell, S., Tranter, M., & Raiswell, R. (2004). Stable isotope evidence for microbial sulphate reduction at the bed of a polythermal high Arctic glacier. Earth and Planetary Science Letters, 219(3-4), 341-355.

Wadham, J. L., Tranter, M., Tulaczyk, S., & Sharp, M. (2008). Subgacial methanogenesis: a potential climatic amplifier?. Global Biogeochemical Cycles, 22(2).

Wadham, J. L., Tranter, M., Skidmore, M., Hodson, A. J., Priscu, J., Lyons, W. B., Sharp, M., Wynn, P., & Jackson, M. (2010). Biogeochemical weathering under ice: Size matters. Global Biogeochemical Cycles, 24(3).

Wadham, J. L., Arndt, S., Tulaczyk, S., Stibal, M., Tranter, M., Telling, J., Lis, G.P., Lawson, E., Ridgwell, A., Dubnick, A., Sharp, M.J., Anesio, A.M., & Butler, C. E. H. (2012). Potential methane reservoirs beneath Antarctica. Nature, 488(7413), 633-637.

Waldron, P. J., Petsch, S. T., Martini, A. M., & Nüsslein, K. (2007). Salinity constraints on subsurface archaeal diversity and methanogenesis in sedimentary rock rich in organic matter. Applied and Environmental Microbiology, 73(13), 4171-4179.

Wang, Z., Chang, X., Yang, X., Pan, L., & Dai, J. (2014). Draft genome sequence of Polaromonas glacialis strain R3-9, a psychrotolerant bacterium isolated from Arctic glacial foreland. Genome announcements, 2(4), 10-1128.

Wang, Q., Dore, J. E., & McDermott, T. R. (2017). Methylphosphonate metabolism by Pseudomonas sp. populations contributes to the methane oversaturation paradox in an oxic freshwater lake. Environmental Microbiology, 19(6), 2366-2378.

Wang, R., Lin, J. Q., Liu, X. M., Pang, X., Zhang, C. J., Yang, C. L., Lin, J.Q., & Chen, L. X. (2019). Sulfur oxidation in the acidophilic autotrophic Acidithiobacillus spp. Frontiers in microbiology, 9, 3290.

Wang, Q., Alowaifeer, A., Kerner, P., Balasubramanian, N., Patterson, A., Christian, W., Tarver, A., Dore, J., Hatzenpichler, R., Boothner, B., & McDermott, T. R. (2021). Aerobic bacterial methane synthesis. Proceedings of the National Academy of Sciences, 118(27), e2019229118.

Ward, B. B., Granger, J., Maldonado, M. T., & Wells, M. L. (2003). What limits bacterial production in the suboxic region of permanently ice-covered Lake Bonney, Antarctica?. Aquatic Microbial Ecology, 31(1), 33-47.

Warrier, R. B., Castro, M. C., Hall, C. M., Kenig, F., & Doran, P. T. (2015). Reconstructing the evolution of Lake Bonney, Antarctica using dissolved noble gases. Applied Geochemistry, 58, 46-61.

Weiss, J. V., Rentz, J. A., Plaia, T., Neubauer, S. C., Merrill-Floyd, M., Lilburn, T., Bradburne, C.; Megonigal, J.P., & Emerson, D. (2007). Characterization of neutrophilic Fe (II)-oxidizing bacteria isolated from the rhizosphere of wetland plants and description of Ferritrophicum radicicola gen. nov. sp. nov., and Sideroxydans paludicola sp. nov. Geomicrobiology Journal, 24(7-8), 559-570.

Welch, K. A., Lyons, W. B., Whisner, C., Gardner, C. B., Gooseff, M. N., McKnight, D. M., & Priscu, J. C. (2010). Spatial variations in the geochemistry of glacial meltwater streams in the Taylor Valley, Antarctica. Antarctic Science, 22(6), 662-672.

Weon, H. Y., Yoo, S. H., Hong, S. B., Kwon, S. W., Stackebrandt, E., Go, S. J., & Koo, B. S. (2008). Polaromonas jejuensis sp. nov., isolated from soil in Korea. International journal of systematic and evolutionary microbiology, 58(7), 1525-1528.

Whiticar, M. J. (1999). Carbon and hydrogen isotope systematics of bacterial formation and oxidation of methane. Chemical Geology, 161(1-3), 291-314.

Widdel, F., & Pfennig, N. (1981). Studies on dissimilatory sulfate-reducing bacteria that decompose fatty acids: I. Isolation of new sulfate-reducing bacteria enriched with acetate from saline environments. Description of Desulfobacter postgatei gen. nov., sp. nov. Archives of microbiology, 129, 395-400.

Widdel, F., Kohring, G. W., & Mayer, F. (1983). Studies on dissimilatory sulfate-reducing bacteria that decompose fatty acids: III. Characterization of the filamentous gliding Desulfonema limicola gen. nov. sp. nov., and Desulfonema magnum sp. nov. Archives of microbiology, 134, 286-294.

Willis, M. J., Herried, B. G., Bevis, M. G., & Bell, R. E. (2015). Recharge of a subglacial lake by surface meltwater in northeast Greenland. Nature, 518(7538), 223-227.

Winkler, G. R., Silberman, M. L., Grantz, A., Miller, R. J., & MacEvitt Jr, E. M. (1981). Geologic map and summary geochronology of the Valdez quadrangle, southern Alaska, 1 sheet, scale 1: 250,000. US Geol. Surv. Open File Rep, 80-892.

Winslow, L. A., Dugan, H. A., Buelow, H. N., Cronin, K. D., Priscu, J. C., Takacs-Vesbach, C., & Doran, P. T. (2014). Autonomous year-round sampling and sensing to explore the physical and biological habitability of permanently ice-covered Antarctic lakes. Marine Technology Society Journal, 48(5), 8-17.

Wolin, E. A., Wolin, M., & Wolfe, R. S. (1963). Formation of methane by bacterial extracts. Journal of Biological Chemistry, 238(8), 2882-2886.

Xing, T., Yao, T., Liu, Y., Wang, N., Xu, B., Shen, L., Gu, Z., Gu, B., Liu, H., & Zhou, Y. (2016). Polaromonas eurypsychrophila sp. nov., isolated from an ice core. International Journal of Systematic and Evolutionary Microbiology, 66(7), 2497-2501.

Xu, Y., & Schoonen, M. A. (1995). The stability of thiosulfate in the presence of pyrite in low-temperature aqueous solutions. Geochimica et Cosmochimica Acta, 59(22), 4605-4622.

Yagi, J. M., Sims, D., Brettin, T., Bruce, D., & Madsen, E. L. (2009). The genome of Polaromonas naphthalenivorans strain CJ2, isolated from coal tar-contaminated sediment, reveals physiological and metabolic versatility and evolution through extensive horizontal gene transfer. Environmental microbiology, 11(9), 2253-2270.

Yarnes, C. (2013). δ13C and δ2H measurement of methane from ecological and geological sources by gas chromatography/combustion/pyrolysis isotope-ratio mass spectrometry. Rapid Communications in Mass Spectrometry, 27(9), 1036-1044

You, K., & Flemings, P. B. (2018). Methane hydrate formation in thick sandstones by free gas flow. Journal of Geophysical Research: Solid Earth, 123(6), 4582-4600.

Zhang, J., Liu, R., Xi, S., Cai, R., Zhang, X., & Sun, C. (2020). A novel bacterial thiosulfate oxidation pathway provides a new clue about the formation of zero-valent sulfur in deep sea. The ISME Journal, 14(9), 2261-2274.

Zhang, S., Yang, G., Wang, Y., & Hou, S. (2010). Abundance and community of snow bacteria from three glaciers in the Tibetan Plateau. Journal of Environmental Sciences, 22(9), 1418-1424.